

#45

**GEOLOGY OF THE MAIN DRIFT - STATION 28+00 TO 55+00,
EXPLORATORY STUDIES FACILITY, YUCCA MOUNTAIN PROJECT,
YUCCA MOUNTAIN, NEVADA**

**by A.L. Albin, W.L. Singleton, T.C. Moyer, A.C. Lee, R.C. Lung, G.L.W.
Eatman, and D.L. Barr**

Bureau of Reclamation and U.S. Geological Survey

**Prepared in cooperation with the
NEVADA FIELD OFFICE,
U.S. DEPARTMENT OF ENERGY,
under Interagency Agreement DE-AI08-92NV10874**

040059

**Denver, Colorado
1997**

9803050057 971231
PDR WASTE
WM-11 PDR



DF03
0/1
102
WM-11

TABLE OF CONTENTS

PREFACE	ix
ABSTRACT	1
INTRODUCTION	4
Tunnel Terminology	9
Geology of the Yucca Mountain Area	10
Site-Characterization Techniques	11
Full-Periphery Geologic Mapping	11
Detailed Line Surveys	11
Stereophotographic Coverage	14
Rock Sampling	14
LITHOSTRATIGRAPHY	15
Topopah Spring, Crystal-Poor Member	15
Middle Nonlithophysal Zone (Tptpmn) - Rock Unit and Contact descriptions	15
Lower Lithophysal Zone (Tptpll)	19
Stratigraphic and Depositional Features	20
Welding Features, Secondary Crystallization, and Alteration	20
STRUCTURE	22
Fractures	22
Cooling joints	24
Analysis of Fracture Data	26
Domains Defined by Fracture Characteristics	34
Comparison of DLS Data, 30cm min. versus 1 m min. Trace Length	40
Faults and Shears	45
Analysis of Fault-and-Shear Data	47
Domains Defined by Fault-and-Shear Characteristics	53
Fracture zone between Sta. 42+00 and 51+50	57
Fracture Zone Characteristics	58
Faults and Shears in the Fracture Zone	63
Origin of the Fracture Zone	64
Age relations	65
Summation	65
Comparative Cross Section	67
STATISTICAL ANALYSIS	69
Cluster Analysis	69
Domain Selection	70
Analysis	71

The First Domain, Sta. 28+00 to 37+00	71
The Second Domain, Sta. 37+00 to 42+00	72
The Third Domain, Sta. 42+00 to 51+50	73
The Fourth Domain, Sta. 51+50 to 55+00	74
Results	75
Set 1 and Set 2	75
Set 3	80
Set 4	80
Multivariate Statistical Analysis	82
Data Processing	82
Descriptive Statistics	83
R-mode, maximum variance, principal component analysis results	83
Structural heterogeneities within the Tptpmn as identified by factor 1 scores ..	84
Structural heterogeneities within the Tptpmn as identified by factor 2 scores	100
Correlations between strike and factor 1 and 2 scores	100
CHLORINE-36	101
GEOTECHNICAL CHARACTERIZATION	102
Background	102
Stratigraphic Unit	103
Physical Features	103
Hydrology	104
Introduction to RQD, RMR, and Q	104
Rock Quality Designation (RQD)	105
Summary of RQD	106
Rock Mass Rating (RMR)	110
Rating for Compressive Strength	110
Rating for RQD	111
Rating for Spacing of Discontinuities	111
Rating for Condition of Discontinuities	111
Joint-Condition Length, continuity	111
Joint-Condition Separation, aperture	111
Joint-Condition Roughness	112
Joint-Condition Filling, gouge	112
Joint-Condition Weathering	112
Rating for Groundwater	113
Adjustment for Orientation of Discontinuities	113
Summary of RMR	114
RMR Very Unfavorable and Favorable Azimuth Frequency	118
Norwegian Geotechnical Institute Rock Quality Q System	119
RQD Rating	120

Jn Rating	120
Observational Jn	120
Joint-Set Orientation	122
Jr Rating	122
Joint-Alteration Rating	123
Joint-Water Rating	123
Stress-Reduction-Factor Rating	123
Summary of Rated Q	125
Ratios	129
Orientation of Critical Joint Sets For Rated Q	136
Ground Support	138
General	138
Classes of Support	140
Installed versus Rated Ground Support	140
Summary of Ground Support	145
Stations 28+00 - 34+00	146
Stations 34+00 - 37+00	146
Stations 37+00 - 39+00	147
Stations 39+00 - 42+00	147
Stations 42+00 - 44+00	148
Stations 44+00 - 51+50	148
Stations 51+50 - 55+00	149
Summary And Conclusions	149
Rock Mass Quality	149
RQD	149
RMR	150
Q	150
Conclusions	151
 REFERENCES	 158
 APPENDIX 1	 162
 APPENDIX 2	 166
 APPENDIX 3	 210

FIGURES

1. Location Map of the Yucca Mountain Project
2. Yucca Mountain and the Exploratory Studies Facility
3. Lithostratigraphic column of the Paintbrush Group
4. Stereonets of fracture data from Sta. 33+00 to 36+00
5. Azimuth distribution in the Main Drift
6. Fracture density in the Main Drift
7. Fracture density of Set 1 versus the remaining fractures
8. Azimuth distribution, First, Second, and Fourth Domains
9. Terzaghi correction of Main Drift data
10. Azimuth distribution, First Domain
11. Azimuth distribution, Second Domain
12. Stereonets of fracture data from Sta. 46+00 to 50+00
13. Stereonets of fracture data from Sta. 51+00 to 54+00
14. Fracture density of 30 cm to 1 m long versus 1 m and longer data
15. Bivariate factor 1 versus fracture length
16. Bivariate factor 1 versus fracture length
17. Bivariate factor 2 versus fracture length
18. Stereonet, FPGM fault data
19. Stereonets, FPGM fault data by domain
20. Fracture density, fracture zone in the Main Drift
21. Fracture density, fracture sets plotted separately
22. Azimuth distribution in the fracture zone
23. Fault density in the fracture zone
24. The ESF and the Ghost Dance fault
25. Azimuth distribution of each domain
26. Azimuth distribution, Sta. 27+00 to 28+00
27. Azimuth distribution, alcove 5

28. Azimuth distribution, South Ramp Sta. 59+35 to 63+08
29. Azimuth distribution, alcove 6
30. Factor score versus stationing, Sta. 35+30 to 37+50
31. Factor score versus stationing, Sta. 50+00 to 55+00
32. Factor score versus stationing, Sta. 33+00 to 35+90
33. Factor score versus stationing, Sta. 38+00 to 43+00
34. Factor score versus stationing, Sta. 47+00 to 48+20
35. Factor score versus stationing, Sta. 48+40 to 50+60
36. Factor score versus stationing, Sta. 40+00 to 44+00
37. Factor score versus stationing, Sta. 50+00 to 53+00
38. Factor 1 score versus strike, 000° to 130°
39. Factor 1 score versus strike, 131° to 260°
40. Factor 1 score versus strike, 261° to 360°
41. Factor 2 score versus strike, 000° to 130°
42. Factor 2 score versus strike, 131° to 260°
43. Factor 2 score versus strike, 261° to 360°
44. Frequency of RQD Ratings
45. Rock Quality Description Values
46. Domain One RQD, Sta. 28+00 to 37+00
47. Domain Two RQD, Sta. 37+00 to 42+00
48. Domain Three RQD, Sta. 42+00 to 51+50
49. Domain Four RQD, Sta. 51+50 to 55+00
50. Rock Mass Rating Results for the Main Drift
51. Rock Mass Rating Results for the Main Drift
52. Domain One RMR, Sta. 28+00 to 37+00
53. Domain Two RMR, Sta. 37+00 to 42+00
54. Domain Three RMR, Sta. 42+00 to 51+50
55. Domain Four RMR, Sta. 51+50 to 55+00
56. Frequency of Azimuths Used to Calculate the Lowest RMR

57. Frequency of Azimuths Used to Calculate the Highest RMR
58. Frequency of Joint Set Ratings in the Main Drift
59. Value of Rated Q for the Main Drift
60. Maximum Value of Q for the Main Drift
61. Rock Quality Rated Q for the Main Drift
62. Main Drift rated Q and Q Max. For Domain One, Sta. 28+00 to 37+00
63. Main Drift rated Q and Q Max. For Domain Two, Sta. 37+00 to 42+00
64. Main Drift rated Q and Q Max. For Domain Three, Sta. 42+00 to 51+50
65. Main Drift rated Q and Q Max. For Domain Four, Sta. 51+50 to 55+00
66. Block-Size-Ratio Comparisons For Domain One, Sta. 28+00 to 37+00
67. Block-Size-Ratio Comparisons For Domain Two, Sta. 37+00 to 42+00
68. Block-Size-Ratio Comparisons For Domain Three, Sta. 42+00 to 51+50
69. Block-Size-Ratio Comparisons For Domain Four, Sta. 51+50 to 55+00
70. Shear-Strength-Ratio Comparisons For Domain One, Sta. 28+00 to 37+00
71. Shear-Strength-Ratio Comparisons For Domain Two, Sta. 37+00 to 42+00
72. Shear-Strength-Ratio Comparisons For Domain Three, Sta. 42+00 to 51+50
73. Shear-Strength-Ratio Comparisons For Domain Four, Sta. 51+50 to 55+00
74. Active-Stress-Ratio Comparisons For Domain One, Sta. 28+00 to 37+00
75. Active-Stress-Ratio Comparisons For Domain Two, Sta. 37+00 to 42+00
76. Active-Stress-Ratio Comparisons For Domain Three, Sta. 42+00 to 51+50
77. Active-Stress-Ratio Comparisons For Domain Four, Sta. 51+50 to 55+00
78. Frequency of Azimuths Used to Calculate Rated Q
79. Frequency of Azimuths Used to Calculate Q Max.
80. Installed Support Frequency
81. Rated Support Frequency
82. Installed-versus-Rated Ground-Support Requirements Sta. 28+00 to 37+00
83. Installed-versus-Rated Ground-Support Requirements Sta. 37+00 to 42+00
84. Installed-versus-Rated Ground-Support Requirements Sta. 42+00 to 51+50
85. Installed-versus-Rated Ground-Support Requirements Sta. 51+50 to 55+00

TABLES

1. Fracture Sets by domain
2. FPGM Fault data
3. FPGM Fault offset data
4. Descriptive statistical analysis
5. Station Coordinates at Stratigraphic Contacts Along Main Drift DLS Tape
6. Fracture Sets By Domain
7. Percentages of RQD
8. RMR Ratings for Joint Orientation in Tunnels
9. Percentages of RMR
10. Q system Joint-Number Rating
11. Q system Stress-Reduction-Factor Rating
12. Percentages of Rated Q
13. Summary of Rock Mass Classification Averages
14. YMP Design Ground-Support Classes
15. Rated and Installed Ground Support in the Main Drift
16. Ground-Support Summary

DRAWINGS

Drawing OA-46-291: Comparative Geologic Cross Section Along the Main Drift

Drawing OA-46-295: Azimuth and dip versus stationing, Main Drift

Drawing OA-46-296: Fracture statistics diagrams, Domain 1

Drawing OA-46-297: Fracture statistics diagrams, Domain 2

Drawing OA-46-298: Fracture statistics diagrams, Domain 3

Drawing OA-46-299: Fracture statistics diagrams, Domain 4

PHOTOS

- 1 YM8085: The TBM near the ESF portal
- 2 YM11095: Geologic mapping from the TBM trailing gear also showing the gantry
- 3 YM12625: Entrance to Alcove 5
- 4 YM13139: Initial excavation of Alcove 7
- 5 PG15552: Tunnel walls showing variation in the color of the matrix
- 6 PG9788: Vapor-phase alteration in the upper Tptpmn
- 7 PG15558: Curved cooling joint
- 8 PG11423, PG11424, PG11418, PG11419: Conical shape formed from intersecting fractures
- 9 PG9817: Cooling joint with perpendicular vapor-phase partings
- 10 PG12057: Slickensides on the Sundance fault
- 11 YM11731: Intense fracturing in the fracture zone
- 12 YM11739: Close-up of intense fracturing
- 13 PG16263, PG16264: Fracturing obvious on walls but not in the crown
- 14 EG&G88b187L: Aerial photo, Yucca Mountain

PREFACE

This report is being submitted to the U.S. Department of Energy to fulfill Level 3 Milestone SPG42AM3: Report on the Geology North/South Main Drift Station 28+00 to 55+00. The Planning and Scheduling Account Number is 1.2.3.2.2.1.2 for the Summary Account titled: Geologic Mapping of the Exploratory Studies Facility. It is the summarization of the U.S. Bureau of Reclamation's mapping of the stratigraphy and structure of the Main Drift from Stations 28+00 to 55+00. Included in the report are statistical analyses of fractures and the geotechnical characterization which presents rock mass quality ratings and rock mass mechanical properties. This report enhances the map and data deliverable for the same interval presented earlier as Level 3 Milestone 3GGF603M.

Table 1 of this preface is the PACS description/completion criteria of Milestone SPG42AM3 in outline form. The table is provided as a guide for DOE reviewers in verifying completion of the milestone. Documentation attached to this preface as part of the milestone requirements include copies of Technical Data Information Forms identifying acquired and developed data generated for this report (Attachment 1) and copies of the transmittal letters to the GENISES Administrator describing the data submitted for entry into the Technical Data Base (Attachment 2).

All the data used in the development of this report were collected and the report was prepared in accordance with approved quality assurance procedures which implement requirements of the Quality Assurance Requirements Descriptions. Therefore, the developed data from this report and all data used have a Q status.

TABLE 1 - Description/completion criteria location summary for U.S. Department of Energy Level 3 Milestone: SPG42AM3 - Geology of the Main Drift, Station 28+00 to 55+00, Exploratory Studies Facility, Yucca Mountain Project, Yucca Mountain, Nevada

CRITERIA	LOCATION/COMPLETION INFORMATION
TECHNICAL REQUIREMENTS	
<p>1. This report will integrate all mapping and other data, including, as appropriate, data from the north ramp report, to present a complete description of the geology of the north/south main drift of the ESF.</p>	<p>The report integrates all mapping and data obtained from Stations 28+00 through 55+00 of the Main Drift. Data obtained from the North Ramp is referenced as appropriate within the report.</p>
<p>2. Maps included with the report will cover from station 28+00 to 55+00, and be presented at a scale of 1:125.</p>	<p>All Full Periphery Geotechnical Maps (FPGM) covering Stations 28+00 to 55+00 are presented at a scale of 1:125.</p>
<p>3. These full-periphery geotechnical maps will show:</p> <p>A. Mapped geologic units and subunits, fractures, faults, and other important structural features (as appropriate),</p> <p>B. The location of all samples collected by the mapping group (or collected by the Pls and/or the ESF Technical Coordination Office), and</p> <p>C. As-constructed installed ground support and type.</p>	<p>The full periphery geotechnical maps incorporate Items A, B, and C of this criteria. These maps have been submitted earlier to the DOE Technical Data Base as part of the data packages identified by the ATDT Data Tracking Numbers below. See Attachments 1 and 2 of the Preface for copies of the TDIFs and GENISES transmittal letters.</p> <p style="text-align: center;"> GS960808314224.012 GS960908314224.015 GS960908314224.016 GS960908314224.017 </p>

TABLE 1 (Continued) - Description/completion criteria location summary for U.S. Department of Energy Level 3 Milestone: SPG42AM3 - Geology of the Main Drift, Station 28+00 to 55+00, Exploratory Studies Facility, Yucca Mountain Project, Yucca Mountain, Nevada

CRITERIA	LOCATION/COMPLETION INFORMATION
<p>4. The deliverable will supply fracture analysis for the north/south main drift in the form of tabulated data sets, stereo plots, and statistical treatment of fracture information (by stratigraphic unit, or some selected interval along the course of tunnel excavation).</p>	<p>Within the report the sections on Structure and Statistical Analysis supply the statistical treatment of the fracture analysis. Additional fracture analyses are provided by the stereonets graphically presented on the FPGMs identified above in Item 3. Detailed Line Surveys (DLS) present tabulated fracture data. The DLSs for Stations 28 + 00 to 55 + 00 have been submitted earlier to the DOE Technical Data Base as part of the data packages identified by ATDT DTNs below. See Attachments 1 and 2 of the Preface for copies of the TDIFs and GENISES transmittal letters.</p> <p style="text-align: center;"> GS960608314224.007 GS960708314224.008 GS960708314224.010 GS960808314224.011 GS960808314224.013 GS960908314224.014 </p>
<p>5. A cross section comparing the predicted geology of the north/south main drift and as-determined structural and stratigraphic interpretations will be presented.</p>	<p>See Drawing OA-46-291 provided in a pocket at the back of the report. This drawing has been submitted earlier to the DOE Technical Data Base as part of the data package identified by the ATDT DTN GS960908314224.022. See Attachments 1 and 2 of the Preface for copies of the TDIF and the GENISES transmittal letter.</p>
<p>6. Predicted and actual stratigraphic, structural and other key features will be discussed in the report.</p>	<p>See Drawing OA-46-291 and the information provided in the section titled "Comparative Cross Section" within the Structure section of the report.</p>

TABLE 1 (Continued) - Description/completion criteria location summary for U.S. Department of Energy Level 3 Milestone: SPG42AM3 - Geology of the Main Drift, Station 28+00 to 55+00, Exploratory Studies Facility, Yucca Mountain Project, Yucca Mountain, Nevada

CRITERIA	LOCATION/COMPLETION INFORMATION
7. Important sampling and testing activities will be identified and discussed, as appropriate.	Funding for the USBR's systematic sampling program in the ESF was terminated in September 1995, prior to excavation of the Main Drift. Location of samples collected by LANL in the Main Drift are identified on the FPGMs (see Item 3).
8. A general discussion of the stratigraphy and structure will be provided that will include characterization of predicted locations of known or suspected fault features such as the Sundance and Ghost Dance faults.	See the Lithostratigraphy and Structural sections.
9. The report will also include a description of rock characteristics associated with features that do not lend themselves well to graphical presentations contained in the report such as fault gouge and breccia.	See the Lithostratigraphy section.
10. Results of the detailed line survey and appropriate graphical and tabular presentation of data will be included in the report.	See the Structure section.
11. A summary of photographic work conducted in support of the mapping exercise will be provided as part of the report.	See "Stereophotographic Coverage" in the Introduction and Appendix 3 for photographs with captions.

TABLE 1 (Continued) - Description/completion criteria location summary for U.S. Department of Energy Level 3 Milestone: SPG42AM3 - Geology of the Main Drift, Station 28+00 to 55+00, Exploratory Studies Facility, Yucca Mountain Project, Yucca Mountain, Nevada

CRITERIA	LOCATION/COMPLETION INFORMATION
12. The stereophotography will be identified within the report (photo numbers, current archive location) for future reference.	See Appendix 2 (Photogrammetric Negative Numbers and Camera Locations).
13. The report will briefly describe any unusual features observed in the mapping, detailed line survey, photogrammetry, or sampling exercises.	See "Fractures (Cooling Joints)" and "Faults and Shears" within the Structure section. See also Photograph #13 in Appendix 3.
14. Results of the RQD and Q&RMR analyses will also be provided and integrated into map or other graphical presentations of related data.	The results are provided on FPGMs (see Item 3) and within the Geotechnical Characterization section of the report.
15. Simple statistical treatment or qualitative assessment of the results of the subject survey will be provided.	See Statistical Analysis section.
16. The following will be included in the report: <ul style="list-style-type: none"> A. Alcove maps (for constructed portions of Alcove 5, the thermal test facility, and Alcove 6, the north Ghost dance Alcove), B. A summary of detailed line survey data, C. Stereo photographic information, D. Tabulations and assessment of structural data from alcove mapping investigations, and E. Statistical treatment of alcove fracture data. 	<p>The detailed line survey for Alcove 5 has been submitted earlier to the DOE Technical Data Base as part of the data package identified by the ATDT DTN GS960908314224.018. See Attachments 1 and 2 of the Preface for copies of the TDIF and the GENISES transmittal letter.</p> <p>The FPGM for Alcove 5 and the DLS and FPGM for Alcove 6 are in process but have not been completed because of inability to fully access the alcoves due to construction requirements. When completed, the data for the alcoves will be submitted as part of the South Ramp report due in August 1997 as Level 3 Milestone SPG42CM3.</p>

TABLE 1 (Continued) - Description/completion criteria location summary for U.S. Department of Energy Level 3 Milestone: SPG42AM3 - Geology of the Main Drift, Station 28+00 to 55+00, Exploratory Studies Facility, Yucca Mountain Project, Yucca Mountain, Nevada

CRITERIA	LOCATION/COMPLETION INFORMATION
REGULATORY REQUIREMENTS:	
1. This deliverable shall be prepared in accordance with OCRWM approved quality assurance procedures implementing requirements of the Quality Assurance Requirements Description.	See the Preface.
2. The product shall be developed on the basis of the best technical data, including both Q and non-Q data. The Q status of the data used and cited in the report shall be appropriately noted.	See the Preface.
3. OPTIONAL: Stratigraphy used shall be consistent with the Reference Information Base section 1.12(a): Stratigraphy-Geologic Lithologic Stratigraphy.	Stratigraphy used is in compliance with the RIB section 1.12(a).
4. Within the report's Reference Section, references to data used in the report shall include record Accession Numbers or Data Tracking Numbers when available.	Data used for development of this report are identified by DTN in Appendix 1 (Data Tracking Numbers for Review Packages). Reports or publications identified in the Reference section were not used as data sources but for corroborative or informational purposes only.

TABLE 1 (Continued) - Description/completion criteria location summary for U.S. Department of Energy Level 3 Milestone: SPG42AM3 - Geology of the Main Drift, Station 28+00 to 55+00, Exploratory Studies Facility, Yucca Mountain Project, Yucca Mountain, Nevada

CRITERIA	LOCATION/COMPLETION INFORMATION
<p>5. Technical data contained within the deliverable and not already incorporated in the Geographic nodal Information Study and Evaluation System (GENISES) shall be submitted for incorporation into the GENISES in accordance with YAP-SIII.3Q.</p>	<p>The developed data generated from this report is identified in the ATDT system under TDIF DTN GS970208314224.005. See Attachments 1 and 2 of the Preface for copies of the TDIF and the GENISES transmittal letter.</p>
<p>6. Verification of technical data submittal compliance shall be demonstrated by including as part of the deliverable:</p> <ol style="list-style-type: none"> 1. A copy of the Technical Data Information Form generated identifying the data in the Automated Technical Data Tracking system, and 2. A copy of the transmittal letter attached to the technical data transmittal to the GENISES Administrator. 	<p>See Attachments 1 and 2 of the Preface.</p>
<p>7. This deliverable shall be processed in accordance with YAP-5.1Q.</p>	<p>See YAR accompanying this milestone deliverable.</p>

PREFACE

ATTACHMENT 1

Technical Data Information Forms

YMP-023-R4
05/06/96

YUCCA MOUNTAIN SITE CHARACTERIZATION PROJECT TECHNICAL DATA INFORMATION

(Check one): ACQUIRED DATA (complete Parts I and II)
Data Tracking Number (DTN): _____

DEVELOPED DATA (complete Parts I, II and III)
Data Tracking Number (DTN): GS960608314224.007

PART I Identification of Data

Title/Description of Data: PROVISIONAL RESULTS: GEOTECHNICAL DATA FOR STATION 26+00 TO 30+00, NORTH RAMP AND MAIN DRIFT OF THE ESF: DETAILED LINE SURVEY DATA

Principal Investigator (PI): BEASON, S C
Last Name First and Middle Initials

PI Organization: U.S. BUREAU OF RECLAMATION

Are Data Qualified?: Yes No Governing Plan: SCPB

SCPB Activity Number(s): 3.3.1.4.2.2.4

WBS Number(s): 1.2.3.2.2.1.2

PART II Data Acquisition/Development Information

Method: TECHNICAL PROCEDURE NWM-USGS GP-32.R0, "UNDERGROUND GEOLOGIC MAPPING", AND SCIENTIFIC NOTEBOOK SN-0084, "COLLECTION OF UNDERGROUND SITE CHARACTERIZATION DATA"

Location(s): ESF - NORTH RAMP AND MAIN DRIFT: RIGHT RIB

Period(s): 11/8/95 to 12/1/95
From: MM/DD/YY To: MM/DD/YY

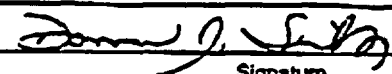
Sample ID Number(s): _____

PART III Source Data DTN(s)

<u>MO950000000005.009</u>	_____	_____
_____	_____	_____
_____	_____	_____

Comments

DATA WERE COLLECTED BY R. LUNG, G. EATMAN, D. BARR, A. ALBIN, A. LEE, AND G. TURLINGTON

Checked by:  12/3/96
Signature Date

YMP-023-R4
05/06/96

YUCCA MOUNTAIN SITE CHARACTERIZATION PROJECT TECHNICAL DATA INFORMATION

(Check one):

ACQUIRED DATA (complete Parts I and II)

Data Tracking Number (DTN): _____

DEVELOPED DATA (complete Parts I, II and III)

Data Tracking Number (DTN): GS960708314224.008

PART I Identification of Data

Title/Description of Data: PROVISIONAL RESULTS: GEOTECHNICAL DATA FOR STATION 30+00 TO STATION 35+00.

MAIN DRIFT OF THE ESF: DETAILED LINE SURVEY DATA

Principal Investigator (PI): BEASON, S C

Last Name

First and Middle Initials

PI Organization: U.S. BUREAU OF RECLAMATION

Are Data Qualified?: Yes No

Governing Plan: SCPB

SCPB Activity Number(s): 8.3.1.4.2.2.1

WBS Number(s): 1.2.3.2.2.1.2

PART II Data Acquisition/Development Information

Method: TECHNICAL PROCEDURE NWM-USGS GP-32, RO. "UNDERGROUND GEOLOGIC MAPPING"; AND SCIENTIFIC

NOTEBOOK SN-0084. "COLLECTION OF UNDERGROUND SITE CHARACTERIZATION DATA"

Location(s): ESF - MAIN DRIFT, RIGHT RIB

Period(s): 12/1/95 to 1/5/96

From: MM/DD/YY

To: MM/DD/YY

Sample ID Number(s): _____

PART III Source Data DTN(s)

M0950000000005.009

Comments

DATA WERE COLLECTED BY R.LUNG, G.EATMAN, A.ALBIN, D.BARR, A.LEE, J.ROGERS, G.TURLINGTON, AND J.BOWEN

Checked by: _____

Donna J. Sultz
Signature

10/3/96

Date

YMP-023-R4
05/06/96YUCCA MOUNTAIN SITE CHARACTERIZATION PROJECT
TECHNICAL DATA INFORMATION

Page 1 of 1

(Check one): ACQUIRED DATA (complete Parts I and II)
Data Tracking Number (DTN): _____

DEVELOPED DATA (complete Parts I, II and III)
Data Tracking Number (DTN): GS960708314224.010

PART I Identification of Data

Title/Description of Data: PROVISIONAL RESULTS: GEOTECHNICAL DATA FOR STATION 40+00 TO STATION 45+00,
MAIN DRIFT OF THE ESF: DETAILED LINE SURVEY DATA

Principal Investigator (PI): BEASON, S C
Last Name First and Middle Initials

PI Organization: U.S. BUREAU OF RECLAMATION

Are Data Qualified?: Yes No Governing Plan: SCPB

SCPB Activity Number(s): 8.3.1.4.2.2.4

WBS Number(s): 1.2.3.2.2.1.2

PART II Data Acquisition/Development Information

Method: TECHNICAL PROCEDURE MW-USGS G2-32.R0. "UNDERGROUND GEOLOGIC MAPPING", AND SCIENTIFIC
NOTEBOOK SN-0084. "COLLECTION OF UNDERGROUND SITE CHARACTERIZATION DATA"

Location(s): ESF - MAIN DRIFT, RIGHT RIB

Period(s): 2/2/96 to 3/21/96
From: MM/DD/YY To: MM/DD/YY

Sample ID Number(s): _____

PART III Source Data DTN(s)

MO960000000005.010 _____

Comments

SUBJECT TO REVISION. DATA WERE COLLECTED BY ROB LUNG, GEORGE EATMAN, ALTON ALBIN, DEBBIE BARR, ARTHUR
LEE, JIM ROGERS, GARY TURLINGTON, JIM BOWEN, AND DONNA SINKS

Checked by: _____

Signature

10/3/96

YMP-023-R4
05/06/96

YUCCA MOUNTAIN SITE CHARACTERIZATION PROJECT TECHNICAL DATA INFORMATION

(Check one): ACQUIRED DATA (complete Parts I and II)
Data Tracking Number (DTN): _____

DEVELOPED DATA (complete Parts I, II and III)
Data Tracking Number (DTN): GS960808314224.011

PART I Identification of Data

Title/Description of Data: PROVISIONAL RESULTS: GEOTECHNICAL DATA FOR STATION 35+00 TO STATION 40+00, MAIN DRIFT OF THE ESP: DETAILED LINE SURVEY

Principal Investigator (PI): BEASON, S C
Last Name First and Middle Initials

PI Organization: J.S. BUREAU OF RECLAYATION

Are Data Qualified?: Yes No Governing Plan: SCP8

SCP8 Activity Number(s): 2.3.1.4.2.2.4

WBS Number(s): 1.2.3.2.2.1.2

PART II Data Acquisition/Development Information

Method: TECHNICAL PROCEDURE NWM-USGS GP-32.R0, "UNDERGROUND GEOLOGIC MAPPING", AND SCIENTIFIC NOTEBOOK SN-0084, "COLLECTION OF UNDERGROUND SITE CHARACTERIZATION DATA".

Location(s): ESP - MAIN DRIFT, RIGHT RIB

Period(s): 1/5/96 to 2/2/96
From: MM/DD/YY To: MM/DD/YY

Sample ID Number(s): _____

PART III Source Data DTN(s)

<u>00950000000005.009</u>	_____	_____
_____	_____	_____
_____	_____	_____

Comments

SUBJECT TO REVISION. DATA WERE COLLECTED BY ROB LUNG, GEORGE EATMAN, ALTON ALBIN, DEBBIE EARR, ARTHUR LEE, JIM ROGERS, GARY TURLINGTON, JIM BOWEN, AND FRANK CALCAGNO

Checked by: *Donna J. Silva*
Signature

10/3/96
Date

YMP-023-R4
05/06/96

YUCCA MOUNTAIN SITE CHARACTERIZATION PROJECT TECHNICAL DATA INFORMATION

(Check one): ACQUIRED DATA (complete Parts I and II)
Data Tracking Number (DTN): _____

DEVELOPED DATA (complete Parts I, II and III)
Data Tracking Number (DTN): GS960808314224.012

PART I Identification of Data

Title/Description of Data: PROVISIONAL RESULTS: GEOTECHNICAL DATA FOR STATION 26+00 TO 30+00, NORTH RAMP AND MAIN DRIFT OF THE ESF, FULL-PERIPHERY GEOTECHNICAL MAPS (DRAWINGS OA-46-222 THROUGH OA-46-226) AND ROCK MASS QUALITY RATINGS REPORT

Principal Investigator (PI): BEASON, S C
Last Name First and Middle Initials

PI Organization: U.S. BUREAU OF RECLAMATION

Are Data Qualified?: Yes No Governing Plan: SCPB

SCPB Activity Number(s): 8.3.1.4.2.2.4

WBS Number(s): 1.2.3.2.2.1.2

PART II Data Acquisition/Development Information

Method: TECHNICAL PROCEDURE NWM-USGS G7-32,80, "UNDERGROUND GEOLOGIC MAPPING", AND SCIENTIFIC NOTEBOOKS SN-0083, "COLLECTION AND PROCESSING OF GEOTECHNICAL DATA", AND SN-0084, "COLLECTION OF UNDERGROUND SITE CHARACTERIZATION DATA"

Location(s): ESF - MAIN DRIFT

Period(s): 11/8/95 to 11/30/95
From: MM/DD/YY To: MM/DD/YY

Sample ID Number(s): _____

PART III Source Data DTN(s)

<u>GS960608314224.007</u>	_____	_____
<u>SNF32020196001.001</u>	_____	_____
<u>SNF32120393001.019</u>	_____	_____

Comments

DATA WERE COLLECTED BY ROBERT LUNG, DEBORAH BARR, GEORGE EATMAN, ARTHUR LEE, ALTON ALBIN, JOHN STEIGNER, BILL SINGLETON, AND JEANNE MAJOR. TDIF REVISED 10/3/96.

Checked by: *Donna Smith* Signature 10/3/96 Date

YMP-023-R4
08/31/95

**YUCCA MOUNTAIN SITE CHARACTERIZATION PROJECT
TECHNICAL DATA INFORMATION
CONTINUATION SHEET**

Location(s) (continued)

ESF - NORTH RAMP

YMP-023-R4
05/06/96

YUCCA MOUNTAIN SITE CHARACTERIZATION PROJECT TECHNICAL DATA INFORMATION

(Check one): ACQUIRED DATA (complete Parts I and II)
Data Tracking Number (DTN): _____

DEVELOPED DATA (complete Parts I, II and III)
Data Tracking Number (DTN): GS960808314224.013

PART I Identification of Data

Title/Description of Data: PROVISIONAL RESULTS: GEOTECHNICAL DATA FOR STATION 45+00 TO 50+00, MAIN DRIFT OF ESF: DETAILED LINE SURVEY DATA

Principal Investigator (PI): BEASON, S C
Last Name First and Middle Initials

PI Organization: U.S. BUREAU OF RECLAMATION

Are Data Qualified?: Yes No Governing Plan: SCPB

SCPB Activity Number(s): 9.3.1.4.2.2.4

WBS Number(s): 1.2.3.2.2.1.2

PART II Data Acquisition/Development Information

Method: TECHNICAL PROCEDURE MWM-USGS GP-32.R0, "UNDERGROUND GEOLOGIC MAPPING"; SCIENTIFIC NOTEBOOK SN-0084, "COLLECTION OF SITE CHARACTERIZATION DATA" (REVISED DEFINITION OF COOLING JOINT (P.11) IMPLEMENTED AT STATION 47+92, REVISED DATA COLLECTION FORMAT (P.15) IMPLEMENTED AT STATION 47+51.40

Location(s): ESF - MAIN DRIFT, RIGHT RIB

Period(s): 3/21/96 to 6/5/96
From: MM/DD/YY To: MM/DD/YY

Sample ID Number(s): _____

PART III Source Data DTN(e)

<u>MO960000000005.010</u>	_____	_____
_____	_____	_____
_____	_____	_____

Comments

SUBJECT TO REVISION. DATA WERE COLLECTED BY R. LUNG, G. ZATMAN, D. BARR, A. ALBIN, A. LEE, J. ROGERS, G. TURLINGTON, J. BOWEN, D. SINKS. BLANKS APPEAR IN DATA COLLECTED PRIOR TO REVISION OF THE FORM. TDFI

Checked by: Donna J. Jiles 10/3/96
Signature Date

YMP-023-R4
08/31/95

**YUCCA MOUNTAIN SITE CHARACTERIZATION PROJECT
TECHNICAL DATA INFORMATION
CONTINUATION SHEET**

Comments (continued)

REVISED 9/24/96

YMP-023-R4
05/06/96

YUCCA MOUNTAIN SITE CHARACTERIZATION PROJECT TECHNICAL DATA INFORMATION

(Check one): ACQUIRED DATA (complete Parts I and II)
Data Tracking Number (DTN): _____

DEVELOPED DATA (complete Parts I, II and III)
Data Tracking Number (DTN): GS960908314224.014

PART I Identification of Data

Title/Description of Data: PROVISIONAL RESULTS - ESF MAIN DRIFT, STATION 50+00 TO STATION 55+00: DETAILED LINE SURVEY DATA

Principal Investigator (PI): BEASON, S C
Last Name First and Middle Initials

PI Organization: U.S. BUREAU OF RECLAMATION

Are Data Qualified?: Yes No Governing Plan: SCPB

SCPB Activity Number(s): 6.3.1.4.2.2.4

WBS Number(s): 1.2.3.2.2.1.2

PART II Data Acquisition/Development Information

Method: TECHNICAL PROCEDURE NWM-USGS GP-32.R0, "UNDERGROUND GEOLOGIC MAPPING"; SCIENTIFIC NOTEBOOK SN-0084, "COLLECTION OF SITE CHARACTERIZATION DATA"

Location(s): ESF - MAIN DRIFT, RIGHT RIB

Period(s): 3/21/96 to 6/5/96
From: MM/DD/YY To: MM/DD/YY

Sample ID Number(s): _____

PART III Source Data DTN(s)

<u>X0960000000005.010</u>	_____	_____
_____	_____	_____
_____	_____	_____

Comments

SUBJECT TO REVISION. DATA WERE COLLECTED BY ALTON ALBIN, DEBBIE BARR, JIM BOWEN, GEORGE EATMAN, ARTHUR LEE, ROB LUNG, JIM ROGERS, DONNA SINKS, AND GARY TURLINGTON

Checked by: Donna J. Sinks
Signature

10/3/96
Date

YMP-023-R4
05/06/96

YUCCA MOUNTAIN SITE CHARACTERIZATION PROJECT TECHNICAL DATA INFORMATION

(Check one): ACQUIRED DATA (complete Parts I and II)
Data Tracking Number (DTN): _____

DEVELOPED DATA (complete Parts I, II and III)
Data Tracking Number (DTN): GS960908314224.015

PART I Identification of Data

Title/Description of Data: PROVISIONAL RESULTS: GEOTECHNICAL DATA FOR STATIONS 30+00 TO 40+00, MAIN DRIFT OF THE ESF, FULL-PERIPHERY GEOTECHNICAL MAPS (DRAWINGS OA-46-227 THROUGH OA-46-238) AND ROCK MASS QUALITY RATINGS REPORT

Principal Investigator (PI): BEASON, S C
Last Name First and Middle Initials

PI Organization: U.S. BUREAU OF RECLAMATION

Are Data Qualified?: Yes No Governing Plan: SCPB

SCPB Activity Number(s): 8.3.1.4.2.2.4

WBS Number(s): 1.2.3.2.2.1.2

PART II Data Acquisition/Development Information

Method: TECHNICAL PROCEDURE NWM-USGS GP-32.R0, "UNDERGROUND GEOLOGIC MAPPING"; AND SCIENTIFIC NOTEBOOKS SN-0083, "COLLECTION AND PROCESSING OF GEOTECHNICAL DATA", AND SN-0084, "COLLECTION OF UNDERGROUND SITE CHARACTERIZATION DATA"

Location(s): ESF - MAIN DRIFT

Period(s): 12/1/95 to 2/13/96
From: MM/DD/YY To: MM/DD/YY

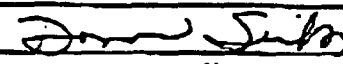
Sample ID Number(s): _____

PART III Source Data DTN(s)

<u>GS960708314224.008</u>	<u>SNF32020196001.002</u>	_____
<u>GS960908314224.011</u>	<u>SNF32020196001.004</u>	_____
<u>SNF32020196001.001</u>	<u>SNF32020196001.005</u>	_____

Comments

DATA WERE COLLECTED BY ALTON ALBIN, DEBBIE BARR, STEVE BEASON, F. CALCAGNO, GEORGE EATMAN, ARTHUR LEE, ROB LUNG, JEANNE MAJOR, BILL SINGLETON, AND JOHN STEIGNER. TDIF REVISED 10/3/96.

Checked by:  10/3/96
Signature

YMP-023-R4
05/06/96

YUCCA MOUNTAIN SITE CHARACTERIZATION PROJECT TECHNICAL DATA INFORMATION

(Check one): ACQUIRED DATA (complete Parts I and II)
Data Tracking Number (DTN): _____

DEVELOPED DATA (complete Parts I, II and III)
Data Tracking Number (DTN): GS960906314224.016

PART I Identification of Data

Title/Description of Data: PROVISIONAL RESULTS: GEOTECHNICAL DATA FOR STATION 40+00 TO 50+00, MAIN DRIFT OF THE ESF, FULL-PERIPHERY GEOTECHNICAL MAPS (DRAWINGS OA-46-239 THROUGH OA-46-250) AND ROCK MASS QUALITY RATINGS REPORT

Principal Investigator (PI): BEASON, S C
Last Name First and Middle Initials

PI Organization: U.S. BUREAU OF RECLAMATION

Are Data Qualified?: Yes No Governing Plan: SCPB

SCPB Activity Number(s): 8.3.1.4.2.2.4

WBS Number(s): 1.2.3.2.2.1.2

PART II Data Acquisition/Development Information

Method: TECHNICAL PROCEDURE MAM-USGS-GP-32, RO "UNDERGROUND GEOLOGIC MAPPING"; SCIENTIFIC NOTEBOOK SN-0063, "COLLECTION AND PROCESSING OF GEOTECHNICAL DATA"; AND SN-0064, "COLLECTION OF UNDERGROUND SITE CHARACTERIZATION DATA"

Location(s): ESF - MAIN DRIFT

Period(s): 2/6/96 to 5/7/95
From: MM/DD/YY To: MM/DD/YY

Sample ID Number(s): _____

PART III Source Data DTN(s)

<u>GS960708314224.010</u>	<u>SNF32020196001.007</u>	<u>SNF32020196001.011</u>
<u>GS960808314224.013</u>	<u>SNF32020196001.008</u>	_____
<u>SNF32020196001.006</u>	<u>SNF32020196001.009</u>	_____

Comments

DATA WERE COLLECTED BY ALTON ALBIN, DEBBIE BARR, F. CALCAGNO, GEORGE EATMAN, ARTHUR LEE, ROB LUNG, JEANNE MAJOR, BILL SINGLETON, AND JOHN STEIGHNER.

Checked by: *Don J. J...* 10/3/96
Signature Date

YMP-023-R4
05/06/96

YUCCA MOUNTAIN SITE CHARACTERIZATION PROJECT TECHNICAL DATA INFORMATION

(Check one): ACQUIRED DATA (complete Parts I and II)
Data Tracking Number (DTN): _____

DEVELOPED DATA (complete Parts I, II and III)
Data Tracking Number (DTN): GS960908314224.017

PART I Identification of Data

Title/Description of Data: PROVISIONAL RESULTS: GEOTECHNICAL DATA FOR STATIONS 50+00 TO 55+00, MAIN DRIFT OF THE ESF, FULL-PERIPHERY GEOTECHNICAL MAPS (DRAWINGS OA-46-251 THROUGH OA-46-256) AND ROCK MASS QUALITY RATINGS REPORT

Principal Investigator (PI): BEASON, S C
Last Name First and Middle Initials

PI Organization: U.S. BUREAU OF RECLAMATION

Are Data Qualified?: Yes No Governing Plan: SCPB

SCPB Activity Number(s): 8.3.1.4.2.2.4

WBS Number(s): 1.2.3.2.2.1.2

PART II Data Acquisition/Development Information

Method: TECHNICAL PROCEDURE MWM-USGS-GP32.R0, "UNDERGROUND GEOLOGIC MAPPING"; SCIENTIFIC NOTEBOOK SN-0083, "COLLECTION AND PROCESSING OF GEOTECHNICAL DATA"; AND SN-0084, "COLLECTION OF UNDERGROUND SITE CHARACTERIZATION DATA"

Location(s): ESF - MAIN DRIFT, RIGHT RIB

Period(s): 5/1/96 to 6/14/96
From: MM/DD/YY To: MM/DD/YY

Sample ID Number(s): _____

PART III Source Data DTN(s)

<u>GS960908314224.014</u>	_____	_____
<u>SNF32020196001.011</u>	_____	_____
<u>SNF32020196001.012</u>	_____	_____

Comments

DATA WERE COLLECTED BY ALTON ALBIN, DEBBIE BARR, DOUG BENNETT, ROB BURT, GEORGE EATMAN, ARTHUR LEE, ALLEN LOCKHART, ROB LUNG, JEANNE MAJOR, BILL SINGLETON, AND JOHN STEIGHNER

Checked by: *Don Silva* 10/3/96
Signature Date

YMP-023-R4
05/06/96

YUCCA MOUNTAIN SITE CHARACTERIZATION PROJECT TECHNICAL DATA INFORMATION

(Check one): ACQUIRED DATA (complete Parts I and II)
Data Tracking Number (DTN): _____

DEVELOPED DATA (complete Parts I, II and III)
Data Tracking Number (DTN): GS960908314224.018

PART I Identification of Data
 Title/Description of Data: PROVISIONAL RESULTS: GEOTECHNICAL DATA FOR ALCOVE 5 (DWFA), MAIN DRIFT OF THE
ESF: DETAILED LINE SURVEY DATA: 1) THERMOMECHANICAL ALCOVE EXTENSION, BEARING OF 108; 2)
THERMOMECHANICAL ALCOVE EXTENSION, BEARING OF 198; 3) ACCESS/OBSERVATION DRIFT, BEARING 108.

Principal Investigator (PI): BEASON, S C
Last Name First and Middle Initials

PI Organization: U.S. BUREAU OF RECLAMATION

Are Data Qualified?: Yes No Governing Plan: SCPB

SCPB Activity Number(s): S.3.2.4.2.2.4

WBS Number(s): 1.2.3.2.2.1.2

PART II Data Acquisition/Development Information
 Method: TECHNICAL PROCEDURE NMM-USGS-GF-32,R0, "UNDERGROUND GEOLOGIC MAPPING"; SCIENTIFIC NOTEBOOK
SN-0084, "COLLECTION OF UNDERGROUND SITE CHARACTERIZATION DATA"

Location(s): ESF - ALCOVE 5 (DWFA)

Period(s): 2/26/96 to 8/1/96
From: MM/DD/YY To: MM/DD/YY

Sample ID Number(s): _____

PART III Source Data DTN(s)
M0960000000005.011

Comments
DATA WERE COLLECTED BY GARY TURLINGTON, DAVID CHURCHILL, ARTHUR LEE, JIM ROGERS, KENT DOW AND DOUG
BENNETT

Checked by: *Donna Smith* 10/3/96
Signature Date

YMP-023-R4
05/06/96

YUCCA MOUNTAIN SITE CHARACTERIZATION PROJECT TECHNICAL DATA INFORMATION

(Check one): ACQUIRED DATA (complete Parts I and II)
Data Tracking Number (DTN): _____

DEVELOPED DATA (complete Parts I, II and III)
Data Tracking Number (DTN): GS960908314224.022

PART I Identification of Data

Title/Description of Data: EXPLORATORY STUDIES FACILITY - MAIN DRIFT, COMPARATIVE GEOLOGY CROSS SECTION
ALONG MAIN DRIFT, STATION 28+94.76 TO STATION 55+00 (DRAWING OA-46-291)

Principal Investigator (PI): EEASON, S C
Last Name First and Middle Initials

PI Organization: U.S. BUREAU OF RECLAMATION

Are Data Qualified?: Yes No Governing Plan: SCPB

SCPB Activity Number(s): 8.3.1.4.2.2.4

WBS Number(s): 1.2.3.2.2.1.2

PART II Data Acquisition/Development Information

Method: TECHNICAL PROCEDURE NWM-USGS G7-32.R0, "UNDERGROUND GEOLOGIC MAPPING" AND SCIENTIFIC NOTEBOOK
SN-0084, "COLLECTION OF UNDERGROUND SITE CHARACTERIZATION DATA"

Location(s): ESF - MAIN DRIFT

Period(s): 11/20/96 to 7/16/96
From: MM/DD/YY To: MM/DD/YY

Sample ID Number(s): _____

PART III Source Data DTN(s)

<u>GS960808314224.012</u>	<u>GS960908314224.017</u>	_____
<u>GS960908314224.015</u>	_____	_____
<u>GS960908314224.016</u>	_____	_____

Comments

CROSS-SECTION WAS COMPILED BY ROB LONG. DATA FROM SAND95-0488 AND SAND95-2193 ARE USED ON THIS
DRAWING FOR COMPARISON ONLY.

Checked by: Don Silva
Signature

10/3/96
Date

YMP-023-R4
05/06/96

YUCCA MOUNTAIN SITE CHARACTERIZATION PROJECT TECHNICAL DATA INFORMATION

(Check one): ACQUIRED DATA (complete Parts I and II)
Data Tracking Number (DTN): _____

DEVELOPED DATA (complete Parts I, II and III)
Data Tracking Number (DTN): GS970208314224.005

PART I Identification of Data

Title/Description of Data: GEOLOGY OF THE MAIN DRIFT - STATION 28+00 TO 55+00, EXPLORATORY STUDIES FACILITY, YUCCA MOUNTAIN PROJECT, YUCCA MOUNTAIN, NEVADA, BY A.L. ALBIN, W.L. SINGLETON, T.C. MOYER, A.C. LEE, R.C. LUNG, G.L.W. EATMAN, AND D.L. BARR. (INCLUDES DRAWINGS OA-46-295 THROUGH OA-46-299)

Principal Investigator (PI): BEASON, S C
Last Name First and Middle Initials

PI Organization: U.S. BUREAU OF RECLAMATION

Are Data Qualified?: Yes No Governing Plan: SCP

SCPB Activity Number(s): 8.3.1.4.2.2.4

WBS Number(s): 1.2.3.2.2.1.2

PART II Data Acquisition/Development Information

Method: COMPILATION OF DATA FROM FULL PERIPHERY GEOTECHNICAL MAPS AND DETAILED LINE SURVEYS FROM THE MAIN DRIFT STATIONS 28+00 TO 55+00. INCLUDES DISCUSSION OF SIGNIFICANT GEOLOGIC AND STRUCTURAL FEATURES AND STATISTICAL ANALYSIS OF THE DATA AS WELL AS GEOTECHNICAL CHARACTERIZATION.

Location(s): ESF - ALCOVE 5

Period(s): 10/1/96 to 2/18/97
From: MM/DD/YY To: MM/DD/YY

Sample ID Number(s): _____

PART III Source Data DTN(s)

<u>GS960608314224.007</u>	<u>GS960808314224.011</u>	<u>GS960908314224.014</u>
<u>GS960708314224.008</u>	<u>GS960808314224.012</u>	<u>GS960908314224.015</u>
<u>GS960708314224.010</u>	<u>GS960808314224.013</u>	<u>GS960908314224.016</u>

Comments

Checked by: *Patricia G. Shaffer* 2/24/97
Signature Date

YMP-023-R4
08/31/95

YUCCA MOUNTAIN SITE CHARACTERIZATION PROJECT
TECHNICAL DATA INFORMATION
CONTINUATION SHEET

Page 2 of 2

Location(s) (continued)

ESF - MAIN DRIFT
USER, ESF

Source Data DTN(s) (continued)

GS960908314224.017
GS960908314224.018
GS960908314224.021
GS960908314224.022

PREFACE

ATTACHMENT 2

Data Transmittal Letters to the GENISES Administrator



United States Department of the Interior

U. S. GEOLOGICAL SURVEY
Box 25046 M.S. 725
Denver Federal Center
Denver, Colorado 80225

IN REPLY REFER TO:

October 04, 1996

QA: N
WBS: 1.2.5.3.5
Page 1 of 2

Joanna L. Wiggins
Technical Data Base Administrator
M&O/TRW
Yucca Mountain Project Office
101 Convention Center Drive, Suite 527
Las Vegas, NV 89109

SUBJECT: Yucca Mountain Site Characterization Project (YMP) Technical Data Base (TDB)
Data Transmittal -- Provisional Results: Main Drift ESF Detailed Line Survey
for Stations 26+00 to 55+00 and Alcove 5.

DTNs	GS960608314224.007	TDIFs	305555	DLS	26+00 - 30+00
	GS960708314224.008		305556		30+00 - 35+00
	GS960808314224.011		305624		35+00 - 40+00
	GS960708314224.010		305554		40+00 - 45+00
	GS960808314224.013		305638		45+00 - 50+00
	GS960908314224.014		305645		50+00 - 55+00
	GS960908314224.018		305647		ALCOVE 5

The subject Data Transmittal Package is being submitted to the YMP TDB in accordance with YMP Administrative Procedure (YAP)-SIII.3Q, Revision 1, ICN 0. All data have been technically reviewed as required. This TDB submittal partially fulfills Milestones 3GGF600M and 3GGF603M. The following items are enclosed:

1. Technical Data Information Forms (7), 8p.
2. Example of the submitted data annotated with parameters and attributes, 2p.
3. Hard Copy of Subject Data. Due to the volume of data, in most cases only a sample of the submitted data are enclosed for verification purposes:

26+00 - 30+00	2p
30+00 - 35+00	2p
35+00 - 40+00	2p
40+00 - 45+00	2p
45+00 - 50+00	2p
50+00 - 55+00	21p
Alcove #5 Bearing 108 +04 - 1+36	38p
Bearing 198 +03 - +14	7p
Bearing 108 +02 - +11	3p

4. GENISES Data Transfer Form, 1p.
5. Six (6) 3½" diskettes containing the subject data in ASCII format.
NOTE: Alcove 5 DLS data are submitted in hard copy only.
6. Abbreviations and Definitions, Filename: ABB-DEFI.ASC (disk #6), 5p.

Joanna Wiggins
Technical Data Base Administrator

October 05, 1996

QA:N
WBS: 1.2.5.3.5
Page 2 of 2

Please capture the annotated supporting information in the TDB.

If you have any questions, please contact me at (303) 236-0516, X271, or Ann Lezark at X229.

Sincerely,


Patrick W. McKinley
Data Management Coordinator
Yucca Mountain Project Branch
U.S. Geological Survey

PWM:al

Enclosures

Copy w/o enc. to: C.M. Newbury, DOE/YMP, Las Vegas
S.J. Bodnar, M&O/TRW, Las Vegas
R.W. Craig, USGS, Las Vegas
S.C. Beason, USBR, Las Vegas
D. Sinks, PWT, Denver
C.D. Miller-Corbett, USGS, Denver
R.R. Arnold, USGS, Denver

Copy w/ enc. to: Records Processing Center, Las Vegas, Items 2 & 4

dlw:ile



United States Department of the Interior

U. S. GEOLOGICAL SURVEY
Box 25046 M.S. 425
Denver Federal Center
Denver, Colorado 80225

IN REPLY REFER TO:

October 04, 1996

QA:N
WBS: 1.2.5.3.5
Page 1 of 2

Joanna L. Wiggins
Technical Data Base Administrator
M&O/TRW
Yucca Mountain Project Office
101 Convention Center Drive, Suite 527
Las Vegas, NV 89109

SUBJECT: Yucca Mountain Site Characterization Project (YMP) Technical Data Base (TDB) Data Transmittal -- Provisional Results: North Ramp and Main Drift ESF Full Periphery Geotechnical Maps (FPGM) and Rock Mass Quality Ratings for Stations 26+00 to 55+00, and Alcove 5 along with the Comparative Geology Cross Section along Main Drift, Station 28+94.76 to 55+00.

DTN	TDIFS	FPGM & ROCK MASS QUALITY RATINGS	MILESTONE
GS960808314224.012	305625	26+00 - 30+00, R0	3GGF600M & 3GGF603M
GS960908314224.015	305650	30+00 - 40+00, R0	3GGF603M
GS960908314224.016	305651	40+00 - 50+00, R0	3GGF603M
GS960908314224.017	305652	50+00 - 55+00, R0	3GGF603M
GS960908314224.021	305649	ALCOVE 5 (FPGM only)	3GGF603M
GS960908314224.022	305676	Geology Cross-Section Stations 28+94.76 to 55+00	3GGF603M

The subject Data Transmittal Package is being submitted to the YMP TDB in accordance with YMP Administrative Procedure (YAP)-SIII.3Q, Revision 1, ICN 0. All data have been technically reviewed as required. This TDB submittal partially fulfills Milestones 3GGF600M and 3GGF603M. The submitted data consist of the following:

Hard copy of Rock Mass Quality: Rated Q (minimum), Rated RMR (minimum), and RQD Line Survey for Stations 26+00 to 55+00.

Hard copy of Maps: Geologic Explanations and Notes and Full Periphery Maps (FPGM) for Stations 26+00 to 55+00 and Alcove 5.

Hard copy of Comparative Geology Cross Section: Along Main Drift, Stations 28+94.76 to 55+00.

The following items are enclosed:

1. Technical Data Information Forms (6), 7p.

DATA FOR SEP INCLUSION:

2. Hard Copy of Rock Mass Quality Ratings for SEP Submittal:

Stations	Q (min), RMR (min), and RQD Data
26+00 to 30+00	3 pages
30+00 to 35+00	4 pages
35+00 to 40+00	4 pages
40+00 to 45+00	4 pages
45+00 to 50+00	4 pages
50+00 to 55+00	4 pages
Alcove #5	Not Reported

Joanna Wiggins
Technical Data Base Administrator

October 05, 1996

QA:N
WBS: 1.2.5.3.5
Page 2 of 2

NOTE: The data being submitted to the TDB/SEP are: Begin and End Stations, Geologic Units, ROD, Rated Q, and Rated RMR. The submitted data are hi-lited on the first page of each data grouping for ease in identification. For Alcove 5 the Q, RMR, and ROD Data reported in the drawing header under Rock Mass Classification (OA-46-290 and 292) are being submitted under item #6 below.

3. Photocopied data sheet for #2 above annotated with parameters and attributes, 1p.
4. Description of "Stratigraphic Units" reported in #2 above, 1p.
5. "Introduction" sheets, 7 pages. These sheets include detailed procedures and qualitative descriptions for determining Q, RMR, and ROD. Included in these procedures and descriptions are disclaimers and limitations on the data. Please capture this information in the TDB.

DATA FOR GIS INCLUSION:

6. Hard Copy of Maps for GIS Submittal:

Stations	Geologic Explanation	Maps
26+00 to 30+00	OA-46-222 (1 plate)	OA-46-223 to 226 (4 plates)
30+00 to 35+00	OA-46-227 (1 plate)	OA-46-228 to 232 (5 plates)
35+00 to 40+00	OA-46-233 (1 plate)	OA-46-234 to 238 (5 plates)
40+00 to 45+00	OA-46-239 (1 plate)	OA-46-240 to 244 (5 plates)
45+00 to 50+00	OA-46-245 (1 plate)	OA-46-246 to 250 (5 plates)
50+00 to 55+00	OA-46-251 (1 plate)	OA-46-252 to 256 (5 plates)
Alcove #5	Not Reported	OA-46-290 & 292 (2 plates)

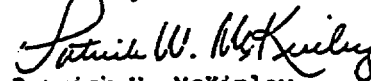
NOTE: The Scanline Q and RMR data acquired by Agapito and reported on the drawing headers are not being submitted by the USGS/USER with this TDB submittal. The Agapito data were collected under Sandia National Laboratory and are identified by the source data tracking numbers reported on the subject TDIFs. See also the annotated drawings OA-46-222 and OA-46-223, Stations 26+00 to 30+00 for these Agapito data exclusions. For Alcove 5 see drawings OA-46-290 & 292 for annotations of Agapito data exclusions.

7. Hard Copy of the Comparative Geology Cross Section along Main Drift, Stations 28+94.76 to 55+00 for GIS Submittal; drawing OA-46-291.

NOTE: The preconstruction cross section is not being submitted to the TDB. Additionally, data identified on the cross section from stations 55+00 to 59+36.89 are not being submitted to the TDB with this package. See annotated subject drawing.

If you have any questions, please contact me at (303) 236-0516, X271, or Ann Lezark at X229.

Sincerely,



Patrick W. McKinley
Data Management Coordinator
Yucca Mountain Project Branch
U.S. Geological Survey

PWM:al

Enclosures

Copy w/o enc. to: C.M. Newbury, DOE/YMP, Las Vegas
S.J. Bodnar, M&O/TRW, Las Vegas
R.W. Craig, USGS, Las Vegas
S.C. Beason, USBR, Las Vegas
D. Sinks, FWT, Denver
C.D. Miller-Corbett, USGS, Denver
R.R. Arnold, USGS, Denver



United States Department of the Interior

U. S. GEOLOGICAL SURVEY
Box 25046 M.S. 425
Denver Federal Center
Denver, Colorado 80225

IN REPLY REFER TO:

February 26, 1997

QA: N
WES:1.2.5.3.5
Page 1 of 1

Joanna L. Wiggins
Technical Data Base Administrator
M&O/TRW
Yucca Mountain Project Office
1180 Town Center Drive
Las Vegas, NV 89134

SUBJECT: Yucca Mountain Site Characterization Project (YMP) Technical Data Base (TDB) Data Transmittal - Geology of the Main Drift - Station 28+00 to 55+00, Exploratory Studies Facility, Yucca Mountain Project, Yucca Mountain, Nevada.

DTN: GS970208314224.005 TDIF: 306035

The subject Data Transmittal Package is being submitted to the YMP TDB in accordance with YMP Administrative Procedure (YAP)-SIII.3C, Revision 1, ICN 0. All data have been technically reviewed as required. This TDB partially fulfills Milestone SPG42AM3. The following items are enclosed for GIS inclusion:

1. Technical Data Information Form (1), 2p.
2. Definition Page, 1p.
3. Hard Copy of Subject Data, Drawings: OA-46-295
OA-46-296
OA-46-297
OA-46-298
OA-46-299

The USGS has not assigned a parameter to the diagrams because an appropriate parameter could not be found. The drawings consist of several statistical representations for fractures and are labeled on the diagrams as "fracture statistics".

Please capture the definitions page as supporting information.

If you have any questions, please contact me at (303) 236-0516, X271, or Craig R. Walker at X278.

Sincerely,

Patrick W. McKinley
Patrick W. McKinley
Data Management Coordinator
Yucca Mountain Project Branch
U.S. Geological Survey

FWM:CRW

Enclosures

Copy w/o enc. to: C.M. Newbury, DOE/YMP, Las Vegas
S.J. Bodnar, M&O/TRW, Las Vegas
R.W. Craig, USGS, Las Vegas
S.C. Beason, USBR, Mercury
A.L. Albin, USBR, Mercury
R. Arnold, USGS, Denver
P.G. Sheaffer, PWT, Denver

ABSTRACT

The Exploratory Studies Facility (ESF), under construction at Yucca Mountain, is being studied to determine its suitability as a permanent high-level nuclear waste-repository. This report presents a summary of data collected by U.S. Bureau of Reclamation (USBR) personnel on behalf of the U.S. Geological Survey (USGS) for the Department of Energy (DOE) in the Main Drift of the ESF from Sta. 28+00 to 55+00. Included in this report are descriptions of lithostratigraphic units, an analysis of data from full-periphery geologic maps (FPGM) and detailed line survey (DLS) data, an analysis of the geotechnical and engineering characteristics of the ESF, and a statistical analysis of the DLS data.

The Main Drift is almost entirely within the Topopah Spring crystal-poor, middle nonlithophysal zone (Tptpmn), the proposed repository horizon, with small exposures of the underlying crystal-poor, lower lithophysal zone (Tptpll) beyond Sta. 53+00. The entire Main Drift is in the Topopah Spring welded (TSw2) thermal/mechanical unit. The discontinuities are divided into four sets by orientation, with a significant number of random orientations. Three sets occur throughout the Main Drift. The fourth set occurs only between Sta. 28+00 and 37+00 in the Main Drift. Set 1 is by far the most prominent set consisting of discontinuities striking generally between 100° and 150° and dipping 70° or more. Set 2 consists of discontinuities striking between 200° and 230° and dipping 70° or more. Set 3 consists of discontinuities striking between 280° and 330° and dipping less than 40° . Set 4 strikes similarly to Sets 1 and 3, 270° to 330° , and dips intermediately between those two sets, 40° to 60° .

The Main Drift is divided into four domains based on structural characteristics. The First Domain, extending from Sta. 28+00 to 37+00, is the only domain in which Set 4 fractures are found in significant numbers. The First Domain is also distinguished by having a large proportion of random fractures and shears. In the Second Domain, Sets 1, 2, and 3 are well defined with relatively few random fractures. The beginning of the Third Domain is marked by the beginning

of the fracture zone at Sta. 42+00 and extends to Sta. 51+50. The Third Domain is dominated by Set 1 fractures. The Fourth Domain, from Sta. 51+50 to 55+00, consists predominantly of Sets 1 and 2 fractures and has a high density of Sets 1 and 2 faults and shears.

The comparison of the pre-construction geologic cross section of the Main Drift and the as-built geologic cross section shows strong agreement between the predicted geology and that actually encountered.

Geotechnical characterization of the Main Drift focused primarily on rock mass quality and rock mass mechanical properties. Descriptions are based on two empirical rock mass classification systems, rock quality (Q system) and rock mass rating (RMR). The averages of all the rating systems give the Main Drift a rating of poor to fair. The average rock quality ratings are fair in the First Domain then generally decrease to poor ratings down the Main Drift.

Cluster analysis, performed using the computer program Clustran, identified four sets of data. Three of the sets are in general agreement with the sets identified through other analytical methods. The fourth set (Set 4) was identified by cluster analysis. The chief differences between the cluster analysis and the other methods used are as follows: (1) Clustran grouped all the discontinuities into the four sets, as opposed to having a "random" category; (2) the sets identified by cluster analysis include a wider range of orientations both in terms of strike and dip.

An r-mode, maximum variance, principle component analysis was performed on the Main Drift DLS data. The BMDP (Bio-medical data-processing program) application 4M (Dixon, 1995) was used to identify diagnostic structural heterogeneities. The variables judged to be continuous--maximum aperture, minimum aperture, fracture length, infilling thickness and dip--were selected for multivariate statistical analysis. The analysis indicated that the most useful DLS parameters for characterizing the Tptpmn are maximum aperture, followed by infilling thickness and fracture length. A two-factor solution was obtained. Factor 1 scores are a function of infilling thickness, maximum aperture, and fracture length. Factor 2 scores are a function of fracture dip and

minimum aperture. Both factor 1 and 2 scores were used to identify significant structural heterogeneities within the Main Drift of the ESF. Statistical correlations between strike and factor scores identified strike ranges with similar characteristics.

INTRODUCTION

Yucca Mountain is located approximately 160 km northwest of Las Vegas, Nevada (Fig. 1), on the western edge of the Nevada Test Site (NTS) and the Nellis Air Force Range. The United States Bureau of Reclamation (USBR) in conjunction with the United States Geological Survey (USGS), under the direction of the Department of Energy (DOE), has undertaken the study of the geology of the Exploratory Studies Facility (ESF). This study is part of a larger investigation to determine the suitability of Yucca Mountain as a high-level, permanent, underground nuclear-waste repository.

The North Portal of the ESF originates in an excavation cut into Exile Hill, a small rise on the lower, eastern flank of Yucca Mountain. The starter tunnel, excavated 60 m into Exile Hill by drill and blast methods, is a 10-m high, horseshoe-shaped tunnel that served as a launch chamber for the tunnel-boring machine (TBM). The TBM is a fully shielded machine manufactured by Construction Tunneling Services of Kent, Washington (Photo 1). The TBM trailing gear was constructed with a special 45-m-long section that provides geologists with relatively unobstructed views of the tunnel walls. The trailing gear is also equipped with a self-propelled gantry, permitting access to the tunnel periphery (Photo 2).

The ESF is a 7.62-m-diameter tunnel which will have a total length of approximately 7,800 m forming a broad U-shape in plan view (Fig. 2). The tunnel, along with several alcoves, has been designed to investigate the subsurface geology, hydrology, thermal/mechanical, and other characteristics of Yucca Mountain. The North Ramp of the tunnel extends from the surface on a bearing of 299° and -2.1 percent slope. A 115° curve to the left (south) begins at Sta. 21+87 (2,187 m from the portal) that brings the tunnel parallel to the axis of the mountain and the beginning of the Main Drift at Sta. 28+00. The Main Drift extends from Sta. 28+00 to 55+00 on a bearing of 183° with a +1.35 percent slope. The Main Drift passes gradually downsection through the entire Topopah Springs crystal-poor, middle nonlithophysal zone (Tptpmn), the proposed repository horizon. The Main Drift begins in the uppermost Tptpmn, with the upper

contact being at Sta. 27+20 (right springline). The underlying Topopah Spring crystal-poor, lower lithophysal zone (Tptpl) appears intermittently along the right invert beyond Sta. 53+00. The South Ramp, under construction, contains a 92° curve to the left (east) bringing the tunnel to an orientation of 091°. The South Ramp continues on a +2.6 percent slope to daylight on the east flank of Yucca Mountain at approximately Sta 78+77 providing a second portal to the ESF.

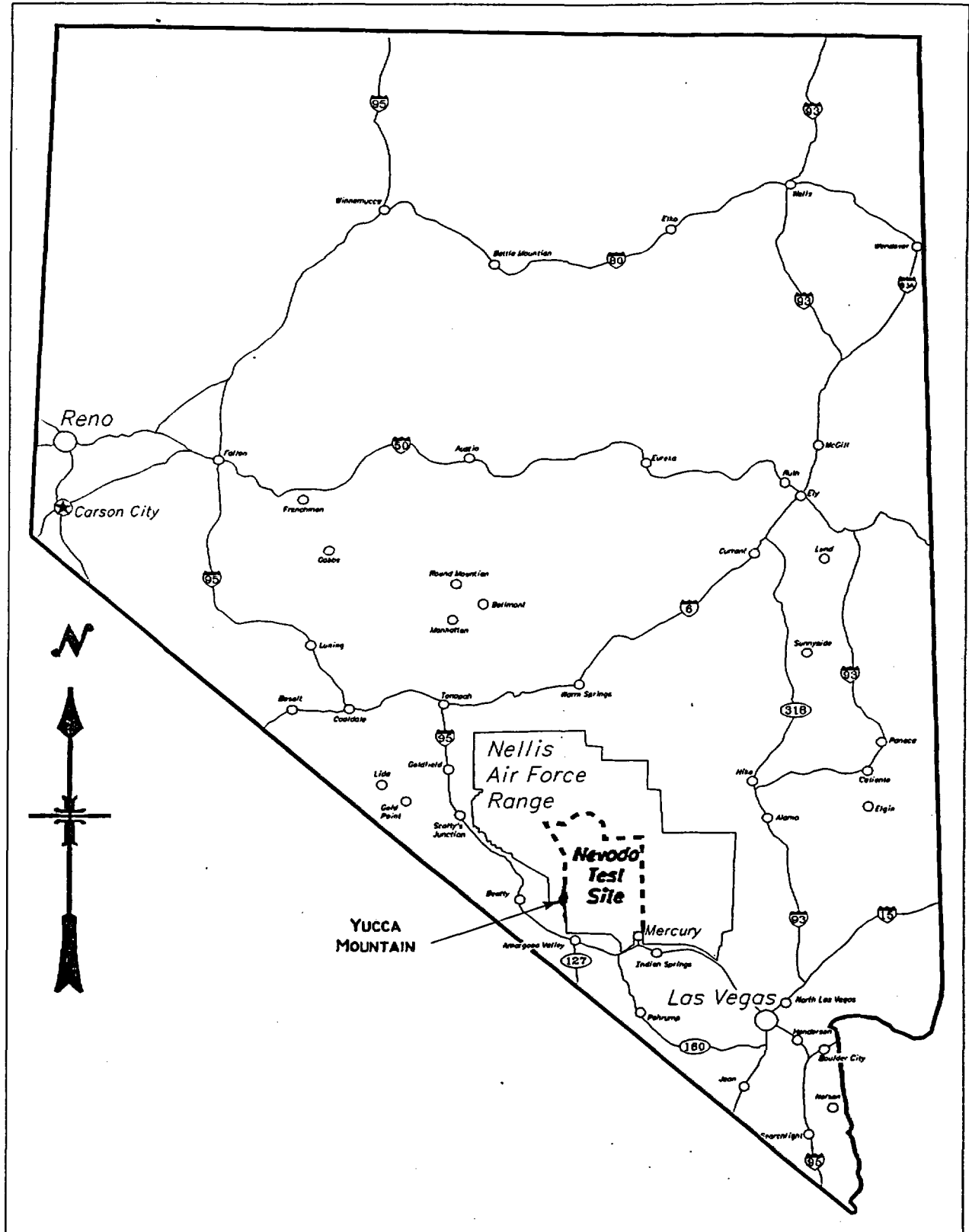


Figure 1. Location map of Yucca Mountain, Nevada (not to scale).

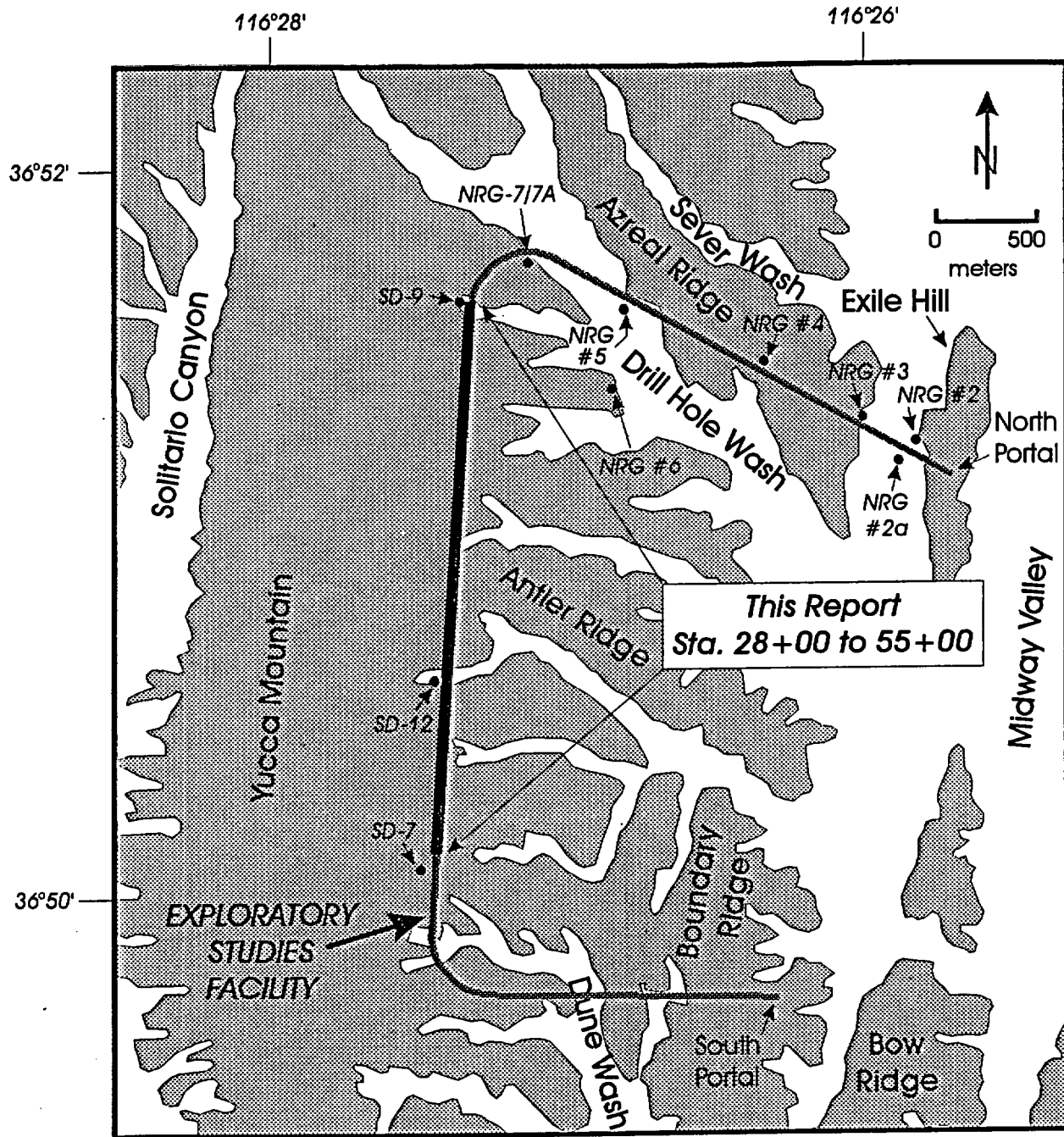


Figure 2. Yucca Mountain in the area of the ESF.
 Note: borehole locations are approximate.

Geologic site characterization in the ESF is by full-periphery geologic mapping (FPGM) at a scale of 1:125 and by detailed line surveys (DLS). A continuous stereo photographic record of the tunnel walls is taken for documentation and possible future photogrammetric analysis.

This report presents analysis, results, and summaries of the data collected in the Main Drift. The methods of analysis include stereonets and histograms concentrating on the orientation, location, and type of discontinuity. The engineering characteristics of the rock are also presented. The engineering characteristics were determined with rock quality (Q system) and rock mass rating (RMR) systems. Statistical analysis of the DLS data was conducted including cluster analysis with the computer program Clustran, and r-mode, maximum variance, principle component analysis with the BMDP (bio-medical data processing program) 4M application.

Test alcoves 5, 6 and 7 are located at Sta. 28+27, 37+37, and 50+64, respectively. As of February 1997, excavation in Test alcove 5 is nearing completion (Photo 3). Test alcove 6 has been excavated to over 100 m in length. Excavation of Test alcove 7 has just begun (Photo 4). A detailed discussion of the geology of the alcoves will appear in a subsequent report.

Tunnel Terminology

The following is a list of the tunnel terms commonly used in this report.

crown	the uppermost part of the tunnel
drift	a horizontal excavation
heading	the excavated face (end) of the tunnel
invert	the bottom (floor) of the tunnel. In the ESF, the precast invert sections are placed in the tunnel to provide a flat working surface
portal	the tunnel entrance
right and left	refers to the right or left when facing the heading
springline	the line at which the tunnel wall breaks from vertical or sloping outward to sloping inward toward the crown. For a round tunnel like the ESF, the springline is midway up the wall
station	the distance from the portal measured in meters e.g. Sta. 28+44 = 2,844 meters from the portal Note: the location of discontinuities in the ESF is given as stationing on the right springline, unless stated otherwise.
wall	the side of the tunnel

Geology of the Yucca Mountain Area

Yucca Mountain lies in the Great Basin in southern Nevada, part of the Basin and Range structural/physiographic province. In the Yucca Mountain area, a thick sequence of Proterozoic and Paleozoic sedimentary rocks underlie approximately 1000 to 3000 m of Miocene volcanic rock (Gibson and others, 1990).

The Miocene volcanic sequence exposed at Yucca Mountain includes units of the Paintbrush and Timber Mountain Groups (Sawyer and others, 1994). The Paintbrush Group consists of pyroclastic rock and lavas originating from the Claim Canyon caldera, located approximately 6 km north of the study area, from 12.8 to 12.7 Ma (Byers and others, 1976; Sawyer and others, 1994). The Paintbrush Group includes a homoclinal sequence consisting of four formations of pyroclastic-flow and pyroclastic-fall deposits with interbedded lavas dipping 5-10° to the east (Byers and others, 1976; Christiansen and others, 1977; Broxton and others, 1993). Two of these formations, the Topopah Spring and Tiva Canyon Tuffs, are voluminous, densely welded, compositionally zoned sheets that grade upward from rhyolite to quartz latite (Lipman and others, 1966; Byers and others, 1976; Schuraytz and others, 1989).

Yucca Mountain is bounded on three sides by alluvium-filled structural valleys consisting mostly of alluvial fan deposits (fluvial and colluvial sediments) and some thin eolian deposits. Yucca Mountain is bounded on the north by the Claim Canyon and Timber Mountain Calderas. The Yucca Mountain area is cut by north-south-striking normal faults which cut the Tertiary volcanics into blocks 1 to 4 km wide (Scott, 1990). Yucca Mountain is bounded by the Solitario Canyon fault to the west and the Bow Ridge fault to the east. Both faults dip steeply toward the west (Scott and Bonk, 1984; Day and others, 1996), and have hundreds of meters of displacement.

Site-Characterization Techniques

Geologic site-characterization activities performed at the (ESF) by the USBR for the USGS include the following techniques.

Full-Periphery Geologic Mapping

Geologic mapping in the ESF records lithostratigraphic and structural features at a scale of 1:125 (refer to Drawings OA-46-222, OA-46-225 through OA-46-239, and OA-46-240 through OA-46-256). These drawings are developed in the full-periphery style in which the tunnel walls, hinged from the crown, are "unrolled" to produce a flat map of the tunnel periphery. Structural discontinuities with trace lengths longer than 1 m and lithostratigraphic contacts were recorded on field sheets along with any other geologically significant features and details of the tunnel support. The field sheets were then digitized into AutoCAD. The resulting maps were field checked for accuracy, consistency, and completeness. The full-periphery geologic maps are located in the Records Processing Center with their associated data tracking numbers listed in Appendix 1.

Detailed Line Surveys

Detailed line surveys (DLS) were conducted along the right wall, normally 0.9 m below the springline. A metric measuring tape was affixed to the wall, and discontinuities that intersect the wall within 30 cm of the tape were documented. Between Sta. 28+00 and 37+80, all fractures with trace lengths longer than 30 cm were reported on the survey. Beginning at Sta. 37+80, the minimum trace length for the DLS was raised to 1 m. Data on the shorter fractures, 30 cm to 1 m, were collected in 50-m intervals every 500 m, between 45+00 and 45+50, and between 50+00 and 50+50. In the Main Drift, Sta. 28+00 to 55+00, over 10,400 fractures, cooling joints, vapor-phase partings, faults, and shears were recorded in the DLS. Of those discontinuities, over 91 percent are fractures, approximately 2 percent are cooling joints, approximately 2 percent are

vapor-phase partings, and approximately 5 percent are faults and shears. The DLS data are located in the Records Processing Center: their data tracking numbers are listed in Appendix 1. Data collected on the following characteristics is recorded in the DLS.

- Station** The location of a discontinuity is measured on the DLS tape to the nearest 0.01 m giving each discontinuity a unique identifier.
- Orientation** The orientation of geologic features is determined with a goniometer for strike azimuth and a Brunton compass for dip values. Orientations are recorded using the right-hand rule where the direction of the dip is 90° to the right (clockwise) of strike.
- Type** Discontinuities are categorized as lithologic contacts, fractures, cooling joints, vapor-phase partings, shears, and faults. Lithologic contacts mark the boundary between lithologic units. Fractures are those discontinuities that have no visible offset. Cooling joints are a class of fracture that presumably formed as a result of stresses in the cooling volcanic sheet, (see **Cooling Joints** p. 24 for further discussion). Vapor-phase partings are discontinuities that consist of roughly linear accumulations of vapor-phase minerals and are parallel to subparallel to lithostratigraphic layering. Shears are those discontinuities having less than 0.1-m offset, or when offset is indeterminate. Faults are those discontinuities with greater than 0.1-m offset.
- Trace length** Trace length is the length of the discontinuity on the wall of the tunnel. The trace length is taken as two measurements, from the DLS survey tape to the upper end of the discontinuity, and from the tape to its lower end. These two measurements allow the discontinuity to be located accurately relative to the DLS tape and other discontinuities.

Height, Width The height and width are measured on an imaginary plane, an extension of the plane of the discontinuity in question. A horizontal line extending on strike from the highest point on the plane defines the upper boundary of the plane. A line parallel to the dip of the discontinuity extending from the point of its greatest lateral extent defines the lateral boundary of the plane. The height and widths are the maximum dimensions of that plane, width being measured parallel to strike and height being measured parallel to dip.

Terminations The number of visible ends (terminations) are counted. The type of termination is also recorded. If the discontinuity extends out of view, such as continuing under the concrete invert sections, or obscured by the tunnels steel support, it is recorded as such. The visible ends are recorded as ending in rock or ending in another discontinuity. The acute angle at which one discontinuity terminates into another is specified as intersecting either at less than or greater than 45°.

Aperture The minimum and maximum open, unfilled space between the surfaces of a discontinuity.

Roughness The quantitative analysis of fracture-surface roughness is based on the scale used by the USBR (Bureau of Reclamation, 1988). Roughness (R) characterizes the small-scale asperities of the fracture surface on a scale from 1 to 6. R1 designates a stepped surface with near-normal steps and ridges. R6 designates a very smooth, shiny, and polished surface.

Infilling type and thickness Mineral coatings and infillings are identified if possible or described by their appearance, color, hardness, reaction to dilute hydrochloric acid, and fluorescence in UV light.

Stereophotographic Coverage

Excavated tunnel walls are photographed from the mapping gantry on the trailing gear of the TBM. The photographs are taken with 60-percent longitudinal overlap and 20-percent circumferential overlap. The photographs provide full stereo photographic documentation of the tunnel walls and for possible future photogrammetric analysis. The photographs are maintained and archived by Science Applications International Corporation (SAIC) Graphics at the Bank of America Building in Las Vegas, Nevada.

Rock Sampling

Funding for the USBR's systematic sampling program in the ESF was terminated in September 1995, prior to the excavation of the Main Drift. Los Alamos National Laboratories (LANL) has since collected samples at the request of the individual Principal Investigators. The sample locations are shown on the FPGMs.

LITHOSTRATIGRAPHY

The lithostratigraphy of the ESF Main Drift is described using the nomenclature and unit divisions of Sawyer and others (1994), and Buesch and others (1996) (Fig. 3). Lithologic descriptions record compositional data, rock color and texture, features of welding, secondary crystallization, alteration, depositional features, and stratigraphic relationships. The percentages of pumice clasts, matrix phenocrysts, lithic fragments, and lithophysae are visual estimates determined using charts produced by the American Geological Institute. The percentages of matrix (including porosity) are subsequently computed by subtraction of the other rock components from 100 percent. Colors are determined on dry surfaces under tunnel lighting conditions using a standard Munsell rock-color chart (Geological Society of America, 1991). Unless otherwise noted, all stratigraphic stationings are given at springline on the right wall of the tunnel. For descriptions of the lithostratigraphy in particular locations, see the FPGMs.

Topopah Spring, Crystal-Poor Member

The Main Drift exposes primarily the crystal-poor, middle nonlithophysal zone of the Topopah Spring Tuff. Small exposures of the underlying crystal-poor, lower lithophysal zone occur intermittently near the right invert from Sta. 53+00 to 55+00. This section provides summary rock unit and contact descriptions, outlines the stratigraphic and depositional features observed in the tunnel walls, and describes general features of welding, secondary crystallization, and alteration for the zones encountered from Sta. 28+00 to 55+00 of the ESF.

Middle Nonlithophysal Zone (Tptpmn) - Rock Unit and Contact descriptions

This zone comprises moderately to densely welded, devitrified pyroclastic-flow material. The zone is generally composed of 1 to 7 percent pumice, 1 to 2 percent phenocrysts, 1 to 3 percent lithic fragments, 0 to 3 percent lithophysae, and 85 to 97 percent matrix. The unit varies from a heterogeneous mix of grayish orange-pink and grayish red-purple to comparatively homogeneous

General Lithostratigraphic Column at Yucca Mountain, Nevada

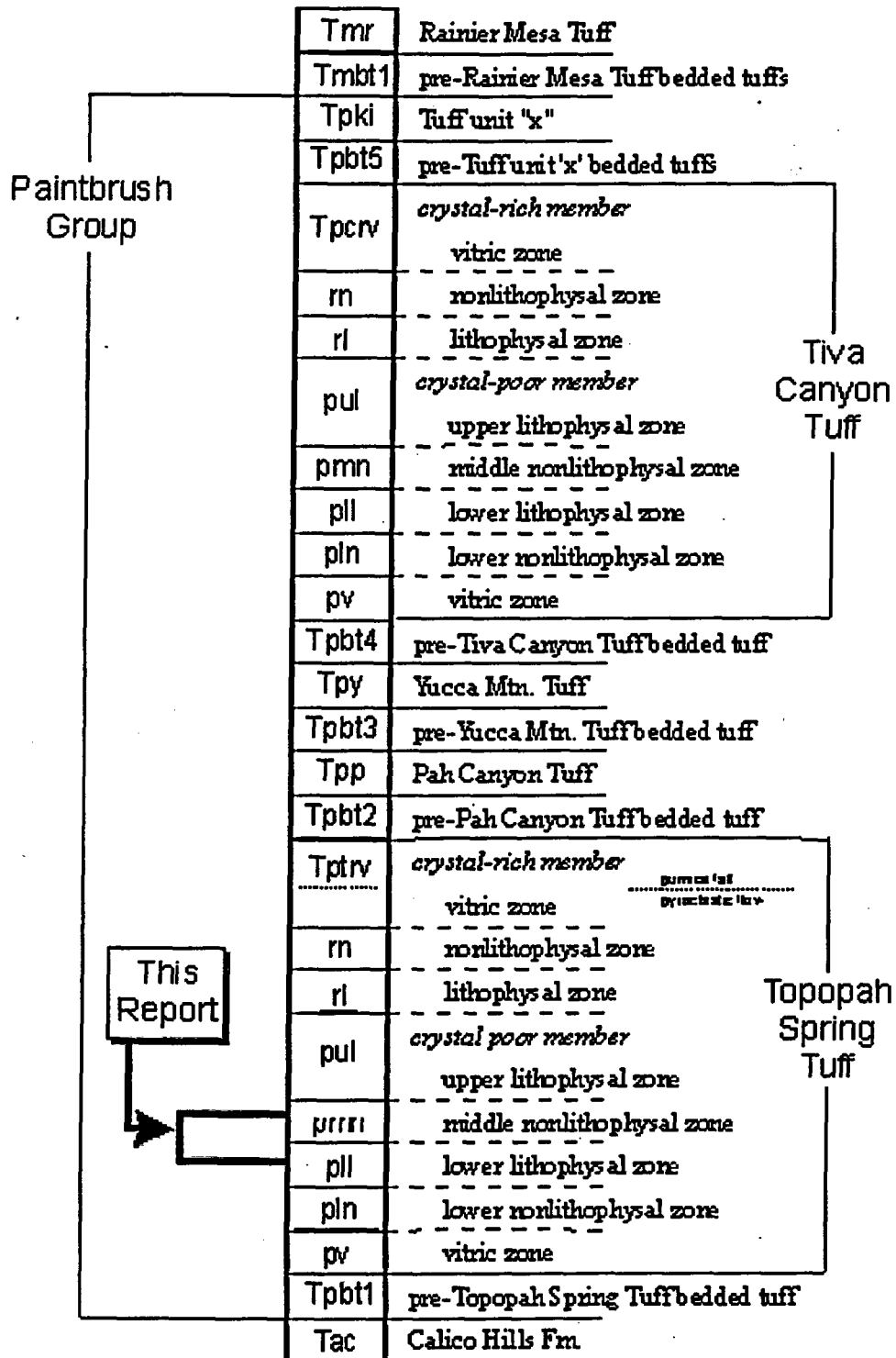


Figure 3. Lithostratigraphic column of the Paintbrush Group at Yucca Mountain showing the stratigraphic interval described in this report.

pale brown or pale red.

The abundance of pumice clasts diminishes downward from 3 to 7 percent at Sta. 28+00, to 2 to 4 percent at Sta. 30+00, and to 1 to 2 percent at Sta. 32+00. From Sta. 32+00 to 54+00, pumice content remains relatively constant at 1 to 2 percent. A swarm of comparatively large pumice clasts marks a flow-unit boundary approximately 2 m above the base of the zone (about 0.2 m below the right springline at Sta. 54+00 and 1.5 m above the right invert at Sta. 52+08); pumice clasts compose 15 to 25 percent of the rock within the swarm and from 3 to 7 percent of the rock in the flow unit beneath the pumice swarm. Pumice clasts are slightly to moderately deformed (aspect ratios of 2:1 to 5:1) throughout the zone. The clasts are mostly smaller than 1.5 cm from Sta. 28+00 to 40+00 and smaller than 3.5 cm from Sta. 40+00 to 55+00. Clasts within the pumice swarm are moderately elongate (aspect ratios of 5:1 to 10:1) and slightly larger (3 to 10 cm) than elsewhere. Granophyricallly devitrified pumice clasts (Sta. 28+00 to 45+00) occur in shades of pinkish gray (5YR8/1), light brownish gray (5YR6/1), grayish orange-pink (5YR7/2, 10R8/2), pale red (10R6/2), and grayish pink (5R8/2). Spherulitically devitrified pumice clasts (Sta. 45+00 to 55+00) occur in shades of grayish orange-pink (5YR7/2), pale red (5R6/2), and pale to moderate brown (5YR6/2 to 5YR4/4). Pumice clasts typically have from 5 to 10 percent phenocrysts of sanidine, plagioclase, and biotite.

Phenocrysts are predominantly sanidine and plagioclase and subordinate fresh-, to partially oxidized biotite. Subangular to subrounded lithic fragments are generally smaller than 3 cm. The lithic assemblage is dominated by clasts of light gray to white (N7 to N9), devitrified volcanic rock, some of which have pale red (5R6/2) flow-foliation. Subordinate lithic types include pale red to grayish red (5R6/2 to 5R4/2), feldspar-bearing volcanic rock, pale yellowish brown (10YR7/1), aphanitic volcanic rock, grayish black (N2) volcanic rock, and light gray to white (N7 to N9), finely crystalline, volcanic rock.

Lithophysae form from 1 to 3 percent of the zone from Sta. 28+00 to 34+05, from less than 1 percent to 2 percent of the zone from Sta. 37+62 to 40+83, and less than 1 percent of the zone

from Sta. 53+20 to 55+00. Lithophysae are absent between Sta. 34+05 and 37+62 and Sta. 40+83 and 53+20. Lithophysae have ellipsoidal, lenticular, or irregular shapes and are lined with vapor-phase minerals. Large cavities commonly have tabular calcite crystals as overgrowths on the primary vapor-phase crystals. Most lithophysae have diameters smaller than 15 cm, but cavities with diameters that vary from 20 cm to greater than 75 cm are scattered throughout the zone.

Devitrified material in hues of light brown and red-purple typically forms 75 to 98 percent of the rock matrix, with the remainder composed of pink, vapor-phase alteration. From approximately Sta. 28+00 to 36+50, the tunnel walls have alternating bands of grayish red-purple (5RP5/2, 5RP4/2) and pale red (10R6/2), grayish orange-pink (5YR7/2), or pale to light brown (5YR6/2 to 5YR6/4) (Photo 5). Bands are defined by abrupt color changes that occur across subvertical boundaries and, although varying considerably, have widths commonly from 2 to 10 m. The red-purple and brownish colors each form approximately 50 percent of the exposure through this part of the Main Drift. From Sta. 36+50 to 55+00, the pale to light brown or grayish brown (5YR6/1) rock contains less than 15 percent red-purple material disseminated through the matrix or occurs as bands with diffuse margins. The rock is intensely fractured from approximately Sta. 41+40 to 52+70, with many fracture faces exposed. Fracture faces that have a thin coating of manganese oxide minerals are grayish black to brownish black (N2 to 5YR3/1); those with a thin coating of vapor-phase minerals, opal, or calcite are white (N9); whereas altered surfaces are pale red (5R7/1 to 5R5/2).

Vapor-phase alteration of the rock matrix occurs as grayish pink (5R8/2) to very light gray (N8) spots, wisps, stringers, and partings (Photo 6). Vapor-phase products, which form 10 to 25 percent of the matrix from Sta. 28+00 to 30+00, decrease to 2 to 10 percent from Sta. 30+00 to 45+00 and to 2 to 5 percent from Sta. 45+00 to 55+00. Spots of vapor-phase alteration, which generally have diameters smaller than 1.5 cm, are larger and more abundant near the top of the unit (diameters to 4 cm from Sta. 28+00 to 35+00). Partings and stringers have a characteristic central band of white (N9) a few millimeters thick, vapor-phase minerals, enclosed in a zone of

light gray to grayish pink (N7 to 5R8/2) alteration of variable thickness (centimeters) surrounded by variably thick bands (decimeters) of grayish red-purple alteration. Discontinuous, irregularly shaped stringers of vapor-phase material (10 to 60 cm long) are a prominent feature of the zone from Sta. 28+00 to 32+75. Stringers may occur within unfractured rock or may emanate from high-angle planar fractures. Throughout this interval, the subhorizontal alignment of these stringers defines a crude foliation to the rock body. Stringers are smaller (10 to 30 cm long) and less numerous (less than 2 percent of the rock) in the remainder of the deposit. Vapor-phase partings are typically between 0.5 and 4 m long. The partings are typically subhorizontal, sinuous to braided or irregular, and vertically spaced at intervals of 0.2 to 1 meter. Partings are well formed near the upper contact of the zone (Sta. 28+00 to 30+00), in the central part of the unit (Sta. 36+50 to 40+00), and near the lower zone contact (Sta. 50+00 to 55+00), but are poorly formed or absent elsewhere.

The lower contact of the Tptpmn is sharp and marked by an abrupt increase in the amount of lithophysae from less than 1 percent to between 10 and 25 percent. The contact is also recognized by a downward change that grades over approximately 25 cm from predominantly pale red (10R6/2) to a mix of pale red and grayish red-purple (5RP4/2) matrix.

Lower Lithophysal Zone (Tptpll)

This unit is present from 0 to 0.4 m above the right invert in two exposures that occur between Sta. 53+63 and 54+53, and between Sta. 54+70 and 54+90. The Tptpll in these exposures is composed of densely welded, devitrified pyroclastic-flow material that contains 3 to 5 percent pumice clasts, 1 to 2 percent phenocrysts, 1 to 2 percent lithic fragments, 15 to 25 percent lithophysae, and 66 to 80 percent matrix.

Devitrified pumice clasts are pale to moderate brown (5YR6/2, 5YR4/4), slightly deformed, and smaller than 3 cm. Phenocrysts are predominantly plagioclase and sanidine, and minor biotite. Lithic fragments are primarily white to light gray (N9 to N7) and pale red (5R6/2), foliated

volcanic rocks that are smaller than 2 cm. The matrix is a mottled mix of pale red (5R6/2) and grayish red-purple (5RP4/2) devitrified material (80 to 90 percent) and grayish orange-pink (10R8/2) spots of vapor-phase alteration (10 to 20 percent). Vapor-phase spots, which may exceed 2.5 cm diameter, typically have a central streak of white (N9) vapor-phase minerals. Moderately well-formed, lenticular-to-ellipsoidal lithophysae have diameters of 7 to 16 cm.

Stratigraphic and Depositional Features

The crystal-poor, middle nonlithophysal zone of the Topopah Spring Tuff is composed of two pyroclastic-flow units separated by a thin swarm of pumice. The flow-unit boundary, which occurs approximately 2 m stratigraphically above the contact between the crystal-poor, middle nonlithophysal zone and lower lithophysal zone, is laterally continuous, and serves as a marker horizon that can help identify the zone contact. This flow-unit boundary also present in a similar stratigraphic position at Sta. 57+13 (1.5 m below springline), is not described in borehole logs prepared by the U.S. Geological Survey (Geslin and others, 1994; Geslin and Moyer, 1994; Moyer and others, 1995).

Welding Features, Secondary Crystallization, and Alteration

The Tptpmn and Tptpll are moderately to densely welded and devitrified. The deposits do not contain features which indicate a change in the degree of welding within the ESF exposures. Macroscopic examination of pumice-clast textures indicates a gradational change in the style of devitrification from predominantly granophyric (Sta. 28+00 to 45+00) to spherulitic (Sta. 45+00 to 55+00).

The effects of vapor transport vary stratigraphically downward through the Main Drift exposures. Lithophysae, vapor-phase stringers, and vapor-phase partings are prominent features of the Tptpmn below the contact with the overlying Topopah Spring crystal-poor, upper lithophysal zone (Tptpul) (Sta. 27+20 to 32+75 and Testing Alcove 5) and above the contact with the

underlying Tptpll (Sta. 53+00 to 55+00). These features, greatly diminished in the central part of the zone, occur in minor amounts from approximately Sta. 36+50 to 40+80. The lithophysae-bearing subzone of the crystal-poor, middle nonlithophysal zone (Buesch and others, 1996) has not been identified in Main Drift exposures or in core recovered from borehole SD-12 (Moyer and others, 1995), which penetrates the zone near the Main Drift at Sta. 46+49. The slight increase in vapor-phase features noted between Sta. 36+50 and 40+80, however, occurs in a similar stratigraphic position to the lithophysae-bearing subzone and may be a poorly developed equivalent to this feature.

STRUCTURE

Fractures, cooling joints, faults and shears form in response to stress. Stresses resulting from the emplacement and cooling of the volcanic sheet and tectonic stresses have acted on the rock units of Yucca Mountain. The stresses related to cooling of the rock acted only during a relatively short period following deposition of the rock. Tectonic stresses could have been acting on the rock as it cooled or subsequent to the cooling in one or more episodes. The primary purpose of the various methods of analysis presented below is to identify relationships within the body of data. These relationships include: clusters of orientations (sets) and how the sets relate to each other in space; how and where those relationships change; and how, or if, other characteristics of the recorded discontinuities relate in any systematic way to their orientation or location. The compilation of offset data on faults and shears is necessary to understand how and where the rock has been deformed. Secondly, these analyses provide information that contributes to understanding the deformational history of the study area. This information may also provide direction in identifying areas for future studies.

Fractures

Fractures are by far the most numerous (91 percent) type of discontinuity recorded in the ESF. The vast majority of fractures are planar and have a roughness of R3 or R4. Average trace length is 2.5 m.

Vapor-phase minerals commonly coat fracture surfaces, and secondary minerals are common in several intervals in the Main Drift. Vapor-phase minerals consisting primarily of silica polymorphs, commonly tridymite, coat fracture and cooling joint surfaces up to a few millimeters

thick. Concentrations of vapor-phase minerals form vapor-phase partings and line lithophysal cavities. Fluorite forms roughly circular, amorphous, purple patches on fracture surfaces. Fractures with fluorite coatings were reported from one short interval, between Sta. 52+21 and 53+51 in the Main Drift. Several fluorite-coated fractures also have significant apertures.

Secondary minerals, also common in the Main Drift, are chiefly calcite and opal with manganese oxides and infrequent hematite. Calcite is most commonly found to contain intergrowths of opal. Deposits are sometimes botryoidal with a slightly pearly luster. Calcite and opal commonly fill fractures exposed in the tunnel walls but also occur on the lower surfaces of open fractures, shears, faults and in lithophysal cavities. In some locations, bladed calcite crystals and rarely networks of fine intergrown blades up to 2 cm long stand on the lower surfaces of open fractures and lithophysal cavities.

Calcite in a shear at Sta. 31+08, just below the right springline has a particularly interesting character. The calcite infilling has a total thickness of 2-cm. The lower portion consists of compact, intergrown crystals. The upper part consists of individual but interconnected blades of calcite that terminate on a smooth, flat plane but there is 3 cm of open space between the calcite and the upper surface of the fracture. This occurrence of calcite displays a characteristic often seen in the Main Drift: that of forming only on the lower surface of an opening. In this particular instance, the crystals appear to have grown to the upper surface of the fracture, filling the available space. In addition, the 3-cm open space demonstrates that the fracture opened further, subsequent to the formation of the calcite.

Specular hematite occurs as black, lustrous, tabular to very delicate blades on the upper surfaces of calcite deposits. A lithophysal cavity containing fine blades of specular hematite is located at Sta. 30+18. Hematite occurs in other lithophysal cavities in that general area as well as in other intervals of the Main Drift.

Cooling joints

Cooling joints are a relatively common type of discontinuity encountered in the ESF, despite only accounting for approximately 2 percent of the DLS entries. During early phases of geologic mapping in the ESF, identification of cooling joints was done by general visual determination based on several rather poorly defined characteristics. As the mapping progressed, it became clear that the identification of cooling joints was inconsistent. This inconsistency was due largely to the lack of well-defined and agreed-upon characteristics that distinguish cooling joints from other fractures.

The American Geological Institute Glossary of Geology does not define cooling joints, and a succinct definition in the literature has not been found. In April 1996, the Underground Mapping Team, in consultation with several technical reviewers, attempted to establish a consistent set of criteria that could be applied to distinguish cooling joints from other fractures. A set of characteristics was agreed upon that established a standard the mappers could use to identify cooling joints. The characteristics are planarity, trace length, smoothness, and mineral coating. Cooling joints tend to be very planar. Their trace lengths tend to be long, greater than 5 m. Cooling joints are smooth having a roughness of R5 or R6. Vapor-phase minerals coat cooling joint surfaces. Vapor-phase alteration margins may be associated with a coating of vapor-phase minerals. The margin consists of a pale grayish purple zone of vapor-phase alteration that extends a few millimeters from the face of the cooling joint.

Distinguishing cooling joints from tectonic fractures is difficult even with the criteria outlined above. Although application of the criteria does not conclusively identify cooling joints, it provides a guide to the mappers in their identification of a cooling joint. In addition, there are still some important questions concerning the applicability of the criteria. In particular, discontinuities meeting the cooling joint criteria do not appear to be intersected by cooling joints of markedly different orientations, at least on the scale of the tunnel. In this apparent absence of a cross

cutting set of cooling joints, it is difficult to understand how thermal stresses alone could account for the cooling joints. One explanation is that stresses other than thermal stress were acting on the volcanic sheet as it cooled. The distribution of the cooling joint orientations is similar to that of fractures and shears (discussed below). Since the distribution of cooling joint orientations is similar to that of the other discontinuities, the tectonic regime that resulted in the system of fracturing and faulting was likely active during the emplacement and cooling of the Topopah Spring Tuff.

When assessing the cooling joint data, consider the first half of the Main Drift data set was collected without widely agreed upon or consistently applied cooling joint identification criteria. In addition, where offset is apparent on a cooling joint, the discontinuity is recorded as a shear or fault. The cooling joints in this data set should be considered as being identified correctly but representing only a portion of the cooling joints present in the ESF. Probably the cooling-joint data accurately represent their orientation distribution.

Although the vast majority of fractures and cooling joints are planar, some are curved, undulatory, or conical. These nonplanar features are some of the more unusual and puzzling features in the tunnel. Curved cooling joints extend for some distance in a planar fashion, curve about a well-defined axis over a distance of a few tens of centimeters, and continue as a planar cooling joint at a high angle to the original orientation (photo 7). An example of such a cooling joint is located at Sta. 31+52.5, 0.5 m below right springline. The south limb of the cooling joint is oriented $010^{\circ}/87^{\circ}$, curves about an axis plunging $035^{\circ}/75^{\circ}$, and continues on an orientation of $300^{\circ}/78^{\circ}$. This cooling joint is of particular interest because its north limb, oriented $300^{\circ}/78^{\circ}$, is coated with vapor-phase minerals that extend to just past the axis of the curve. Calcite up to 4 mm thick is also present on that surface. The south limb of the cooling joint has some spots of manganese oxide, but is otherwise clean. The surface of the cooling joint has a network of shallow north-plunging lines of vapor-phase minerals caused by discontinuous planes of vapor-phase minerals (vapor-phase partings) that lie perpendicular to the cooling joint and extend a few centimeters from the cooling joint into the rock. The occurrence of the vapor-phase minerals on the fracture

oriented $300^{\circ}/78^{\circ}$ may be related to the stress field acting on the body of the rock at the time the rock was cooling and while vapor activity was high. If so, the minerals would indicate that the direction of the least principal compressive stress (σ_3) lay in a north northeast-south southwest direction. This orientation of σ_3 is consistent with what is thought to have been the regional stress regime at the time of deposition of these rocks (Minor, 1995).

Gently undulating cooling joints have also been observed that curve to intersect other cooling joints. Such relationships occur between Sta. 34+40 and 34+55, where cooling joints oriented $330^{\circ}/23^{\circ}$ and $295^{\circ}/54^{\circ}$ curve to terminate on each other at nearly right angles. A similar relationship is observable at Sta. 36+60.

Broad, conical forms are visible in the tunnel walls, mostly between Sta. 30+00 and 36+00. The conical forms are defined by several fractures or cooling joints that intersect at low angles and cumulatively form flat, irregular conical shapes. In some instances, there is a layering effect caused by overlapping, roughly concentric fractures. Some of these features are bounded by shears, many of which are reactivated cooling joints. The best example of such a feature occurs at Sta. 34+12 on the right rib (photo 8). The significance of these features is open to speculation.

Other features of note are cooling joints with sets of vapor-phase partings extending from them. Along these fractures, short (usually less than 10 cm), closely and evenly spaced vapor-phase partings are arrayed perpendicular to the fracture. Such sets of vapor-phase partings have been observed to extend 3 to 4 m along a fracture (photo 9). A cooling joint oriented $060^{\circ}/75^{\circ}$ at Sta. 31+09, above the right springline, is a good example of such a feature. Other, similar occurrences are visible sporadically in the same general area.

Analysis of Fracture Data

The detailed line survey (DLS) data from the Main Drift, Sta. 28+00 to 55+00, sampled over 10,100 fracture, cooling joints, and vapor-phase parting entries. Of these entries, 7360 have trace

lengths of 1 m or longer. The data discussed in this section include all fractures, cooling joints, and vapor-phase partings with trace lengths of 1 m or greater. Of this data, fractures make up over 95 percent; cooling joints and vapor-phase parting account for approximately 2 percent each. For a discussion of the fractures with trace lengths less than 1 m versus those with longer trace lengths, see **Comparison of DLS Data, 30 cm Minimum versus 1 m Minimum Trace Length**, p. 40. The term "fracture" as used in this section includes fractures, cooling joints, and vapor-phase partings unless stated otherwise.

The DLS data were analyzed using stereonet projections, azimuth distribution, and fracture density histograms, as well as a variety of other plots. Stereonet projections were generated using the computer program Dips. Stereonets of data grouped by 100-meter intervals in the Main Drift were used to identify fracture sets. The other plots, generated using the computer application Excel, were used to confirm and refine the definition of the fracture sets and determine their boundaries. The centers of the sets were identified using a combination of; locating the centers of the contours generated by the Dips contour plots, the peak occurrence in orientation, and the numerical averages identified in Excel.

The entire DLS data set and various smaller intervals were analyzed to identify the fracture sets, their relationships, and how those relationships change. All the pole plots show to greater and lesser degrees, clusters of poles establishing the primary fracture sets. Typical changes in clustering occur between Sta. 35+00 and 38+00 (Fig. 4). The most prominent and well-defined cluster of poles represents a set of fractures oriented approximately $120^{\circ}/80^{\circ}$, designated Set 1. A second cluster of poles represents a set of fractures oriented approximately $220^{\circ}/80^{\circ}$, designated Set 2. This set is well defined in some intervals of the Main Drift but in some intervals is less well defined. A third cluster of poles represents fractures oriented approximately $310^{\circ}/30^{\circ}$, designated Set 3. This set is represented on most of the stereonet. The exception is the interval between Sta. 42+00 and 50+00 where there is nearly complete absence of Set 3 fractures. Between Sta. 28+00 and 37+00, a fourth set of fractures was identified in the cluster analysis. Set 4 strikes similarly to Sets 1 and 3, between 270° and 330° , and dips intermediately

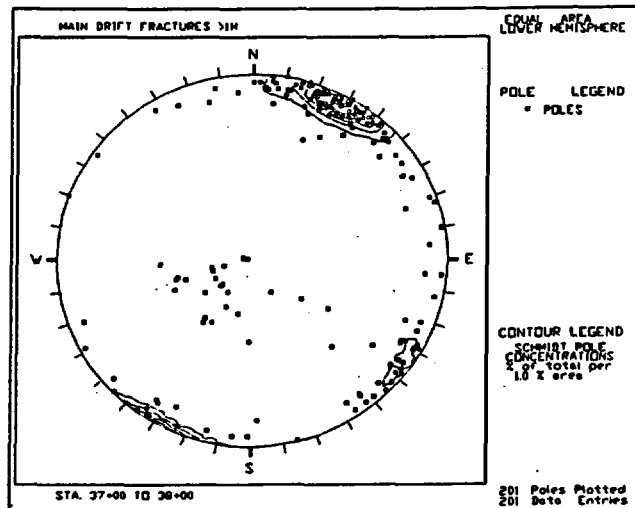
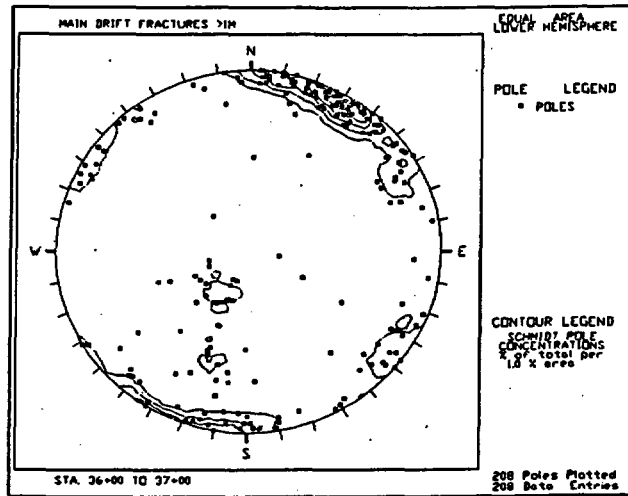
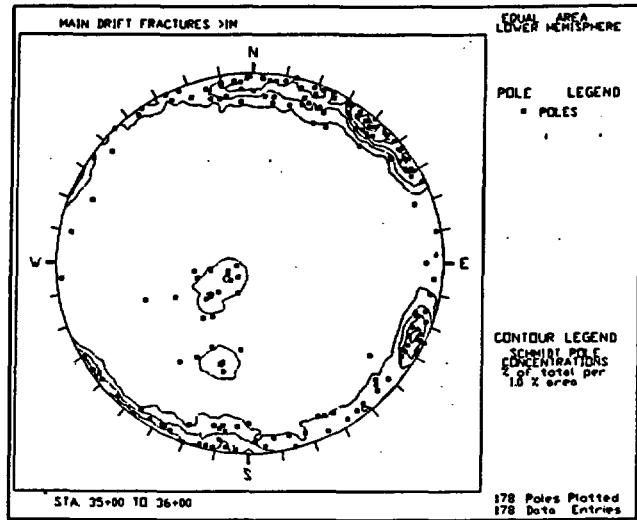


Figure 4 Stereonets of fractures from Sta. 35+00 to 36+00, 36+00 to 37+00, and 37+00 to 38+00.

between Sets 1 and 3, 40° to 60° . On most of the stereonet, the fracture sets are relatively well defined. There are intervals, however, where the fracture sets are represented by more diffuse clusters with poorly defined boundaries between sets (discussed below). A significant number of fractures, especially between Sta. 28+00 and 42+00, cannot be included in any of the fracture sets within geologically significant limits. These fractures are designated random fractures.

The azimuth-distribution histogram also shows a very strong concentration of fractures between 100° and 155° (Fig. 5). Another, more subtle and broader concentration between 200° and 310° is also apparent in the histogram. This concentration is a combination of what is seen in the stereonet as the cluster of steeply dipping fractures striking in the 220° range and the cluster of moderately dipping fractures striking in the 300° range.

The fracture-density histogram of the Main Drift (Fig. 6) shows a strong concentration of fractures between Sta. 42+00 and 51+50 which identifies the fracture zone. In the remainder of the Main Drift, the fracture density is much more even. A fracture-density histogram comparing Set 1 with the remaining data (Fig. 7) demonstrates that Set 1 consistently comprises the majority of fractures in the Main Drift; and that Set 1 fractures make up the vast majority of fractures in the fracture zone between Sta. 42+00 and 51+50. The azimuth-distribution histogram which excludes the data between Sta. 42+00 and 51+50 (Fig. 8) still shows a strong peak between 100° and 150° , although not nearly as extreme as in figure 5.

Defining Set 2 is more problematic. The edge of this concentration at 200° is only 17° from the bearing of the tunnel, 183° . Anticipated is a decrease in the numbers of fractures recorded as their strikes become closer to paralleling the axis of the tunnel because of a sampling direction bias. The Terzaghi correction was applied to the data to compensate for the decreased probability of encountering fractures nearly parallel to the tunnel. The Terzaghi method applies a factor of $1/\cosine$ of the angle between the strike of the fracture and a line perpendicular to the transect, the axis of the tunnel (Terzaghi, 1965). This factor was used to weight the occurrence of fractures based on their orientations (Fig. 9). Within a few degrees of the axis of the tunnel, the correction factor becomes

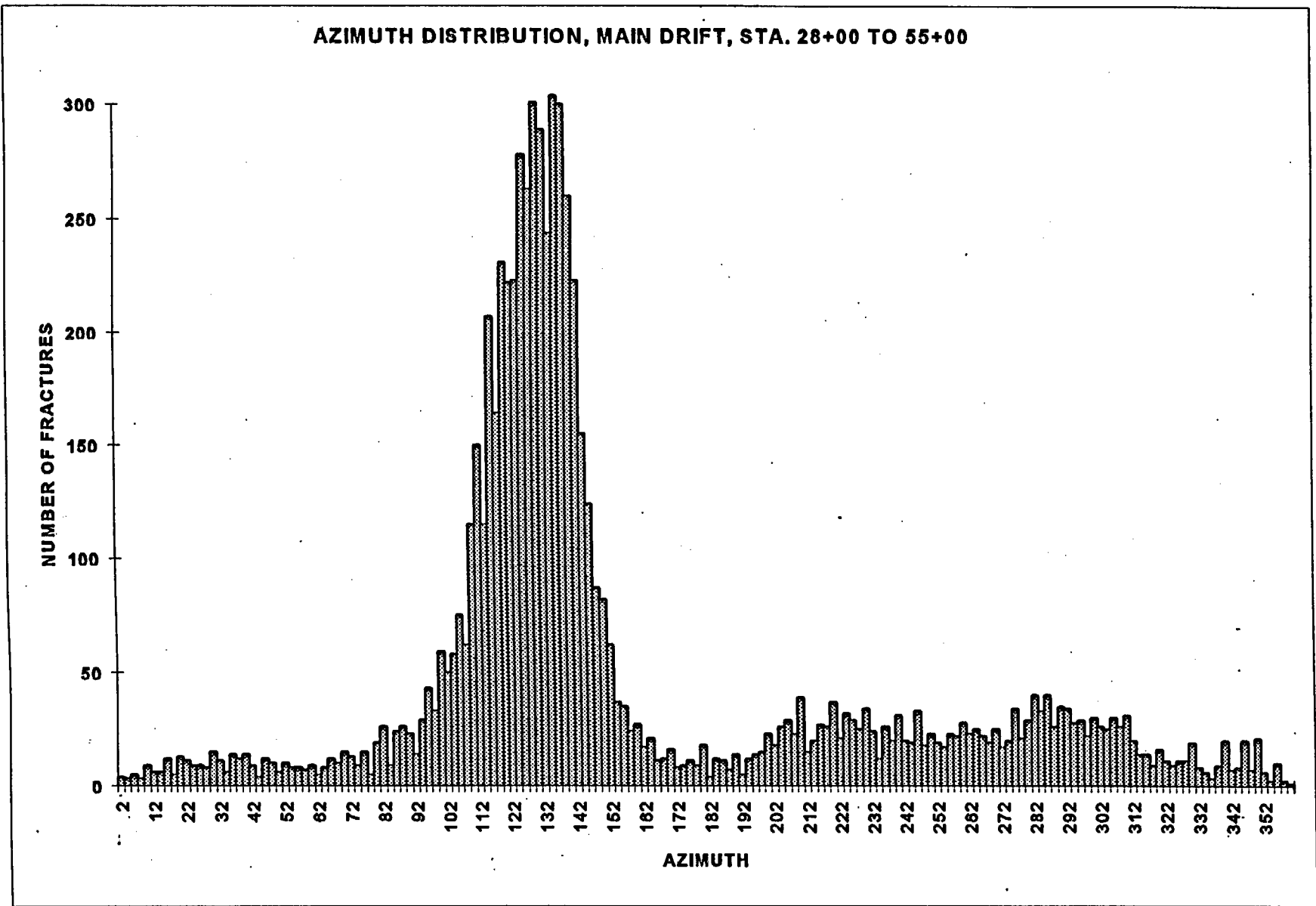


Figure 5 Distribution of fracture, cooling joint, and vapor-phase partings by azimuth in the Main Drift.

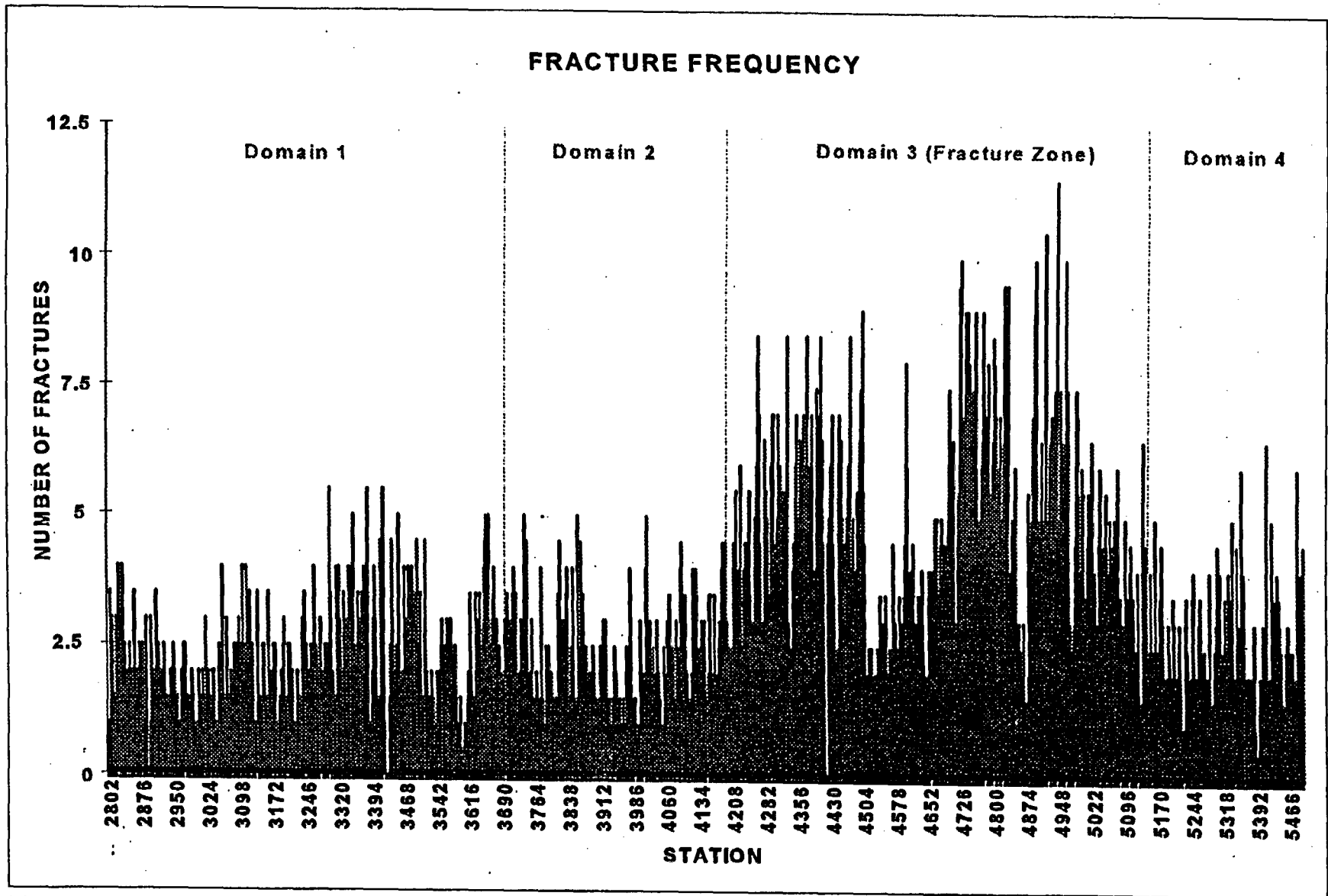


Figure 6. This fracture-density histogram plots the number of fractures, cooling joints, and vapor-phase partings per meter in each 2 meter interval along the Main Drift.

C-01

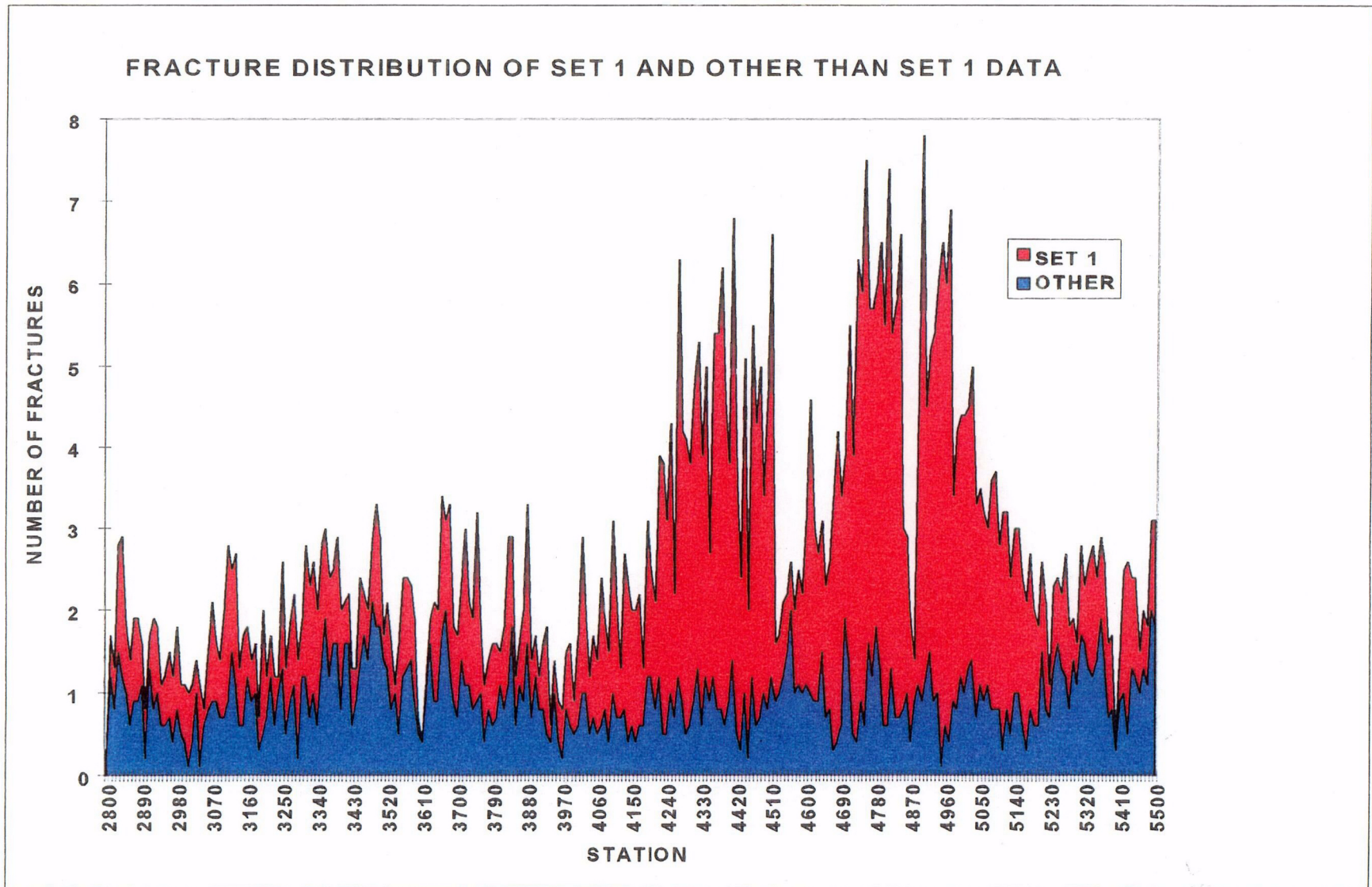


Figure 7. The fracture density of Set 1 (Red) plotted with all other fractures (Blue) clearly shows the predominance of Set 1 in the Main Drift. Figure also shows the more uniform density of other than Set-1 fractures. The X axis is in fractures/meter over a 10 meter average.

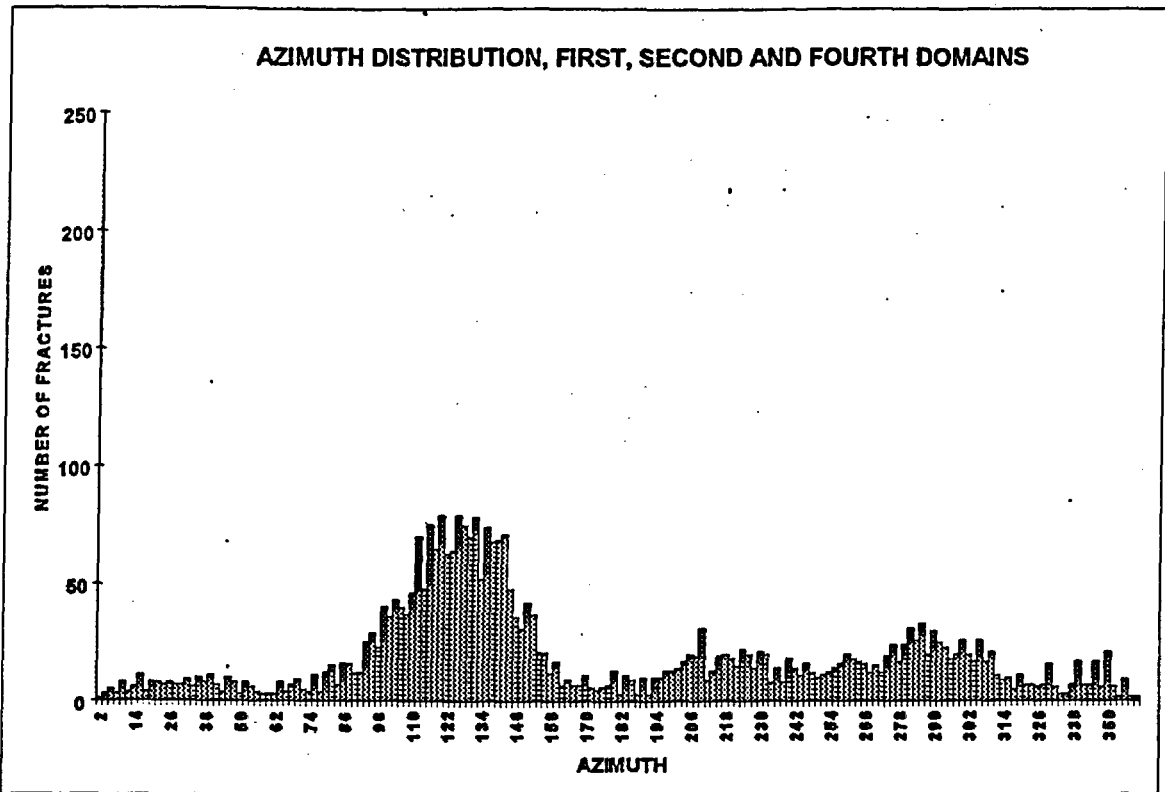


Figure 8. The Azimuth distribution of the First, Second, and Fourth Domains (excluding data from the fracture zone) show a strong concentration of Set-1 fractures. The Y axis is scaled for comparability with figure 5.

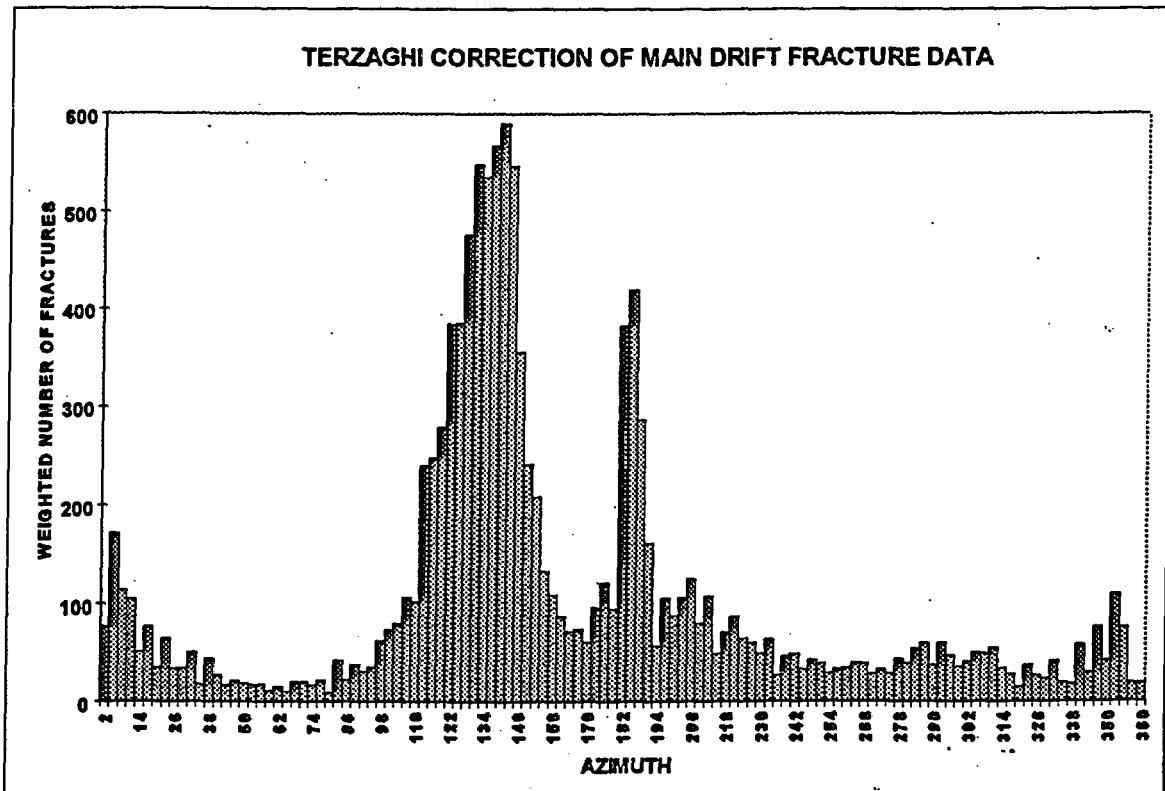


Figure 9. Weighted numbers of fractures from the application of the Terzaghi correction to the Main Drift fracture data.

exceedingly high. This effect is demonstrated by the spikes on the histogram centered on 183° and 003°. To moderate the effect of this exceedingly high correction factor, the data were separated by azimuth into groups on 3° intervals. The correction factor was established based on the azimuth of the center of each group.

The Terzaghi correction plot shows the concentration between azimuths 100° and 150° as essentially unchanged from the plot of the uncorrected data. The plot also shows that the distributions on either side of the spike at 183° have somewhat different shapes. The slope on the right side of the peak, toward the higher azimuths, is broader and flatter than the slope on the left side of the peak. This relationship suggests an actual separation between the concentration beginning at approximately 200° and the data with azimuths less than 180°.

This simple exercise provides another way of seeing the data which may assist in determining the validity of placing data-set boundaries near the axis of the tunnel. Simply applying the Terzaghi correction to the strike angle alone cannot be accepted as a complete correction of the data set.

Domains Defined by Fracture Characteristics

An assessment of the various histograms and projections mentioned above reveals the presence of four large domains in the Main Drift. The four domains are distinguished by structural characteristics. Following are the primary characteristics: (1) the occurrence or absence of fracture sets; (2) changes in fracture distribution and/or density; and (3) changes in the relative numbers of fractures in the fracture sets (Table 1).

The First Domain is between Sta. 28+00 and 37+00. The azimuth-distribution histogram displays the characteristics that set the First Domain apart from the rest of the Main Drift (Fig. 10). This domain is characterized by a more even distribution of fracture orientations resulting in a more diffuse clustering of the data, and less well-defined fracture sets. The First Domain has a greater

TABLE 1 FRACTURE SETS BY DOMAIN

FIRST DOMAIN, STA. 28+00 TO 37+00						
	STRIKE	RANGE	DIP, AVG	RANGE	NUMBER	% TOTAL
SET 1	115	082 - 132	82	>70	798	47%
SET 2	210	195 - 245	83	>70	230	14%
SET 3	310	282 - 350	22	<40	86	5%
SET 4	292	280 - 320	51	40 - 60	62	4%
RANDOM					506	30%
TOTAL					1682	

SECOND DOMAIN, STA. 37+00 TO 42+00						
	STRIKE	RANGE	DIP, AVG	RANGE	NUMBER	% TOTAL
SET 1	125	100 - 140	84	>70	540	57%
SET 2	210	200 - 242	84	>70	134	14%
SET 3	331	290 - 350	18	<40	51	5%
RANDOM					215	23%
TOTAL					940	

THIRD DOMAIN, STA. 42+00 TO 51+50						
	STRIKE	RANGE	DIP, AVG	RANGE	NUMBER	% TOTAL
SET 1	138	100 - 145	83	>70	2951	74%
SET 2	220	200 - 250	84	>70	215	5%
SET 3	316	295 - 345	22	<40	21	1%
RANDOM					785	20%
TOTAL					3972	

FOURTH DOMAIN, STA. 51+50 TO 55+00						
	STRIKE	RANGE	DIP, AVG	RANGE	NUMBER	% TOTAL
SET 1	141	120 - 150	81	>70	428	56%
SET 2	231	215 - 265	84	>70	168	22%
SET 3	340	305 - 355	12	<35	26	3%
RANDOM					145	19%
TOTAL					767	

Table 1 presents the orientations of fracture sets and related information determined through analysis of DLS data. Values for strike, dip, and ranges were obtained primarily through the use of stereonet plots, azimuth distribution histograms, and fracture density histograms. The DLS data analyzed includes fractures, cooling joints, and vapor-phase partings.

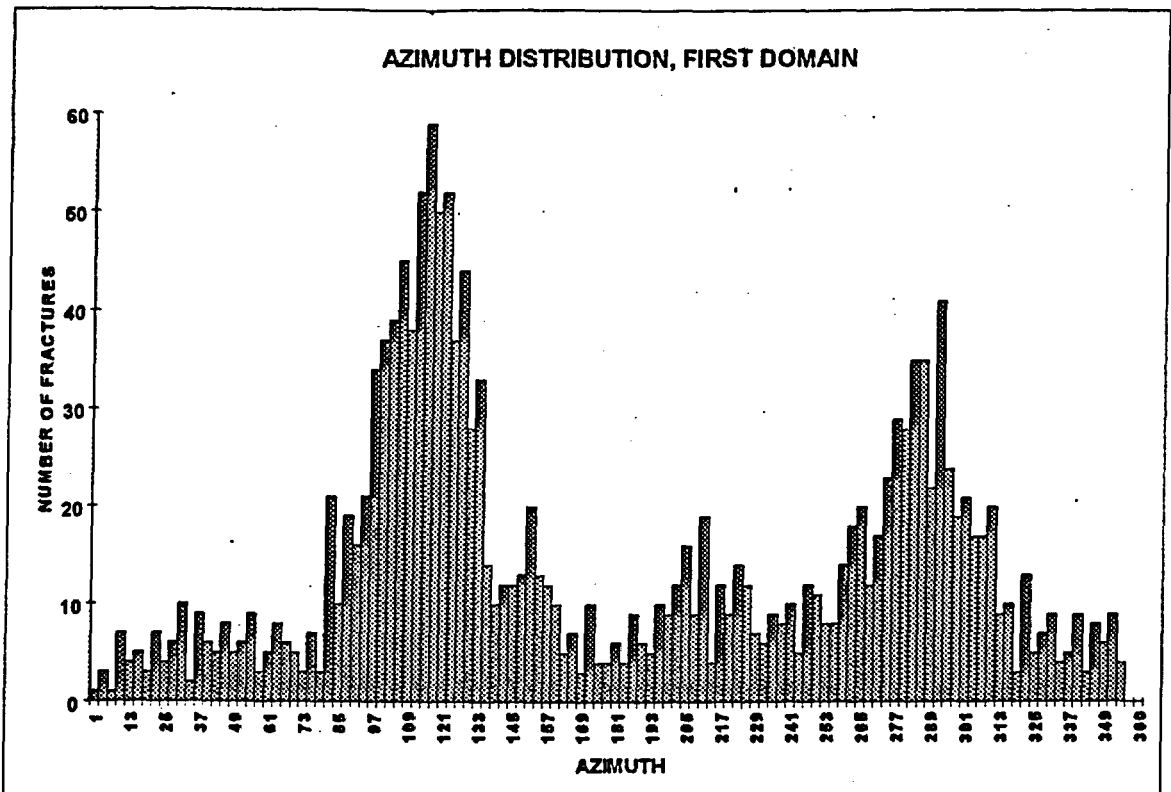


Figure 10. The distribution of fractures in the First Domain is more evenly distributed than in the other Domains.

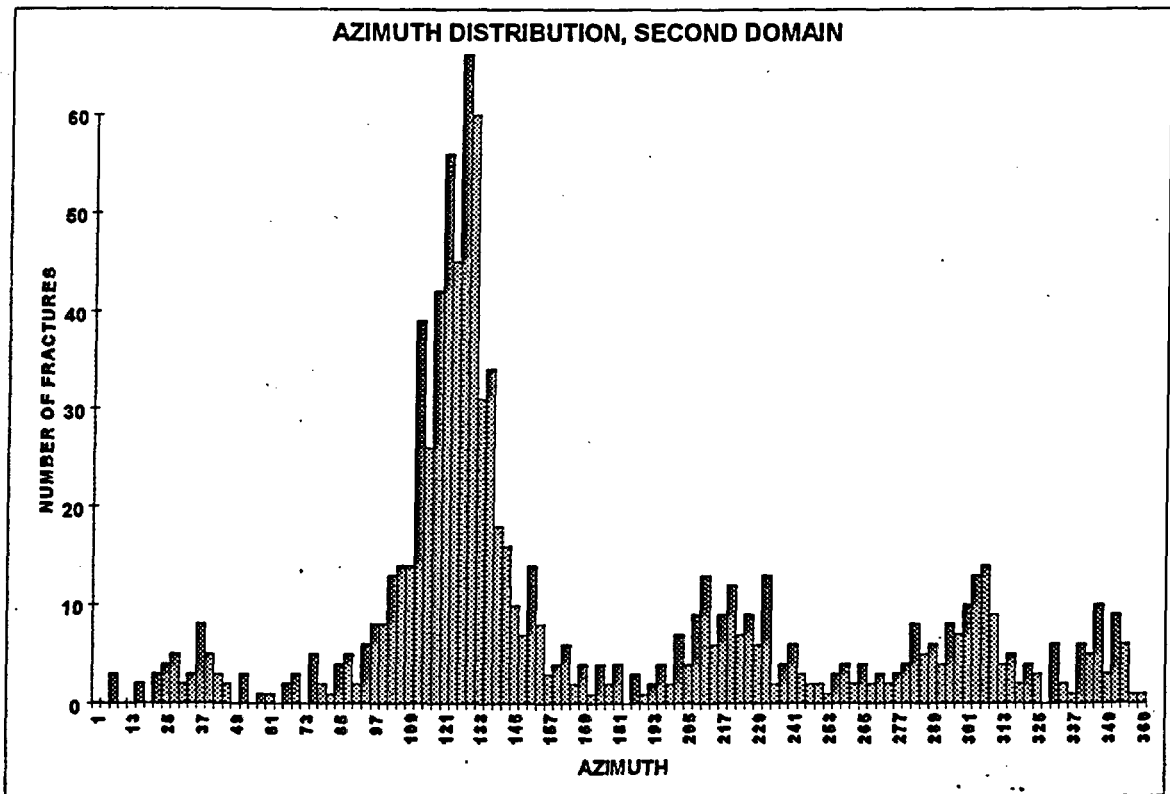


Figure 11. The azimuth distribution of fractures in the Second Domain shows a strong peak in Set 1 and does not have the more even distribution seen in the First Domain.

percentage of random fractures than seen elsewhere in the Main Drift. Random fractures are those that do not fall into any of the sets within geologically significant limits. Set 1 is prominent in the First Domain but not to the extent found elsewhere in the tunnel. The distribution of the fractures is markedly different in the Second Domain (Fig. 11). The Second Domain, between Sta. 37+00 and 42+00, is characterized by well-clustered and well-defined fracture sets. Set 1 fractures clearly predominate and are tightly clustered.

The Third Domain is the fracture zone between Sta. 42+00 and 51+50. This portion of the Main Drift is also discussed in **Fracture Zone Between Sta. 42+00 and 51+50**, below. The fracture zone is made up predominantly of Set 1 fractures with an average fracture density of over five fractures per meter, as shown in figure 6. Set 2 fractures are also present and have a rather wide diversity in orientations. The fracture density histogram shows two zones within the fracture zone with markedly fewer fractures. The first zone, between Sta. 45+30 and 46+55, is a quiet zone with a fracture density similar to that of areas outside the fracture zone. The second zone, between Sta. 48+55 and 48+80, is not a quiet zone but a zone containing 10 shears and intense random fracturing. Thus the second lull is an artifact of the fractures having too low a continuity (trace length less than 1 m) to be recorded in the DLS.

The clusters of Sets 1 and 2 rotate clockwise in the Third Domain (Fig. 12). Between Sta. 46+00 and 49+00, the center of Set 1 rotates clockwise 20° and maintains this orientation to at least Sta. 55+00. Set 2 fractures are less numerous, and their clusters are generally less well defined than Set 1 fractures; however, there is a discernible clockwise rotation of Set 2 data. The concentration of Set 2 fractures is generally between $200^\circ/80^\circ$ and $220^\circ/80^\circ$. Beginning at Sta. 48+00, the Set 2 data shifts to the right, probably because of a decrease in the numbers of

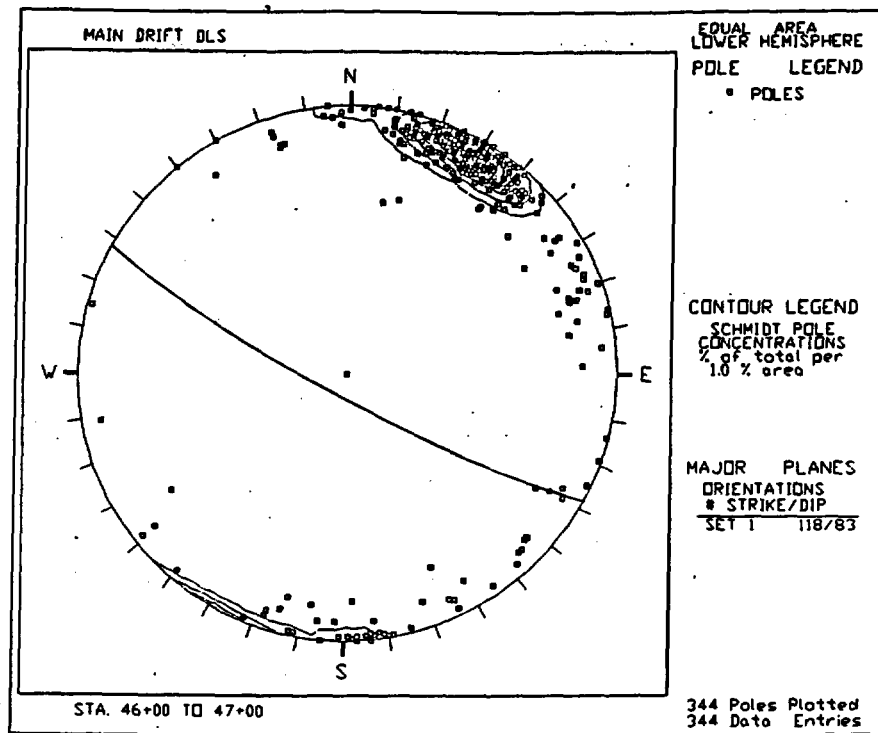


Figure 12a Stereonet of fracture from Sta. 46+00 to 47+00

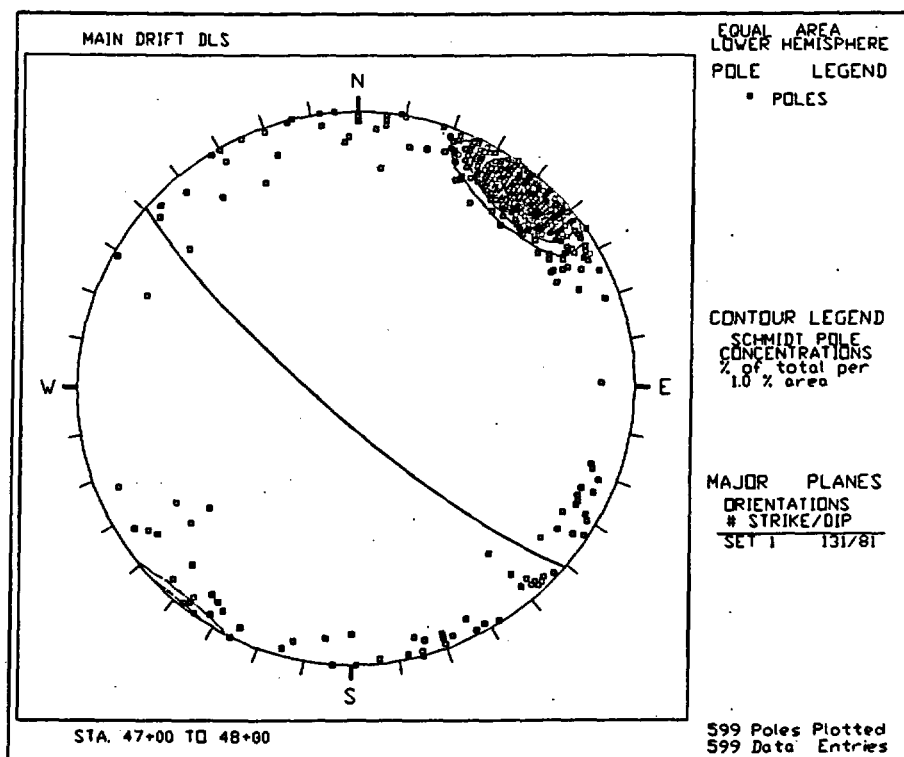


Figure 12b Stereonet of fractures from Sta. 47+00 to 48+00.

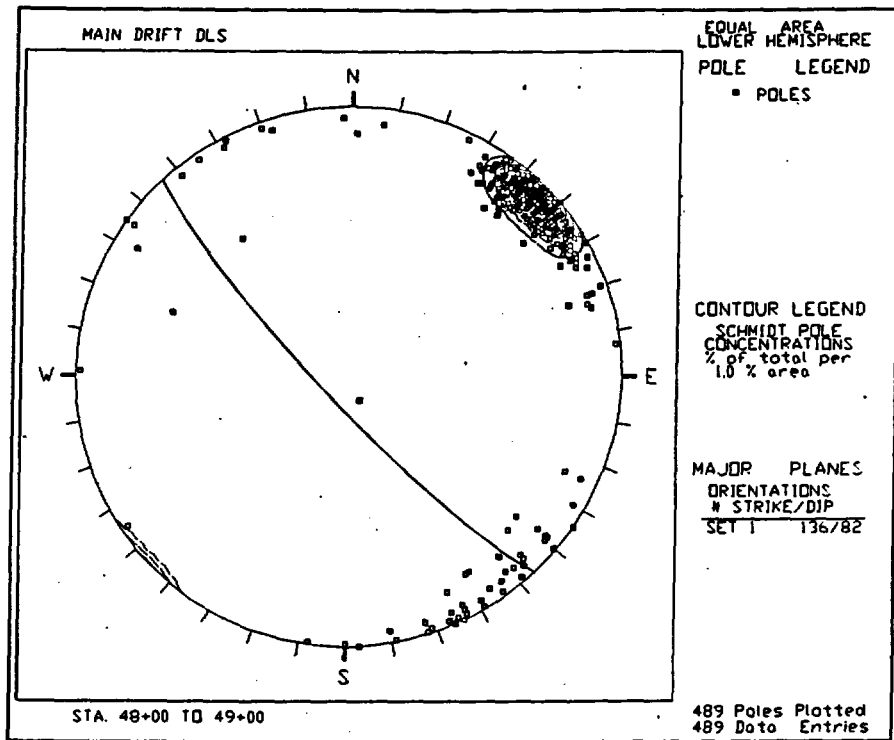


Figure 12c Stereonet of fractures from Sta. 48+00 to 49+00.

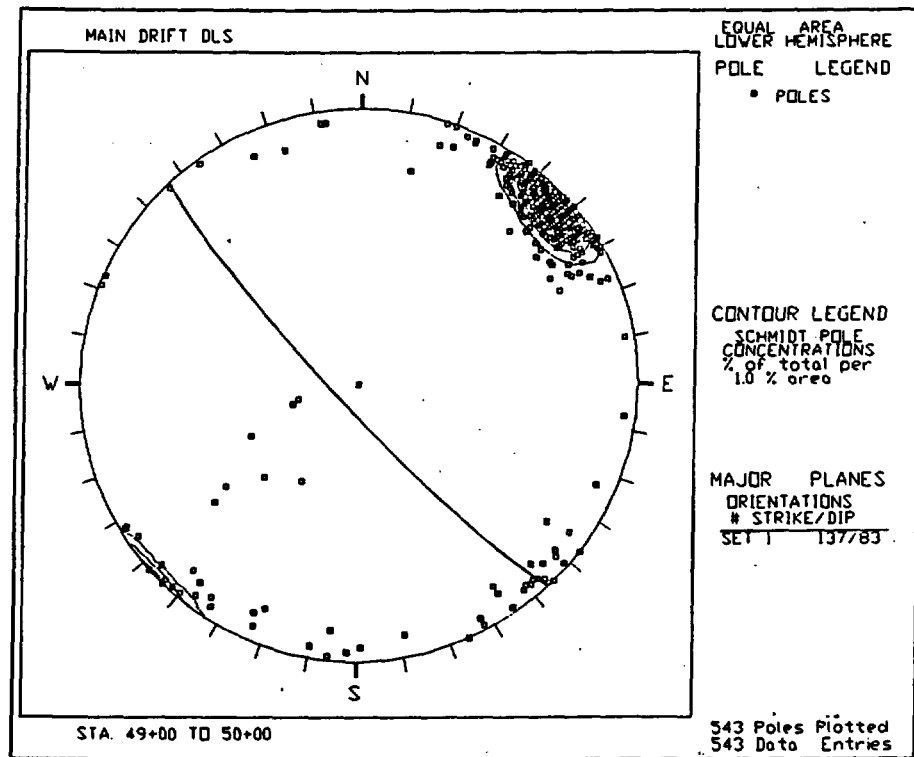


Figure 12d Stereonet of fractures from Sta. 49+00 to 50+00.

fractures striking between 200° and 230°. Beyond Sta. 49+00, the cluster of Set 2 data becomes more well defined and begins shifting to the right becoming centered between 240° and 250°. Because of this clockwise rotation, when large blocks of data are plotted, the sets become less well defined and less distinct from each other.

The Fourth Domain is between Sta. 51+50 and 55+00 and is distinguished by a distinctly lower fracture density than in the fracture zone. The azimuth distribution is much the same as in the Third Domain with a very strong concentration of Set 1 centering on 140°. This orientation represents an approximate 20° clockwise rotation from the orientation of Set 1 in the Third Domain. Set 2 rotates clockwise as well (Fig. 13). Set 3 fractures are present in small numbers, the majority being represented by vapor-phase partings.

Comparison of DLS Data, 30cm min. versus 1 m min. Trace Length

The DLS originally recorded any discontinuity with a trace length of 30 cm or greater. A collective decision by members of the underground mapping team and USGS and DOE personnel was made to increase the minimum trace length from 30 cm to 1 m. The decision was prompted by feedback from the users of the DLS data that questioned the usefulness of the data collected on the short fractures and the need to make the most effective use of manpower resources. At Sta. 37+80, the change to the 1-m-minimum trace length was implemented. Every 500 m, a 50-m section of DLS was collected using the 30-cm-minimum trace-length criterion. The 30-cm criterion was used from Sta. 45+00 to 45+50 and from Sta. 50+00 to 50+50.

A comparison was made between DLS data with trace lengths between 30 cm and 1 m and those with trace lengths 1 m and longer. The most obvious difference between the two sets of data is the difference in the number of data points. Where the DLS data were collected using the 30 cm criterion, the fractures with trace lengths less than 1 m accounted for an average of 53 percent of the data entries. A variety of histograms and projections--including stereonets,

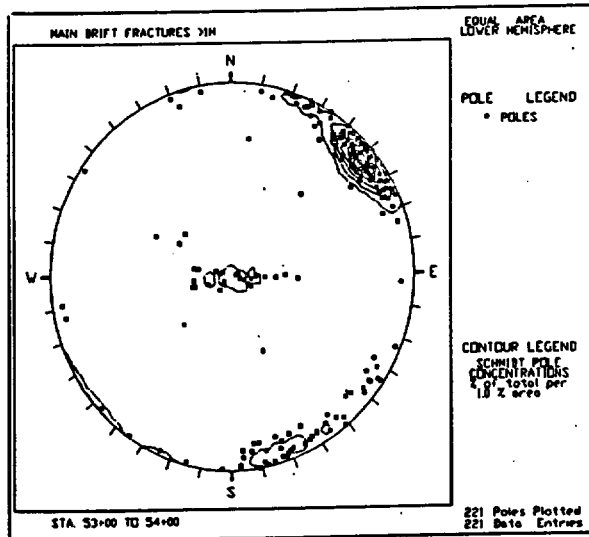
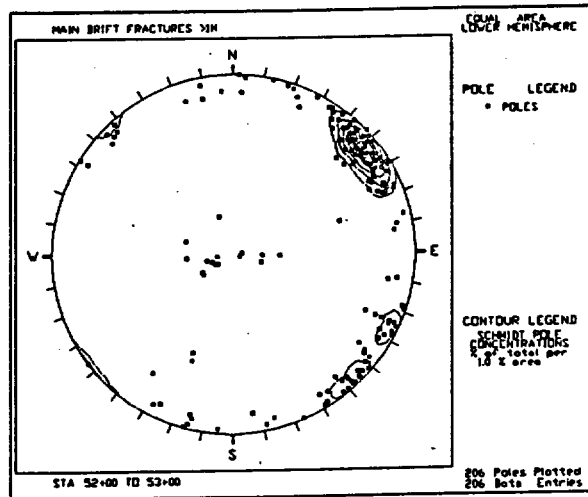
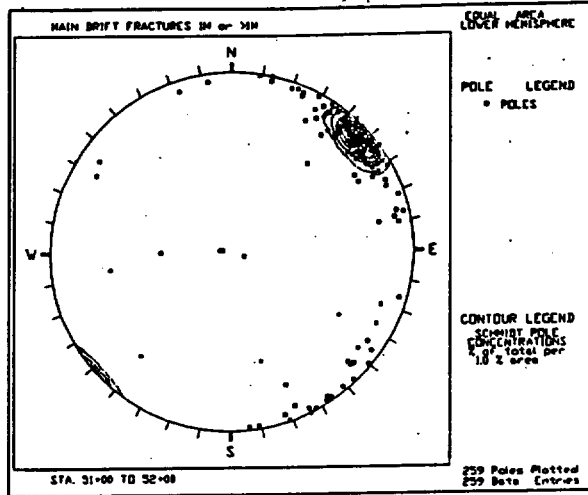


Figure 13

Stereonets of fractures from Sta. 31+00 to 32+00, 32+00 to 33+00, and 33+00 to 34+00.

fracture-

density histograms, and fracture-density histograms--was used to compare the data sets primarily in terms of orientation and location. The various methods of comparison show the two data sets have the same general pattern of azimuth distribution and fracture density (Fig. 14). At the azimuths representing fracture Sets 1 and 3, the fractures 1 m and greater are more numerous than the shorter fractures. Aside from those orientation ranges, the fractures having less than 1 m trace lengths generally are more numerous than the longer fractures. Although the two data sets have the same general distribution, the fractures shorter than 1 m long have a more even distribution, thus a greater proportion of random fractures than the 1 m and greater data.

A comparison of other characteristics including maximum aperture, minimum aperture, infilling thickness, dip, and fracture length was performed through statistical analysis. Factor 1 and 2 scores are a function of maximum aperture, minimum aperture, infilling thickness, dip, and fracture length. Bivariate factor 1 and 2 versus fracture length scatter plots (Figs. 15 to 17) were produced to determine if significant bias is produced when the 30-cm minimum trace length criterion is used, as opposed to the 1-meter minimum trace length. If significantly different structural data are being collected using the 30-cm criterion, then significantly different factor 1 and/or 2 scores should be seen in the data with trace lengths between 30 cm and 1 m versus the data with greater trace lengths. Figure 15 clearly shows a positive correlation between factor 1 scores and fracture length. This correlation is to be expected, because factor 1 scores are a function of fracture length. The fit is not linear, in that factor 1 scores are also a function of the maximum aperture of the fracture and the thickness of its infilling. Figure 16 shows that the distribution of factor 1 scores differs little regardless of whether a 30-cm criterion is used. Figure 17 shows that the distribution of factor 2 scores differs little regardless of which minimum trace length criterion is used. Since the distribution of factor 1 and 2 scores is not affected by the use of the 30-cm criterion, the use of the 1-m criterion saves time and produces similar results for maximum aperture, minimum aperture, infilling thickness, dip, and fracture length.

The comparison of data collected from fractures with trace lengths of 30 cm to 1 m with those having longer trace lengths shows no significant differences either in terms orientation; location or

C-02

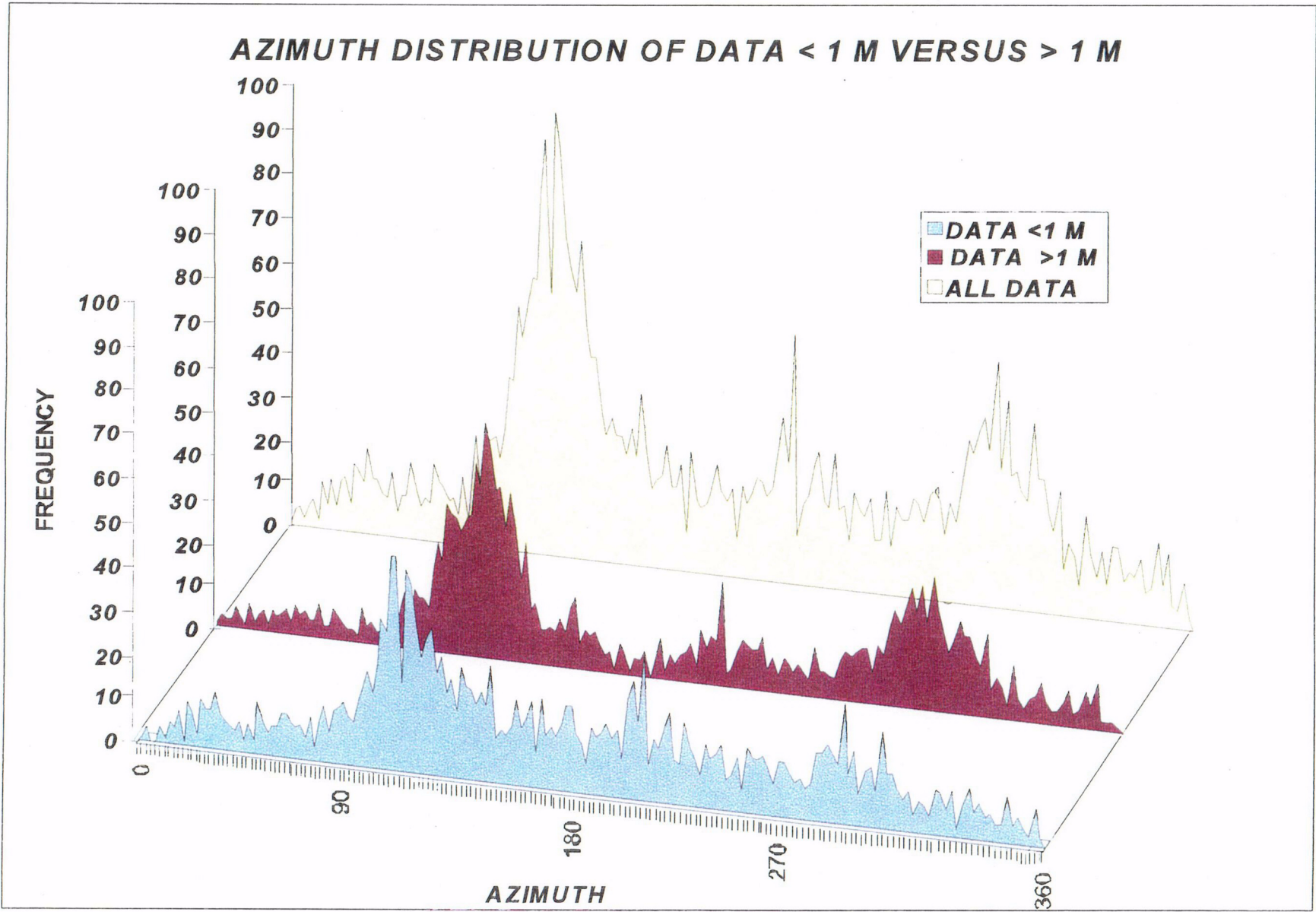


Figure 14. Azimuth distribution of data collected between Sta. 28+00 to 37+80 separated by trace length.

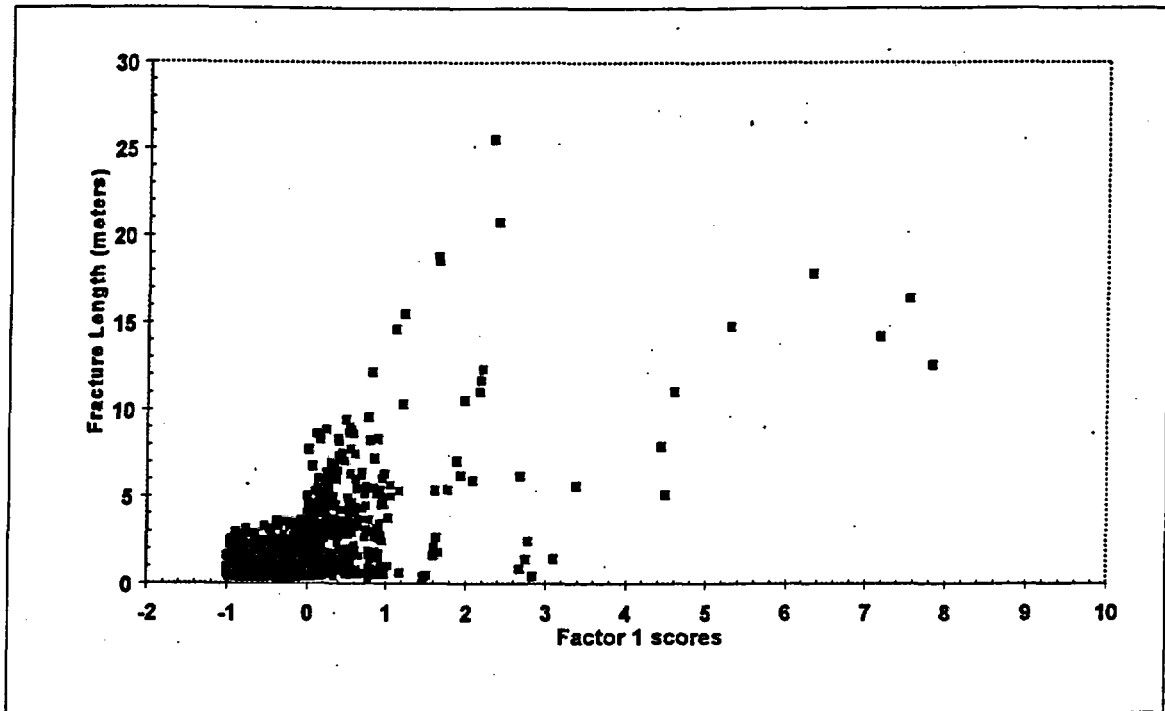


Figure 15. A Factor-1 plot showing a general positive correlation between Factor-1 scores and fracture length.

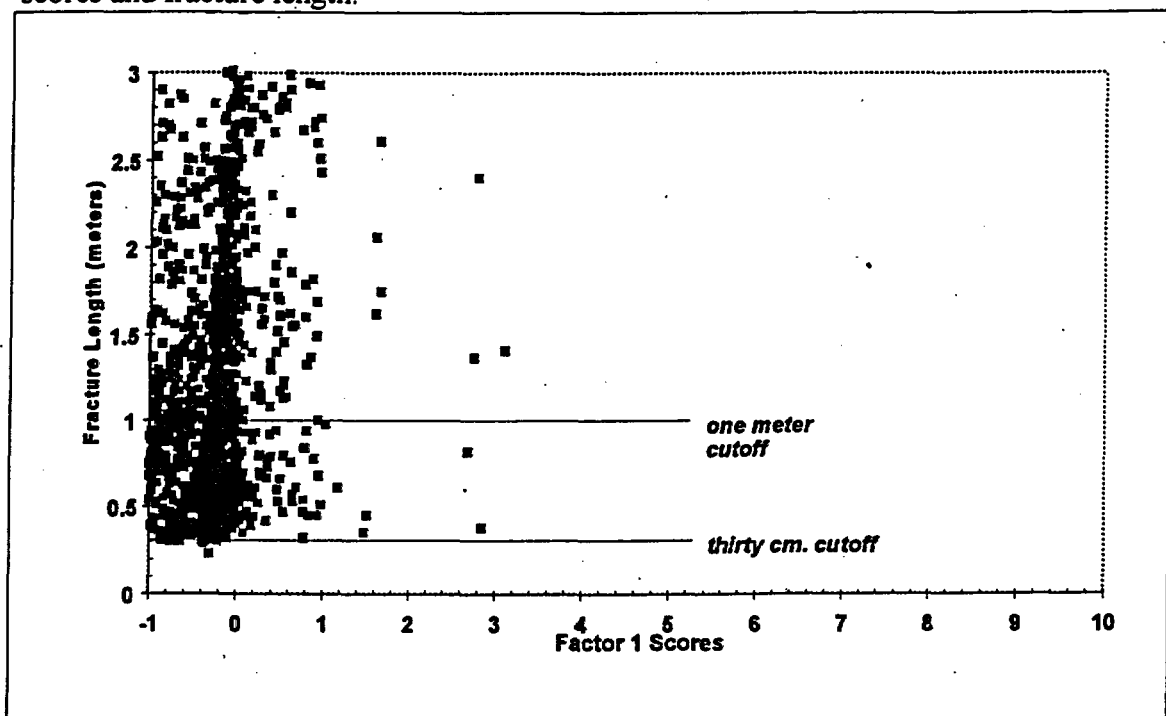


Figure 16. A Factor-1 score versus fracture-length plot showing that, for fractures 0.3 to 3.0 meters in length, similar Factor-1 scores are obtained regardless of whether a 0.3- or 1.0-meter cutoff was used.

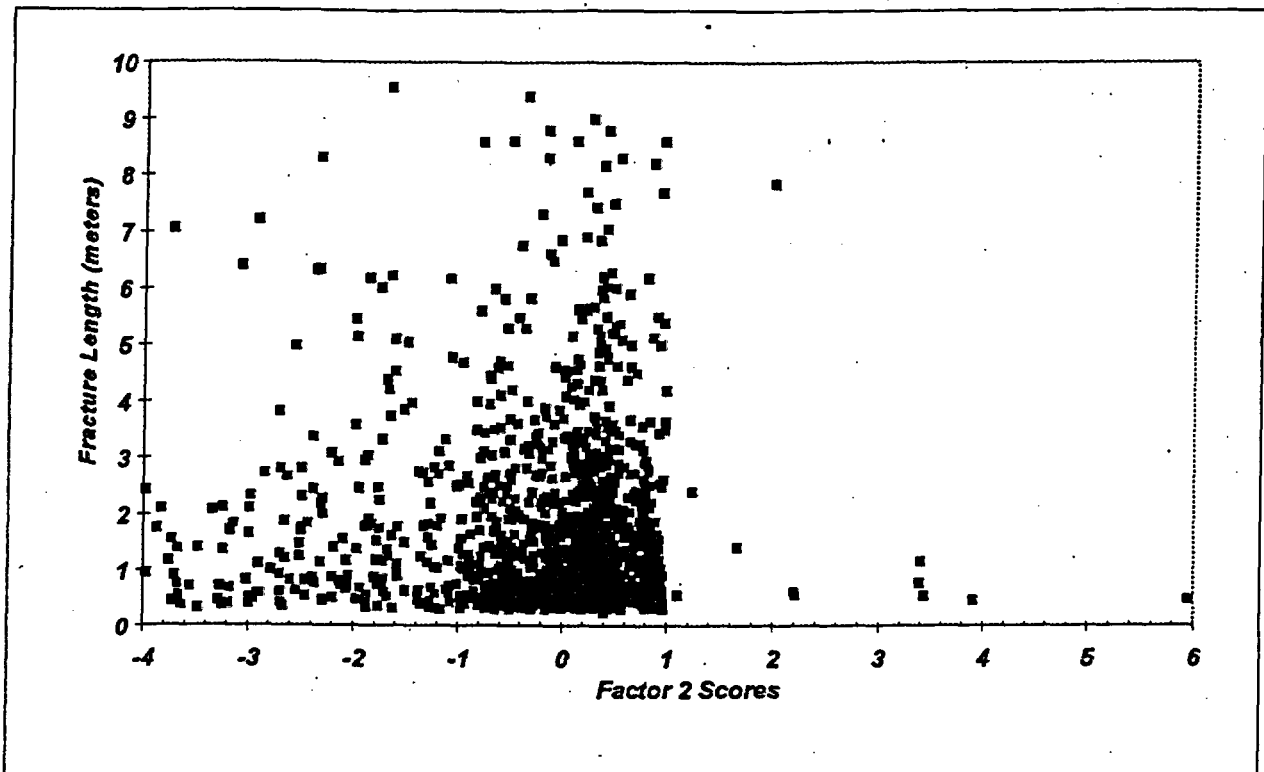


Figure 17. A Factor-2 score versus fracture-length plot showing that Factor-2 scores are not a function of fracture length.

other recorded characteristics between the two sets of data. To the extent determinable by the analysis conducted as part of this study, the collection of data on fractures 1 meter and longer is satisfactory.

Faults and Shears

Faults are defined by technical procedure GP-32 (Beason and others, 1994) as discontinuities displaying more than 0.1 m of offset, and shears are those having less than 0.1 m of offset or an undetermined offset. The DLS record contains 66 faults and 255 shears in the Main Drift portion of the tunnel. The only named fault in the Main Drift is the Sundance fault. Although the fault plane has distinct horizontal slickensides, the magnitude and sense of the offset could not be determined (Photo 10). Of the 31 faults with measured offsets, the largest is 0.63 m; the next largest is 0.34 m. Seven faults have offsets between 0.2 and 0.3 m, and 21 faults have offsets between 0.1 and 0.2 m. Slickensides were observed on a small minority of Sets 1 and 2 faults and

shears.

One of the most consistent characteristics of the faults and shears in the Main Drift is their lack of continuity. Only a few faults and shears are continuous around the entire circumference of the tunnel. Common relationships include faults and shears that extend part way around the tunnel, then die out. In such cases, an echelon faults or shears may or may not be present. In many cases, offset appears to occur in zones containing discontinuous shears and/or faults with markedly different orientations that appear unconnected. The best example is in the Sundance fault zone, exposed between Sta. 35+90 (right wall) and 36+30 (left wall), where Sets 1, 2, and 3 faults and shears are present but do not appear interconnected. The traces of shears visible in the tunnel wall sometimes become untraceable for some distance and then reappear. In some instances, a fracture passing through the space between the visible traces of the shear is offset, indicating that shearing is occurring in the zone where the trace of the shear is not visible. At Sta. 28+83, a shear oriented $290^{\circ}/83^{\circ}$ is composed of an echelon segments. Offset is apparent on each segment, but there is no visible connection or offset in the approximately 10-cm space between the segments. Offset also occurs within systems of shears of differing orientation. Offset is transferred from one shear to another shear with a markedly different orientation. The intersecting shears form wedges which are offset relative to the adjacent body of rock. An example of such an intersection occurs between Sta. 28+00 and 28+50 where a fault striking 206° (Set 2) terminates on a Set 3 shear forming a low angle wedge. High-angle wedges are more common. Good examples are located between Sta. 40+00 and 43+00.

Kinematic indicators observed in the Main Drift contributed to determining offset. At Sta. 29+23, fractures spaced 1 to 2 cm apart and oriented $050^{\circ}/25^{\circ}$ are confined between two low angle shears oriented $284^{\circ}/08^{\circ}$ and $310^{\circ}/10^{\circ}$. The orientation of these fractures suggests right-lateral offset (top to the east) on these shears. Where the strike-slip component of offset on Set 3 shears has been identified with confidence, the offset is right-lateral, top to the east. Slickensides are almost invariably on fault or shear surfaces striking between 150° and 230° and they invariably plunge less than 10° . In most cases, the slickensides remain bidirectional indicators, as the sense of offset could not be determined.

Analysis of Fault-and-Shear Data

The sense of offset is determined visually by identifying features which have been offset across the shear or fault. The sense of offset can sometimes be inferred from kinematic indicators within and/or adjacent to the fault or shear. Determining offset in the middle, nonlithophysal zone is often problematic, for there are few features that can be used reliably as markers. Overall, at least one component of offset, either strike-slip or dip-slip, was determined on 80 percent of faults and shears. Both strike-slip and dip-slip components of offset were determined on only 5 percent of faults and shears. And for 20 percent of faults and shears, the sense of offset could not be determined. In some cases, neither the magnitude nor the sense of offset could be determined, even though quite obvious indicators of offset were present. Indicators of offset such as gouge or brecciated rock may be present, or features that appear to be truncated and/or offset by a shear may not be convincingly identified on the other side of the shear.

Determining the sense and magnitude of offset on faults and shears was given careful attention during field reviews of the FPGMs as part of the preparation of this report. Additional data collected during this process do not appear on the FPGM. Shear and fault data compiled from the FPGM of the Main Drift and field reviews were tabulated and analyzed (Table 2). The distribution of faults and shears shows essentially the same sets present in the fracture distribution (Fig. 18) but the relative abundance of faults and shears within those sets is different. In addition, the relative abundance of faults and shears in each set changes along the Main Drift (Table 3).

Set 1 faults and shears are oriented $120^{\circ}/82^{\circ} \pm 20^{\circ}$ and dip 75° or more, with a few falling slightly outside this range. This set also includes a few shears dipping steeply in the opposite direction, e.g. $290^{\circ}/86^{\circ}$. The orientation of Set 1 faults and shears coincides with that of the most numerous and densely clustered set of fractures and cooling joints. Set 1, however, is the least numerous group of faults and shears.

TABLE 2 SHEAR AND FAULT SETS, STA. 28+00 TO 55+00																
STA.	SET 1				SET 2				SET 3				RANDOM			
	Str.	Dip	offse	slics	Str.	Dip	offse	slics	Str.	Dip	offse	slics	Str.	Dip	offse	slics
2800					206	85	LL									
					26	82	LL									
					42	83	RL									
					221	82	LL		305	43	R?					
									290	46	R					
2850									313	28	R					
					210	83	LL		307	31	R?					
	120	84	R						310	45	R					
									307	59	R					
													248	34	R	
2900					247	80	LL,N									
									302	26	R					
									284	8	R					
									310	10	R					
													43	38	R?	
													314	65	RL	
3000																
									260	7	R					
	288	78			191	87	LL									
									310	33	R,LL?					
	132	85			214	88	LL		332	47	R,LL?					
	139	81	R		235	89	N		297	15	R					
					220	78	LL						360	8	LL	
					206	72	LL									
3200					203	86	LL									
					209	88	LL									
													50	18	R	
3250					222	63	LL									
	119	81	N													
	287	68	R										45	27	R	
3300	290	86	N													
					225	78	N									
3400																
	107	80	N						301	39	R					
									295	37	R					
									322	37	R					
3500									305	35	R					
	278	65	R						314	33	R					
									304	25	R			14	79	LL
	103	86	RL													
	280	86	N		205	87	N?		292	30	R					
	127	78	RL,R		210	83	N		327	26	R,RL					
3600	155	84		0	45	86			290	45	R					
	154	87	LL	0												
	337	88	R													
	122	84							314	32	R			43	25	R?
									297	17	R					
									301	32	R					
									293	24	R					
3650	98	88							284	11	R					
	124	75	R						330	7	R					
3700	117	80	N						324	24	R					
									320	17	R					
									305	15	R					
					258	88	N		285	34	R					
					239	89			316	31	R					
					208	78	N		310	23	R?					
3800					65	86										
	120	89	N		227	84										
					215	77	LL,N									
					211	79	N									
					230	83	N?									
					44	87	R									
					218	87	N									
3900					215	88	N						70	40	R	
	141	86	LL		37	86	R		360	18			70	30	N?	
4000					205	85	N									
					217	84	N									

STA.	SET 1				SET 2				SET 3				RANDOM			
	Str.	Dip	offse	slics	Str.	Dip	offse	slics	Str.	Dip	offse	slics	Str.	Dip	offse	slics
					221	78							245	10	R	
					213	71	LL						220	13	R	
	165	80		5					298	23	R					
	155	78	N?													
	125	74			60	60	LL									
4100					60	80			295	25						
	128	83	N		219	87	LL?,N?		286	16			211	45	R	
					225	83	R									
4250	113	89	R													
	149	78	N		219	81	N		326	12	R					
	105	90	N						319	25	R					
									325	34	R					
4300					245	88	N									
					199	77	LL?	0								
					247	73	LL									
	140	85		170	240	80	LL									
													180	78	176	
													175	76	165	
	122	82			210	77		170								
					30	85										
4400																
4450					40	90	LL									
					215	80	LL									
					230	85	LL?	168								
					242	84	N,LL?									
					215	80	LL?	4								
4500					196	88	LL									
					197	81	LL									
	170	80	RL		195	80	LL									
	145	85	RL,N		205	81	LL?									
					220	80	R									
					244	80	LL									
					240	71										
4550					192	78	LL?									
					207	82										
					223	86										
4600													271	88	R	
4650					208	80	LL									
	158	85	RL		220	80	LL						262	87	RL	
					236	87	LL									
4700					237	82										
					214	77	RL									
	145	80	R		43	86										
					228	82	LL									
					23	65	LL									
4800					225	81	LL									
4850					259	85										
					245	88	LL									
					245	88	LL									
					234	88	LL									
					224	87	RL									
					222	84	RL									
					215	87	RL									
					230	76	RL									
					247	88	LL									
					236	84	LL									
4900					242	88	N						276	78	N	
4950	142	79	N		209	82	LL									
					240	83										
5000	130	85	R													
	143	86	R		238	82	N									
5050	144	82	R													
	120	85	R													
	158	81	N?		249	88	N									
5150					241	83	N,LL?									
					224	80	R									
					229	72										
					244	84	LL,N									
5200	143	81	RL		212	75	R									
	141	87	R,EL?													
	100	80	N													
	136	87	N		239	86	N									
	130	77	N		259	79										

**TABLE 3 COMPILED SENSE OF OFFSET
ON FAULTS AND SHEARS BY DOMAIN**

FIRST DOMAIN, STA. 28+00 TO 37+00				
OFFSET	N	R	RL	LL
SET 1	3	4	2	0
SET 2	5	0	0	12
SET 3	0	22	1	2

SECOND DOMAIN, STA. 37+00 TO 42+00				
OFFSET	N	R	RL	LL
SET 1	6	3	0	2
SET 2	12	3	0	9
SET 3	0	19	0	0

THIRD DOMAIN, STA. 42+00 TO 51+50				
OFFSET	N	R	RL	LL
SET 1	3	5	3	0
SET 2	5	1	2	23
SET 3*	0	0	0	0

FOURTH DOMAIN, STA. 51+50 TO 55+00				
OFFSET	N	R	RL	LL
SET 1	18	5	8	1
SET 2	17	7	0	9
SET 3*	0	0	0	0

OFFSET

N normal

R reverse

RL right lateral

LL left lateral

* no Set 3 faults or shears recorded

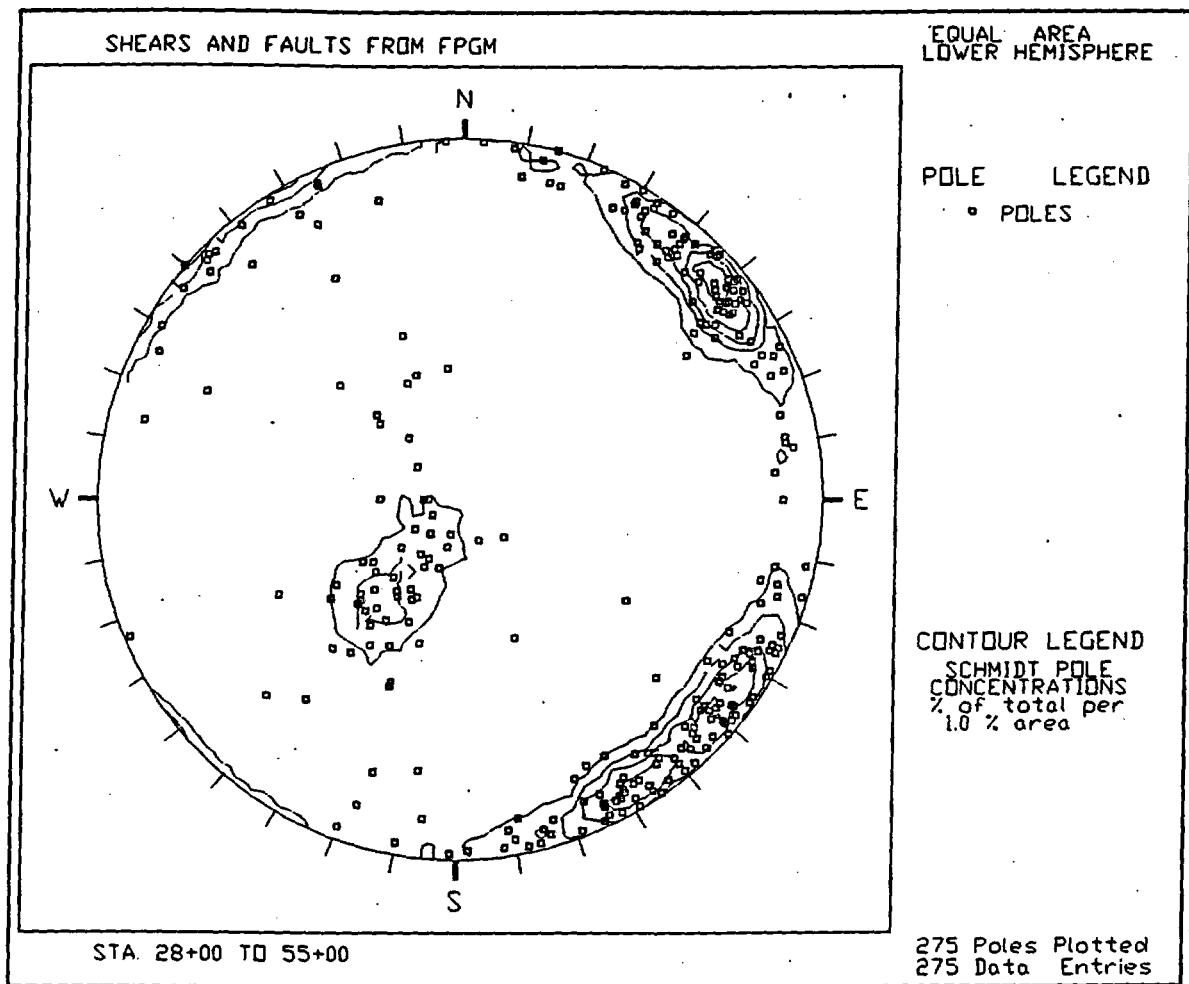


Figure 18. Stereonet plot of all the faults and shears in the Main Drift, compiled from the FPGMs. The plot shows the same general distribution as seen in the plots of fracture data.

Set 2 faults and shears are oriented $210^{\circ}/83^{\circ} \pm 20^{\circ}$ and dip 75° or more. This set also includes faults and shears dipping in the opposite direction, e.g. $044^{\circ}/87^{\circ}$. Faults and shears of this set are the most numerous overall. They are commonly rougher, more irregular, and have more gouge infilling than faults and shears belonging to the other sets.

Set 3 faults and shears strike $310^{\circ} \pm 30^{\circ}$ and dip moderately, less than 40° . They are almost exclusively reactivated cooling joints.

The shear and fault sets are oriented similarly to the fracture sets; and like them, the fault sets rotate clockwise going down the Main Drift. As with the fracture analysis, changes in the pattern of shearing in the Main Drift resulted in identifying four domains. The domain boundaries are the same or very close to the domain boundaries established by changes seen in fracturing.

Domains Defined by Fault-and-Shear Characteristics

Changes in the pattern of shearing and faulting identifies four domains having the same or very similar boundaries to those identified in the fracture analysis. The precise location of the domain boundaries differ due to the specific criteria used to define the boundaries as discussed below. The changes that set the domains apart from each other are the relative abundance, occurrence or absence of faults and shears in the three sets, and changes in the pattern of offset. As with the fractures, the orientations of the fault and shear Sets 1 and 2 rotate clockwise south along the Main Drift. Stereonet projections of the shear and fault data display the characteristics that define the four domains (Fig. 19).

The First Domain extends from Sta. 28+00 to 37+00, ending just beyond the Sundance fault. The plot of these data shows three well-defined sets oriented $120^{\circ}/81^{\circ}$, $208^{\circ}/82^{\circ}$ and $305^{\circ}/32^{\circ}$. Here, Set 3 faults and shears are the most numerous, and Set 2 faults and shears are distinctly more numerous than those of Set 1. Only one Set 1 shear was mapped between Sta. 28+00 and 30+50, and only three were mapped between Sta. 30+50 and 32+50. This absence of Set 1 is distinctly different from the fracture data where Set 1 fractures clearly and consistently outnumber the other fracture sets. Data points representing faults and shears of the Sundance fault zone which strike approximately 155° cluster separately from other Set 1 faults and shears. Set 3 consists largely of reactivated cooling joints, some of which display vapor-phase minerals. A subset of Set 3 is present only in the First Domain. This subset strikes similarly to Set 3 shears (290° to 335°) but dips more steeply, between 40° and 60° . In the Second Domain, the steepest Set 3 shear dips 34° . The data set in the First Domain is also distinguished from the rest of the

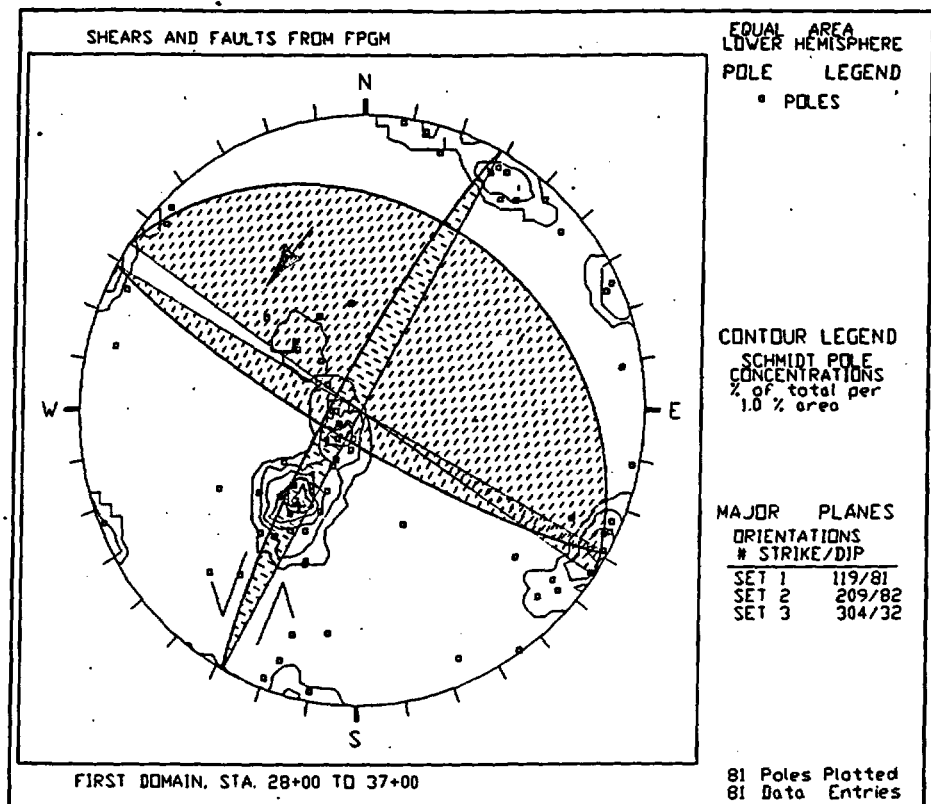


Figure 19a. Stereonet plots of faults and shears by domain (figure 19a is the First Domain). The patterned planes represent the orientation of the peak concentration in the fault and shear sets in each domain. The arrows indicate the predominate sense of offset. The predominate dip-slip, and strike-slip components are shown where applicable. The offset data is also presented in Table 3.

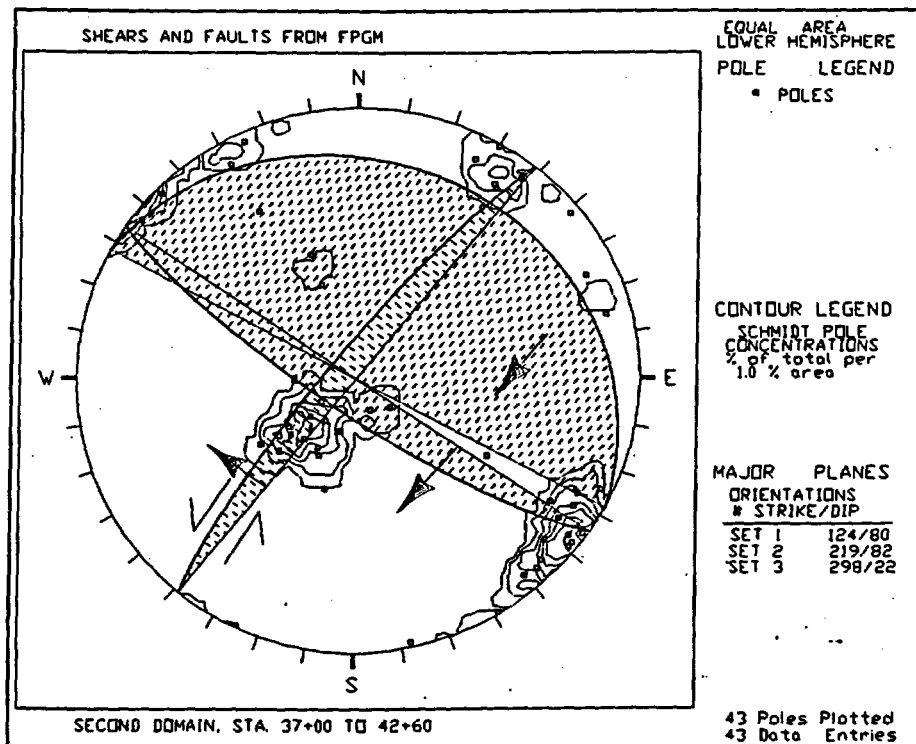


Figure 19b Faults and shears of the Second Domain.

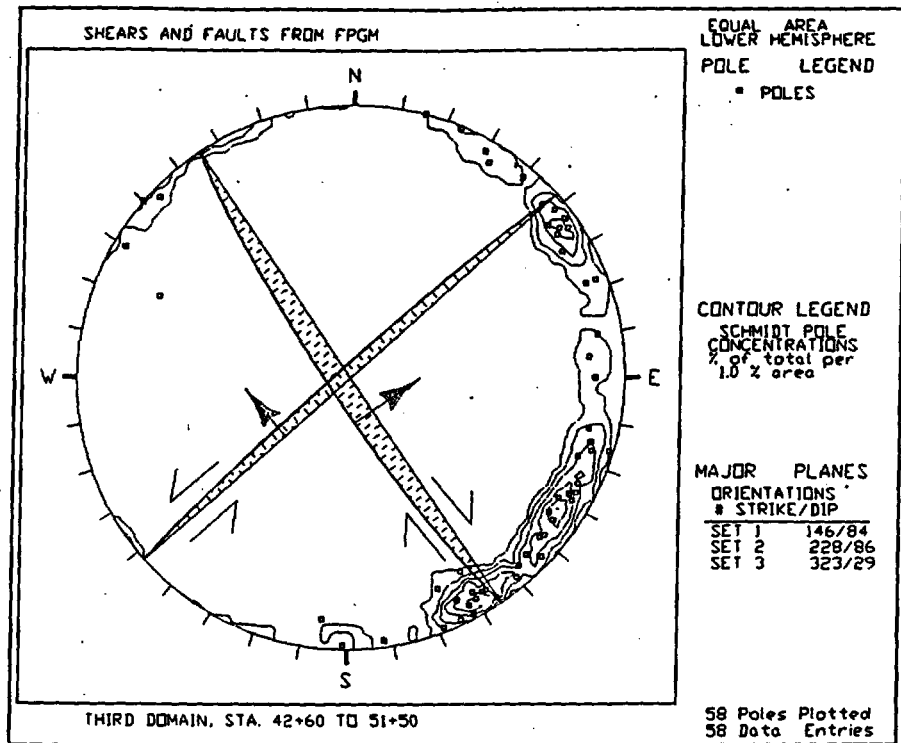


Figure 19c. Faults and shears of the Third Domain.

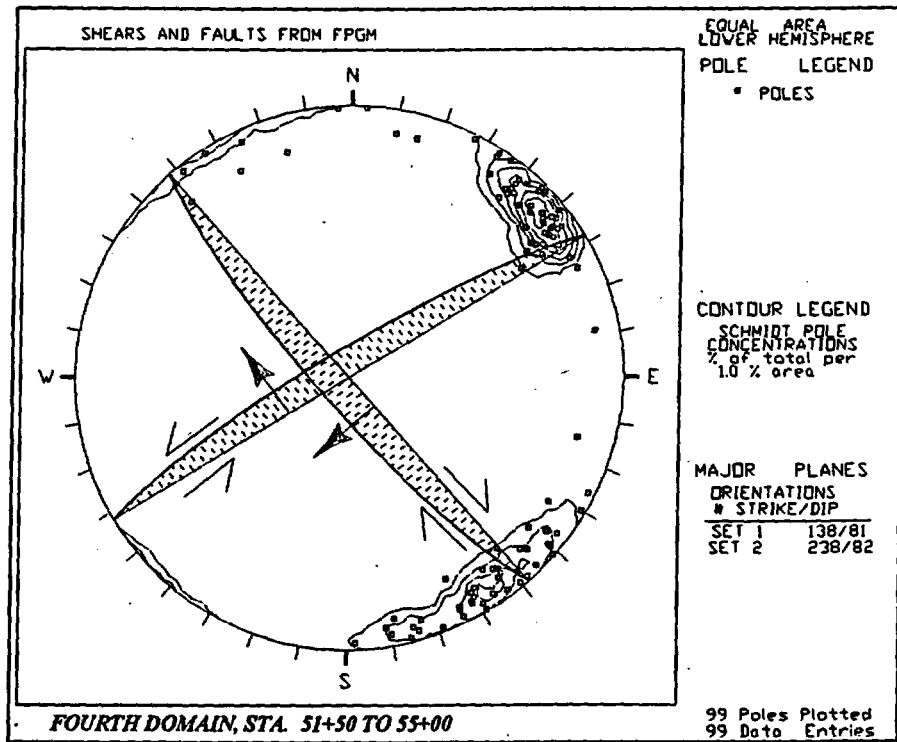


Figure 19d. Faults and shears of the Fourth Domain

Main Drift in that 20 percent of the faults and shears do not fall into one of the three established sets and are thus classified as random. The number of random faults and shears in the First Domain (13) is nearly three times that found in the Second Domain and six times that found in the Third and Fourth Domains.

The predominant offsets from Table 3 are also shown on the stereonets (Fig. 19). The compilation of offsets shows mixed normal and reverse offsets on Set 1 shears with some right-lateral offsets; an overall left-lateral offset on Set 2, west side to the south southwest with some normal offsets; and invariably reverse offsets on Set 3, top (hanging wall) to the south southwest with two left-lateral offsets and one right-lateral offset.

The Second Domain, Sta. 37+00 to 42+60, begins in the area of the Sundance fault and ends just inside the fracture zone. The end of the Second Domain is marked by the last occurrence of a Set 3 shear. Fractures and cooling joints of this orientation occur beyond approximately Sta. 50+00, but none are shears. Set 1 faults and shears plot similarly to those in the First Domain. The cluster of Set 2 data has rotated clockwise approximately 10° from its position in the First Domain. The relative abundance of data points in the three sets has also changed. Set 2 faults and shears are slightly more numerous than those of Set 3. Set 1 faults and shears are the least numerous.

In the Second Domain, Set 1 faults and shears have twice as many normal offsets as reverse with some left-lateral offsets. Set 2 offsets are predominantly normal with a few reverse offsets. Left-lateral offsets are the only strike-slip displacements recorded. Set 3 faults and shears have exclusively reverse offset. The predominant offsets shown on the stereonet (Fig. 19b) show a similar pattern to that of the First Domain but with more normal offsets on Set 1 and a much stronger normal component on Set 2. The composite offset shows a strong left-lateral shearing (west side to the south southwest) and normal offsets on Set 2. Reverse offset on Set 3 results in an overall offset of the top (hanging wall) to the south southwest.

The Third Domain as defined by the distribution of faults and shears is between Sta. 42+60 to

51+50. A major change occurs at the beginning of the Third Domain. Set 3 shears are not present beyond this point. In the Third Domain, Set 2 faults and shears are still in the majority, but the relative number of Set 1 faults and shears increases significantly. The clusters of Set 1 and particularly Set 2 data are not as well defined as in the First and Second Domains, and the distinction between the two sets is not as clear. The data clusters continue their clockwise rotation. The Set 2 cluster has a bimodal character with a concentration of faults and shears striking approximately 215° and another at approximately 240° . The overall rotation of the Set 2 data is the result of an increase in the number of faults and shears striking approximately 240° .

In the Third Domain, offsets of Set 1 faults and shears remain mixed with a slightly greater number of reverse than normal offsets. Right-lateral offsets on Set 1 shears have replaced left-lateral offsets recorded in the Second Domain. Offsets on Set 2 faults and shears are overwhelmingly left-lateral. Normal offsets are the predominant dip-slip offset.

The Fourth Domain, Sta. 51+50 to 55+00, 350 m long, is much shorter than the other domains. Despite the shorter length, this domain has nearly twice as many faults and shears as any of the others. Almost all the faults and shears are in Set 1 or 2. The numbers of data points in Sets 1 and 2 are nearly equal, and the two sets are well concentrated and distinct from each other. Set 1 is oriented $140^{\circ}/80^{\circ}$, quite similar to that of the Third Domain. Set 2 is oriented $240^{\circ}/82^{\circ}$, which is similar to one of the concentrations in the Third Domain. Only three shears are categorized as random. The number of shears oriented in the 215° range are greatly reduced in the Fourth Domain, resulting in a continued clockwise rotation of Set 2.

The offset on Set 1 faults and shears is predominantly normal and right-lateral with some reverse offsets. Set 2 offsets are predominantly normal, with a substantial number of reverse offsets and left-lateral offset was the only strike-slip offset recorded.

Fracture zone between Sta. 42+00 and 51+50

The fracture zone between Sta. 42+00 and 51+50 is a zone of intense Set 1 fracturing. This zone

appears to be strata bound within the Tptpmn. The zone does not crop out on the surface. Down-hole video from drill hole SD-12, located 39.4 m west of tunnel Sta. 46+49, shows a similar zone of intensely fractured rock only within the Tptpmn. The Main Drift in the area of the fracture zone is parallel to the Ghost Dance Fault and is approximately 100 m west of and in the hanging wall of the fault. It is not known whether the fracture zone is continuous across the Ghost Dance fault as only limited information exists east of the Main Drift.

The DLS in this interval of tunnel contains 4561 discontinuities. Of these, 4443 were recorded as fractures and cooling joints, 106 as faults or shears, and 11 as vapor-phase partings. The fracture density averages 5.2 fractures per meter but ranges as high as 19 fractures per meter (photo 11 and 12) (Fig. 20). The average spacing for all fractures in this zone is 0.21 m, and the average fracture length is 2.19 m.

Fracture Zone Characteristics

Four fracture sets (Sets 1, 2, 3, and random) have been identified in the fracture zone through statistical analysis of the DLS data. The location and character of the fracture zone are illustrated by the azimuth distribution and fracture-density histograms of the entire data set (Figs. 5 and 6). The predominance of Set 1 is evident in the fracture-density histograms with the sets plotted separately (Fig. 21), and the azimuth distribution histogram of the fracture zone (Fig. 22).

On the full-periphery geologic maps of the fracture zone, the intense fracturing appears to occur only on the ribs or walls of the tunnel. This impression results from the cross-cutting, steeply dipping Set 1 and 2 fractures forming prisms with nearly vertical axes which are prone to be plucked out of the tunnel walls during excavation. This plucking results in a myriad of fracture faces on the tunnel walls giving them a tabular to an elongated, blocky appearance. These prisms are present in the crown of the tunnel, but they have been cut across their axes and plucking does

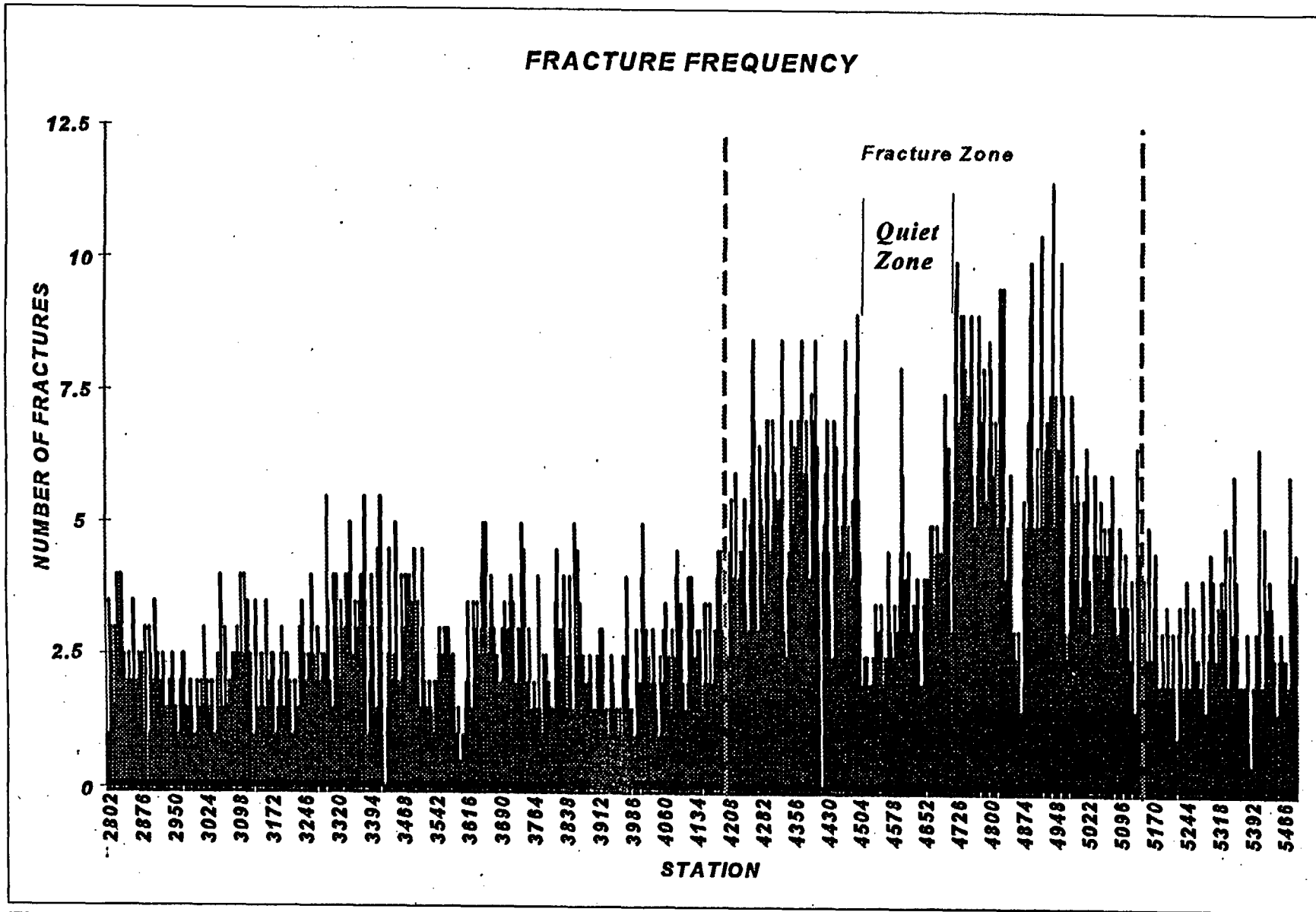


Figure 20. Fracture-density histogram of Main Drift and Fracture Zone

FRACTURE ZONE FROM STATION 42+00 TO 51+50 FRACTURE DENSITY

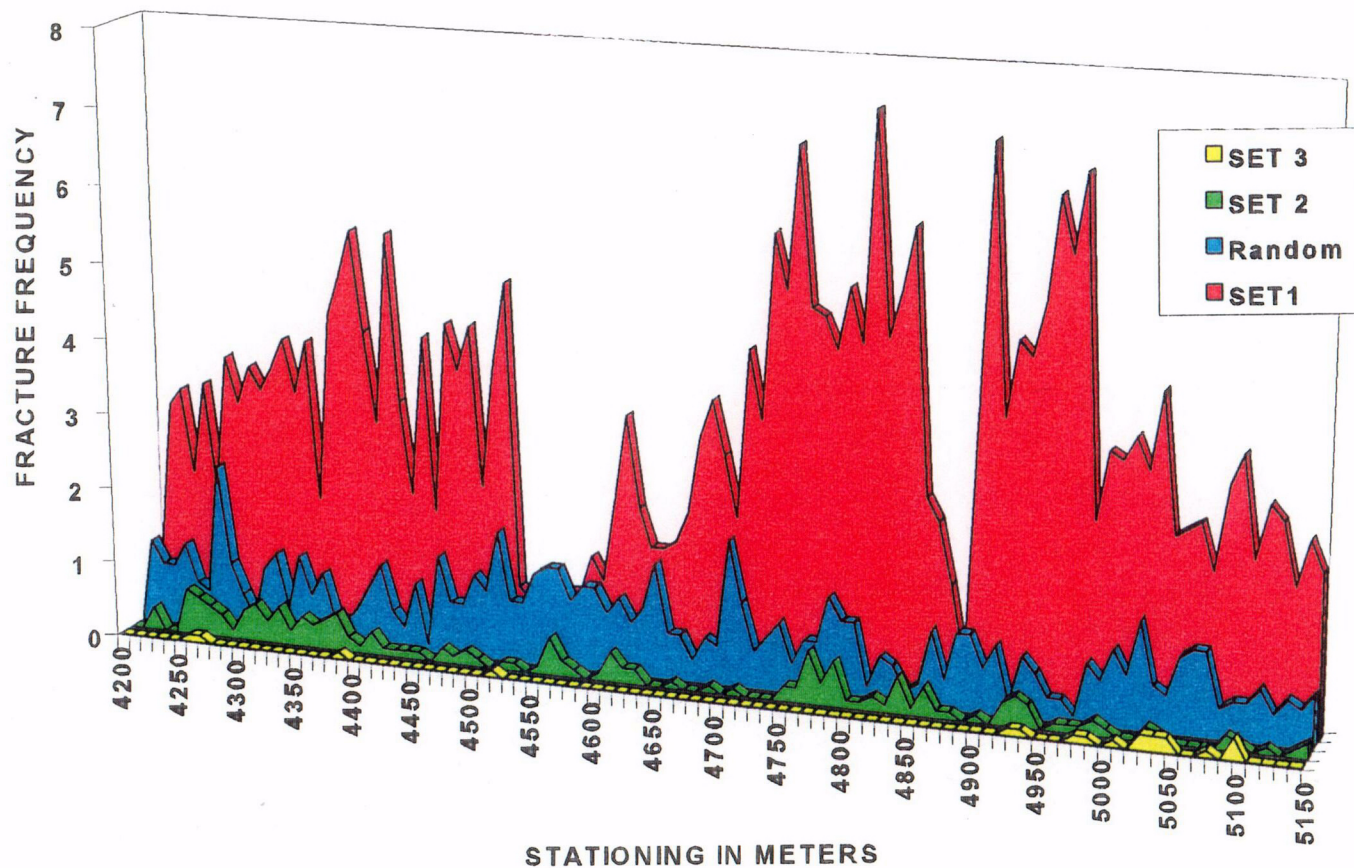


Figure 21. Fracture-density histogram showing fractures/meter, averaged over 10-meter intervals, of Sets 1, 2, 3, and Random.

C-03

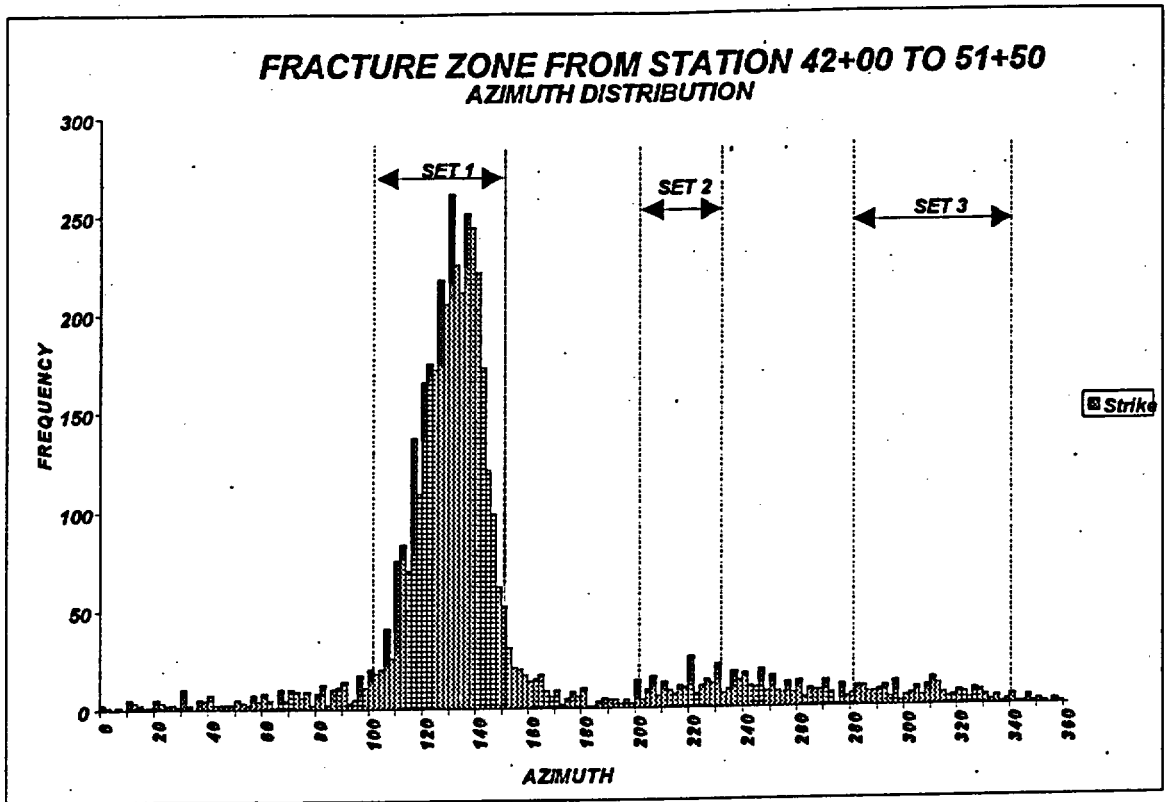


Figure 22. Azimuth-distribution histogram showing the fracture frequency for Set 1, 2, and 3 of the fracture zone.

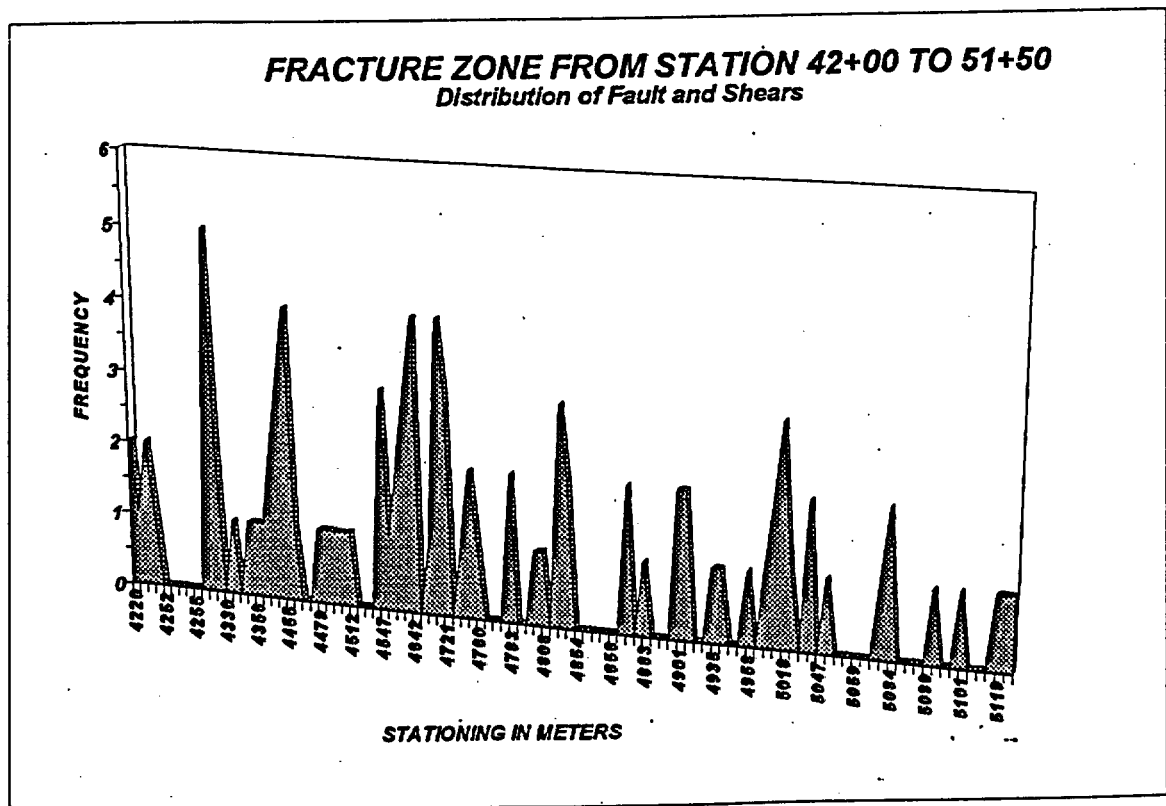


Figure 23 Histogram showing the frequency of faults and shears, in the Fracture Zone, plotted against stationing.

not occur (Photo 13). This geometry causes the crown of the tunnel to appear relatively unfractured. Close examination, however, reveals the crown to be just as intensely fractured as the walls.

The fracture-density histogram (Fig. 20) shows the fracture zone is made up of three subzones, two zones of intense fracturing separated by a quiet zone. The first subzone of intense fracturing, Sta. 42+00 to 45+30, has a very strong concentration of Set 1 fractures oriented between 110° and 135° , with the peak at 120° . The average fracture density for fractures of all orientations in this subzone is 4.8 per meter. The second subzone is a quiet zone between Sta. 45+30 and 46+55, with a fracture distribution very similar to that of the first subzone but with a fracture density similar to that outside the fracture zone, 2.9 fractures per meter. In the third subzone, between Sta. 46+55 and 51+50, the peak orientation of Set 1 fractures rotates clockwise approximately 20° . Set 1 is clustered between 120° and 150° with the peak at 138° . The fracture density for all fractures in this subzone is 5.1 per meter. The fracture-density histogram (Fig. 20) also shows a short zone of apparent lower fracture density within the third subzone between Sta. 48+55 and 48+80. This is not a quiet zone but an intensely fractured zone with 10 Set 2 shears. Because of the intense fracturing and shearing, the trace lengths of most fractures are below the 1-m minimum DLS criterion, and not recorded, resulting in the apparent lower fracture density.

Set 1 is the dominant fracture set throughout the fracture zone and is oriented 100° to 150° and dips from 70° to 90° . These fractures are smooth (R5) and tight with manganese oxide coatings and some vapor-phase mineralization. The fractures in this set are closely spaced, averaging 17 cm (all spacing measurements have been corrected to true spacing calculated from the DLS spacing). Fracture densities on Set 1 fractures have been recorded as high as 19 per meter. Fracture continuity in this set ranges from 1 m (minimum cut-off length) to more than 20 m. The average length of fractures in this set is 2.42 m.

Set 2 fractures in the fracture zone are oriented 200° to 230° , averaging 217° , and dip from 70° to 90° , averaging 82° . Fracture infilling in this set consists predominately of a combination of

calcite and silica which has a white, powdery appearance and effervesces with difficulty when exposed to dilute HCl. The fractures in this set are widely spaced, averaging 4.86 m apart. Fracture densities for this set are less than 1 per meter. Fracture continuity in this set ranges from 1 to 11.5 m. The average length of fractures in this set is 2.50 m.

Set 3 fractures in the fracture zone are oriented 280° to 340° , averaging 322° , and dip less than 40° , averaging 20° . Almost all these fractures occur beyond Sta. 50+00. Fracture infilling is dominantly vapor-phase mineralization, thin coatings primarily consisting of silica polymorphs. The very low-angle fractures in this set include vapor-phase partings, cooling joints, and fractures. The vapor-phase partings define a foliation in the rock which is more or less parallel to lithostratigraphic layering. These low-angle cooling joints may result from stresses related to contraction of the cooling volcanic sheet. These fractures, rare in most of the fracture zone, are more common between approximately Sta. 50+00 and 51+00 where average spacing is 6 m. Fracture continuity in this set ranges from 1 to 6.5 m. The average fracture length in this set is 2.39 m.

The random set contains 791 fractures that are outside the defined limits of the other three sets.

Faults and Shears in the Fracture Zone

The fracture zone contains 107 faults and shears with an average spacing of 8.65 m (Fig. 23). Offsets of Set 1 faults and shears is mixed with a slight majority of reverse offsets. Offsets on Set 2 faults and shears are consistently left-lateral with a few normal offsets. Only 6.5 percent of the faults and shears have offset greater than 0.10 m. For a further discussion of the faults in the fracture zone see the discussion of the Third Domain, p.56.

There are no major faults in the fracture zone. One hypothesis for this apparent lack of structural movement is that there is simply very little offset across this zone. Another hypothesis is that movement occurs as micro-movement on a multitude of the Set 1 fractures. If micro-movement has occurred on these fractures, determining the sense of offset would be important, specifically

whether micro offsets are similar to the mixed offsets recorded on Set 1 faults and shears in the fracture zone. A greater understanding of the fracture zone's extent, structure, and origin can be obtained with further study. A program of detailed, microscopic thin section-work would be required to explore this hypothesis.

Origin of the Fracture Zone

The two likely hypotheses for the origin of this zone are tectonic and/or cooling of the ash-flow sheet. Evidence points to a combination of tectonic and genetic origin. One possible explanation for the strata-bound nature of the zone is that the Tptpmn is brittle, while the lithophysal zones above and below are mechanically much different. The Tptpul generally contains 10 to 30 percent lithophysae and locally up to 40 percent (Barr and others, p. 60, 1996). The Tptpll exposed in the Main Drift contains 15 to 20 percent lithophysae. Lithophysae are elliptical to irregular and generally from 4- to 50-cm long. In addition to the lithophysae, other expressions of vapor-phase alteration are spots, stringers, and vapor-phase partings which result in the lithophysal zones being mechanically much weaker than the nonlithophysal zones. The difference in mechanical characteristics is demonstrated by the fracture characteristics of the two units. Fracturing in the lithophysal zones is largely controlled by the lithophysae and the other discontinuities which inhibit the formation of continuous fractures. Fractures that extend from the Tptpmn into the Tptpul typically splay and dissipate into broad zones of fracturing that die out a few meters into the Tptpul. The lithophysal zones accommodate stress by internal deformation, through the crumbling and rotation of the matrix between lithophysae.

The only information on the western extent of the fracture zone is from drill hole SD-12. Alcove 7 (Sta. 50+64) is being excavated through the Ghost Dance fault, into the footwall of the fault. The geology of Alcove 7 will be reported in a subsequent report. Based on what is known about the fracture zone at this time, it appears that the fracture zone may result from the combined cooling stresses in the ash-flow sheet and tectonic stresses. The orientation of Set 1 fracturing in the fracture zone is perpendicular to what is thought to have been the least principal compressive stress (σ_3) in the regional stress regime at the time of deposition (Minor, 1995).

Certainly, if the origin of this zone were entirely due to regional tectonics, it would likely be seen in other densely welded units. But the Main Drift and drill hole SD-12 are the only places where the fracture zone has been observed.

Age relations

In some instances a Set 3 shear has offset both cooling joints with vapor-phase mineralization and fractures with no coatings. In these areas, the cooling joints have greater offset than the uncoated fractures. Many examples are present in the Main Drift of Set 3 faults and shears being offset by Sets 1 and 2 faults. One good example is at Sta. 39+30 where two Set 3 shears are offset by a Set 2 fault oriented 037°/86°.

Summation

Moderately dipping shears with orientations averaging 300°/30° are largely reactivated cooling joints. These faults and shears are found only between Sta. 28+00 and 42+60, where they are relatively common. The faults and shears invariably have reverse offset, top (hanging wall) to the south. Although there are similarly oriented fractures and cooling joints between approximately Sta. 50+00 and the end of the Main Drift, none are shears. The presence of these shears indicates that the Tptpmn in the First and Second Domains experienced compressional stress oriented generally in a north northeast-south southwest direction. Compressional stress with this orientation is contrary to what the regional paleo-stress regime is thought to have been (Minor, 1995).

The proximity of the Ghost Dance fault to the Main Drift suggests a relationship between movement on the fault and features in the tunnel. Figure 24 shows the ESF and its more prominent geologic features in relation to the Ghost Dance fault as mapped on the surface of Yucca Mountain by Day and others (1996). Figure 24 also contains a graph of the normal offset on the Ghost Dance fault. The fault has minimal offset in the area of the boundary between the First and Second Domains. Offset increases in either direction from that point. Compressional

Exploratory Studies Facility Yucca Mountain Project

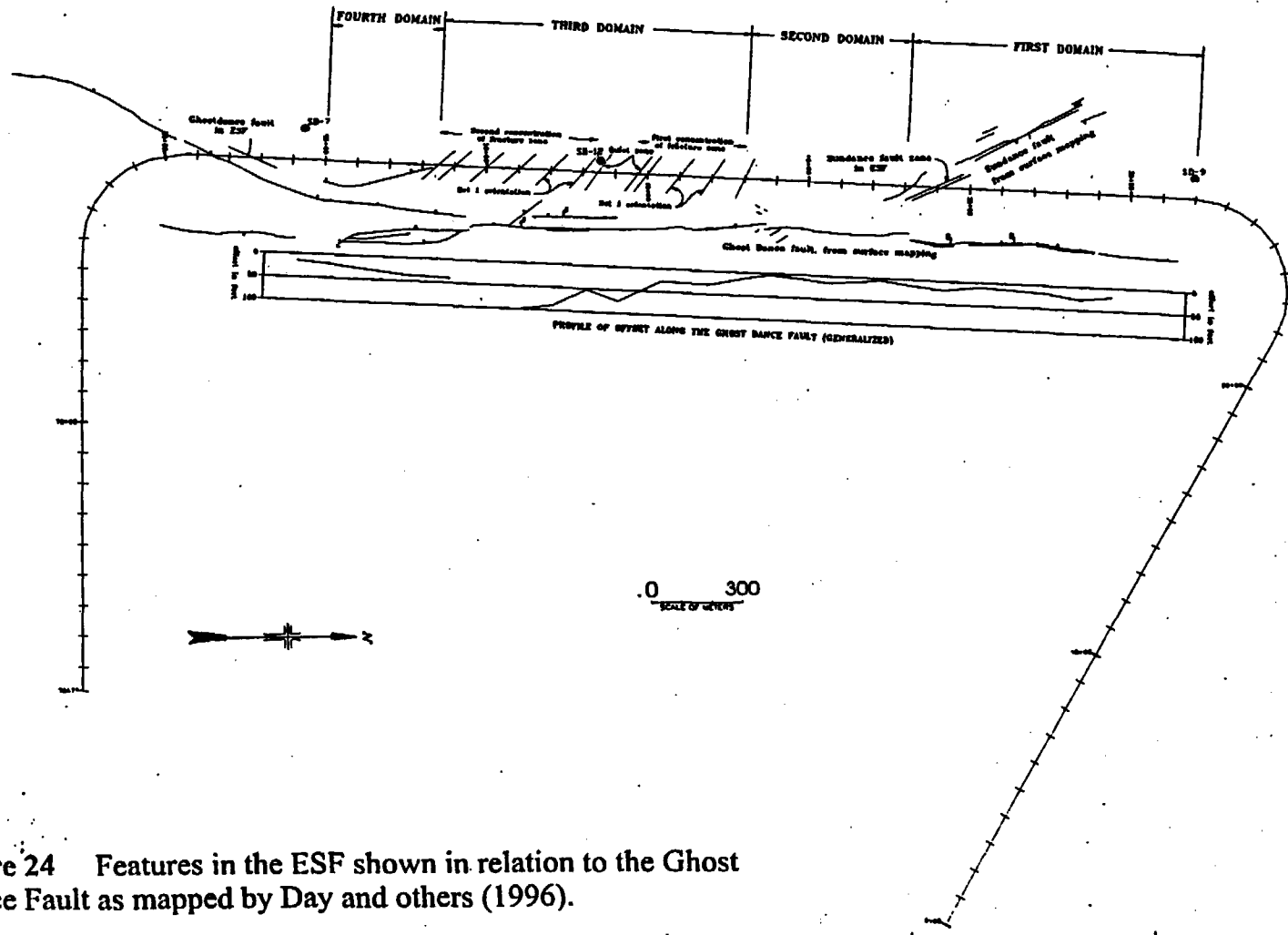


Figure 24 Features in the ESF shown in relation to the Ghost Dance Fault as mapped by Day and others (1996).

stress could have resulted, locally, from flexure in the hanging wall (west side) of the fault.

The pattern of fracturing and faulting in the Main Drift, and in particular, the fracture zone may also be related to the Ghost Dance fault. The fracture zone occurs adjacent to the section of the fault with the greatest offset. And the orientation of Set 1 fractures, $\pm 120^\circ$, is approximately 60° from the orientation of the Ghost Dance fault, $\pm 180^\circ$. This angular relationship is consistent with the formation of Set 1 as tensile fractures resulting from possible left-lateral movement on the Ghost Dance fault (Ramsey and Huber, 1983)(Suppe, 1985).

The pattern of fracturing, shearing, and faulting observed in the Main Drift is consistent with the pattern seen along the Ghost Dance fault, which in turn is also seen in the faulting and rotation of blocks in Yucca Mountain. The most persistent sense of offset in the Main Drift is the left-lateral offset of Set 2 faults and shears. This pattern of offset is consistent with the clockwise rotation visible in aerial photos of Yucca Mountain (photo 14). Large blocks on the flanks of the mountain show increasing offset to the south. And, toward the southern end of the mountain, large blocks have been noticeably rotated to the right (clockwise)(Rosenbaum, and others, 1991; Hudson, and Sawyer, 1994).

Comparative Cross Section

The Comparative Geology Cross Section Along The Main Drift was developed by the underground mapping team from the as-built geology mapped in the Main Drift (Drawing OA-46-291). The as-built cross section was compared to the pre-construction cross section, Stratigraphic Cross Section Along the ESF Main Drift, assembled by Agapito and Associates (Kicker and others, 1995). The pre-construction cross section is largely based on three drill holes along the alignment of the Main Drift. Drill hole USW SD-9 is projected 71.0 m east to Sta. 28+20, USW SD-12 is projected 39.4 m east to Sta. 46+50, and USW SD-7 is projected 102.6 m east to Sta. 55+70. The stratigraphic unit predicted through the Main Drift is the Tptpmn. Structure predicted in the Main Drift consists of the Sundance fault zone at approximately Sta. 36+35 and the Abandoned Wash fault at Sta. 57+20. Note: subsequent mapping (Day and others,

1996) has identified this fault crossing the Main Drift at approximately Sta. 57+20 as the Ghost Dance fault.

The stratigraphy of the as-built cross section is Tptpmn with small exposures of the underlying Topopah Spring Tuff, lower lithophysal zone (Tptpll) exposed along the invert from Sta. 53+00 to 55+00. The Sundance fault zone was encountered at Sta. 35+94, within 50 m of the pre-construction cross section prediction. The general orientation of the zone is 155°/84°. Both ESF and surface mapping suggest that the Sundance fault zone is not a single, continuous plane. The Sundance fault zone, is described on the cross section, as a 10-m-wide zone of short, discontinuous, 3- to 4-m-long faults and shears. The pre-construction cross section and the as-built cross sections agree very closely. The as-built cross-section also shows the location of the Northern Ghost Dance Fault Alcove (Alcove #6) at Sta. 37+37.

STATISTICAL ANALYSIS

Statistical analysis of the DLS data was conducted to identify relationships between the location, orientation, and characteristics of the discontinuities in the Main Drift. Cluster analysis was applied to the orientation data to identify statistically significant clusters (fracture sets). Multivariate statistical analysis was performed on those DLS characteristics judged to be continuous variables to identify diagnostic structural heterogeneities.

Cluster Analysis

Cluster analysis was performed with the use of the computer program Clustran, a commercially available software package. Clustran mathematically groups the orientation data into clusters. The clusters thus derived are free of the subjective judgment or bias that may be present in other means of analysis. The clusters identified by statistical analysis were compared to clusters identified by other means. The comparison helped substantiate relationships and identify relationships that might otherwise have been overlooked. The Clustran program can analyze a maximum of 2000 entries. Because of the size of the data set (7681 entries with greater than 1 m trace length), separating the data into smaller groups for analysis was necessary. Structural features in the Main Drift were considered when the smaller data groups were formed. All discontinuities recorded in the DLS were included in this analysis; therefore, the sets do not distinguish among fractures, shears, faults, cooling joints, or vapor-phase partings.

Fractures oriented parallel or subparallel to the tunnel alignment will tend to be poorly represented in the DLS record. For the purposes of this cluster analysis, the azimuth range affected by this "blind zone" was chosen to be 20 degrees, 10 degrees on either side of the axis of the Main Drift. On the stereonet pole plots, the "blind zone" is the region perpendicular to the axis of the Main Drift, because a pole is perpendicular to the plane it represents. This "blind zone" is shown between two lines on drawings OA-46-296 to 299. The "blind zone" is intended only as a range of influence, and not to precisely quantify that range.

Clustran initially tests the orientation data for randomness by the chi-square test, Poisson analysis, and log likelihood ratio test for quality of fit. Data from the ESF are found to be nonrandom. This nonrandomness is expected because the poles plotted show clusters, not a uniform scatter. Thus, the data can be analyzed for clusters, outlying data removed and statistically significant clusters selected.

The user specifies different clustering radii for the algorithm that result in identifying clusters using an "objective function" that is minimized at the "best" radius. Statistical fits made by Clustran to the extracted clusters of data include their means and confidence intervals. Clustran allows the user to write the clusters into new data files, which may be used for further analysis (Gillett, 1987).

Cluster analysis provides a statistical approach to resolving sets, but cannot apply a knowledge of geological concepts. Sets derived from cluster analysis must then be viewed in terms of geological relevance. If sets derived by using the "best radius" as determined by the minimized "objective function" are not geologically significant, it may be necessary to choose the next higher "minimized function" and its corresponding radius. In the cluster analysis completed for this report, it was sometimes necessary to select the next higher "objective function" to produce meaningful sets.

Domain Selection

The Main Drift is divided into four domains based on structural characteristics. The domains were identified and their boundaries refined by the use of a variety of analytical methods including cluster analysis. The First Domain (Sta. 28+00 to 37+00) is distinguished by northwest-striking, intermediate-dipping (approximately 35° to 65°) fractures (Set 4). These fractures are relatively abundant before Sta. 37+00, but, nearly totally absent beyond that point (Drawing OA-46-295). The First Domain is also characterized by a more even distribution of orientations than seen in the other domains. The Second Domain is the interval between Sta. 37+00 and the beginning of the fracture zone at Sta. 42+00. The Second Domain is characterized by well defined clusters and a

strong concentration of Set 1 orientations. The Third Domain is the fracture zone from Sta. 42+00 to 51+50. The Third Domain is characterized by a dramatic increase in fracture density. The Fourth Domain, between Sta. 51+50 and 55+00, is the interval between the fracture zone and the end of the Main Drift. The Fourth Domain is characterized by well defined clusters in Sets 1 and 2 and fracture densities near those of the First and Second Domains.

Analysis

Variations in the Main Drift DLS data were evaluated by analyzing data subsets containing numbers of entries suited to Clustran's capabilities (2000 entries maximum). The DLS data in each domain was divided into subsets containing 300 to 500 fractures and analyzed separately in Clustran. The subsets of data presented below were chosen because the cluster analysis on each of these subsets produced consistently similar cluster characteristics as that of the domain it represents. The analysis includes all discontinuities; fractures, cooling joints, vapor-phase partings, faults, and shears. The term "fracture" as used in this section includes all discontinuities.

The First Domain, Sta. 28+00 to 37+00

The First Domain, Sta. 28+00 to 37+00, has 1751 DLS discontinuities. Drawing OA-46-296 shows a representative subset of this domain from Sta. 28+00 to 31+00, containing 486 entries. Clustran identified four sets of fractures within this subset. Sampled areas within the First Domain consistently produced the same four sets when analyzed with Clustran.

Within this subset of data, a peak in fracture density is centering on an orientation of $114^{\circ}/83^{\circ}$, Set 1, with 348 of the 486 total number of fractures falling into this data subset. Throughout the First Domain, no appreciable change is noted in the orientation of the peak fracture density. The azimuths range from 069° to 185° , and the dips range from 65° to 90° in the southwest dipping fractures and 37° to 90° in the northeast dipping fractures.

Set 2 contains 69 fractures centering on an orientation of $215^{\circ}/88^{\circ}$. Azimuths range from 191° to 250° , and the dips range from 65° to 90° .

Set 3 contains 35 fractures centering on an orientation of $325^{\circ}/13^{\circ}$. Set 3 azimuths vary widely because a cluster of shallow-dipping fractures, plotting near the center of the stereonet, will include a wider range of azimuths than the same size cluster of steep-dipping fractures. The dips range from 3° to 56° . This set contains discontinuities mapped as low-angle vapor-phase partings, fractures, and cooling joints generally subparallel to the foliation.

Set 4 contains 34 fractures centering on an orientation of $293^{\circ}/49^{\circ}$. Azimuths range from 247° to 323° , and the dips range from 34° to 61° . These intermediate-dipping fractures are found almost exclusively in the Tptpmn between Sta. 27+20 and approximately Sta. 37+00.

The Second Domain, Sta. 37+00 to 42+00

The Second Domain, Sta. 37+00 to 42+00, contains 961 DLS entries. Drawing OA-46-297 shows a representative subset of this domain from Sta. 37+00 to 39+00 that contains 407 fractures. Clustran identified three sets within this interval.

The peak fracture density is at an orientation of $125^{\circ}/84^{\circ}$, Set 1, with 262 of the 407 total number of fractures in this data subset. Throughout the Second Domain, is a minor amount of variation in the highest concentration strike and dip of this set, ranging from $118^{\circ}/84^{\circ}$ to $128^{\circ}/85^{\circ}$. The azimuths in the Sta. 37+00 to 39+00 subset range from 074° to 175° . The majority of the fractures have dips ranging from 58° to 90° , with only one fracture dipping as low as 44° .

Set 2 contains 86 fractures centering on an orientation of $216^{\circ}/87^{\circ}$. The azimuths range from 179° to 253° . The majority of the fractures have dips ranging from 65° to 89° , with two fractures dipping as low as 38° .

Set 3 contains 59 fractures centering on an orientation of $333^{\circ}/14^{\circ}$. Azimuths vary widely because this cluster plots near the pole of the stereonet. Most azimuths are between 285° and 360° , and the dips range from 3° to 47° . This set contains vapor-phase partings, fractures, and cooling joints generally subparallel to the foliation.

The Third Domain, Sta. 42+00 to 51+50

The Third Domain, Sta. 42+00 to 51+50, contains 4074 DLS entries. Drawing OA-46-298 shows the two subsets of data analyzed by Clustran. The first subset, from Sta. 42+00 to 43+00, contains 388 fractures. The second, from Sta. 49+00 to 50+00, contains 537 fractures. Clustran identified the same two sets of fractures in both subsets of data.

Sta. 42+00 to Sta. 43+00

The peak fracture density is at an orientation of $111^{\circ}/88^{\circ}$, Set 1. Clustran grouped 345 fractures into Set 1 out of the 388 total number of fractures in this data subset. The azimuths range from 068° to 175° . The majority of the fractures have dips ranging from 66° to 90° , with three fractures dipping from 15° to 33° . Set 2 contains 43 fractures centering on an orientation of $212^{\circ}/83^{\circ}$. The azimuths range from 182° to 245° , and the dips range from 65° to 89° . Not present in this interval are the northwest-striking, moderately dipping Set 3 fractures found in the First, Second, and Fourth Domains.

Abrupt and gradual variations in azimuth in the Main Drift are shown in drawing OA-46-295. A particularly good example is shown on the drawing between Sta. 45+00 and 46+50, in the Third Domain. These variations in azimuth were not detected in a cluster analysis.

Sta. 49+00 to Sta. 50+00

The peak-fracture density is at an orientation of $136^{\circ}/83^{\circ}$, Set 1. Of the 537 total number of

fractures in this data subset, Clustran grouped 506 fractures into Set 1. Most of the Set 1 azimuths in the Sta. 49+00 to Sta. 50+00 subset range from 107° to 157°, with 1 fracture at 082° and 2 fractures with azimuths up to 187°. Set 1 dips range from 65° to 90°, with six fractures dipping between 16° and 58°.

Set 2 contains 31 fractures centering on an orientation of 225°/85°. The azimuths range from 203° to 260°, and the dips range from 72° to 90°.

Only 3 Not present in the this interval are the northwest-striking, moderately dipping Set 3 fractures found in the First, Second, and Fourth Domains.

The Fourth Domain, Sta. 51+50 to 55+00

The Fourth Domain, Sta. 51+50 to 55+00, contains 895 discontinuities. Drawing OA-46-299 shows a representative subset of this domain between Sta. 51+50 and 52+50 containing 239 fractures. Clustran identified three sets of fractures within this subset. Sets 1, 2, and 3 correspond to the sets identified in the other domains with minor differences in peak orientations and ranges.

Set 1 continues to be the dominant set. The peak-fracture density, orientated 138°/82°, contains 172 fractures of the 239 total fractures in this interval. The azimuths of Set 1 fractures range from 085° to 169°, and the majority of the fractures have dips ranging from 66° to 90°, with 2 fractures dipping 52° or less.

Set 2 contains 54 fractures centering on an orientation of 223°/84°. The azimuths range from 190° to 260°. The majority of the fractures have dips ranging from 59° to 88°.

Set 3 contains 13 fractures centering on an orientation of 336°/07°. Most azimuths range from 171° to 360°. Azimuths for the entire set are in all directions because the cluster of these shallow dipping fractures includes the center of the stereonet. The dips range from 03° to 17°. This set

contains vapor-phase partings, fractures, and cooling joints subparallel to the foliation.

Results

Cluster analysis of the Main Drift DLS data has identified four sets. Sets 1 and 2 contain most of the fractures and have consistently appeared in all four domains. Set 3 contains fractures mapped as low-angle vapor-phase partings and other relatively low-angle fractures. The orientation of Set 3 is generally similar to the foliation of the Tptpmn in the Main Drift and does not appear in all the domains. Set 4 strikes similarly to Set 3 and has dips intermediate between Sets 1 and 3, 40° to 60°. Set 4 is restricted to the First Domain of the Main Drift.

Set 1 and Set 2

Set 1 is the predominant fracture set in the Main Drift. The concentration of fractures in this east-southeast-striking and steeply dipping set is shown on the various azimuth-distribution histograms (Figs. 25a - d). In the fracture zone (the Third Domain), Set 1 is clearly and strikingly the dominant fracture set as shown in the azimuth-distribution histogram as well as visually on the tunnel walls.

Set 2 is south-southwest-striking and steeply-dipping. The fracture-density histogram of Set 2 on drawings OA-46-296 to 299 shows that, although a numerically prominent set, the frequency of occurrence is significantly less than Set 1. Ratios between number of fractures in Sets 1

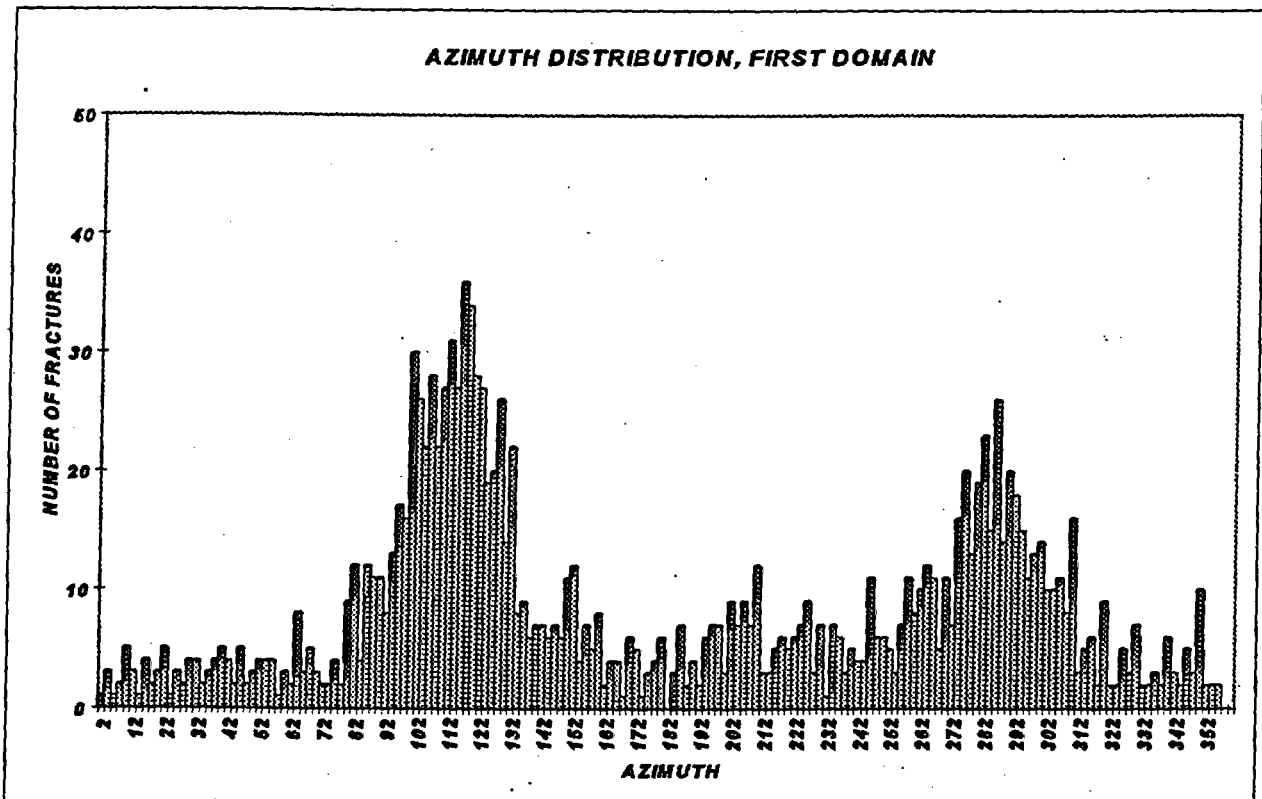


Figure 25 Azimuth distribution in the First Domain.

and 2 range from 3:1 to 6:1, and within the fracture zone the ratio can range up to 16:1. Cluster analysis has been run on subsets of data which include only Set 2 fractures. These subsets do not include any consistent or geologically meaningful smaller sets within Set 2.

The azimuth-range Clustran has identified as the boundary between Sets 1 and 2, as shown on stereonets from drawings OA-46-296 to 299, is within the "blind zone" region. A comparison was conducted to test whether the potential bias introduced by the "blind zone" actually resulted in an under-representation of fractures subparallel to the axis of the Main Drift, 183° , causing an artificial separation of the data by Clustran. The placement of the boundary between the two sets was examined by comparing the results of the cluster analysis of Main Drift data with that of data collected in adjacent areas. The data collected in adjacent areas provide samples of the Tptpmn collected along transects differing in orientation from that of the Main Drift. This data will tend to counter any bias introduced by the orientation of the tunnel.

The North Ramp between Sta. 27+20 and 28+00 exposes the Tptpmn. This portion of the North Ramp changes in orientation from 199° to 183° . Alcove 5, located at Sta. 28+27 and oriented 108° , also exposes Tptpmn. The Tptpmn data from Sta. 27+00 to 28+00 shows a peak orientation at $182^\circ/83^\circ$ (Fig. 26), within the "blind zone" in the Main Drift. Data from Alcove 5 displays a similar peak orientation (Fig. 27). Both of these data sets also have a peak orientation similar to Set 1, but no distinct set corresponding to Set 2, although there are fractures with Set 2 orientations. The comparison suggests that the data collected in the First Domain of the Main Drift may not be completely representative of the Tptpmn in that area; fractures oriented approximately 180° may be under-represented.

The Tptpmn is exposed in the South Ramp curve between Sta. 59+35 and 63+08, where the orientation of the tunnel changes from 183° to 113° . The Tptpmn is also exposed in Alcove 6, located at Sta. 37+37, and oriented 090° . Preliminary data from these locations do not have peak orientations within the "blind zone," although there are fractures present with orientations near 180° azimuth. The azimuth distribution in these sets of data supports the separation of Sets 1 and

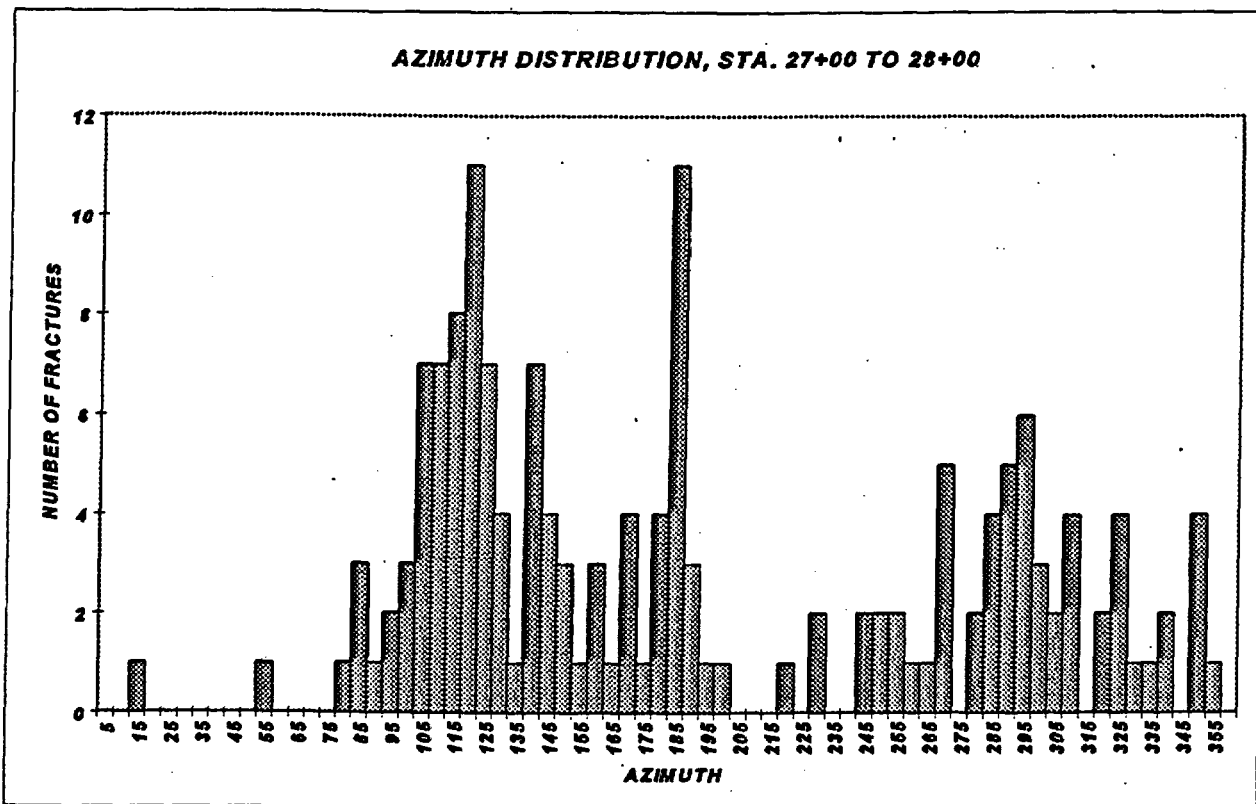


Figure 26. Distribution of azimuth in 5-degree intervals.

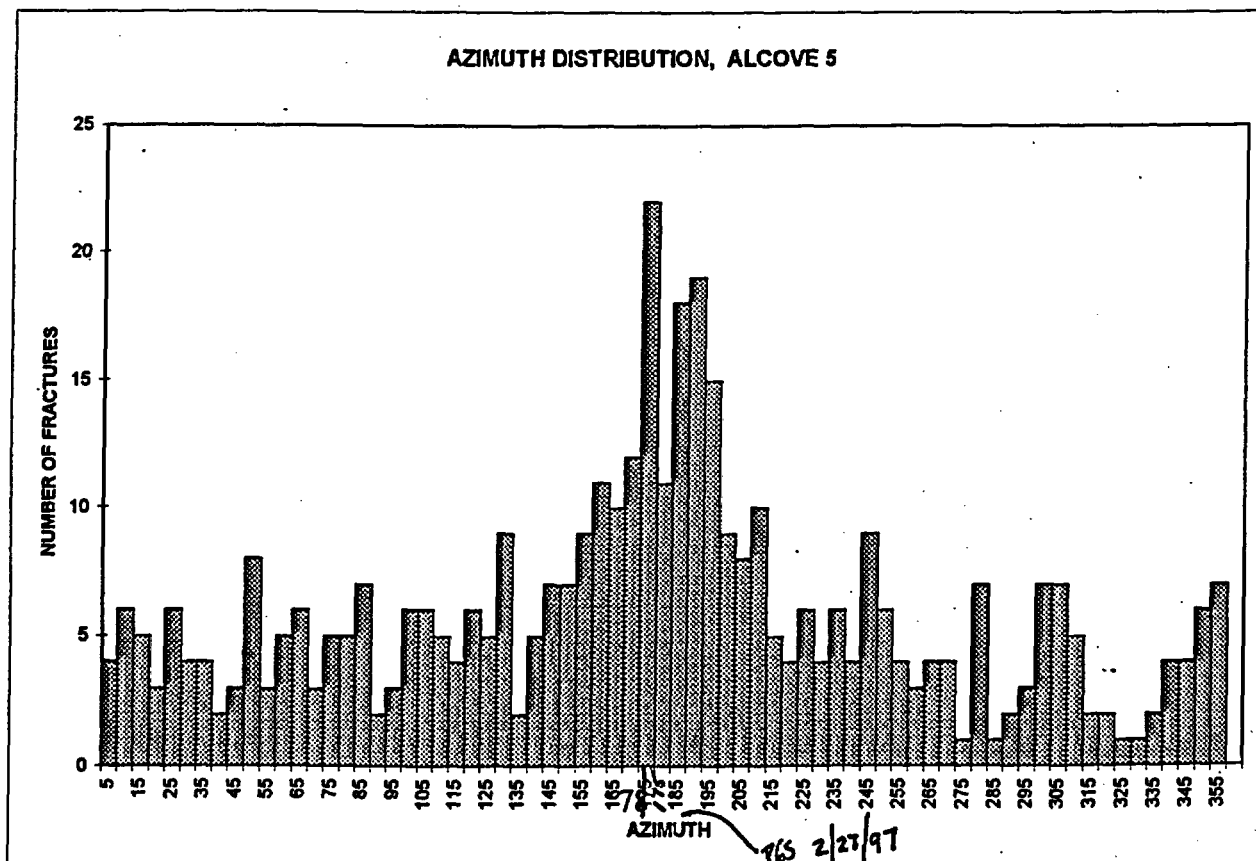


Figure 27. Distribution of azimuth in 5-degree intervals.

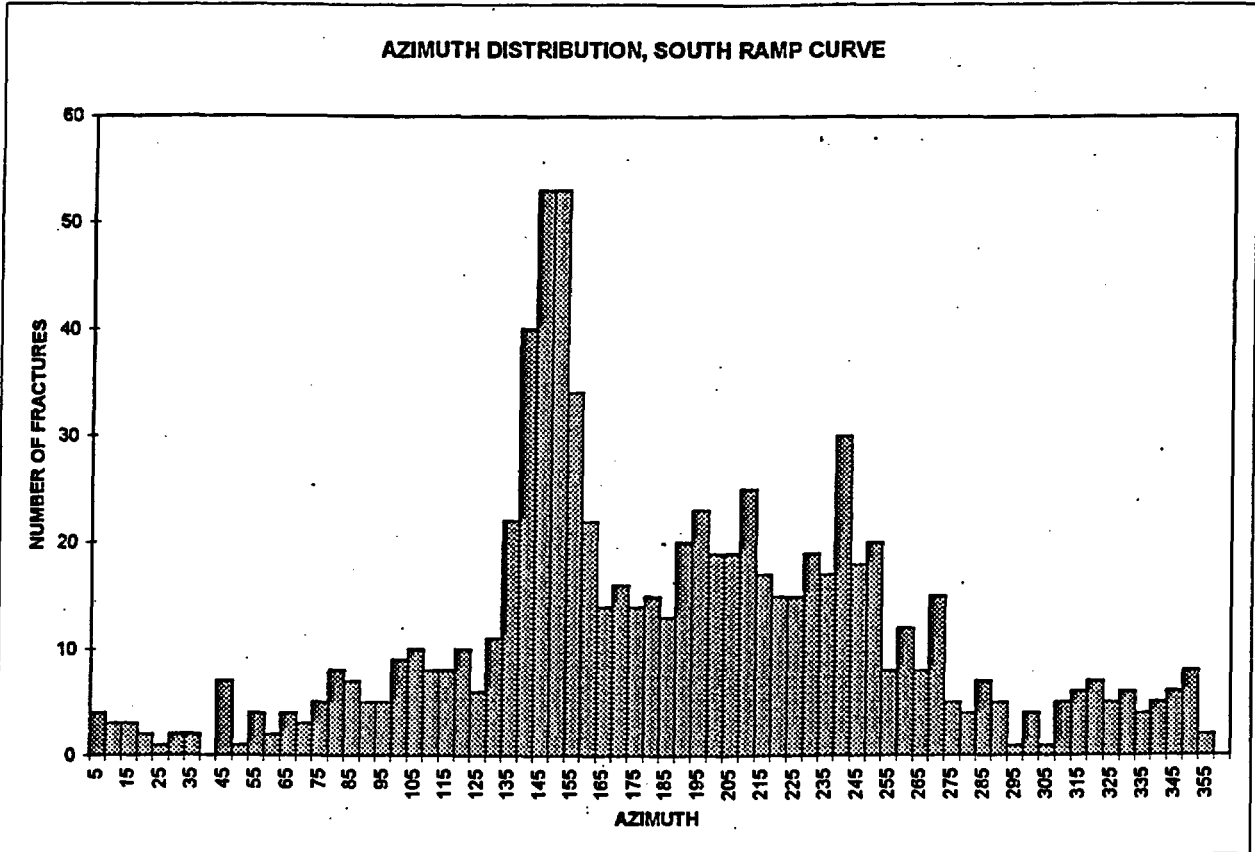


Figure 28. Distribution of azimuth in 5-degree intervals.

2 (Figs. 28, 29). However, the South Ramp data were collected east (in the footwall) of the Ghost Dance fault; thus a direct comparison of these data with data collected in the Main Drift may not be valid.

DLS data collected in units other than the Tptpmn within the North Ramp display a peak orientation at approximately 180° azimuth corresponding to the “blind zone” in the Main Drift, and a secondary peak orientation at approximately 215° to 220° azimuth, corresponding to Set 2. Set 1 first appears in abundance in the Topopah Spring crystal-poor, upper lithophysal zone (Tptpul), near its contact with the underlying Tptpmn and becomes a prominent set at the first occurrence of the Tptpmn in the ESF (Sta. 27+20).

Set 3

Set 3 contains discontinuities mapped as low-angle vapor-phase partings and fractures subparallel to the foliation of the Ttpmn. This set is present in the First, Second and Fourth Domains but is generally not present in most of the Third Domain. Only within the last 150 m of the fracture zone, from Sta. 50+00 to Sta. 51+50, are Set 3 fractures present. The absence of these low-angle fractures throughout most of the fracture zone is not attributed to the truncation of trace lengths by the intense fracturing within the fracture zone. These low-angle fractures also do not appear in the quiet zone within the fracture zone, from Sta. 45+30 to 46+55, where they would not be truncated if present. Set-3 fractures are mapped between 50+00 and 51+50 where fracturing is quite intense.

Set 4

Set 4 consists of northwest-striking, intermediate-dipping (40° to 60°) fractures. The first occurrence of this set, in the vicinity of the Main Drift, is in the North Ramp at Sta. 27+20, in the Ttpul, near the contact with the underlying Ttpmn. Fractures oriented similarly to Set 4 may

AZIMUTH DISTRIBUTION, ALCOVE 6

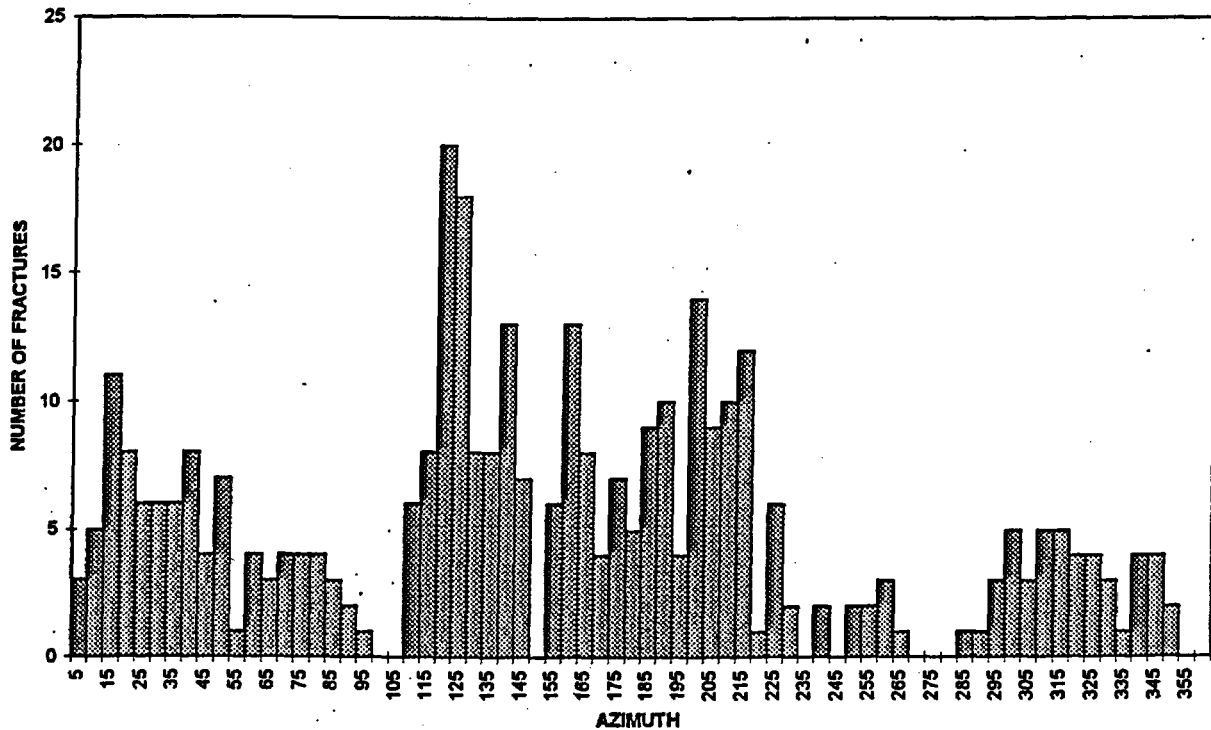


Figure 29. Distribution of azimuth in 5-degree intervals.

also be present in the Tiva Canyon crystal-poor, lower nonlithophysal zone (Tpcpln) exposed in the North Ramp (Barr and others, 1996). Virtually the last occurrence of a Set 4 fracture is at approximately Sta. 37+00, the end of the First Domain. Neither the DLS nor the FPGM record significant numbers of Set 4 fractures in Alcove 5; their absence may be due to intense fracturing and brecciation of the rock exposed in Alcove 5. Drawing OA-46-295 shows that intermediate-dipping fractures occur before Sta. 37+00, with only a few fractures of this orientation occurring after this station. Set 4 fractures are not found in preliminary data from Alcove 6 (Sta. 37+37) or the South Ramp. This absence suggests that Set 4, in the vicinity of the Main Drift, is restricted to either a zone in the upper portion of the middle nonlithophysal zone and the lowermost upper lithophysal zone, or is restricted laterally with the occurrence of these fractures not necessarily related to the lithology.

Multivariate Statistical Analysis

An r-mode, maximum-variance, principal component analysis (Harman, 1976; Jolliffe, 1986; Wackernagel, 1995; Dixon, 1995) was performed on 8061 DLS data entries collected from the Main Drift of the ESF between stations 28+00 and 55+00. These analyses were used primarily to identify diagnostic structural heterogeneities, based on DLS data, for the proposed repository horizon, Tptpmn. Descriptive statistical analysis was also performed to characterize the main drift section of the ESF as a whole.

Data Processing

Only continuous variables can be effectively analyzed by factor analysis. Since maximum aperture, minimum aperture, fracture length, total mineral-infilling thickness, and dip were judged to be continuous in distribution, these variables were selected for multivariate statistical analysis. The mineral-infilling thickness values were summed for each of the 8061 entries. For example, if a particular DLS measurement included recorded values of 1 mm of calcite, 1 mm of quartz, and 2 mm of fluorite, then an $m_{th}=4$ value was used for analysis (where m_{th} represents mineral-infilling thickness in mm). DLS records containing nonnumerical average-infilling-thickness values were not included in the multivariate analysis (for example, thick deposits of calcite, or thin quartz infilling). Since correlations between variables cannot be determined with statistical certainty with missing data values, DLS measurements without a complete set of results for each of the variables were not used for data analysis.

Descriptive Statistics

The descriptive statistical results based on 8061 DLS entries for the main drift are as follows:

Table 4 Descriptive Statistical Results

Variable Name	Mean	Distribution type	Standard Deviation
Dip	78.518	Log normal	15.703
Fracture Length (meters)	2.098	Log normal	4.292
Minimum Aperture (mm)	0.007	Exponential	0.218
Maximum Aperture (mm)	0.582	Log normal	2.824
Infilling thickness (mm)	1.324	Log normal	10.900

R-mode, maximum variance, principal component analysis results

The five DLS parameters analyzed include dip, fracture length, minimum aperture (a_{\min}), maximum aperture (a_{\max}), and mineral-infilling thickness (m_{th}). Factor-score results were also compared against strike measurements to identify any correlations. Squared multiple correlations (R^2) indicate that a_{\max} ($R^2=0.067$) is the most diagnostic DLS parameter, followed by m_{th} ($R^2=0.064$), fracture length ($R^2=0.037$), a_{\min} ($R^2=0.002$), and then dip ($R^2=0.002$).

Sorted rotated factor loadings for factor 1 are $SRFL_{m_{th}}=0.707$, $SRFL_{a_{\max}}=0.688$ and $SRFL_{fracture\ length}=0.600$, indicating that factor 1 scores are a function of m_{th} , followed by a_{\max} and then fracture length. Another way of stating this is that m_{th} , followed by a_{\max} and then fracture length are the most useful DLS parameters for characterizing the crystal-poor middle nonlithophysal zone (Tptpmn). Higher factor 1 scores correlate with more-infilled and/or wider and/or longer fractures, whereas lower factor 1 scores correlate with more sealed and/or short fractures.

Sorted rotated-factor loadings for factor 2 are $SRFL_{Dip}=0.775$ and $SRFL_{a_{\min}}=0.612$, indicating that factor 2 scores are a function of dip, followed by minimum aperture. Higher factor 2 scores correlate well with steeply dipping and/or open fractures, whereas lower factor 2 scores correlate

with more shallow-dipping and/or sealed fractures.

Factor score versus stationing plots, such as those shown in figures 30 through 37, were used to identify statistically significant heterogeneities based on the DLS measurements within the Tptpmn. As may be expected, most of the produced factor 1 and 2 plots are similar to those shown in figures 30 and 31, in that they show no significant changes in factor 1 and 2 scores with stationing. These factor results indicate that the "Tptpmn" is, with the below-listed exceptions, homogenous with respect to the measured DLS variables.

Structural heterogeneities within the Tptpmn as identified by factor 1 scores

The below listed observations, derived from detailed examinations of factor 1 score plots, are the most statistically significant structural heterogeneities identified for the main drift of the ESF. Figure 32 shows that from Sta. 33+80 to 35+00, a sub-zone can be identified where there are more fractures with thicker infilling and/or wider and/or longer fractures, when compared to the rock before Sta. 33+80, and after Sta. 35+00. These more infilled and/or wider and/or longer fractures correlate spatially with the vapor-phase alteration that occurs as greyish pink (5R8/2) to light grey (N8) from Sta. 33+80 to 35+00. Figure 33 shows that at approximately Sta. 41+40, a factor 1 score boundary can be drawn with some high factor 1 score fractures occurring before Sta. 41+40, and lower factor 1 scores after Sta. 41+40. This boundary, at about Sta. 41+40, correlates with the beginning of an intensely fractured zone extending from Sta. 41+40 to 52+70. Figure 34 shows that the section of rock exposed in the ESF located between Sta. 47+55 to 48+00 forms a distinct subzone characterized by a comparatively high number of wider and/or longer fractures with comparatively thick amounts of infilling. Interestingly, the area from Sta. 47+55 to 48+00 is also characterized by a rotation in strike orientations to higher values, and by a comparatively high fracture intensity. Although, the correlation between factor 1 scores, fracture intensity, and a steady rotation of strike orientations is statistically significant, the genetic and/or tectonic rationale for this correlation is unknown at this time and needs to be further examined. The last heterogeneity based on factor 1 scores is a boundary at Sta. 49+50, shown in figure 35, with sections of rock containing higher factor 1 scores forward of Sta. 49+50 to the end of the north

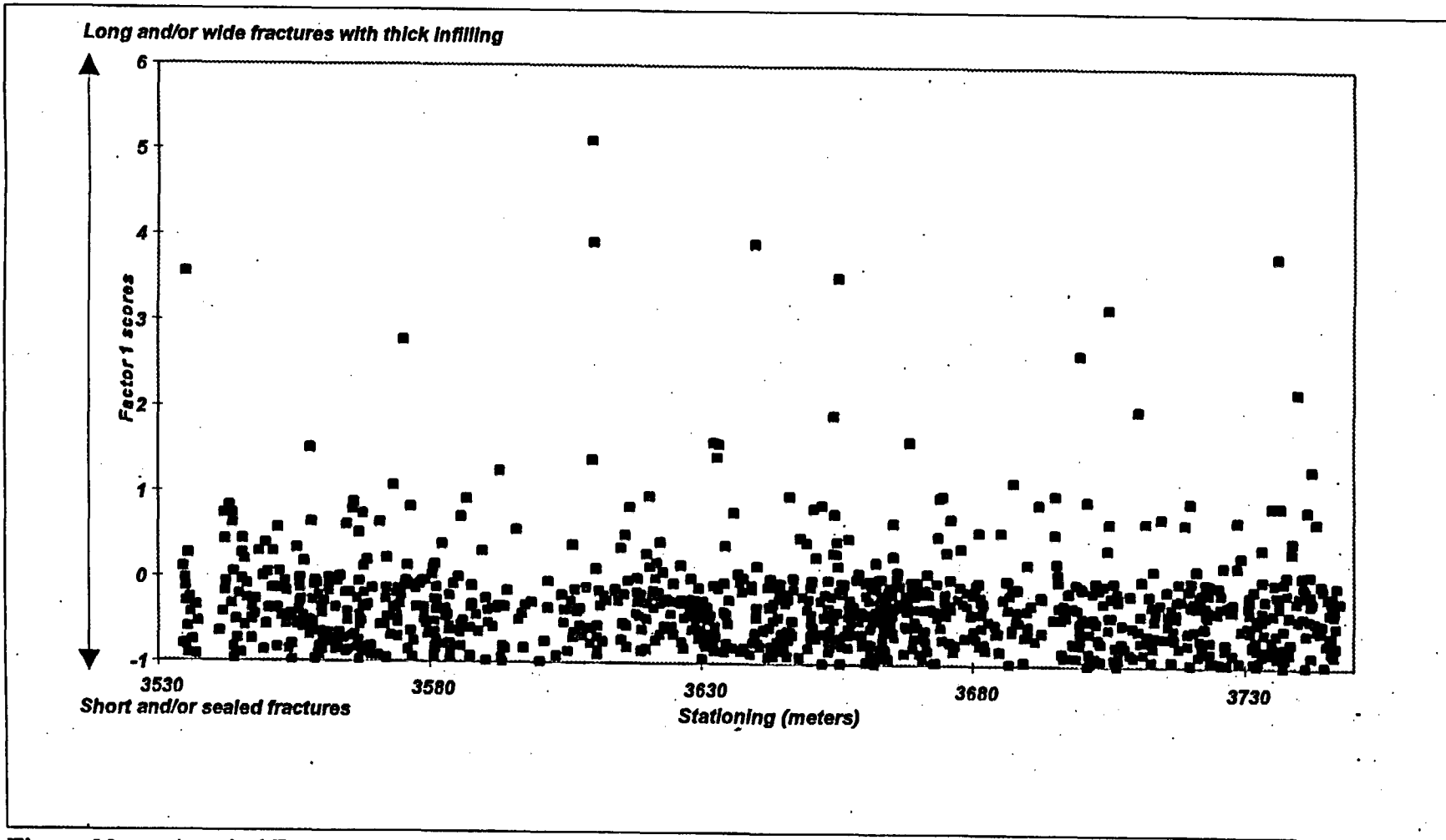


Figure 30 A typical Factor 1 score versus stationing plots showing the general homogeneity of the "Tptpmn".

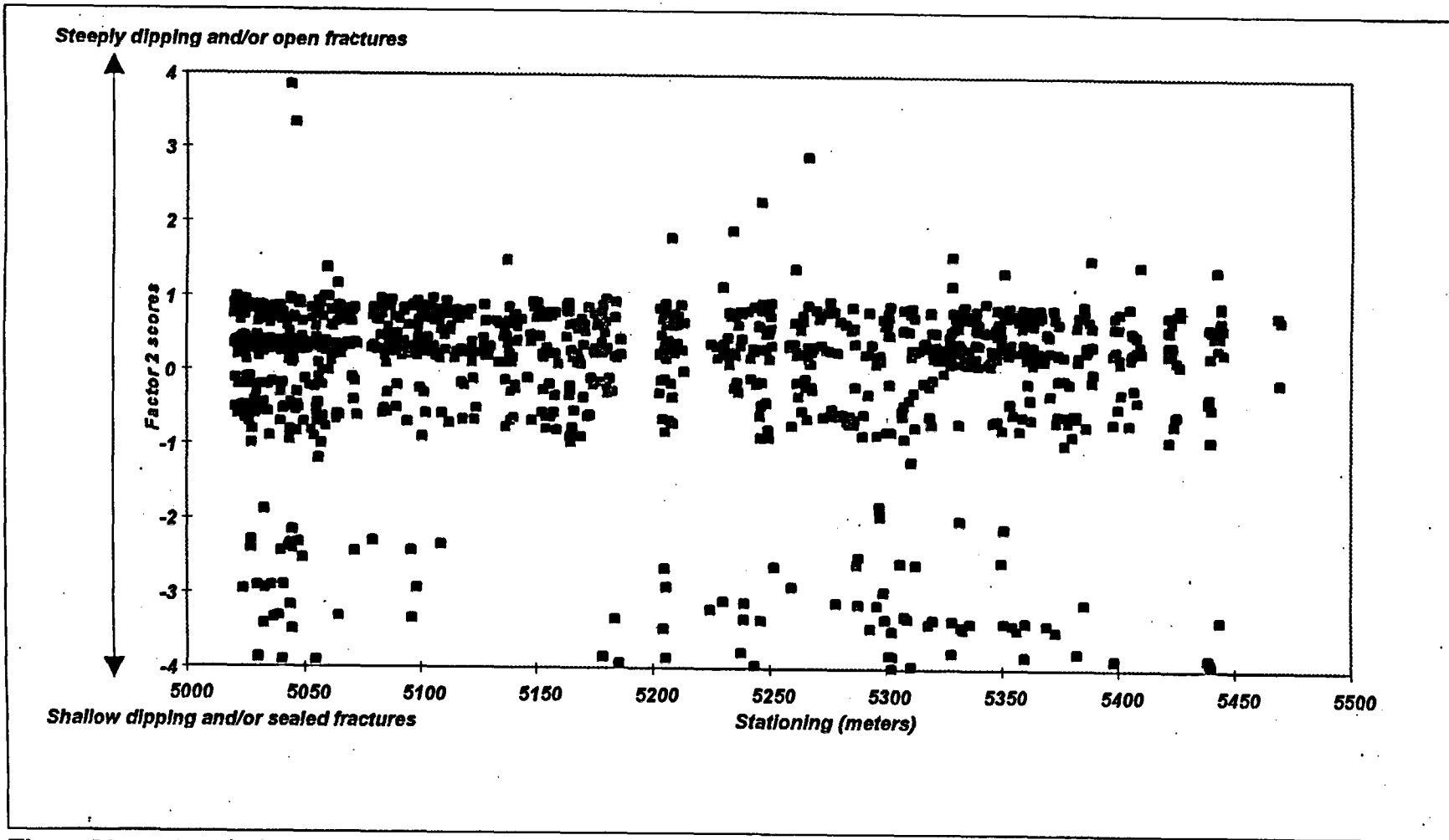


Figure 31 A typical Factor 2 score versus stationing plot showing the general homogeneity of the "Tptpmn".

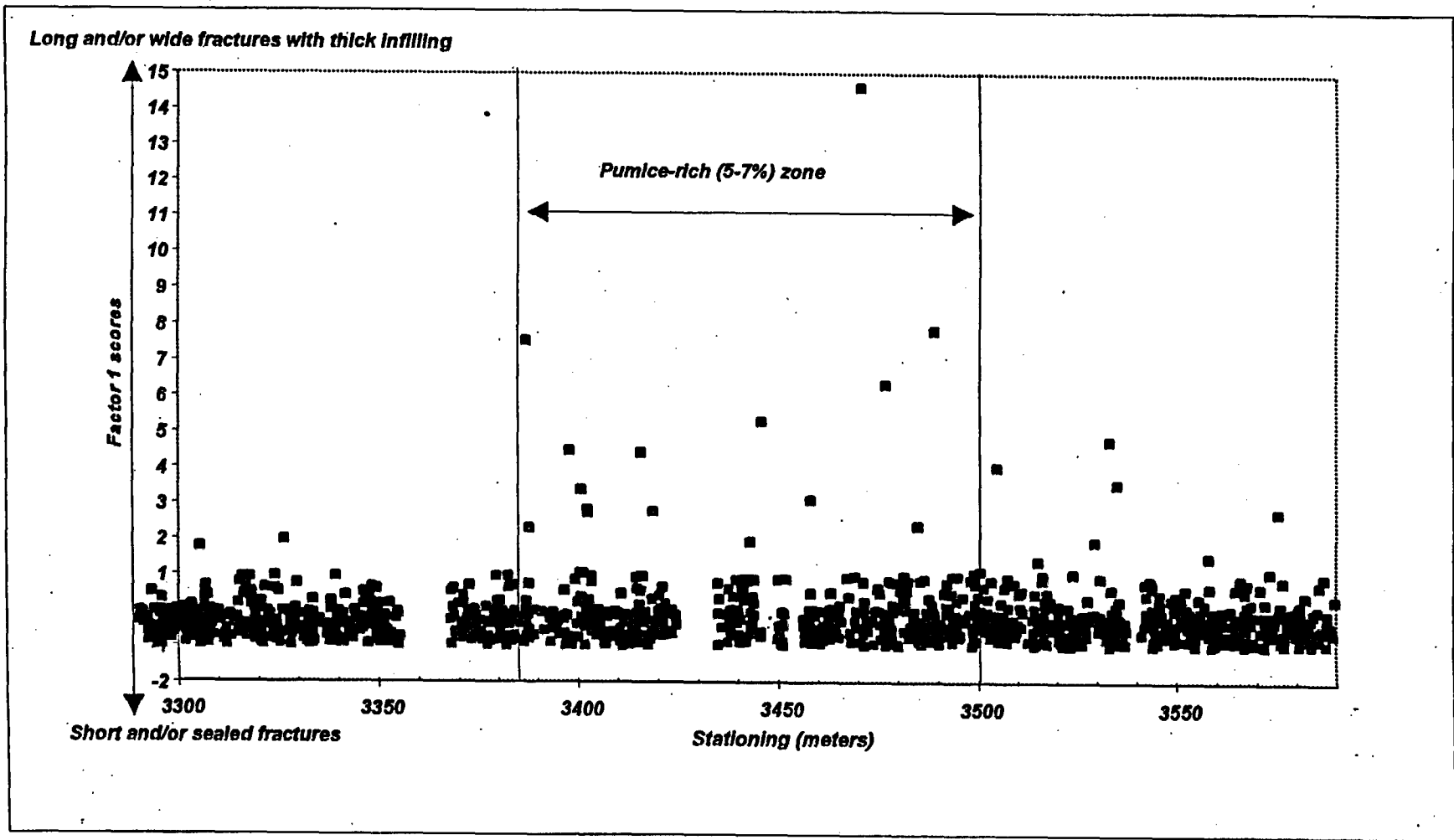


Figure 32 A pumice-rich subzone from 33+85 to 35+00 with higher than average Factor 1 scores.

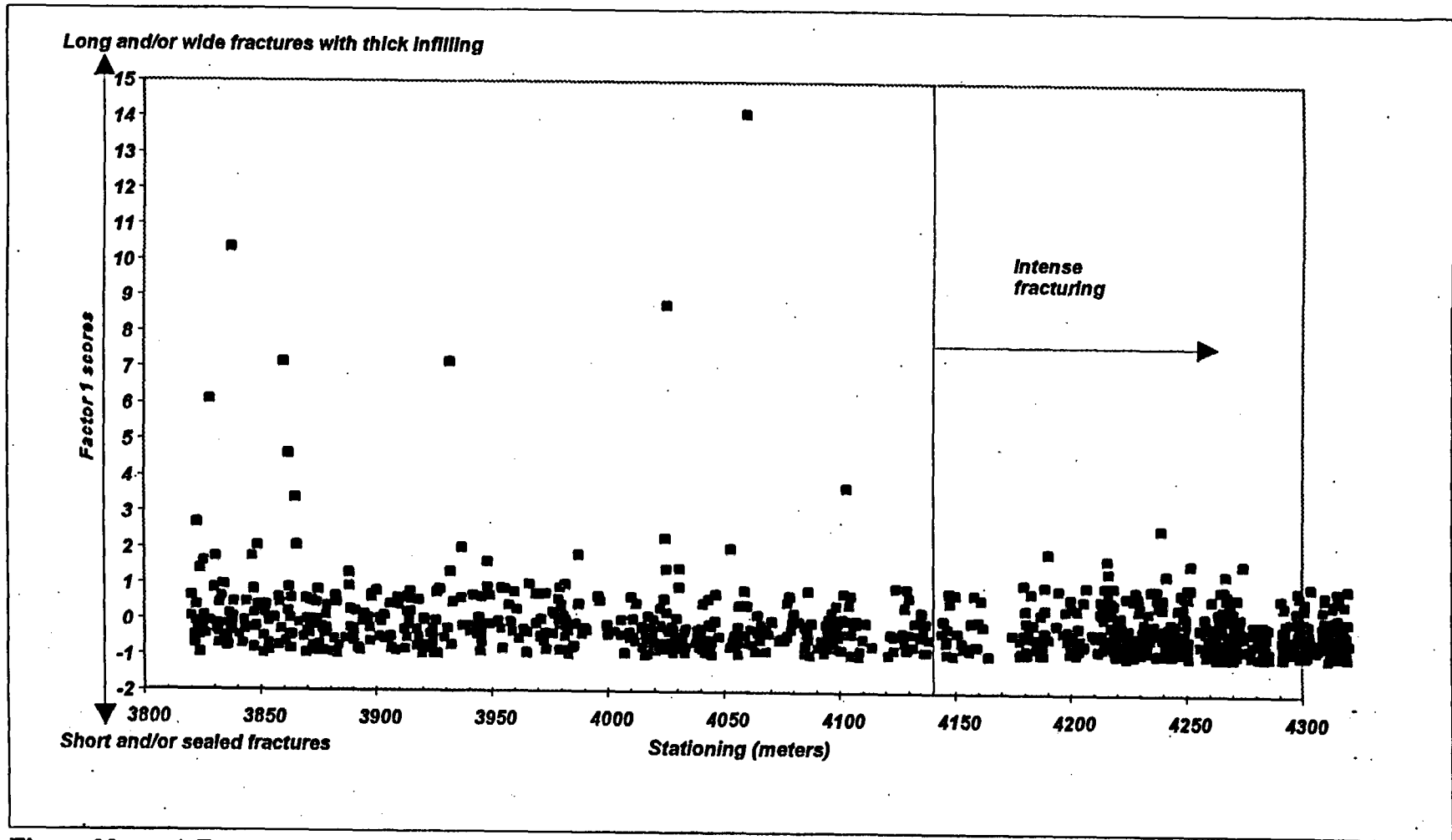


Figure 33 A Factor 1 score boundary at 41+40 which coincides with a boundary between less and more intense fracturing.

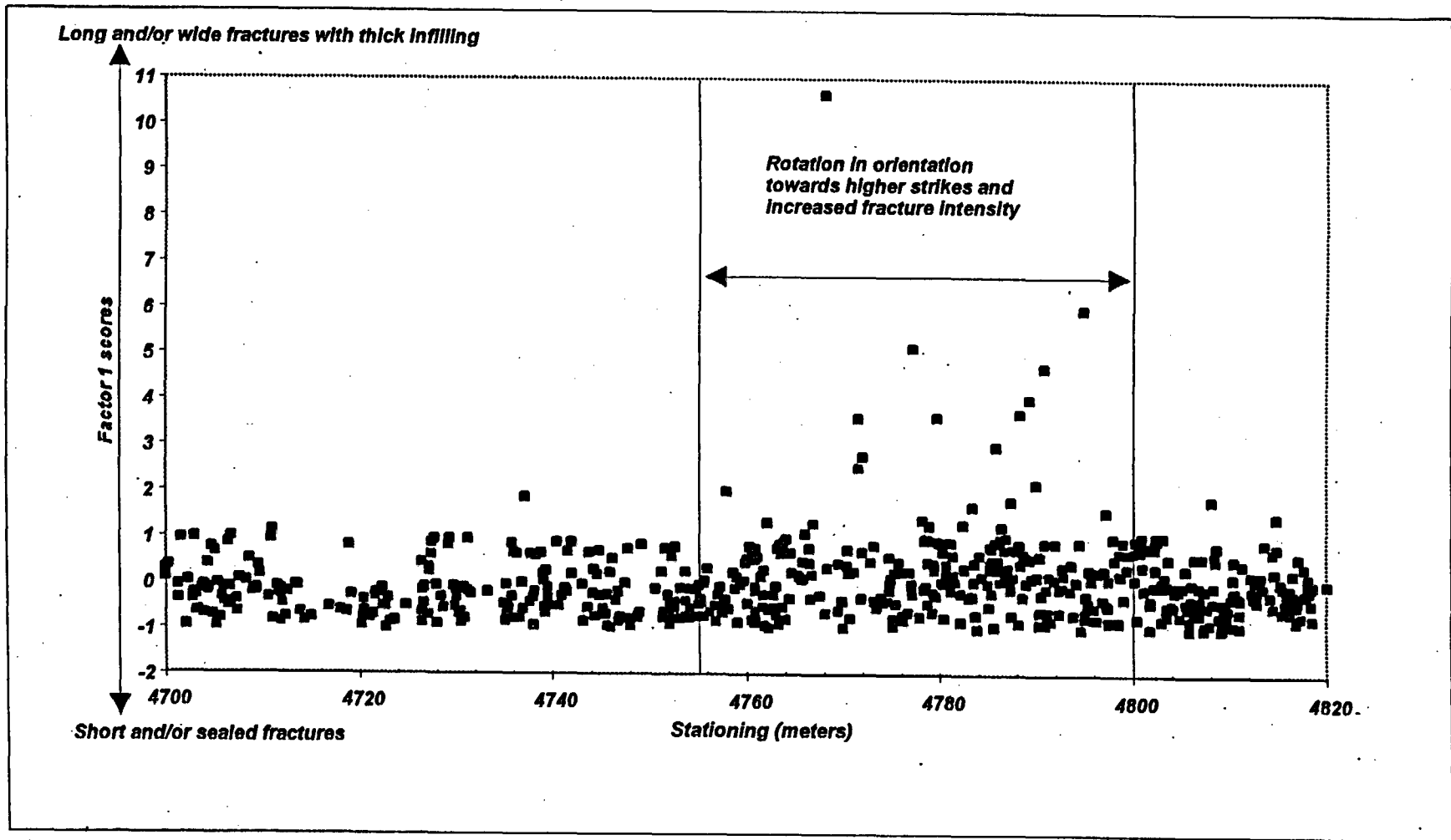


Figure 34 A subzone of higher Factor 1 scores which correlates with a shift towards higher strikes, and increased fracture density.

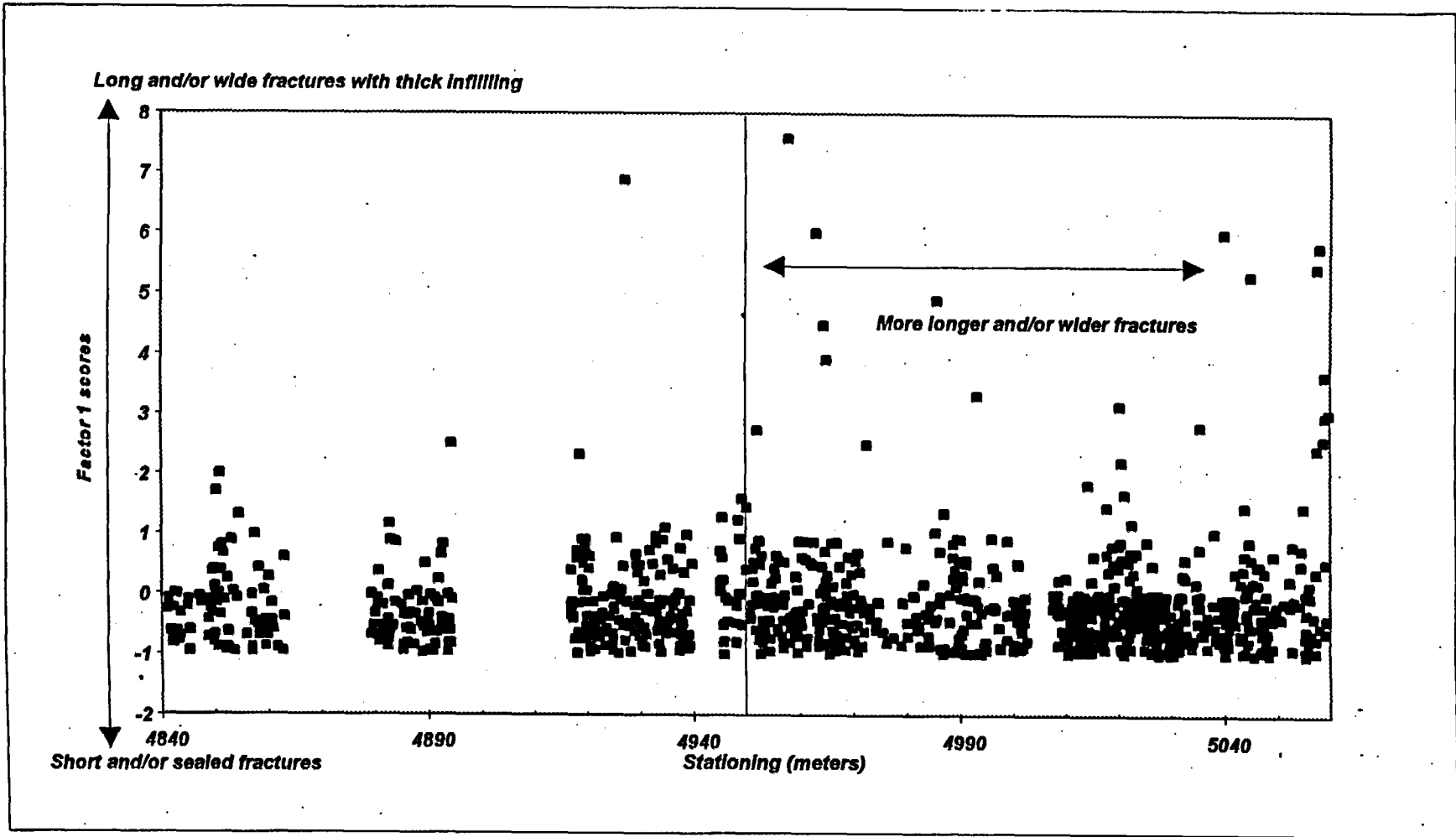


Figure 35 A Factor 1 boundary at 49+50, with longer and/or wider fractures beyond 49+50.

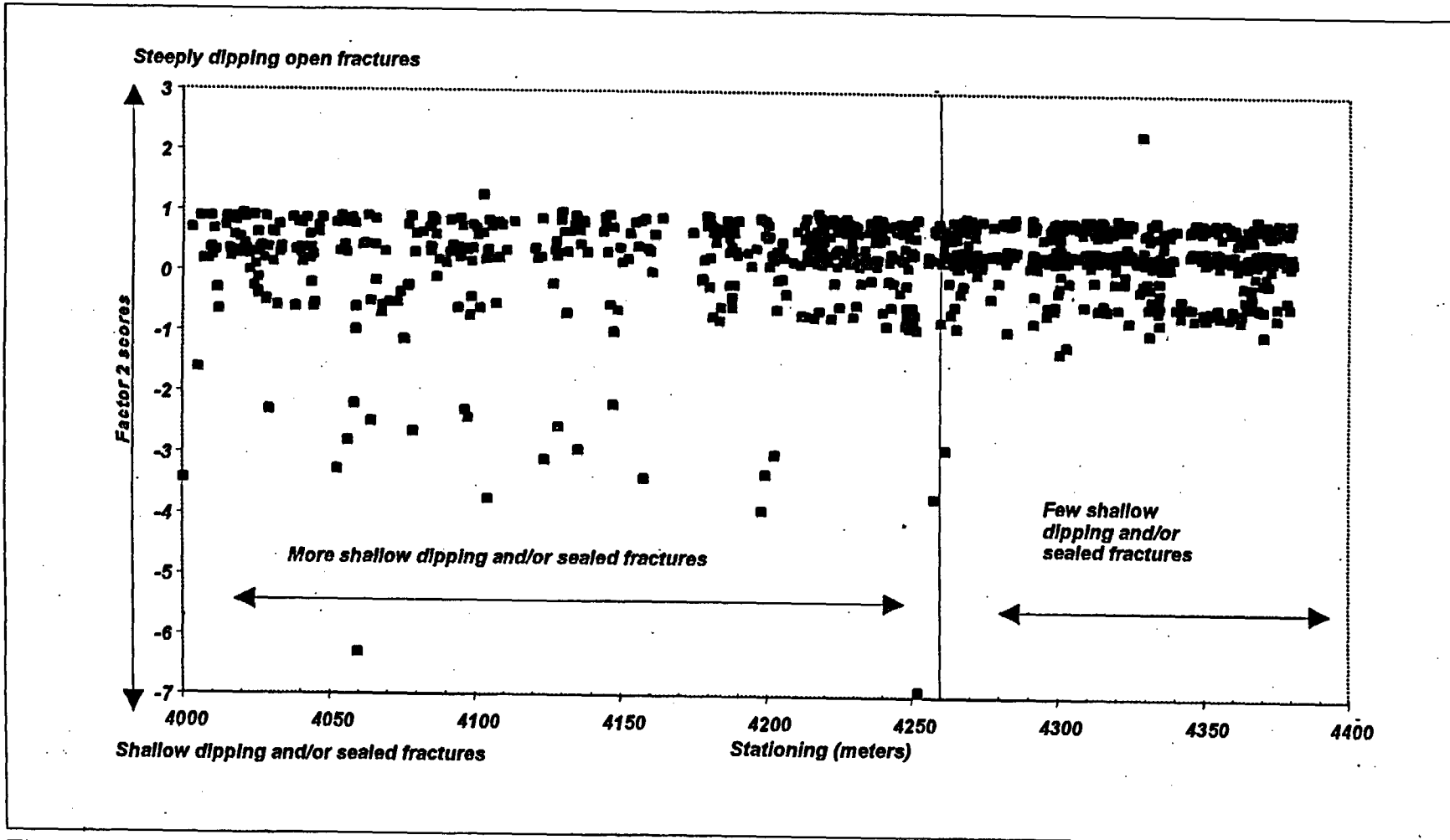


Figure 36 A Factor 2 boundary at 42+60, with less shallow dipping and/or sealed fractures after 42+60.

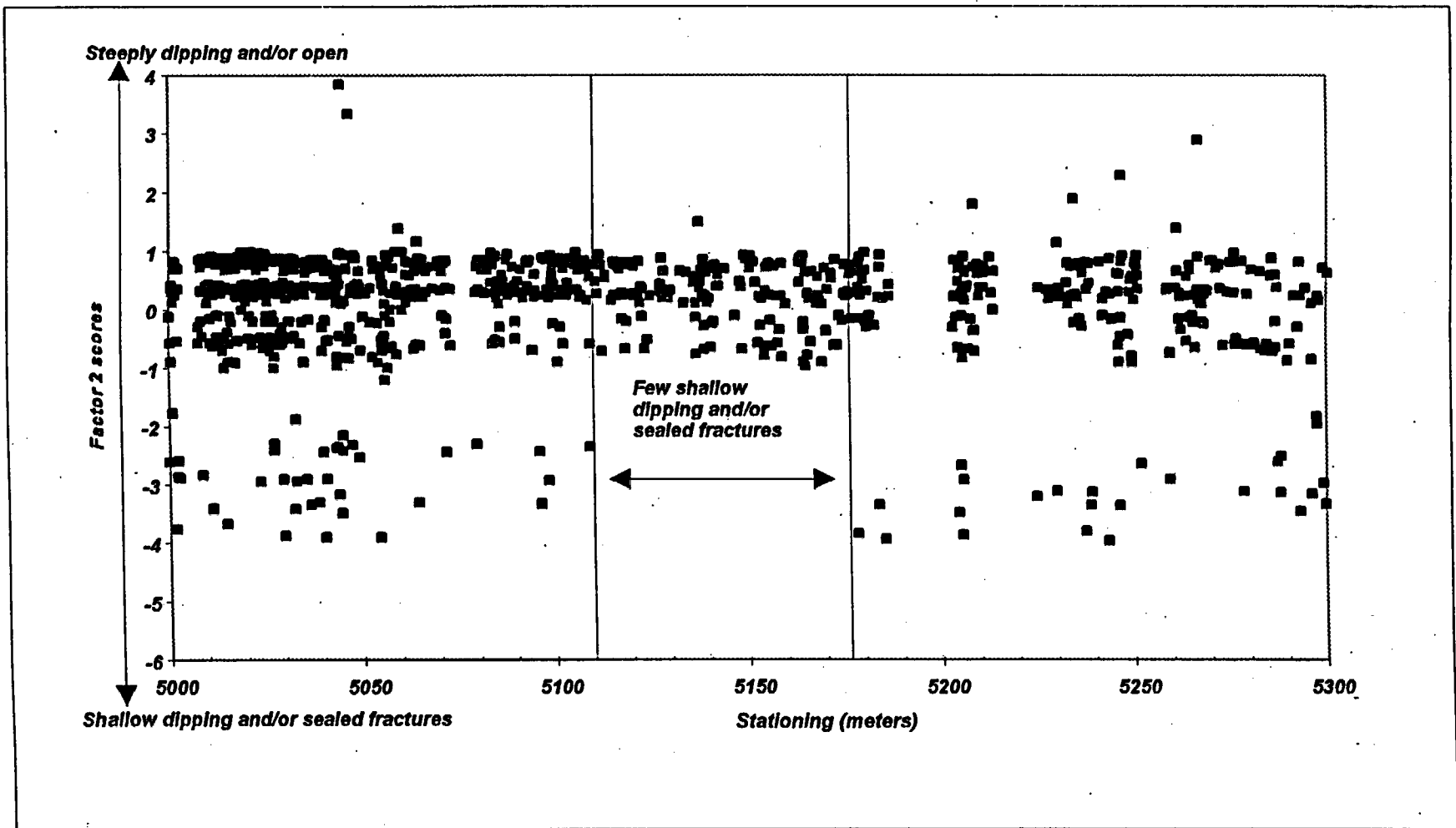


Figure 37 A factor plot showing a zone from 51+10 to 51+75 containing few shallow dipping and/or sealed fractures.

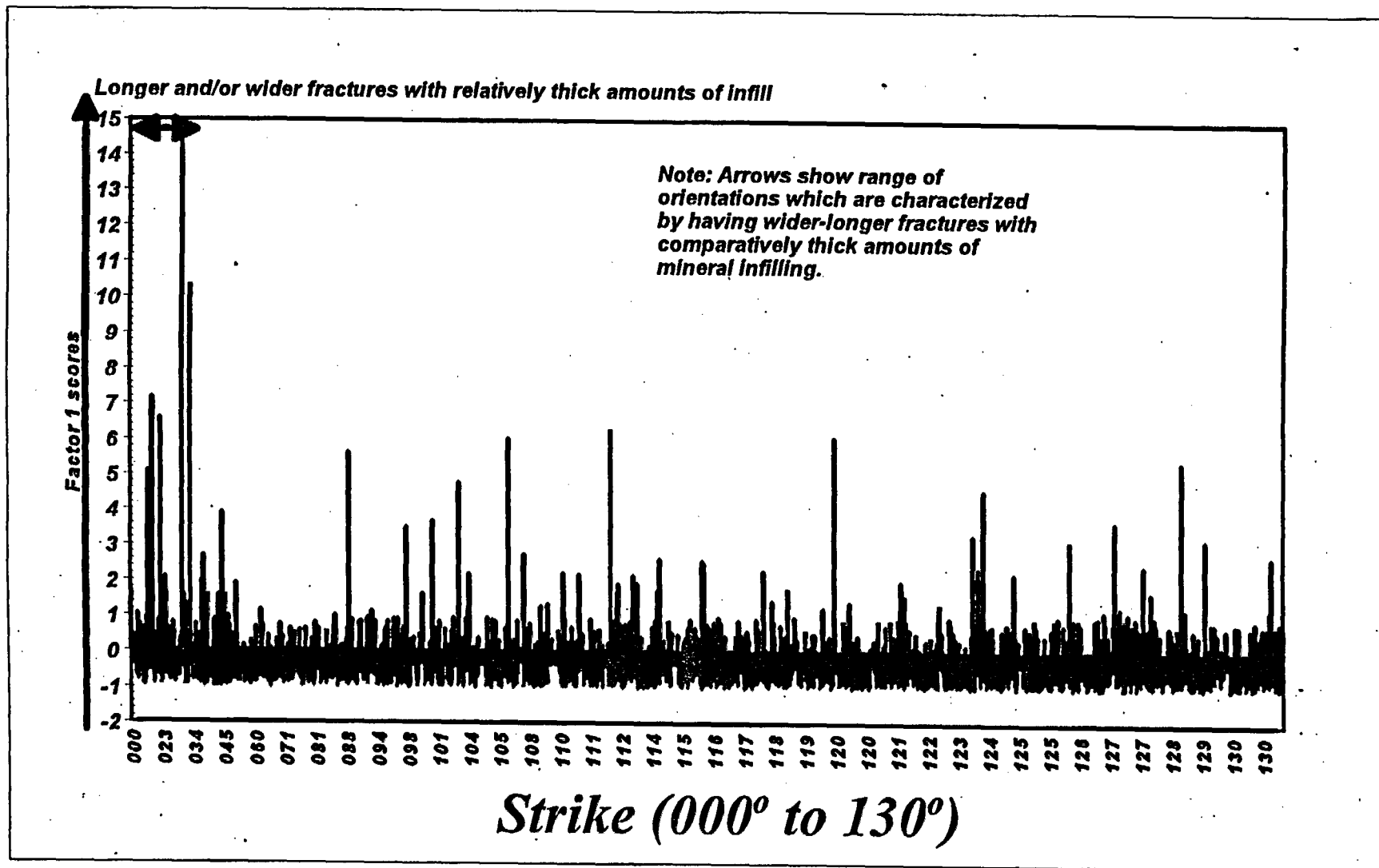


Figure 38. Strike (000° to 130°) versus Factor 1 scores in the Main Drift.

Longer and/or wider fractures with relatively thick amounts of Infill

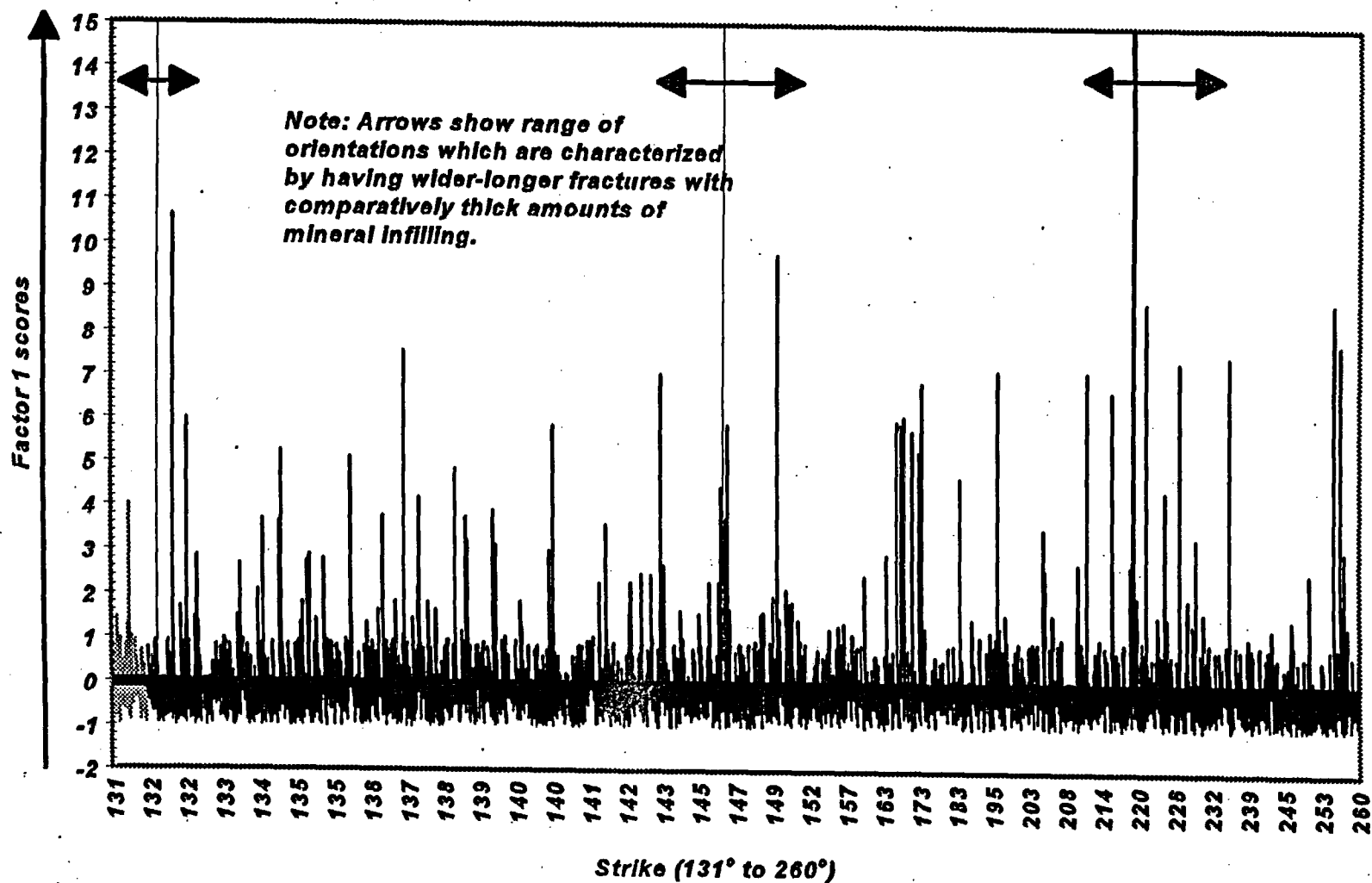


Figure 39. Strike (131° to 260°) versus Factor 1 scores in the Main Drift

Page left intentionally blank

Longer and/or wider fractures with relatively thick amounts of infill

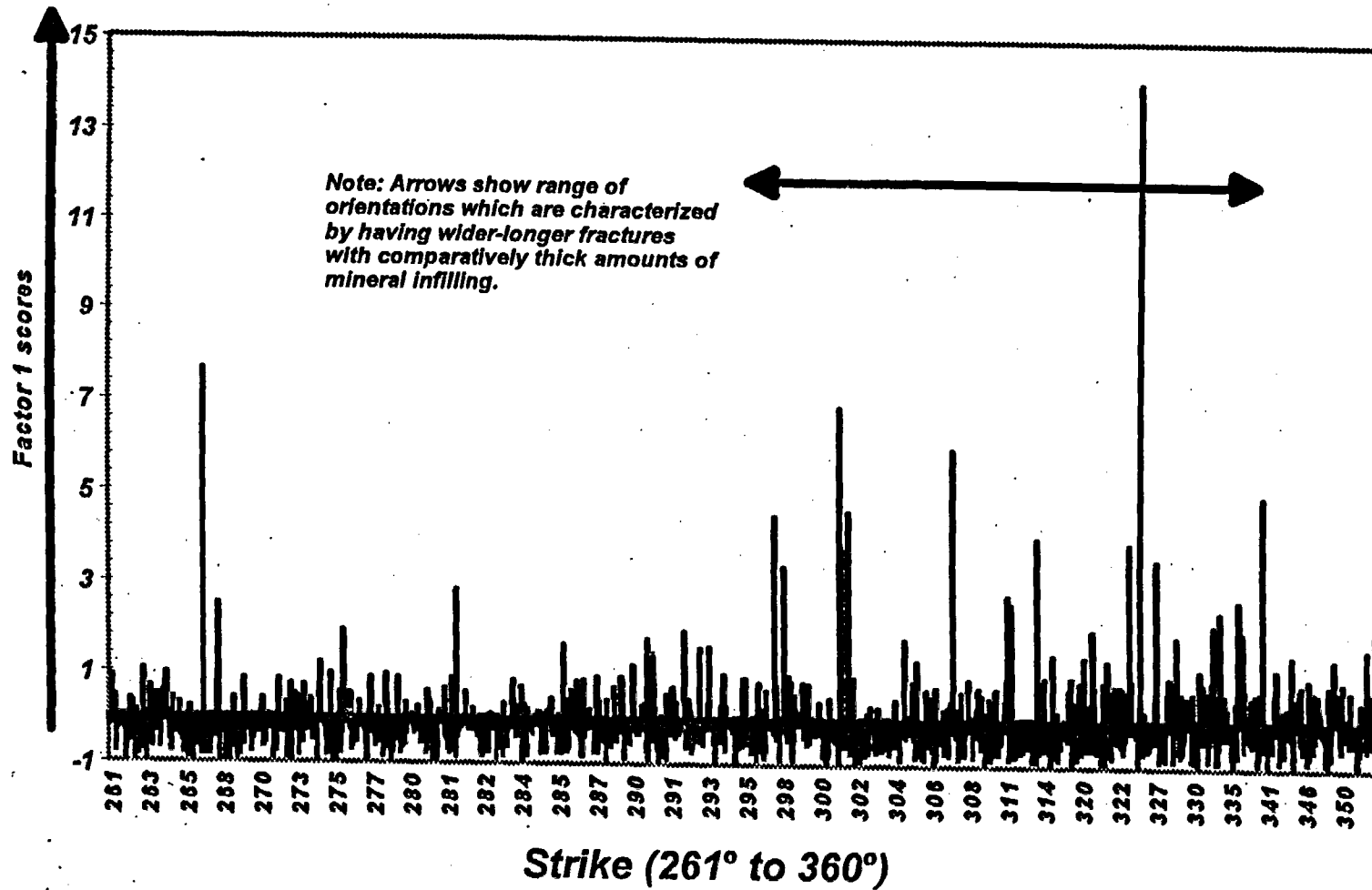


Figure 40. Strike (261° to 360°) versus Factor 1 scores in the Main Drift.

Open and/or steeper dipping fractures

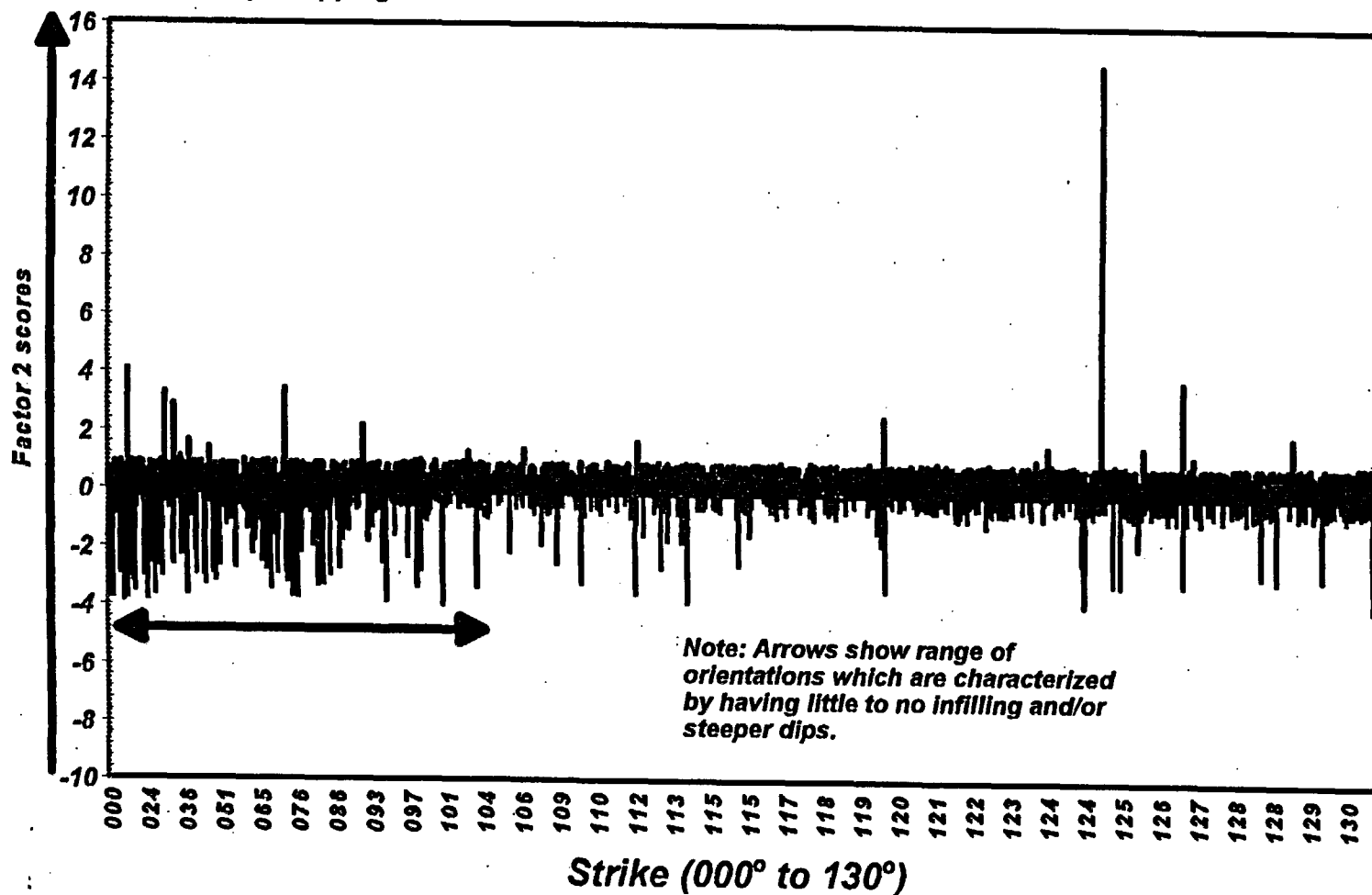


Figure 41. Strike (000° to 130°) versus Factor 2 scores in the Main Drift.

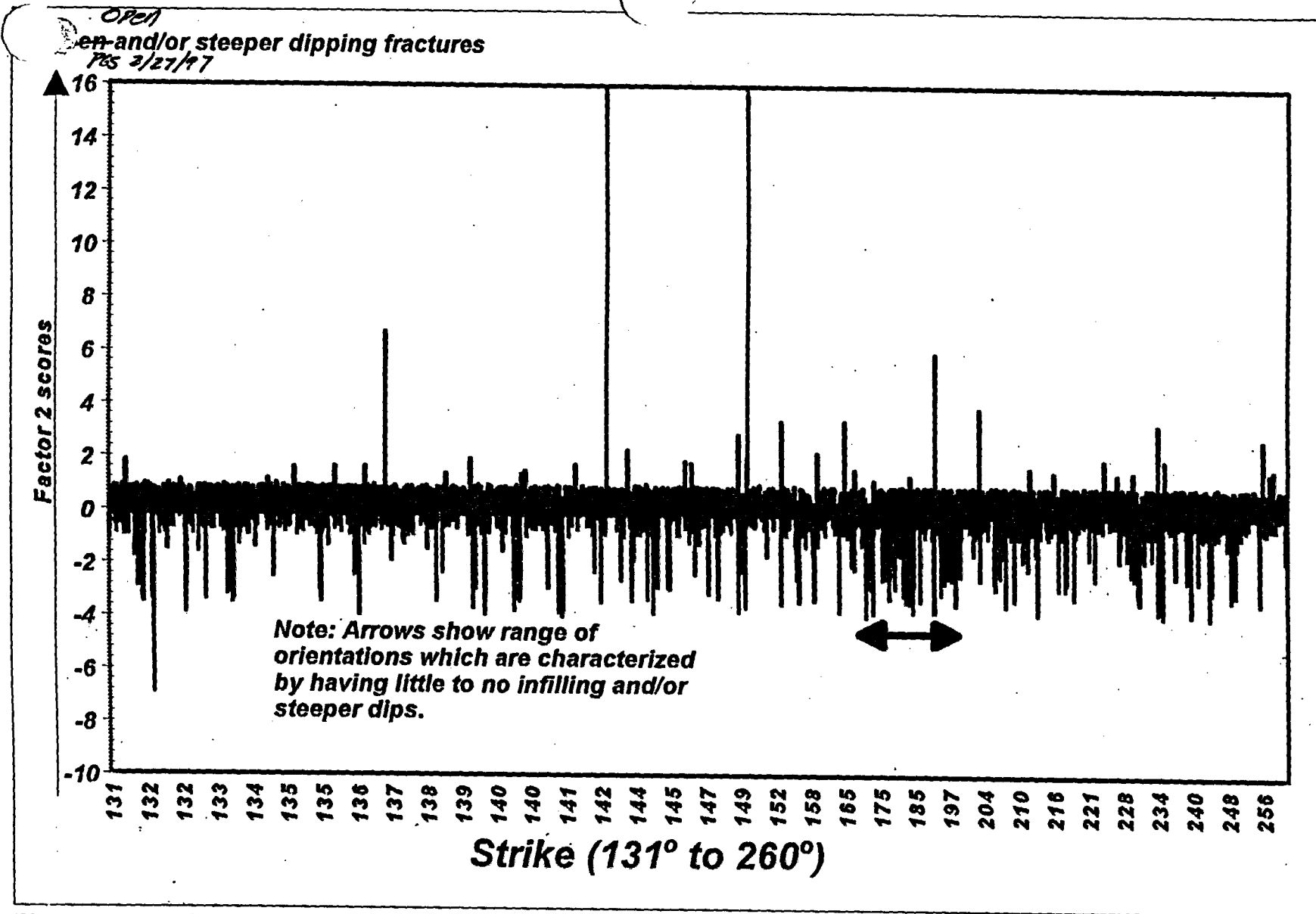


Figure 42. Strike (131° to 260°) versus Factor 2 scores in the Main Drift.

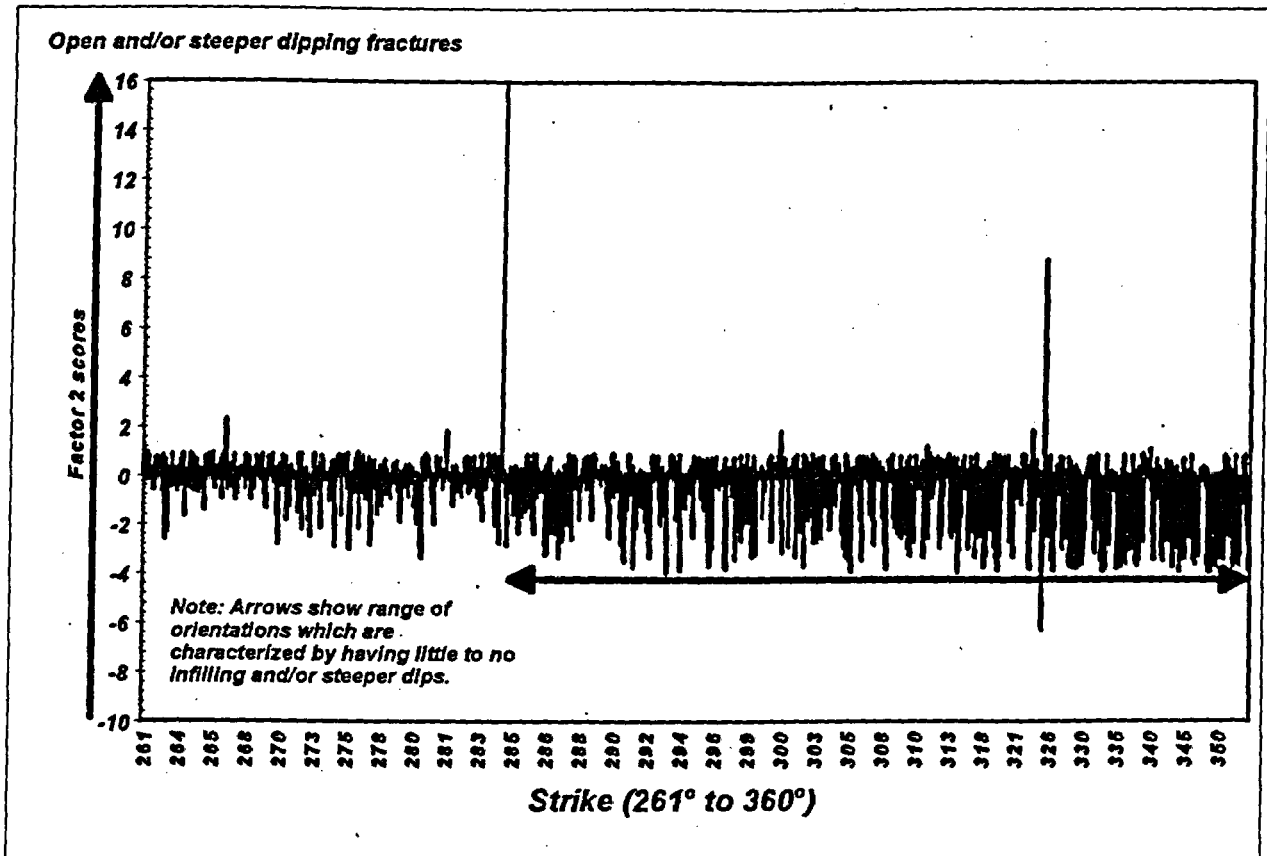


Figure 43. Strike (261° to 360°) versus Factor 2 scores in the Main Drift.

ramp at Sta. 55+00. This information indicates the main drift from Sta. 49+50 to 55+00 contains more longer/wider fractures with thicker amounts of infilling. The genetic and/or tectonic significance of this boundary located at or near Sta. 49+50 is unknown.

Structural heterogeneities within the Tptpmn as identified by factor 2 scores

Two statistically significant structural heterogeneities based on changes in the distribution of factor 2 scores were identified for the main drift of the ESF. Although the factor 2 scores boundary and sub-unit described below are statistically significant, they are not as significant as the above-listed factor 1 heterogeneities. The first significant heterogeneity in the distribution of factor 2 scores with stationing starts at about Sta. 42+60. Figure 36 shows that prior to Sta. 42+60, relatively low factor 2 scores ranging from -2 to -6 are common. In comparison, after Sta. 42+60, low factor 2 scores are very rare. This boundary represents both the end of a zone of "Tptpmn" containing numerous shallow-dipping fractures, and the beginning of a zone containing

more intense fracturing. Figure 37 shows that from Sta. 51+10 to 51+75 a subunit can be identified. This sub-unit represents a zone of rock lacking shallow-dipping fractures and/or containing wider-than-average apertures.

Correlations between strike and factor 1 and 2 scores

Figures 38 through 43 were used to identify the correlations between factor scores and strike for the Main Drift and are listed below. Figures 38 to 40 indicate that fractures with strikes from 000° to 032° , 131° to 133° , 143° to 150° , 209° to 237° , and 297° to 342° have a comparatively high number of wider and/or longer fractures with comparatively thick amounts of infilling when compared to fractures with other orientations. Figures 41 to 43 show that fractures with strikes from 0° to 105° , 167° to 201° , and 284° to 360° , tend to have a greater proportion of fractures with little-to-no infilling and/or steeper dips, when compared to fractures with other orientations. Genetic and/or tectonic interpretations regarding these correlations should be made in the future.

CHLORINE-36

Ground water travel time in the ESF is an important issue as it is a factor in how the Yucca Mountain site would function as a nuclear waste repository. Los Alamos National Laboratory (LANL) is conducting a sampling and testing program to identify potential fast paths of infiltration pathways using ^{36}Cl concentrations in rock pore water. Chlorine-36 is a radioactive isotope produced naturally in the atmosphere as well as by atmospheric nuclear testing which can be carried underground by percolating ground water. During atmospheric nuclear testing in the 1950s, high concentrations of ^{36}Cl were added to meteoric water. A ^{36}Cl concentration significantly higher than levels that occur naturally in the atmosphere is termed a bomb-pulse signal. The presence of a bomb-pulse signal suggests the presence of ground water that has percolated from the surface in the last 50 years along fast ground water transport paths. A LANL milestone report (Fabryka-Martin and others, 1996) characterizes the results of this study.

The ongoing study now has results from samples collected to approximately Sta. 63+00. Analyzed samples from two areas in the Main Drift have elevated ^{36}Cl concentrations. Ten samples between Sta. 34+28 and 35+93, the location of the Sundance fault, have bomb-pulse levels of ^{36}Cl . Three samples between Sta. 43+63 and approximately 45+00, in the fracture zone, have bomb-pulse levels of ^{36}Cl . No samples collected beyond this area have elevated levels of ^{36}Cl (Fabryka-Martin and others, 1996).

GEOTECHNICAL CHARACTERIZATION

This section summarizes the results of geotechnical characterization data collected during excavation of the Main Drift in the ESF from Sta. 28+00 to 55+00. The purpose of this report is to present rock mass quality ratings for the Main Drift. These data may be used to assess the stability of current and proposed underground excavations at Yucca Mountain. The rock mass classification systems used were developed in response to the demand for numerical design tools. Bieniawski (1989) lists the benefits of rock mass classification:

- Improve the quality of site investigations by recognizing parameters important to the geotechnical classification of the rock mass.
- Provide quantitative information for design purposes.
- Enable better engineering judgment and achieve a common standard for more effective communication.

Background

Descriptions of the rock mass are based on two empirical rock mass classification systems: the Norwegian Geotechnical Institute Q rock quality (Q system) and the Geomechanics Rock Mass Rating (RMR) system. The Norwegian Geotechnical Institute Q rock mass classification system (Barton and others, 1974) was selected as a design tool by the underground designers for use in the ESF. This system describes the quality of the rock for engineering purposes as the product of six different numerical parameters. Observations and data for these parameters are collected, documented, and assigned a Q rating under a draft technical procedure titled *Rock Mass Classification YMP-USGS-GP-54, R0 and Scientific Notebook SN-0083 - Collection and Processing of Geotechnical Data*. Additional data are collected under the same procedure and scientific notebook above to describe the rock mass using the Geomechanics Rock Mass Rating (RMR) system developed by Bieniawski (1989). Ratings are assigned to each 5-m length of tunnel using both rock classification systems. Later sections describe the parameters used in the two rock mass rating systems.

Stratigraphic Unit

The Main Drift is one lithostratigraphic unit, Tptpmn. Tptpmn is predominantly a moderately to densely welded tuff, with relatively high intact strengths; containing less than 10 percent lithophysal voids. Stratigraphic units both overlying and immediately underlying the Main Drift (28+00 - 55+00) are listed in Table 5: (below).

Stratigraphic Unit	Top Contact Station (m)	Bottom Contact Station (m)
Topopah Spring crystal-poor, upper lithophysal zone (Ttptul)	17+97	27+20
Topopah Spring crystal-poor, middle nonlithophysal zone (Tptpmn)	27+20	57+30*
Topopah Spring crystal-poor, lower lithophysal zone (Ttptll)	57+30*	**NE

* Fault Contact ** Not encountered by the ESF

Table 5. Station Coordinates at Stratigraphic Contacts Along Main Drift DLS Tape

Physical Features

There are two major geological features encountered in the Main Drift with potential engineering and construction design significance:

- Sundance fault zone at Sta. 36+05.
- Intensely fractured zone from Sta. 42+00 to 51+50.

The Main Drift was excavated on an azimuth of 183°, an upgrade of +1.35 percent, and is 7.62 m in diameter. The tunnel has been divided into four domains: Sta. 28+00 - 37+00, 37+00 - 42+00, 42+00 - 51+50, and 51+50 - 55+00. The actual orientation of the discontinuities within the Main Drift varies slightly from domain to domain. Table 6 lists ranges of peak strikes and average dips:

Domain	Range of Peak Strike	Range of Dip	Notes
Set 1	115° - 141°	81° - 84°	
Set 2	210° - 231°	84°	
Set 3	310° - 350°	12° - 22°	
Set 4	285°	51°	Domain 1 only

Table 6. Fracture Sets By Domain

Hydrology

Dry conditions exist throughout the ESF in the North Ramp portion and along the Main Drift. During excavation, there was no groundwater evident.

Introduction to ROD, RMR, and Q

Q ratings are assigned to each 5-m length of tunnel. The original construction plan was to install ground support based on the Q system. With this objective in mind, the 5-m rating length was selected. However, a uniform rating length and particularly a short, uniform rating length may be at some variance with the spirit of the original rating systems. Bieniawski (1989) suggests an RMR rating should be assigned to structural regions in which certain fractures are more or less uniform. Barton and others (1974) states zones with marked variations in rock parameters should be classified separately; however, where variable zones intersect the excavation for a few meters, a compromise design may be appropriate. It appears from these statements that a single rock mass quality rating could and perhaps should be applied to longer lengths of the tunnel. In short, the final design of a tunnel support system should recognize that using a 5-m rating length causes variations in the assessment of rock mass parameters. As a result, Q system joint number (Jn) and stress reduction factor (SRF) may fluctuate erratically with length.

Rock Quality Designation (RQD)

The rock quality designation (RQD) index is a rating parameter of both the Q and RMR systems for drill core. It was introduced over 20 years ago as a quantitative measure of rock quality (Deere and others., 1988). The total length of core pieces which are 4 inches (about 10 cm) and longer is divided by the length of the core run. RQD is calculated as follows:

$$\text{RQD \%} = \frac{\sum \text{Length of Core Pieces} > 10 \text{ cm}}{\text{Interval Length}} * 100\% \quad \text{Equation 1}$$

Following is the sequence for calculating RQD from observation of the tunnel wall. Lengths of intact rock adjacent to the DLS survey tape are estimated or calculated as the percentage of core pieces 10 cm or longer which would be recovered in an imaginary horizontal drill hole along the right wall of the excavation. The fundamental assumption for RQD calculation with the DLS data is that the length of rock between recorded fractures is intact rock. From that assumption, the total of intact rock pieces longer than 10 cm are determined from the fracture spacing. That length, expressed as a percentage of the total length, is the line survey RQD. Where RQD within a 5-m section is less than or equal to a rating of 10 or less (including 0), a nominal value of 10 is used to evaluate Q.

In areas supported by steel sets, an accurate station for fractures behind the sets cannot be recorded. Where fracturing on either side of the steel sets suggests fracturing behind the steel sets, an estimated station for the inferred fractures is recorded and RQD is calculated using these fractures.

Lithophysae encountered in core drilling produce a length of drill hole with no core recovery. Lithophysae zones are treated as closely spaced fractures and therefore excluded from the theoretical length of intact rock. This procedure of "zeroing out" lithophysal cavities reduces the calculated RQD. Lithophysal voids might not produce sliding planes, which affect stability. The rock mass with a high concentration of lithophysae cavities is not characterized well by the empirical systems. This particular issue is not addressed by Deere (1989) or any other

publications.

Rock mass classification based on RQD alone is recognized as a limited system since it does not take direct account of other factors such as joint orientation. However, RQD still remains an important parameter of Q and RMR rating systems.

Summary of RQD

Both the Q and RMR classification systems use RQD as a major factor in calculating of a rock mass rating. Table 7 below provides a descriptive value along with a numerical index summarizing the RQD values encountered in the Main Drift of the ESF.

RQD Ranges	Rock Quality Description	Percent Present in Main Drift
< 25%	Very Poor	2%
25% - 50%	Poor	24%
51% - 75%	Fair	53%
76% - 90%	Good	18%
91% - 100%	Excellent	3%

Table 7. Percentages of RQD

With the parameters from Table 7, the RQD values which appear most frequently in the Main Drift, range from 51 to 75, which suggests a *fair* rating for the rock quality. (Figure 44).

Main Drift RQD

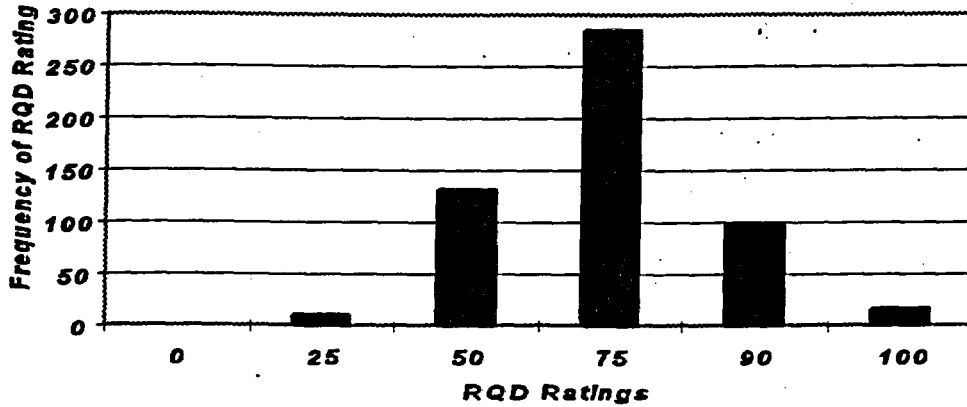


Figure 44. Frequency of RQD Ratings

The theoretical rock quality for the entire Main Drift according to the RQD system (Deere, 1968) is shown in Figure 45. The RQD varies erratically. If an overall average is necessary, then 61 percent or *fair* describes the RQD for the entire Main Drift. Breaking the Main Drift down into its four domains provides a closer look at the actual RQD ratings.

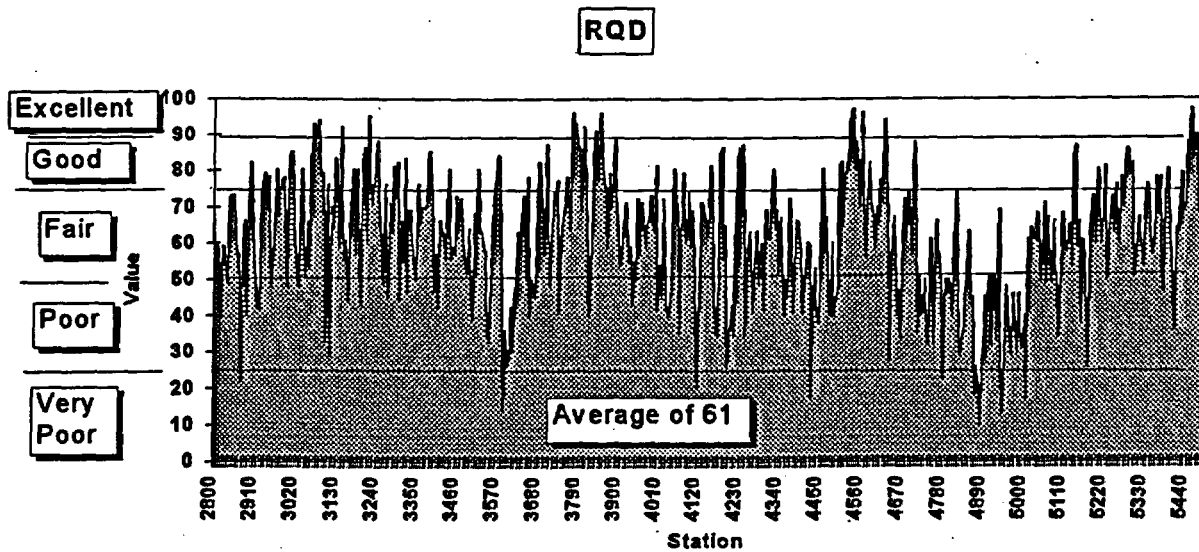


Figure 45. Rock Quality Description Values

Figures 46 through 49 show the RQD values for each of the four domains identified within the Main Drift.

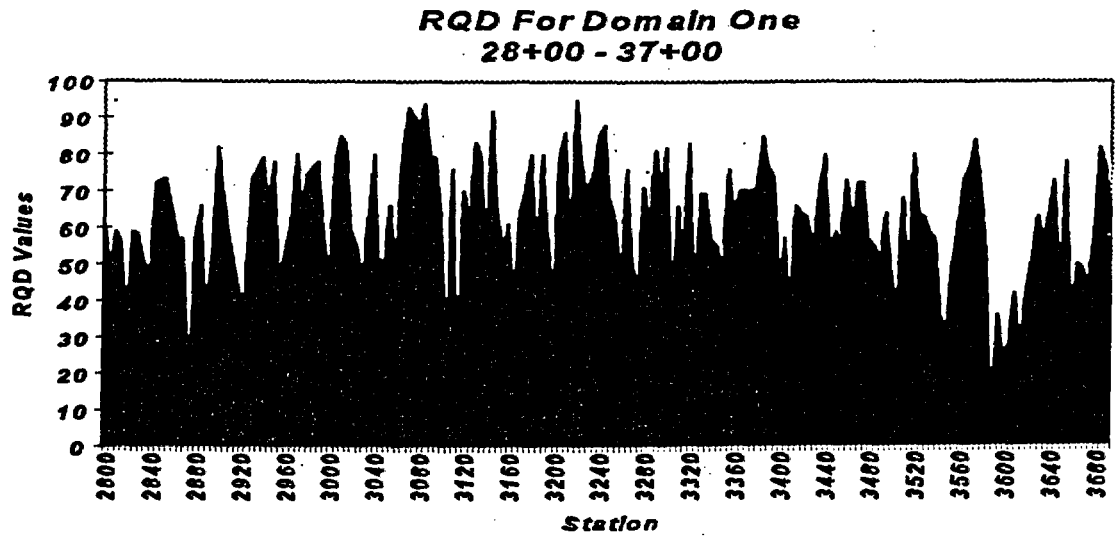


Figure 46. Domain One RQD, Sta. 28+00 to 37+00

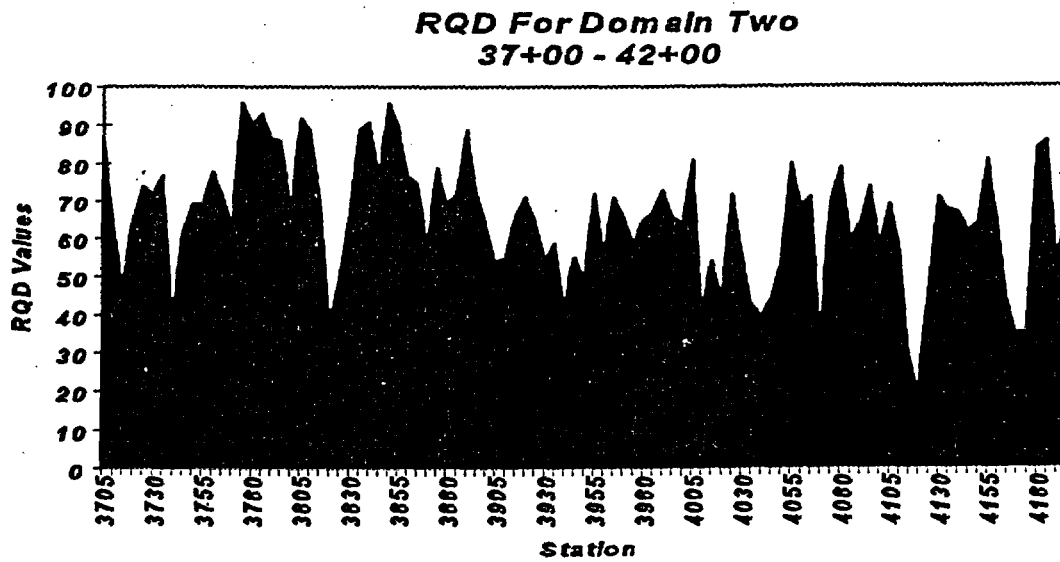


Figure 47. Domain Two RQD, Sta. 37+00 to 42+00

**RQD For Domain Three
42+00 - 51+50**

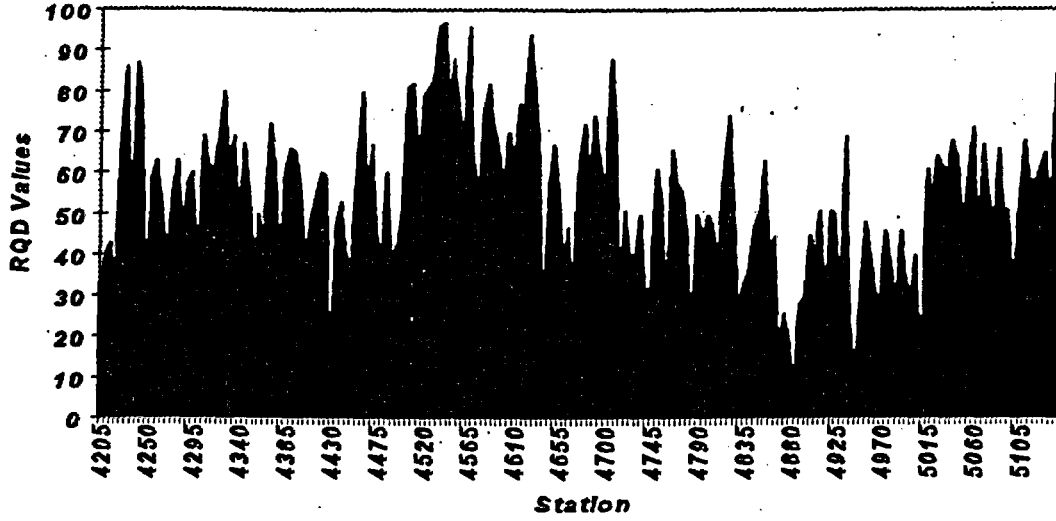


Figure 48. Domain Three RQD, Sta. 42+00 to 51+50

**RQD For Domain Four
51+50 - 55+00**

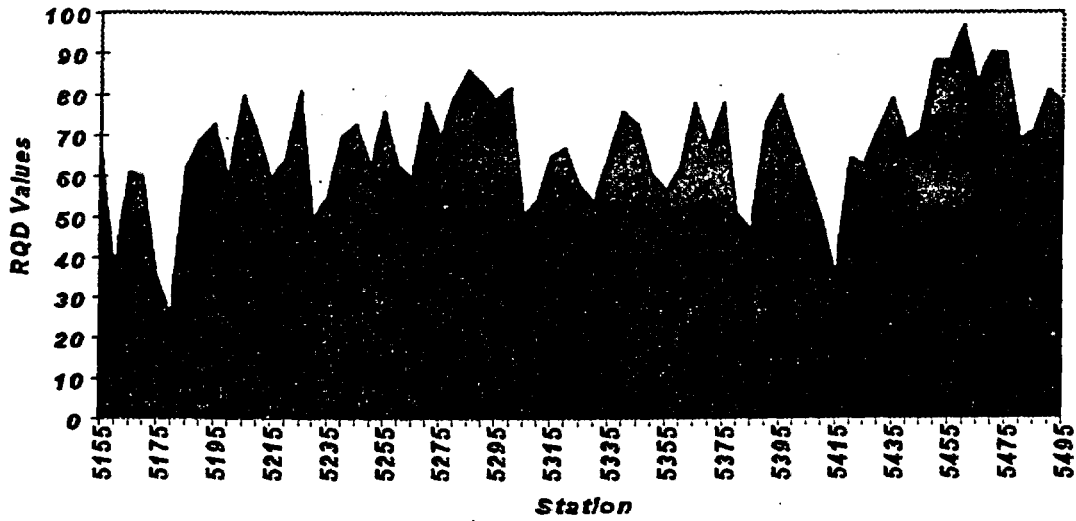


Figure 49. Domain Four RQD, Sta. 51+50 to 55+00

Rock Mass Rating (RMR)

The RMR system, also known as the Geomechanics Classification, is an empirical rating system based on the sum of six rock mass parameters. Bieniawski (1989) developed this system in 1973 and, with the addition of case histories, revised it to its present form. The numerical rock mass rating, RMR, is calculated according to the following equation:

$$\text{RMR} = \text{C} + \text{RQD} + \text{J}_s + \text{J}_{cd} + \text{J}_{wR} + \text{AJO} \quad \text{Equation 2}$$

where

- C is a numerical index associated with the intact-rock compressive strength.
- RQD is a numerical index associated with the rock mass RQD (the index is not the actual RQD value).
- J_s is a numerical index associated with the fracture spacing of a given joint set.
- J_{cd} is a numerical index associated with the condition of discontinuities.
- J_{wR} is a numerical index dependent on groundwater or inflow conditions (the "R" is used to distinguish this rating from the Q system joint water rating).
- AJO is a numerical index associated with the orientation of discontinuities.

Compressive strength, RQD, joint spacing, joint condition, groundwater and joint orientation parameters are divided into five ranges of rated values (see Table 9). The rating numbers reflect the importance of each parameter. For this report, the joint set with the lowest total rating for spacing, joint condition, and orientation is used to calculate the RMR.

Rating for Compressive Strength

The rock-wall compressive-strength rating is assigned using laboratory test data as a reference and sounding the tunnel rib with a rock hammer. This procedure is not sensitive to changes in the numerical index in borderline cases.

Rating for RQD (RQD)

RQD is determined from procedures previously discussed, and a numerical index is assigned based on that RQD.

Rating for Spacing of Discontinuities (Js)

Spacing is the separation of discontinuities in a single joint set, measured normal to the plane of the discontinuity. Spacing affects block size and geometry of loose wedges in the rock mass.

Rating for Condition of Discontinuities (Jcd)

This parameter includes roughness of the discontinuity surfaces, their separation, length or continuity (persistence), weathering of the wall rock of the planes, and the infilling material. The joint condition most often is assigned by rating five individual parameters. The total of length, separation, roughness, joint filling, and weathering ratings yields a Jcd rating as shown below:

$$Jcd = CDl + CDs + CDr + CDf + Cdw \quad \text{Equation 3}$$

Joint-Condition Length, continuity (CDl)

The *continuity* of fractures influences the extent to which the rock material and the discontinuities separately affect the behavior of the rock mass. A discontinuity is considered fully continuous if its length is greater than the dimension of the excavation.

Joint-Condition Separation, aperture (CDs)

Separation, or the distance between the discontinuity surfaces, controls the extent to which the opposing surfaces can interlock as well as the amount of water that can flow through the discontinuity. In the absence of interlocking, the discontinuity filling entirely controls the shear strength of the discontinuity. As the separation decreases, the asperities of the rock wall tend to become more interlocked, and both the filling and the rock material contribute to the discontinuity

shear strength. The shear strength along a discontinuity is therefore dependent on the degree of separation, presence or absence of filling materials, roughness of the surface walls, and the nature of the filling material.

Joint-Condition Roughness (Cdr)

Roughness, or the nature of the asperities on the discontinuity surfaces, is an important parameter characterizing the condition of discontinuities. Asperities that occur on joint surfaces interlock if the surfaces are clean and closed and inhibit shear movement along the joint surface. Asperities usually have a base length and amplitude measured in millimeters and are readily apparent on a core-sized exposure of a discontinuity.

Joint-Condition Filling, gouge (Cdf)

The *infilling* has a twofold influence: (a) depending on the thickness, the filling prevents the interlocking of the fracture asperities; and (b) possesses its own characteristic properties: shear strength, permeability, and deformational characteristics.

Joint-Condition Weathering (CDw)

Weathering of the wall rock, the rock constituting the discontinuity surfaces, is classified in accordance with the recommendations of the ISRM Committee on Rock Classification (1981):

Unweathered (CDw1) No visible signs of weathering are noted. The rock appears fresh and the crystals are bright.

Slightly weathered (CDw2) - Discontinuities are stained or discolored and may contain a thin filling of altered material. Discoloration may extend into the rock from the discontinuity surfaces to a distance of up to 20 percent of the discontinuity spacing.

Moderately weathered (CDw3) - Slight discoloration extends from discontinuity planes for greater than 20 percent of the discontinuity spacing. Discontinuities may contain filling of altered material. Partial opening of grain boundaries may be observed.

Highly weathered (CDw4) - Discoloration extends throughout the rock, and the rock material is partly friable. The original texture of the rock has mainly been preserved, but separation of the grains has occurred.

Decomposed (CDw5) - The rock is totally discolored and decomposed and friable.

Rating for Groundwater (Jw)

Groundwater is an important parameter in most circumstances; however, tunneling conditions are dry throughout the Main Drift.

Adjustment for Orientation of Discontinuities (AJO)

The rating of discontinuity orientations depends on the engineering application. Tunnels, slopes, and foundations use different rating values for joint orientations.

Table 8 below shows ratings for joint orientations in tunnels. (Note: In the table below, *normal* means *perpendicular* to the tunnel centerline). Concentration is on unfavorable and very unfavorable conditions as this is needed for tunnel support.

Orientation of joints with respect to tunnel axis and direction of tunnel excavation	Dip of Discontinuity			Condition for tunneling	Category	AJO _{index}
	0 - 20	20 - 45	45 - 90			
Strike-versus-Tunnel axis			normal	Very Favorable	AJO. 1	0
Drive-versus-Dip direction			with			
Strike-versus-Tunnel axis		normal		Favorable	AJO. 2	-2
Drive-versus-Dip direction		with				
Strike-versus-Tunnel axis	any	parallel	normal	Fair	AJO. 3	-5
Drive-versus-Dip direction	either	either	against			
Strike-versus-Tunnel axis		normal		Unfavorable	AJO. 4	-10
Drive-versus-Dip direction		against				
Strike-versus-Tunnel axis			parallel	Very Unfavorable	AJO. 5	-12
Drive-versus-Dip direction			either			

Table 8. RMR Ratings for Joint Orientation in Tunnels

Summary of RMR

The range of RMR values for the Main Drift is quite small, with most 5-m intervals indicating either a *fair* or *good* rating. These values are calculated according to Equation 2. Table 9 summarizes the percentages of RMR, and Figure 50 portrays a histogram of the frequency of each 5-m rating throughout the Main Drift.

RMR	RMR Description	Percentages of the Main Drift
< 20	Very Poor	0%
20 - 40	Poor	1%
41 - 60	Fair	55%
61 - 80	Good	44%
81 - 100	Very Good	0%

Table 9. Percentages of RMR

Main Drift RMR

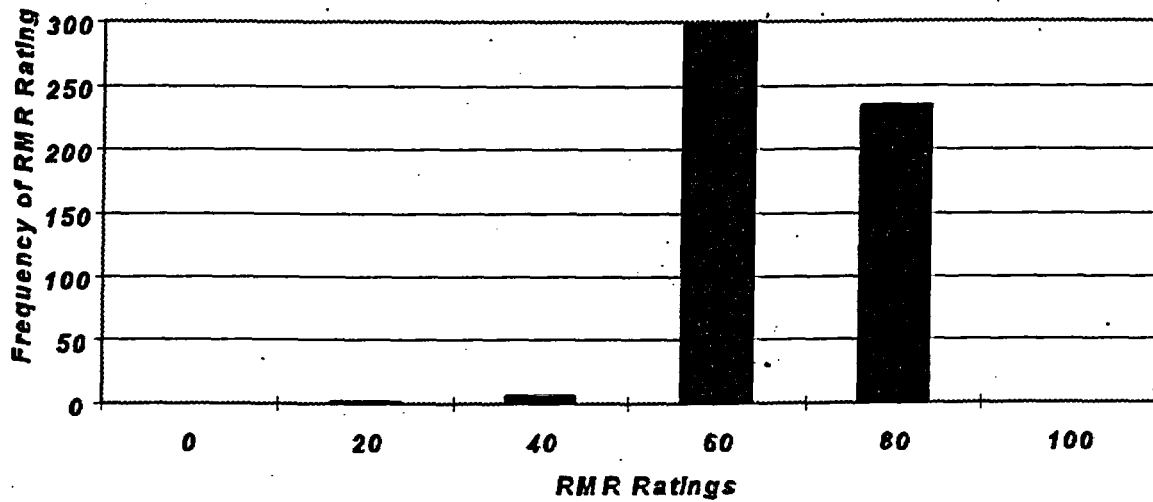


Figure 50. Rock Mass Rating Results for the Main Drift

The overall RMR average for the entire Main Drift, is 59, which warrants a rating of *fair*, almost in the *good* category. See Figure 51 below:

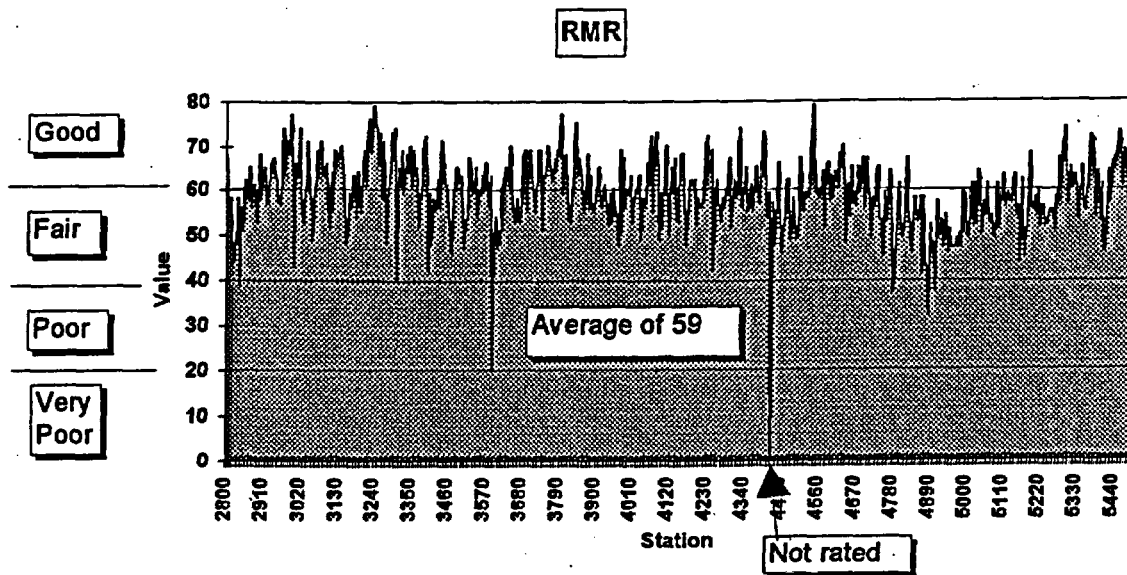


Figure 51. Rock Mass Rating Results for the Main Drift

Figures 52 through 55 show the RMR values for each of the four domains identified within the Main Drift.

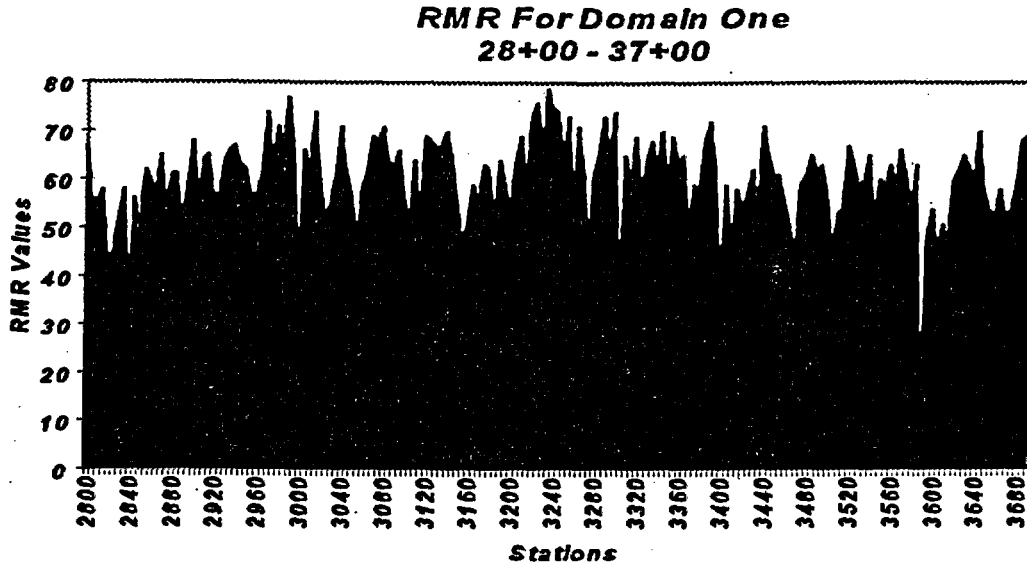


Figure 52. Domain One RMR, Sta. 28+00 to 37+00

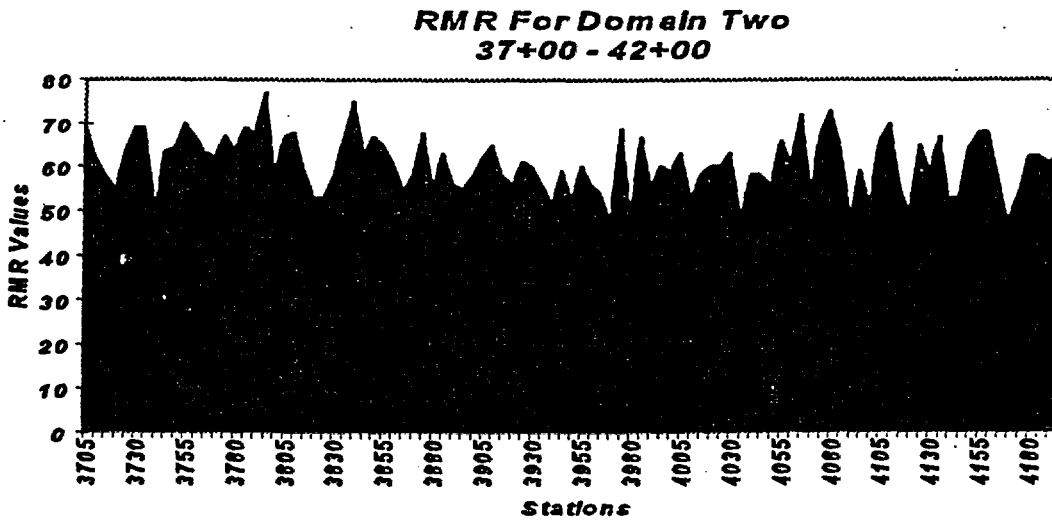


Figure 53. Domain Two RMR, Sta. 37+00 to 42+00

**RMR For Domain Three
42+00 - 51+50**

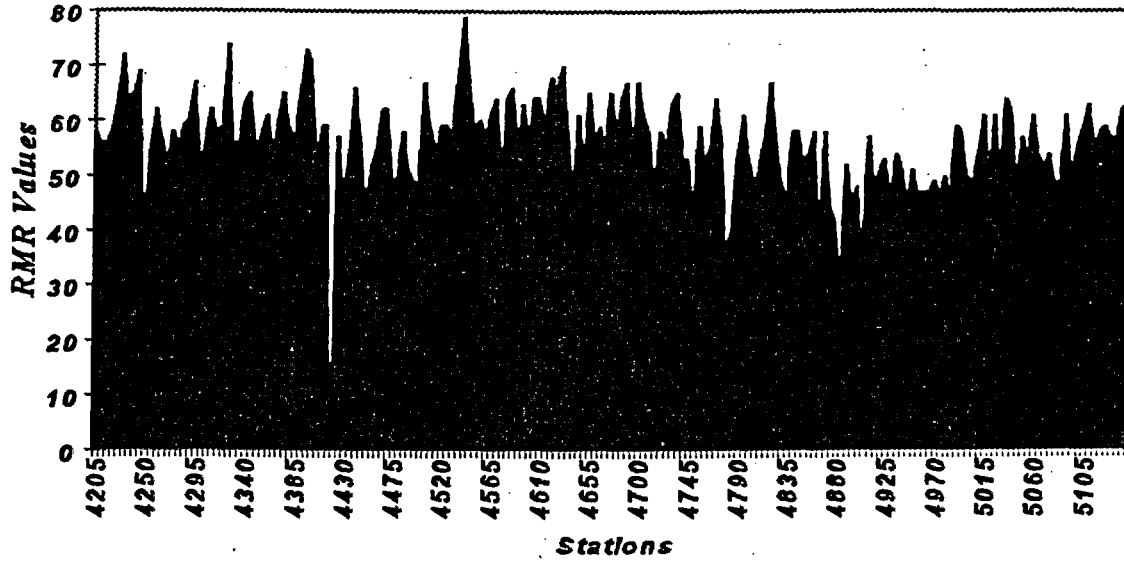


Figure 54. Domain Three RMR, Sta. 42+00 to 51+50

**RMR For Domain Four
51+50 - 55+00**

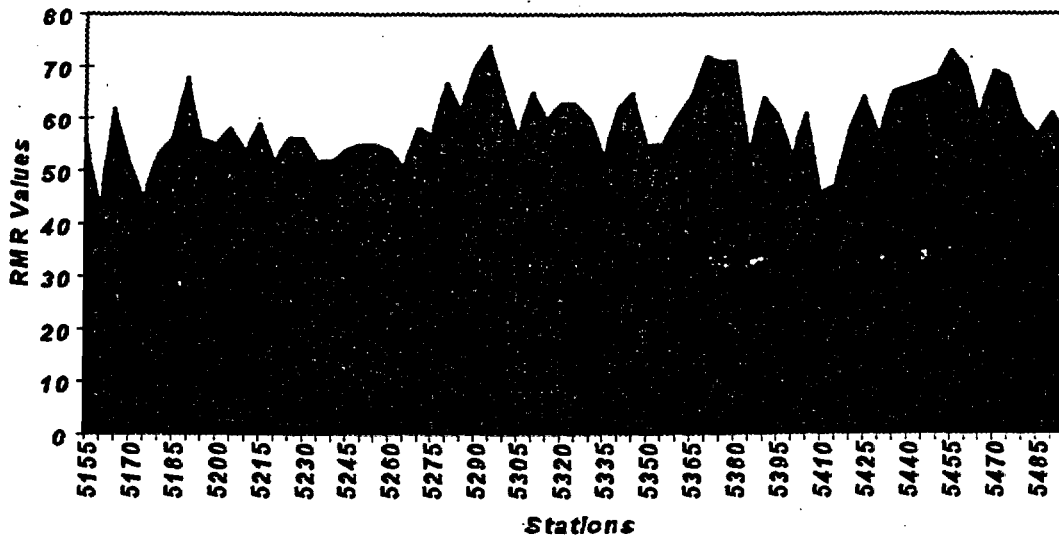


Figure 55. Domain Four RMR, Sta. 51+50 to 55+00

RMR Very Unfavorable and Favorable Azimuth Frequency

The two figures below show the orientations of very unfavorable and favorable RMR. The orientation is used as a parameter in the RMR system, and it is clear that the orientation controls the rating. Figure 56 below is developed based on all the azimuths with dips $> 40^\circ$. This places the joints in the very unfavorable range based upon their joint orientation. The figure depicts the frequency of the most undesirable orientations. Parallel and steep are the worst.

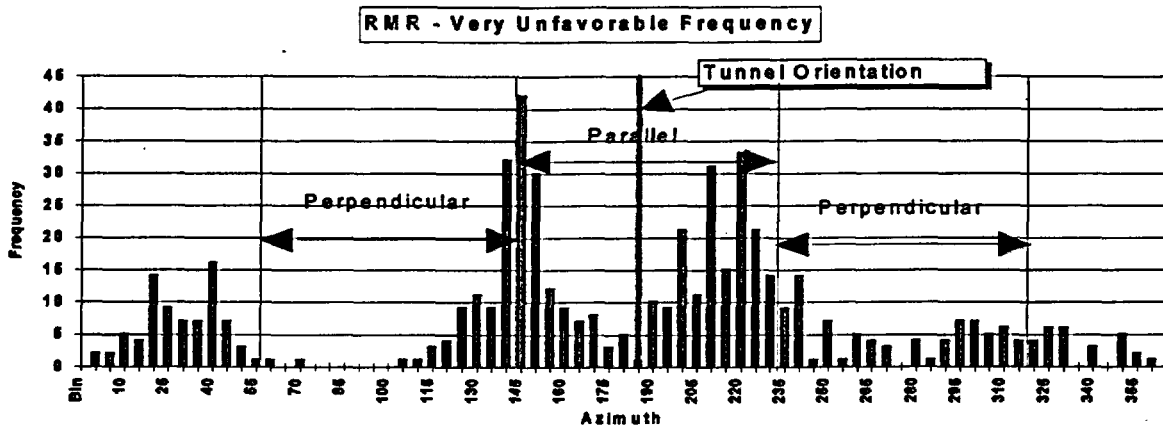


Figure 56. Frequency of Azimuths Used to Calculate the Lowest RMR

Figure 57 shows that the highest RMR value was determined from fractures oriented in a more perpendicular orientation with respect to the tunnel. Perpendicular and steep are most favorable.

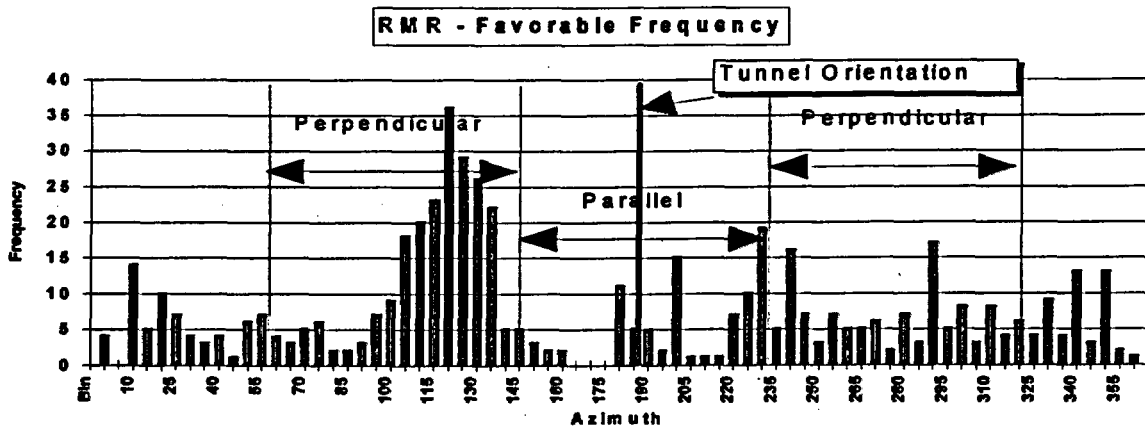


Figure 57. Frequency of Azimuths Used to Calculate the Highest RMR

Norwegian Geotechnical Institute Rock Quality Q System

The Q ratings described as “mapped Q” are a conservative estimate of the rock mass quality in that the ratings are based on the lowest quotient of observed joint roughness, J_r divided by joint alteration, J_a . A less-conservative component of the mapped Q rating results from assigning a rating to each 5-m length of tunnel. For this short length, a stress-reduction factor associated with multiple shears is not often used. If longer lengths of tunnel were rated, a higher stress-reduction factor due to multiple shears would lower the Q ratings.

Observations and data for the six parameters are collected, documented, and assigned a Q rating. The Q value is calculated with the following equation:

$$Q = (RQD/J_n) * (J_r/J_a) * (J_wQ/SRF) \quad \text{Equation 4}$$

where:

RQD is an integer number equal to the RQD percentage. In the equation above, the numerical value of 90 is used for an RQD of 90 percent.

J_n is an index number based on assessment of the number of joint sets within the 5-meter rating length considered.

J_r is an index number representing the roughness of the joint set.

J_a is an index number based on the alteration or filling of a given joint set.

J_wQ is an index number based on groundwater conditions. The “Q” is used to distinguish this index from the RMR system groundwater rating.

SRF is an index number based on in-situ conditions which influence the stability of the excavation.

The procedures used to assign a numerical value to each factor are discussed below.

ROD Rating

The RQD is determined with the procedures described previously. This numerical rating is used directly in calculating the Q value.

Jn Rating

The number of joint sets is a parameter related to the extent of fracturing in the ground mass. The number of joint sets is determined according to the observational procedures described below.

Observational Jn

The number of joint sets for a given 5-m-rating interval is determined primarily from observations of the right rib of the tunnel along the DLS tape. However, discontinuities which are subparallel to the tunnel axis are more easily observed in the crown of the tunnel; therefore the observed Jn includes joint sets evident in the crown. The right rib of the tunnel is emphasized so that observed ratings may be compared with the data gathered in the Detailed Line Survey.

Visual inspection to determine the number of joint sets requires engineering-geological judgment. Ratings are based strictly on observations within a 5-m length. The use of a short length to determine this parameter leads to oscillations in the joint-number rating. Intuitively, one might assume this parameter would be more or less constant in a structural region. That constancy is not the case using a short rating length. Variation in Q ratings between two adjacent lengths of tunnel are most often due to the quotient RQD/Jn and the parameter SRF which is discussed later.

The following guidelines should be used to count the number of joint sets. Fractures about 1 meter and longer are used to select the number of apparent joint sets. If well developed, foliation and bedding planes are counted as a complete joint set. Determining the number of joint sets requires a minimum of two fractures of similar orientation observed within the 5-meter length to

count as a set. These fractures must have similar characteristics (aperture, infilling, roughness, etc.) whose orientations are within 15° of each other; then those joints are considered as a joint set. If the joints with similarly oriented strikes have distinctly different characteristics, then there may be two joint sets present. If a collection of joints exhibits strikingly similar characteristics, but their orientations cannot be contained within 15°, they may be a joint set best characterized as random joints. Joint sets with a spacing along the tunnel axis greater than 5 meters apart would not be counted as a set, but rather as a random set. (This limitation presents a problem in utilizing the 5-m cut-off rule). A random set is counted if at least two fractures not part of an identified set appear in the rating length.

Fracture zones including crushed rock or intensely jointed rock may be evident on the left rib of the tunnel and not on the right. In these cases, notes describing fracture zones or fallout on the left rib are entered on the data form, but the Q rating is based on observations along the right wall. If there are only a few joints visible, the joints are counted as "random joints" when evaluating Jn. Table 10 explains the joint-number rating system.

Fracturing Description	Category Number	Jn Rating
Massive	Jn. 00	1
One joint set	Jn. 10	2
One + random	Jn. 11	3
Two joint sets	Jn. 20	4
Two + random	Jn. 21	6
Three joint sets	Jn. 30	9
Three + random	Jn. 31	12
Four or more sets, heavily jointed, sugar cube	Jn. 40	15
Crushed Rock	Jn. 50	20

Table 10. Q system Joint-Number Rating

The histogram in Figure 58 depicts the frequency of joint-set numbers throughout the Main Drift. There are predominantly three joint sets; sometimes 2 + random (shown below as 6) and 3 +

random (shown below as 12); but for the most part, there are three (shown below as 9).

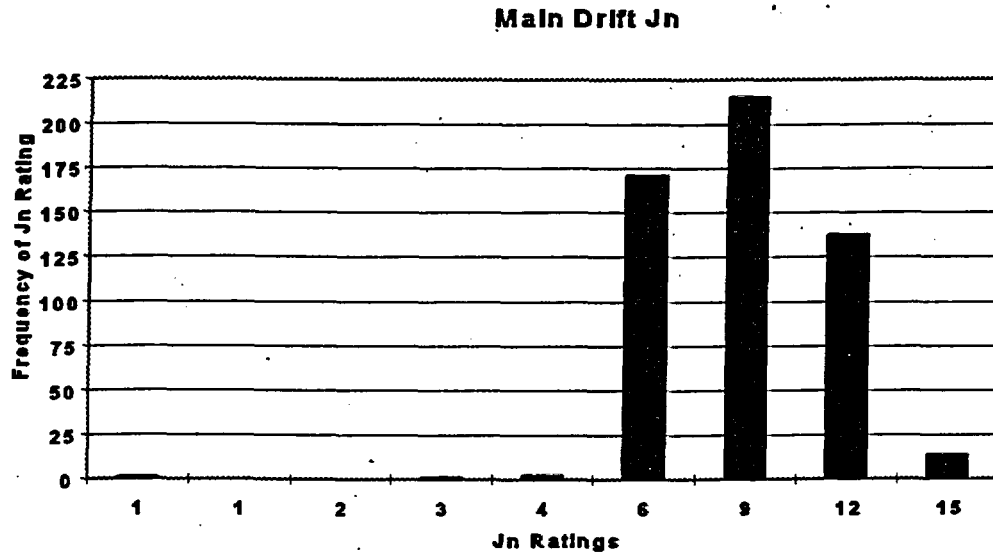


Figure 58. Frequency of Joint Set Ratings in the Main Drift

Joint-Set Orientation

For each joint set identified, the strike (degrees) and dip (degrees) of that set are measured or estimated.

Jr Rating

Joint roughness is related to the shear strength of the rock. The joint-roughness rating considers the small-scale roughness of the fracture surface in combination with the large-scale roughness. Small-scale roughness is divided into three broad categories: rough, smooth and slickensided. Large-scale roughness describes the increase in shear strength of a joint due to undulations of the surface which induce displacements of the rock normal to the direction of movement during shearing. These large scale surface shapes are assigned one of two category descriptions: planar or undulating. Joint roughness is determined for each joint set entered on the field data form. The Jr rating assigned to each set is conservatively based on those fractures which are smoother

than the average for the set. The rating may not include the single worst joint condition but will always indicate roughness below the average for the set.

Joint-Alteration Rating

Joint alteration describes conditions which may reduce the stability of rock blocks in the tunnel. The quotient J_r/J_a describes the inter-block shear strength.

Joint-Water Rating

The Main Drift, as well as the Exploratory Studies Facility excavation is dry.

Stress-Reduction-Factor Rating

The stress reduction factor considers loosening loads, *in situ* stress, and squeezing or swelling loads. For field-form notation, a category, SRF.40, was added to the original system to indicate no related reduction in the rock-quality rating. Stress-reduction factors at Yucca Mountain are most often related to fracture zones intersecting the excavation. As discussed in the introduction, the rating length limits the use of categories SRF. 31 and SRF. 34. The shear zones described in the table are features which influence the surrounding rock. One would expect an influence zone of, for example, 2 meters on either side of the shear. Given that size zone and a rating length of 5 meters, significant multiple shear zones are not a probability. If longer rating lengths were used, multiple shear zones would often be encountered. Table 11 shows the ratings for stress-reduction factor.

Description of the stress condition			Category	SRF
Weakness zones cause loosening of the rock				
Multiple weakness zones containing clay or chemically disintegrated rock, loose surrounding rock			SRF. 31	10
Single weakness zone containing clay (depth < 50 m)			SRF. 32	5
Single weakness zone containing clay (depth > 50 m)			SRF. 33	2.5
Multiple shear zones, competent rock, loose surrounding rock			SRF. 34	7.5
Single shear zone in competent rock (depth < 50 m)			SRF. 35	5
Single shear zone in competent rock (depth > 50 m)			SRF. 36	2.5
Loose open joints, heavily jointed			SRF. 37	5
Competent rock, stress factors	σ_c/σ_1	σ_t/σ_1		
Competent rock no stress problems			SRF. 40	1
Low stress near surface	>200	>13	SRF. 41	2.5
Medium stress	200 - 10	13 - .66	SRF. 42	1
High Stress (range .5 - 2 evaluate case by case)	10 - 5	.66 - .33	SRF. 43	1
Mild rock burst (range 5 - 10 evaluate case by case)	5 - 2.5	.33 - .16	SRF. 44	10
Heavy rock burst (range 10 - 20 evaluate case by case)	< 2.5	<.16	SRF. 45	20
Mild squeezing (range 5 - 10 evaluate case by case)			SRF. 51	10
Heavy squeezing (range 10 - 20 evaluate case by case)			SRF. 52	20
Swelling rock, chemical swelling stress factors				
Mild swelling (range 5 - 10)			SRF. 61	10
Heavy swelling (range 10 - 20)			SRF. 62	20
σ_1 - major principal stress, σ_c - unconfined compressive strength, σ_t - tensile strength				

Table 11. Q system Stress-Reduction-Factor Rating

Summary of Rated Q

Two Q values were calculated for each 5-meter section of the main drift. The value reported as the Q rating for any section is called the Rated Q. This value is determined using the lowest Jr/Ja ratio from within the 5-meter interval. The second Q value, called Q Max is calculated using the highest Jr/Ja ratio within the 5-meter interval. All other parameters, RQD/Jn and Jw/SRF, within equation 4 remain constant for both Rated Q and Q Max.

Table 12 summarizes Rated Q percentages throughout the entire Main Drift. The histogram in Figure 59 shows the distribution of the Rated Q values. The most frequent rating is a value of between 1 and 4, which warrants a *poor* rating.

Rated Q Value	Rock Quality Description	Percentages in the Main Drift
0.1 - 1	Very Poor	12%
1 - 4	Poor	51%
4 - 10	Fair	27%
10 - 40	Good	9%
40 - 100	Very Good	1%

Table 12. Percentages of Rated Q

Main Drift Rated Q

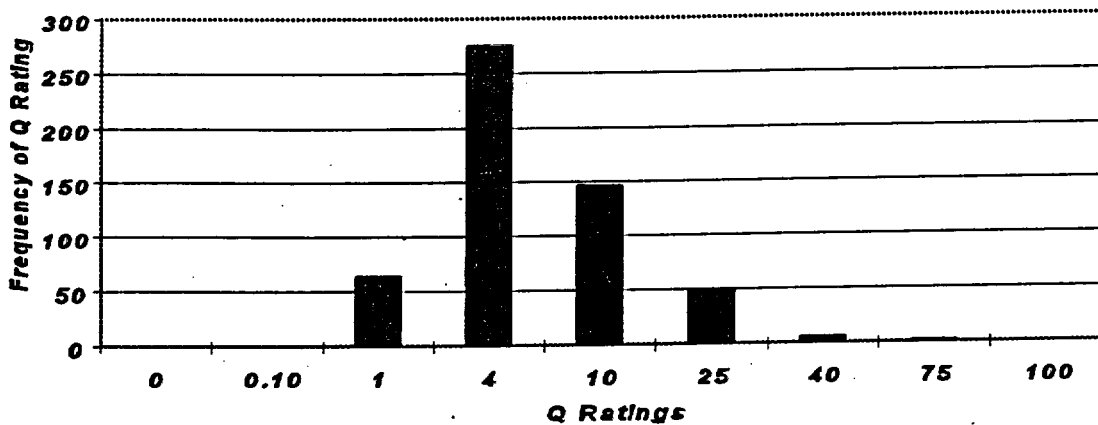


Figure 59. Value of rated Q for the Main Drift

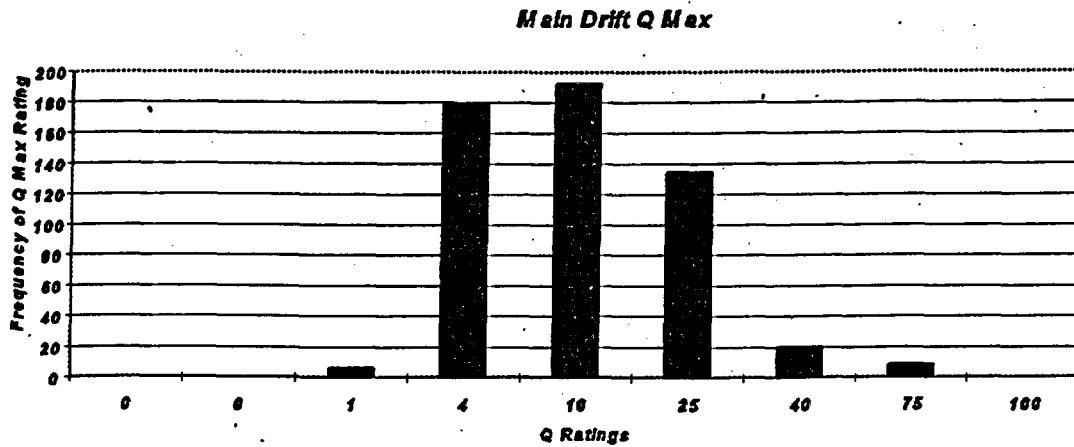


Figure 60. Maximum Value of Q for the Main Drift

The histogram in Figure 60 shows the frequency of Q Max. The most frequent rating for the Q Max value is between 4 and 10, which warrants a *fair* rating.

The overall rock quality Rated Q average for the entire Main Drift is 4.58, or *fair*, see Figure 61. Figures 62 through 65 graphically depict the values of Rated Q and Q Max.

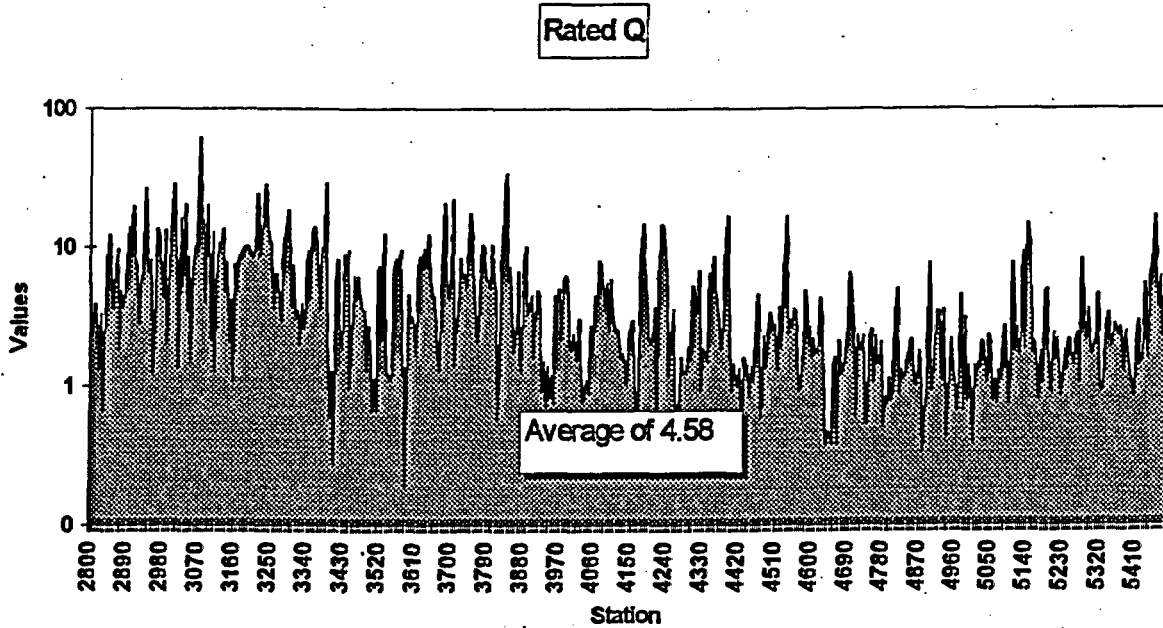


Figure 61. Rock Quality Rated Q for the Main Drift

**Rated Q and Q Max For Domain One
28+00 - 37+00**

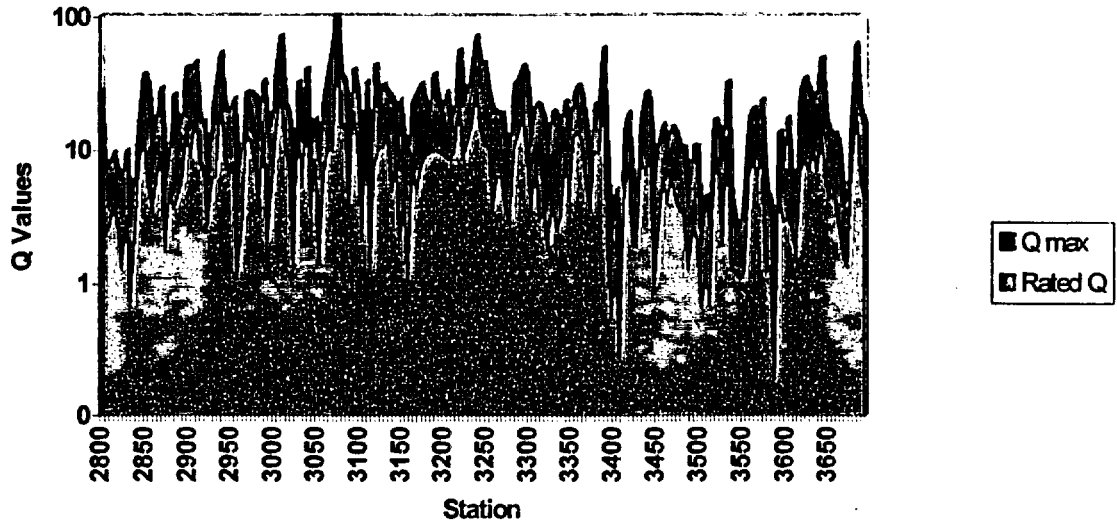


Figure 62. Main Drift rated Q and Q Max. For Domain One, Sta. 28+00 to 37+00

**Rated Q and Q Max For Domain Two
37+00 - 42+00**

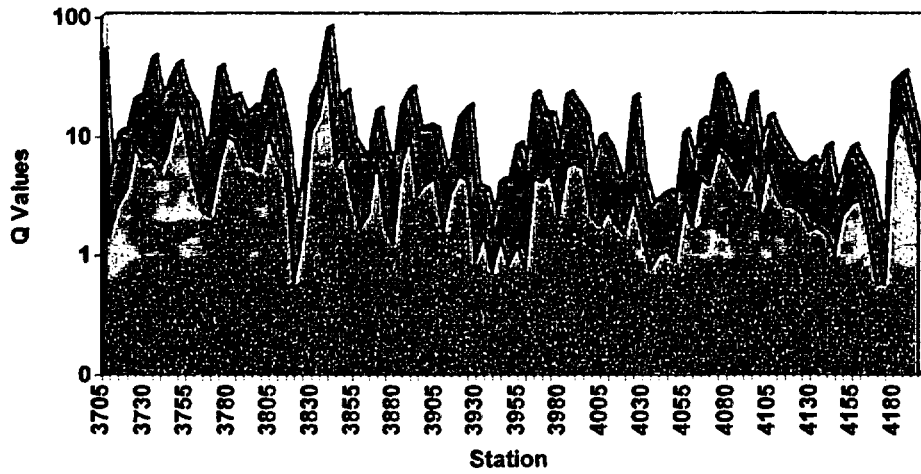


Figure 63. Main Drift Rated Q and Q Max. For Domain Two, Sta. 37+00 to 42+00

**Rated Q and Q Max For Domain Three
42+00 - 51+50**

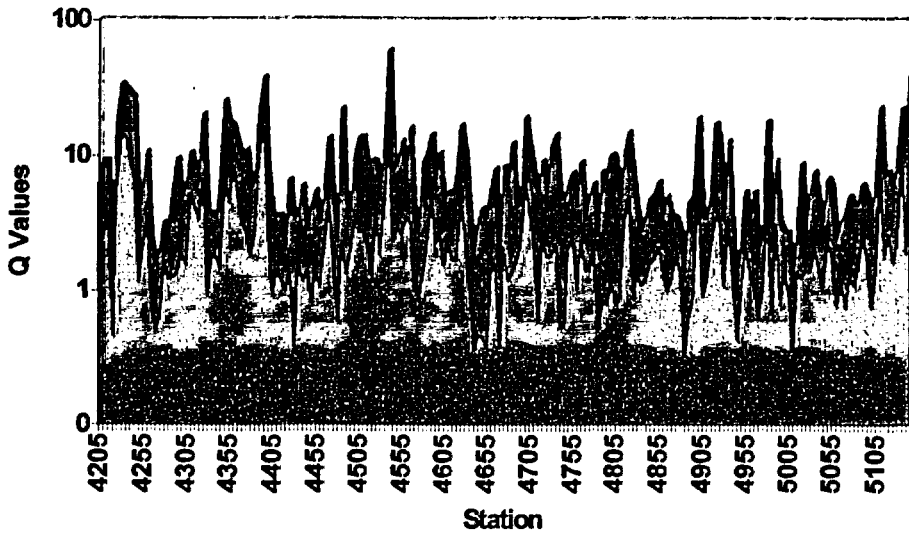


Figure 64. Main Drift Rated Q and Q Max. For Domain Three, Sta. 42+00 to 51+50

**Rated Q and Q Max For Domain Four
51+50 - 55+00**

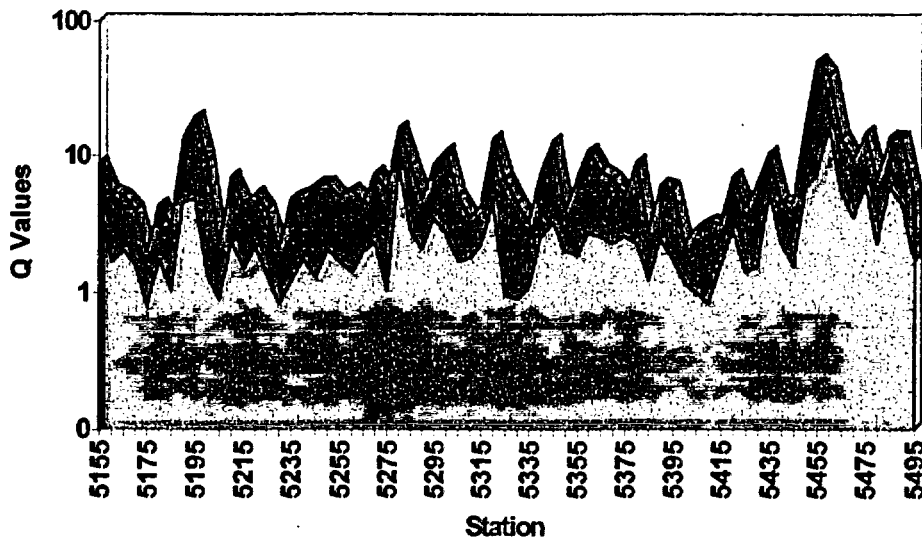


Figure 65. Main Drift Rated Q and Q Max. For Domain Four, Sta. 51+50 to 55+00

Ratios

Equation 4 is used to calculate the Q value which is essentially composed of three significant ratios. These three parameters -- (1) Block size $\{RQD/J_n\}$, (2) Inter-block shearing strength $\{J_r/J_a\}$, (3) Active stress $\{J_w/SRF\}$ -- relate to tunneling conditions described as follows:

- The first quotient, RQD/J_n , represents the overall structure of the rock mass and is a crude measure of the relative *block size*. The larger the ratio, the higher the values.
- The second quotient, J_r/J_a , represents the roughness and frictional characteristics of the joint walls or filling materials. This quotient is weighted in favor of rough, unaltered joints with little or no separation (in direct contact). Such surfaces will be close to peak strength, tend to dilate significantly when sheared and, therefore, be especially favorable to tunnel stability. This quotient is a fair approximation of the actual *shear strength* expected of the various combinations of wall roughness and alteration. The larger the ratio, the higher the values.
- The third quotient, J_w/SRF consists of two stress parameters. J_w is a measure of water pressure, which has an adverse effect on the shear strength of joints because of a reduction in normal stress. The parameter SRF is a measure of (1) loosening load in the case of excavation through shear zones and clay bearing rock, (2) rock stress in competent rock, and (3) squeezing or swelling loads in plastic, incompetent rock. It can be regarded as a total-stress parameter. The quotient (J_w/SRF) is a complicated empirical factor describing the Q-system "active stresses". The term does not refer specifically to the insitu state of stress in the rock, but includes mechanical effects, effects of shears, and chemical behavior, as well as strength of material and insitu stress. The larger the ratio, the lower the values.

Figures 66 through 69 show the *block size* ratios for each of the four domains identified within the

Main Drift Report.

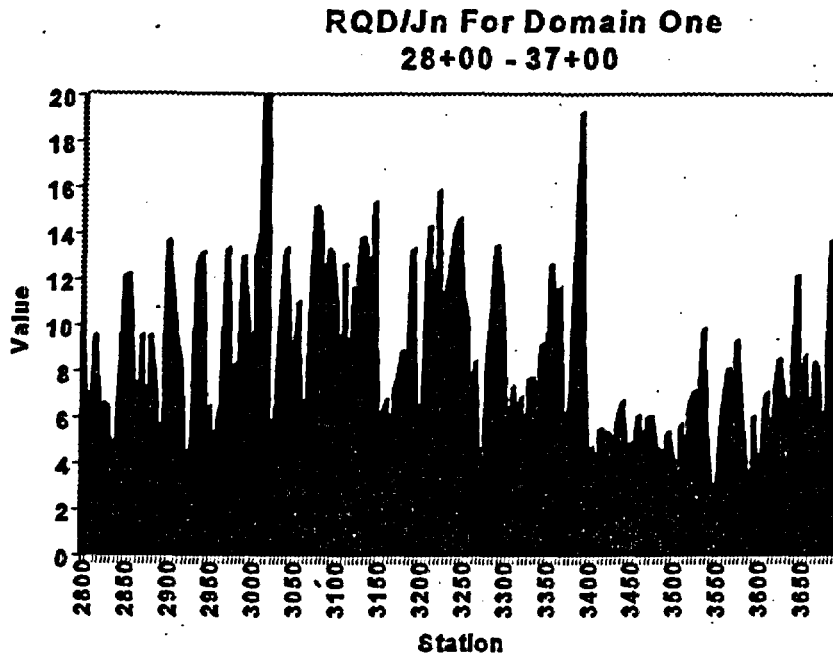


Figure 66. Block-Size-Ratio Comparisons For Domain One, Sta. 28+00 to 37+00

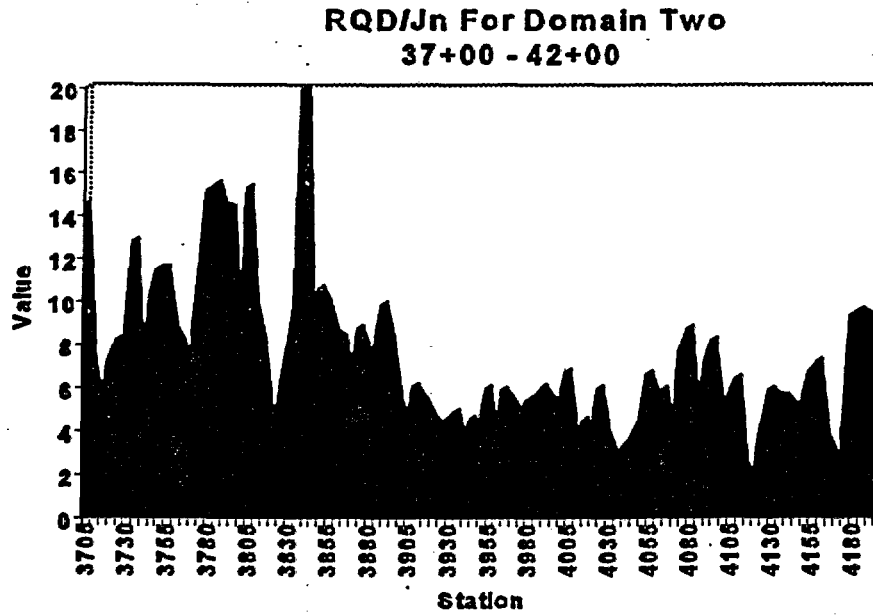


Figure 67. Block-Size-Ratio Comparisons For Domain Two, Sta. 37+00 to 42+00

**RQD/Jn For Domain Three
42+00 - 51+50**

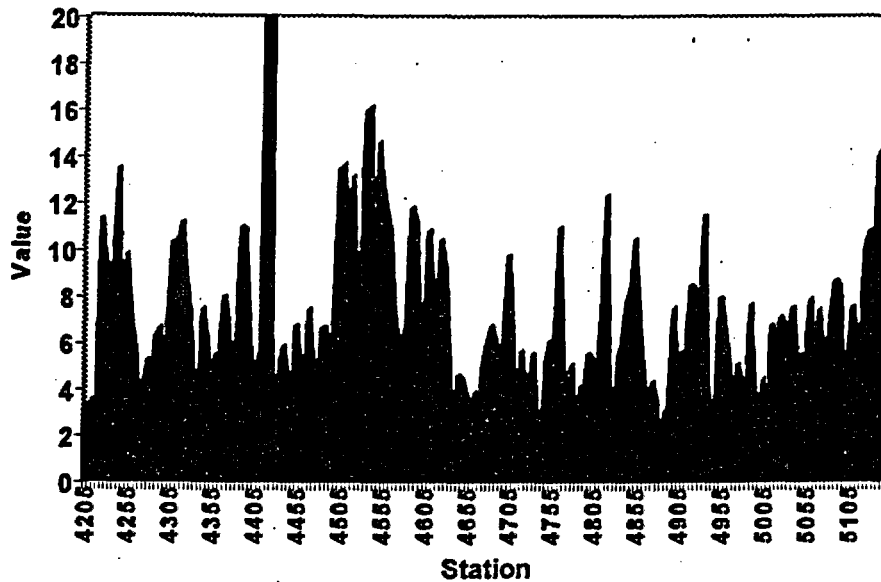


Figure 68. Block-Size-Ratio Comparisons For Domain Three, Sta. 42+00 to 51+50

**RQD/Jn For Domain Four
51+50 - 55+00**

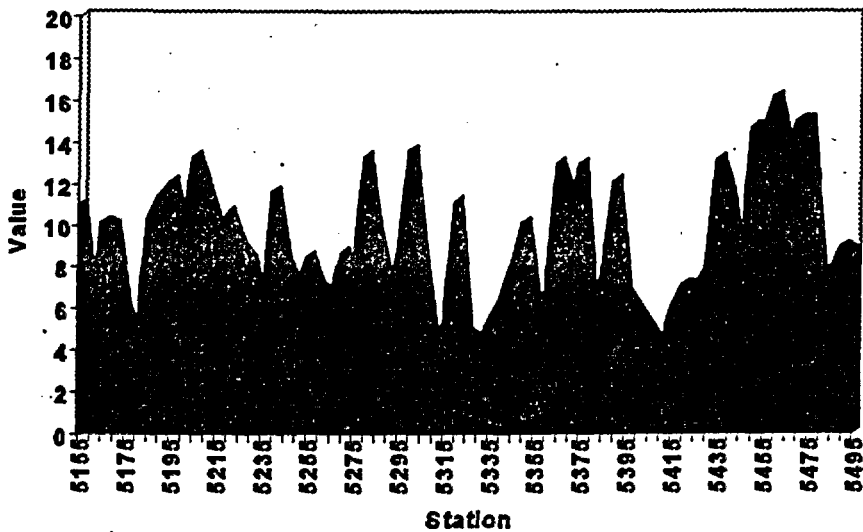


Figure 69. Block-Size-Ratio Comparisons For Domain Four, Sta. 51+50 to 55+00

Figures 70 through 73 show the *shear strength* ratios for each of the four domains identified within the Main Drift Report.

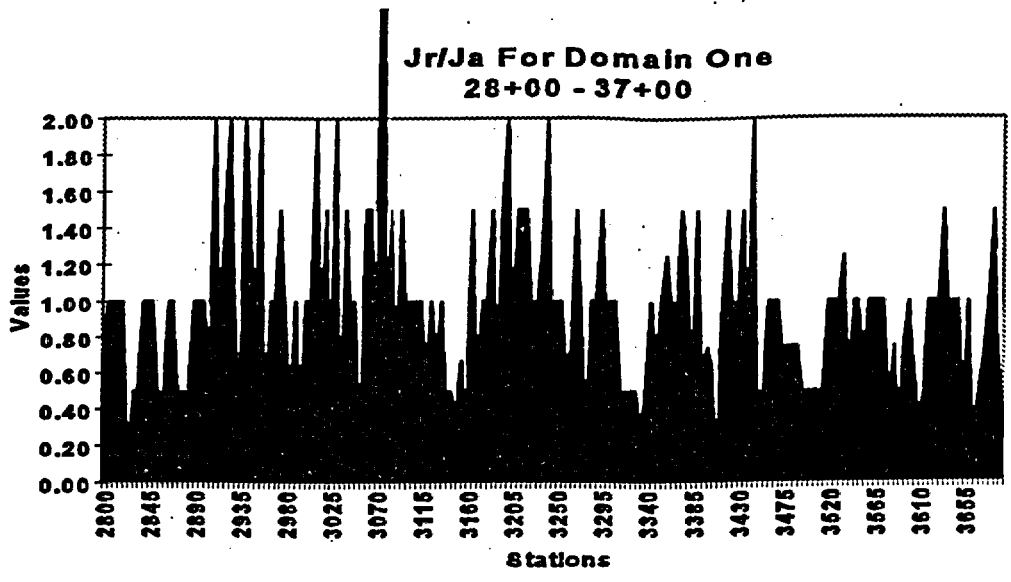


Figure 70. Shear-Strength-Ratio Comparisons For Domain One, Sta. 28+00 to 37+00

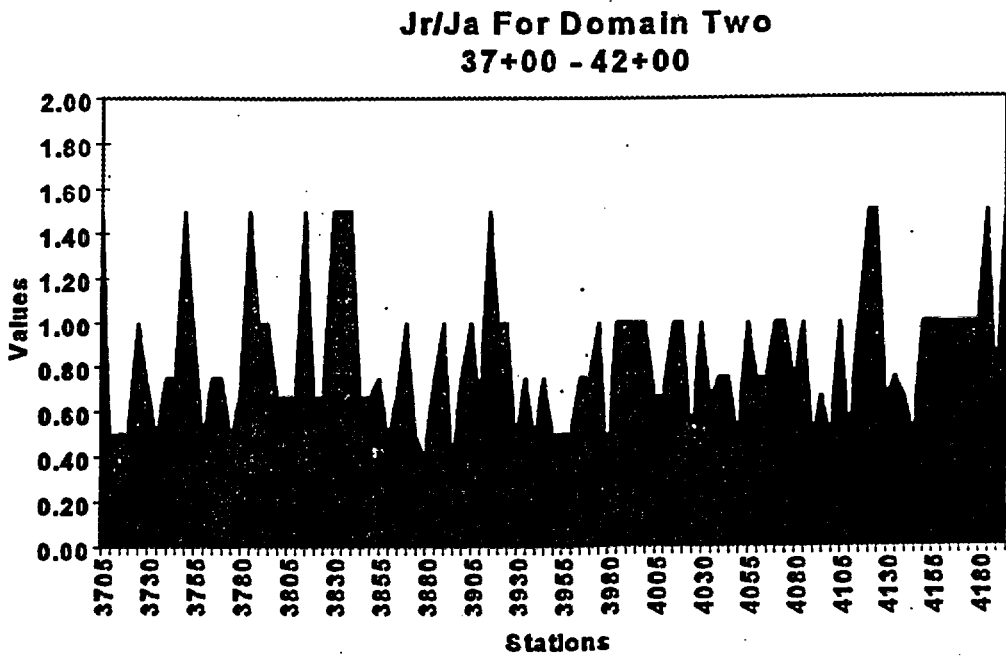


Figure 71. Shear-Strength-Ratio Comparisons For Domain Two, Sta. 37+00 to 42+00

**Jr/Ja For Domain Three
42+00 - 51+50**

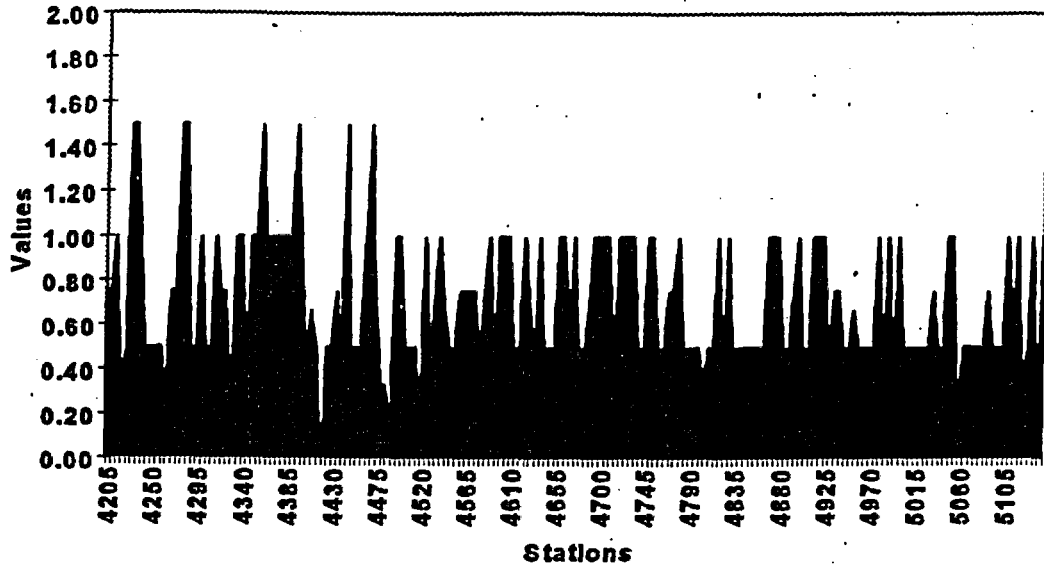


Figure 72. Shear-Strength-Ratio Comparisons For Domain Three, Sta. 42+00 to 51+50

**Jr/Ja For Domain Four
51+50 - 55+00**

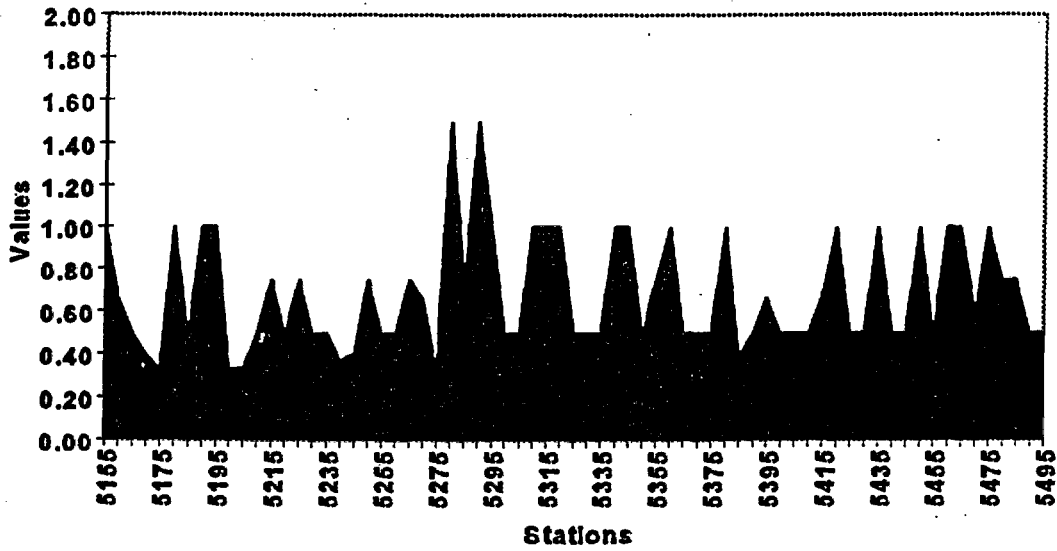


Figure 73. Shear-Strength-Ratio Comparisons For Domain Four, Sta. 51+50 to 55+00

Figures 74 through 77 show the *active stress ratios* for each of the four domains identified within the Main Drift Report.

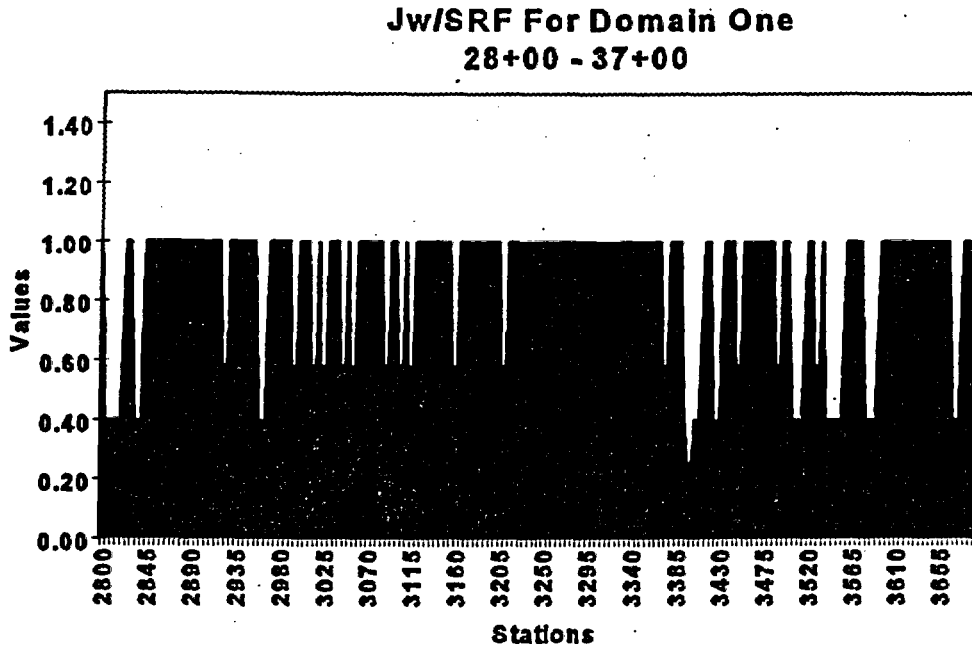


Figure 74. Active-Stress-Ratio Comparisons For Domain One, Sta. 28+00 to 37+00

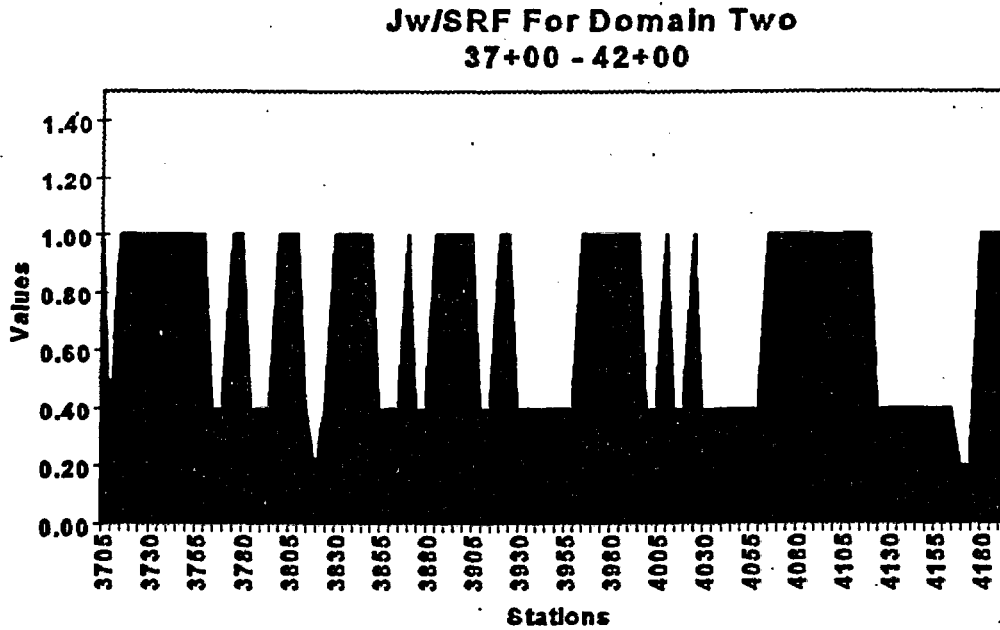


Figure 75. Active-Stress-Ratio Comparisons For Domain Two, Sta. 37+00 to 42+00

**Jw/SRF For Domain Three
42+00 - 51+50**

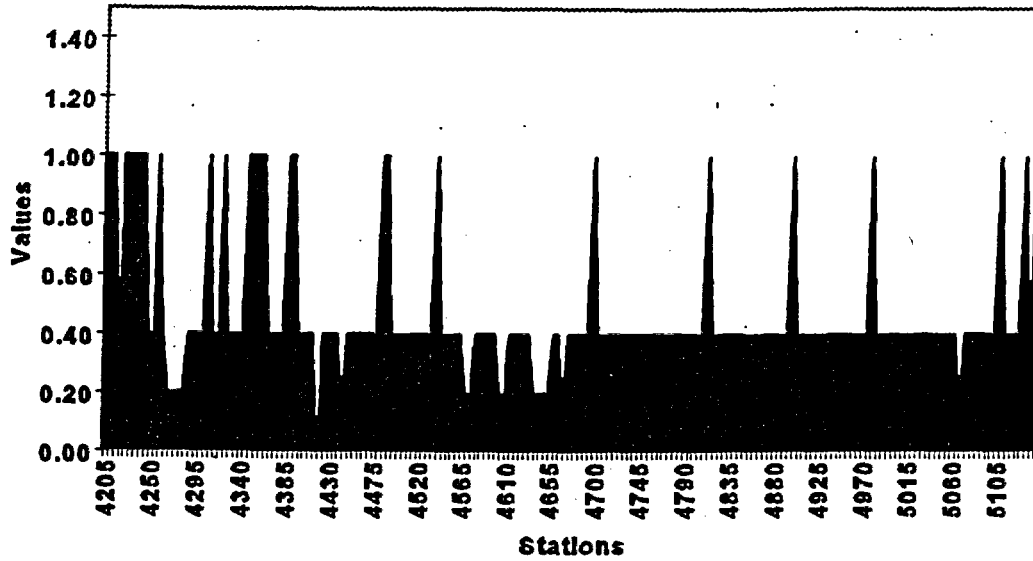


Figure 76. Active-Stress-Ratio Comparisons For Domain Three, Sta. 42+00 to 51+50

**Jw/SRF For Domain Four
51+50 - 55+00**

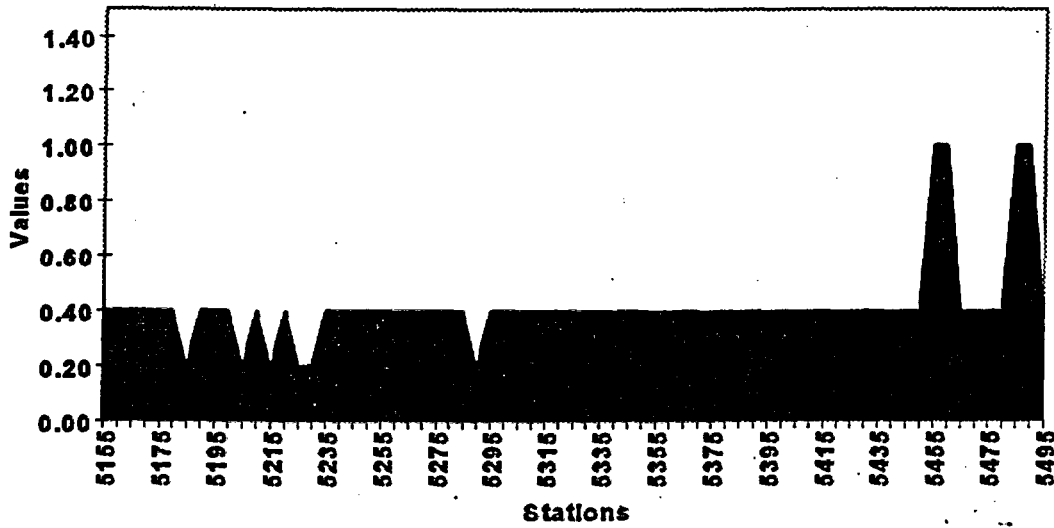


Figure 77. Active-Stress-Ratio Comparisons For Domain Four, Sta. 51+50 to 55+00

Orientation of Critical Joint Sets For Rated Q

The two figures below show the orientations of the Rated Q and Q Max. In calculating Q, fracture orientation is not a specific factor; therefore, the lowest value of the ratio J_r/J_a is used to calculate Rated Q, and the highest ratio is used to calculate Q Max. Figure 78 clearly shows that the most frequent fractures are from 105° to 150° and 200° to 250° . The worst fracture orientations fall either very close to or within the parallel range. Parallel with the tunnel heading and steeply dipping fractures produce the lowest Q ratings.

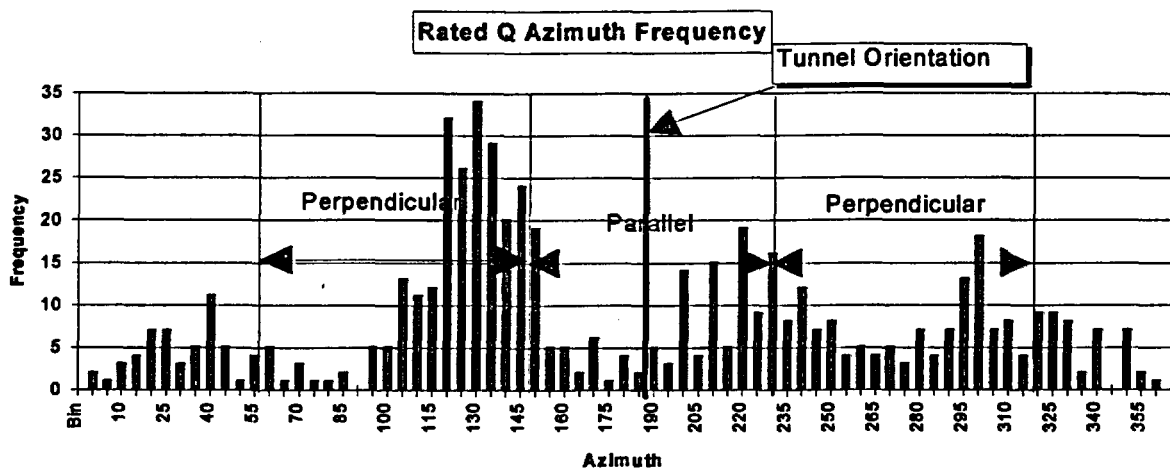


Figure 78. Frequency of Azimuths Used to Calculate Rated Q

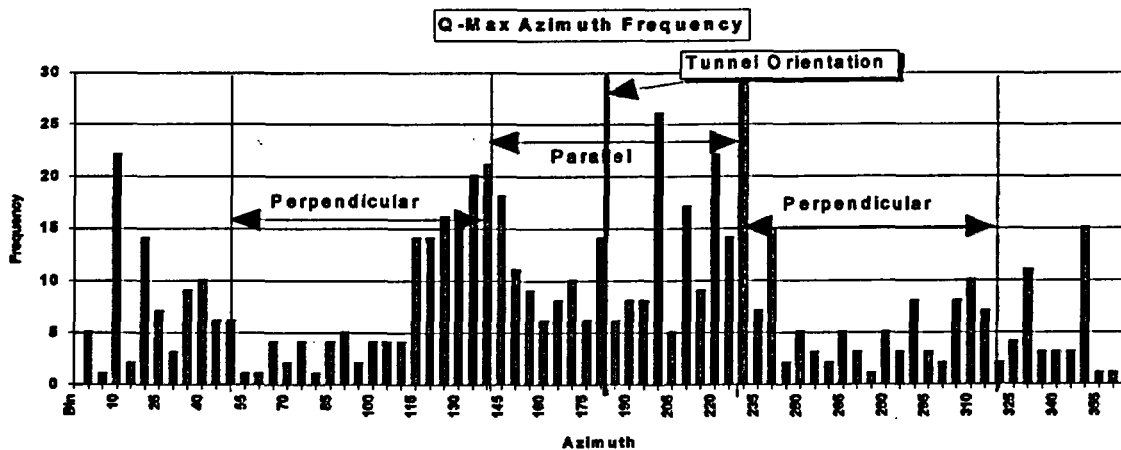


Figure 79. Frequency of Azimuths Used to Calculate Q Max.

Table 13 summarizes the averages of the rock mass classification systems and shows the ratios for each of the domains and sub-domains identified within the Main Drift.

Station	Rated Q	Q Max	RMR	RQD
28 - 37	7.39	13.38	61	63
28 - 34	8.81	15.47	62	66
34 - 37	4.57	9.22	58	57
37 - 42	4.7	9.39	61	66
37 - 39	6.97	13.07	63	74
39 - 42	3.19	6.94	59	60
42 - 51+50	2.48	5.74	57	55
42 - 44	4.13	7.25	60	57
44 - 51+50	2.04	5.33	56	54
51+50 - 55	2.80	5.54	60	67
Station	Rated Q	RQD/Jn	Jr/Ja	Jw/SRF
28 - 37	7.39	8.02	0.97	0.86
28 - 34	8.81	9.07	1.03	0.9
34 - 37	4.57	5.92	0.85	0.80
37 - 42	4.7	7.09	0.84	0.72
37 - 39	6.97	9.74	0.83	0.79
39 - 42	3.19	5.33	0.85	0.67
42 - 51+50	2.48	7.25	0.72	0.47
42 - 44	4.13	6.81	0.86	0.65
44 - 51+50	2.04	7.37	0.68	0.43
51+50 - 55	2.80	9.12	0.69	0.43

Table 13. Summary of Rock Mass Classification Averages

Ground Support

General

Analysis of drill-hole core indicated that low-quality rock would be encountered in the Main Drift excavation. As expected, using the Q system ratings, *poor* to *fair* quality rock was excavated through most of the Main Drift excavation. This section describes the type of support anticipated in the construction documents, and compares the theoretical support based on design documents with the actual ground support installed in the Main Drift.

The design support includes rock support with welded wire fabric (category 1), to rock support with welded wire fabric and shotcrete (category 3), to structural steel supports (steel sets) with lagging (category 4). The actual support installed in the Main Drift was either category 1 or category 3. Shotcrete was not used in the Main Drift. Understanding the reluctance to use shotcrete is critical to a reasonable interpretation of the Figures presented later in this section. Shotcrete was not used in the Main Drift for two reasons:

- 1) For construction convenience and efficiency, the contractor elected to install either rock bolts reinforcement or steel sets and to forego the use of shotcrete for ground support.
- 2) The routine use of shotcrete for ground support would be detrimental to geologic mapping, full periphery photography, and rock-characterization efforts.

The stability of the excavation and, consequently, the required ground support is significantly affected by the method of excavation. Tunnel-boring machine excavation in the Main Drift produces a much more stable excavation than that produced by the drill-and-blast method. Theoretical ground support based on the Q rock mass quality rating does not directly consider the method of excavation. The effects of these two factors, elimination of shotcrete and TBM excavation, explain some of apparent differences in rated and actual support.

One final consideration with regard to ground support is the need to immediately supplement the actual support installed during excavation. Through the tunnel, many 5-m intervals indicate the need for category 3 support (rock reinforcement with shotcrete). Again, this calculation does not consider the beneficial effect of the method of excavation. Based on observation of the stability of the opening, immediate action is not required. Developing performance problems may be detected by simple visual observation of the opening and by interpretation of structural instrumentation data. The decision to install additional shotcrete for ground support should include at least two considerations:

- 1) The final lining requirements for the tunnel should be established before an extensive program of supplemental ground support is undertaken. If a final lining is planned for the entire tunnel, the permanent lining can be designed as supplemental ground support.
- 2) The positive effect of the TBM excavation vs. drill-and-blast excavation should be evaluated. Such an empirical analysis is beyond the scope of this data collection effort; however, the need for additional ground support may be minimized by careful consideration of the data collected in the tunnel, coupled with mathematical models of the excavation.

The following sections describe ground-support elements and discuss the implications of rock mass quality ratings for seven reaches of the Main Drift.

Classes of Support

Support categories used in comparisons of installed versus calculated ground support are described in Table 14 below. These descriptions are taken from drawing BAABEE0000-01717-2100-40151-00, titled "7.2 m Tunnel Ground Support Master Sections" effective April 16, 1996. The original ground-support drawings used the term "category" and did not include Classes 2a and 3a. In this report, the terms "ground-support class" and "ground-support category" are used interchangeably, and both refer to the descriptions in Table 14.

Ground Support Class	Description of Class of Support
1	8 rockbolts 1.5- x 1.5-m spacing with welded-wire fabric (wwf)
2	15 rockbolts 1.0- x 1.0-m spacing with wwf
2a	w6 steel sets 1220-mm spacing with wwf and lagging
3	15 rockbolts 1.0- x 1.0-m spacing with wwf and shotcrete
3a	w6 x 20 steel sets 1220-mm spacing with wwf
4	w8 x 31 steel sets 610 - 1220-mm spacing with wwf and crown lagging
5	w8 x 31 steel sets 610-mm spacing with full lagging

Table 14. YMP Design Ground-Support Classes

Installed versus Rated Ground Support

The theoretically required ground support, designated rated support, is based on a calculation of the rock quality rating, Q and two parameters of the Q rating RQD/Jn and Jr/Ja. The methodology used to determine support is described on drawing BABEAB0000-01717-2100-40151, titled "TS North Ramp Ground Support Master Elevation and Sections," accepted for construction October 13, 1991.

The ground support actually installed in the Main Drift is determined by the excavation contractor. The heading crew selects rock reinforcement or steel sets and lagging for support based on their experience in similar conditions and their estimate of loosening loads. As discussed

previously, shotcrete, and therefore Category 3 support, are not used for routine ground support. Table 15 summarizes the ground support. Note, categories 3a and 5 were not installed or rated in this portion of the tunnel.

Class of Support	Rated %	Installed %
1	22%	78%
2	0%	0%
3	78%	0%
4	0%	22%

Table 15. Rated and Installed Ground Support in the Main Drift

The histograms in Figures 80 and 81 below, depict the frequency of installed and rated ground support in the Main Drift of the ESF. Since the plotting software requires a numerical value for the independent axis of the graph, category 3a is identified as category 3.1.

Frequency of Installed Support

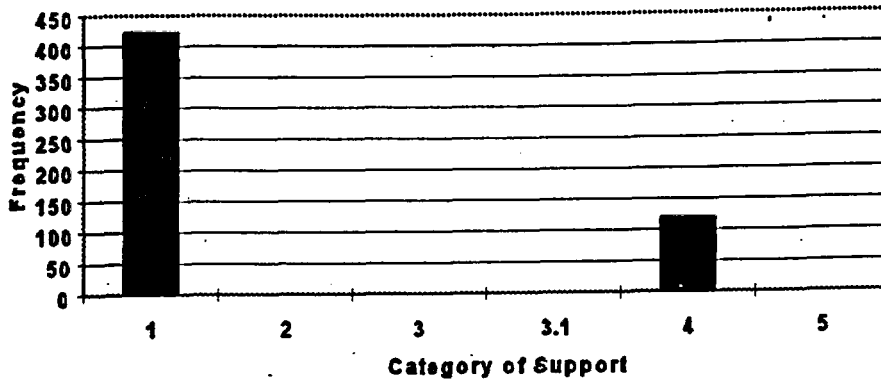


Figure 80. Installed Support Frequency

Rated Ground Support Requirements

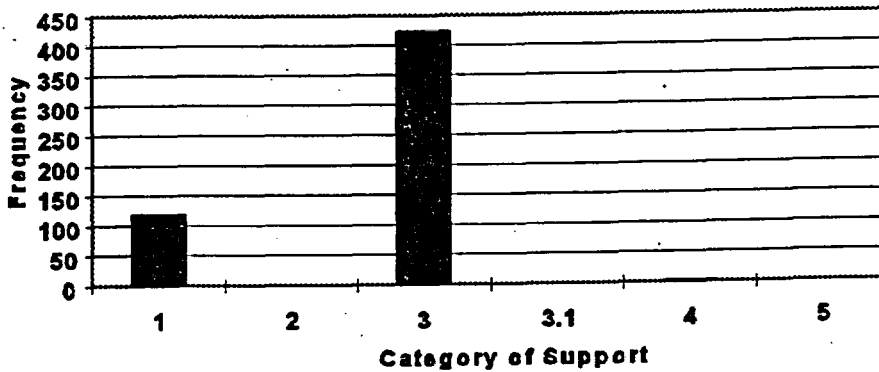


Figure 81. Rated Support Frequency

Ground-support requirements are based on YMP ground support guidelines. These guidelines not only use the calculated Q values, but also are based on the associated Q parameters (RQD/J_n and J_r/J_a). Figures 82 through 85 provide a graphical presentation of installed versus rated ground support for each of the four domains in the Main Drift.

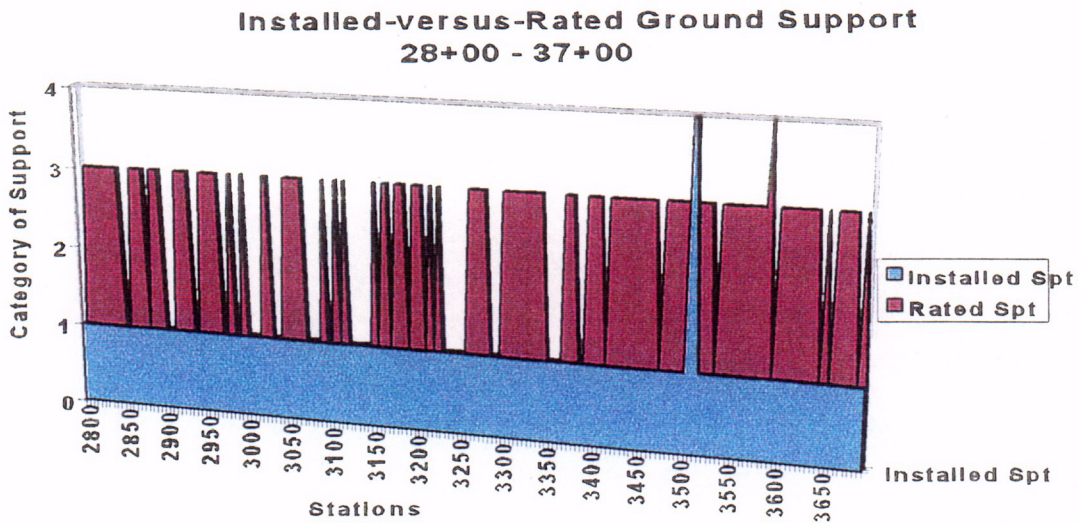


Figure 82. Installed-versus-Rated Ground-Support Requirements Sta. 28+00 to 37+00

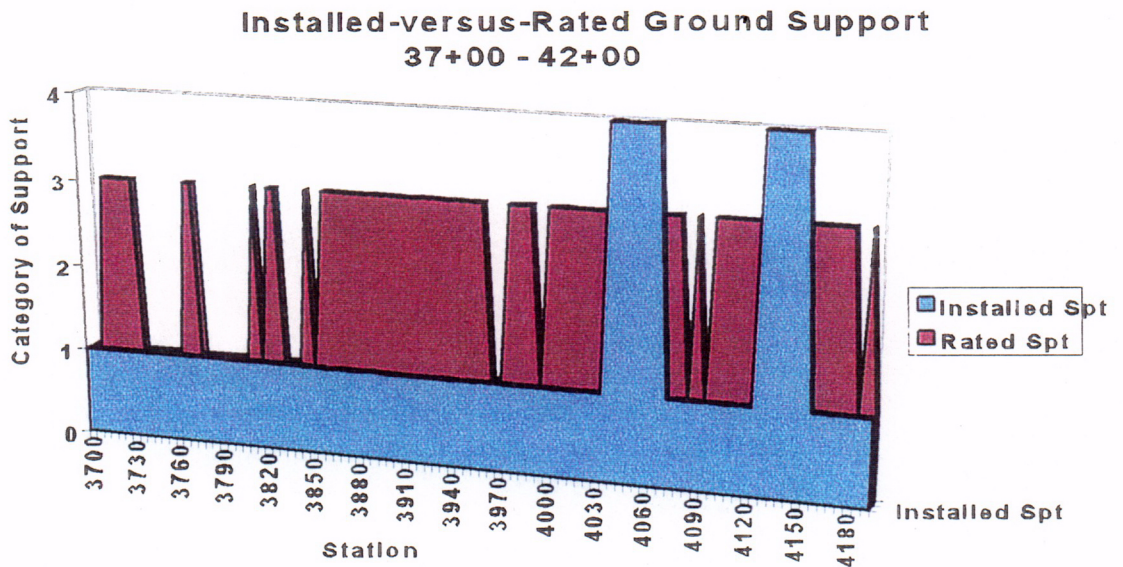


Figure 83. Installed-versus-Rated Ground-Support Requirements Sta. 37+00 to 42+00

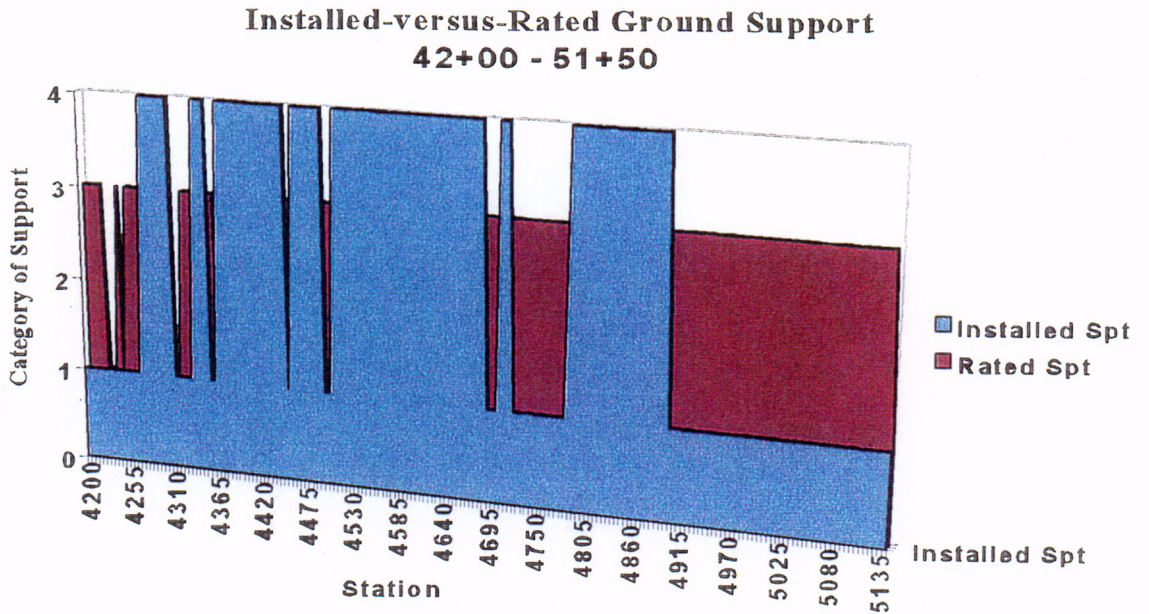


Figure 84. Installed-versus-Rated Ground-Support Requirements Sta. 42+00 to 51+50

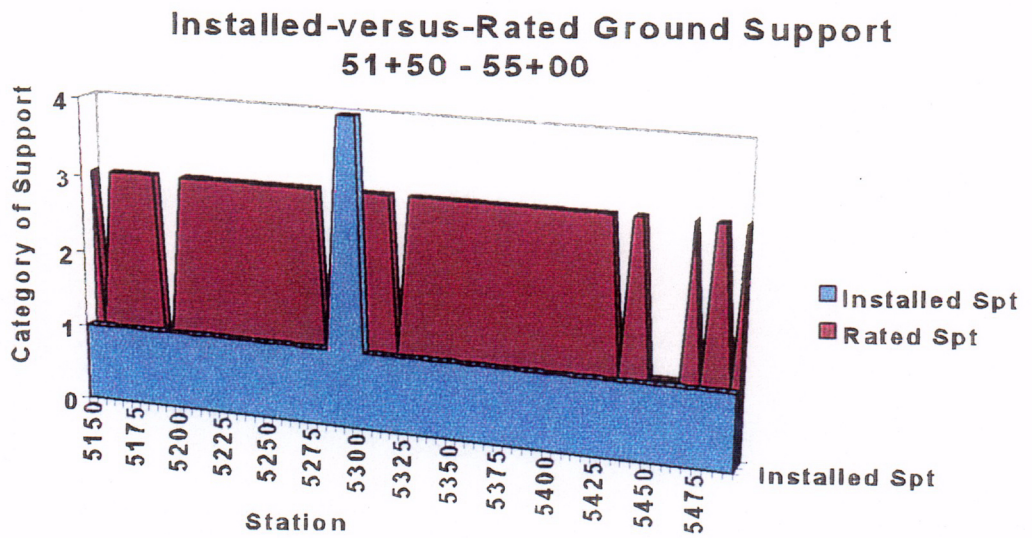


Figure 85. Installed-versus-Rated Ground-Support Requirements Sta. 51+50 to 55+00

C-05

Summary of Ground Support

Table 16 below shows a comparison of installed and rated support for selected reaches of the tunnel. Within the first three domains, subsections were selected which appear to exhibit similar patterns of rock quality ratings and similar patterns of rated support. The fourth domain was not subdivided. These subsections are discussed in more detail in the paragraphs following the table.

Station	Installed Ground Support				Rated Ground Support					
	1		4		1		3		4	
	m	%	m	%	m	%	m	%	m	%
28+00 - 37+00	890	99%	10	1%	305	34%	590	65%	5	1%
28+00 - 34+00	600	100%	--	--	265	44%	335	56%	--	--
34+00 - 37+00	290	97%	10	3%	40	13%	255	85%	5	2%
37+00 - 42+00	435	87%	65	13%	140	28%	360	72%	--	--
37+00 - 39+00	200	100%	--	--	100	50%	100	50%	--	--
39+00 - 42+00	235	78%	65	12%	40	13%	260	87%	--	--
42+00 - 51+50	450	47%	500	53%	80	8%	870	92%	--	--
42+00 - 44+00	110	55%	90	35%	45	23%	155	77%	--	--
44+00 - 51+50	340	45%	410	55%	35	5%	715	95%	--	--
51+50 - 55+00	335	96%	15	4%	60	17%	290	83%	--	--

Table 16. Ground-Support Summary

The following paragraphs discuss various sections of the tunnel to provide more detail on the apparent discrepancy between theoretically rated and installed ground support. These paragraphs broadly describe areas which may warrant consideration for additional ground support. While calculation of the theoretical support requirement suggests a significant length of the tunnel may require additional support, the decision to add ground support should be based on an analysis of the excavation. Considerations include the nearly undamaged periphery due to TBM excavation, the results of tunnel instrumentation, and environmental factors (i.e., long-term dust control).

Stations 28+00 - 34+00

Within domain one, this section has an average Q value of 8.81 (*fair*) and a block-size ratio (RQD/Jn) of 9.07. The summary of 5-meter sections, Table 16, shows 56 percent category 3 ground support is required. ESF TS North Ramp Ground Support Guidelines indicate that for rock quality Q between 5.5 and 10 and RQD/Jn < 10 category 3 support is required. If the block-size ratio were 10 or greater, the recommended category of support would be category 1.

- In 44 percent of this section, the installed support equals the theoretical support; all rated category 1.
- Based on average Q parameters, the rated category 3 support appears to be on the borderline with category 1. Additional ground support will not be required through most of this section.

Stations 34+00 - 37+00

Within domain one, this section has an average Q value of 4.57 (*fair*) and a block-size ratio (RQD/Jn) of 5.92. The ESF TS North Ramp Ground Support Guidelines indicate that for Q ratings between 4.0 and 5.5 and RQD/Jn > 5, category 1 support is required. For the same range of Q values, if the RQD/Jn < 5, category 3 support is required. The summary of 5-meter sections shows 85 percent category 3 ground support is required.

- In 16 percent of this section, the installed support equals or exceeds the theoretical support requirement (13 percent rated category 1, 3 percent installed category 4).
- Average values imply significant lengths of category 1 support in this reach. The difference between rated support and installed support in this section may be resolved by review of the theoretical support-rating system. If a significant portion of the 5 meter Q values are above 5.5, then RQD/Jn values less than 10 would require category 3 support. Q values below 4.0 would also indicate category 3

support. The averages fall in a range from which departure above or below crosses the border to category 3 support. Additional ground support will not be required through most of this section.

Stations 37+00 - 39+00

Within domain two, this section has an average Q value of 6.97 (*fair*) and a block-size ratio (RQD/Jn) of 9.74. These values are very similar to those in subsection 28+00 to 34+00 discussed above and the conclusions are the same.

- In 50 percent of this section, the installed support equals the theoretical support; all rated category 1.
- Based on average Q parameters, the rated category 3 support appears to be on the borderline with category 1. Additional ground support will not be required through most of this section

Stations 39+00 - 42+00

Within domain two, this section has an average Q value of 3.19 (*poor*), a block-size ratio (RQD/Jn) of 5.33, and an inner block shear ratio (Jr/Ja) of 0.85. Based on ESF TS North Ramp Ground Support Guidelines, 13 percent category 1 and 87 percent category 3 ground support would be required. Increases in the values of the block-size ratio to 10 and the inner-block shear ratio to a value above 1.0 would change the recommended support to category 2.

- In 25 percent of this section, the installed support equals or exceeds the theoretical support; 13 percent rated category 1- and 12-percent-installed category 4.
- Seventy-five percent of this reach theoretically could be considered for additional ground support.

Stations 42+00 - 44+00

Within domain three, this section has an average Q value of 4.13 (*fair*) and a block-size ratio (RQD/Jn) of 6.81. The summary of 5-m sections from Table 16 shows 23 percent category 1 and 77 percent rated category 3 ground support. ESF TS North Ramp Ground Support Guidelines recommend category 1 support for rock quality Q between 4.0 and 5.5 with RQD/Jn > 1. From Table 16, based on ESF TS North Ramp Ground Support Guidelines, 13 percent category 1 and 87 percent category 3 ground support is required.

- In approximately 68 percent of this section, the installed support equals or exceeds the theoretical support; 23 percent rated category 1 and 35 percent installed category 4.
- Thirty-two percent of this reach theoretically could be considered for further analysis and additional ground support.

Stations 44+00 - 51+50

Within domain three, this section has an average Q value of 2.04 (*poor*), a block-size ratio (RQD/Jn) of 7.37, and an inner-block shear ratio of 0.68. Based on these average values, category 3 support is required. Table 16 lists a rated support category 1 for only 5 percent of this section.

- In approximately 60 percent of this section, the installed support equals or exceeds the theoretical support; 5 percent rated category 1 and 55 percent installed category 4.
- Approximately 40 percent of this reach theoretically could be considered for further analysis and additional ground support.

Stations 51+50 - 55+00

Within domain four, this section has an average Q value of 2.80 (*poor*), block-size ratio (RQD/Jn) of 9.12, and an inner-block shear ratio (Jr/Ja) of 0.69. With these average values and ESF TS North Ramp Ground Support Guidelines, category 3 support is required. An increase in the block-size ratio to 10 would change the recommended support to category 2.

- In approximately 21 percent of this section, the installed support equals or exceeds the theoretical support; 17 percent rated category 1-and 4-percent-installed category 4.
- Approximately 79 percent of this reach could be considered for further analysis and additional ground support. If the effect of faults and shears is overestimated by the rated stress-reduction factor, then nearly the entire section would be rated for category 1 support.

Summary And Conclusions

Rock Mass Quality

Table 13 shows a summary of the rock mass ratings in the Main Drift. Through the Main Drift, average rock quality varies within a narrow range. Domain three average Q rating of 2.5 is qualitatively described as *poor* rock; the highest average Rated Q of 7.4 in domain one describes a *fair* quality rock. Generally, the average rock quality ratings vary along the tunnel from a high of 8.8 between Sta. 28+00 and 34+00 to a low of 2.0 between Sta. 44+00 and 51+50.

RQD

Figure 45 shows the variation of RQD along the tunnel. Over a 50-m reach of tunnel, the calculated RQD values between a 5-m reach may vary by 30 rating points. Figure 44 and Table 7 summarize the frequency of the various ranges of RQD. Seventy-seven percent of mapped RQD

values fall in the *poor* rock or *fair* rock descriptive categories. From Table 13, average RQD values range from 54 to 74. These averages all descriptively indicate a *fair* rock category.

RQD data presented in Figures 46 through 49 show the variability of fracture spacing along the right rib of the tunnel. At the same time, the pattern of RQD ratings shown in the figures demonstrates a typical pattern throughout all four domains. That is, areas of wide-fracture spacing and high RQD ratings alternate with areas of more highly fractured rock. The average RQD values shown in the Table 13 show relatively uniform rock quality through the four domains.

RMR

Within a 50 meter reach of the Main Drift, the RMR for 5-m sections may vary through a 20-point range. In the Table 13, average RMR ratings vary from 56 to 62. The domain averages are very near 60 for all four domains, so RMR ratings indicate a rock mass of *fair* quality showing little change from domain to domain.

Q

Figures 60 through 75 show the variation in rated Q, Q max, RQD/Jn (block size), Jr/Ja (shear strength), and Jw/SRF (active stress) for each 5-m rating interval along the Main Drift. Table 13 summarizes average values of the same parameters for each domain and for reaches of the tunnel which exhibit a characteristic pattern. Average Q ratings range from the middle range of *poor* to the upper range of *fair* quality rock. Table 12 shows 51 percent of 5-m sections rated are described as *poor* quality rock and 27 percent of the sections rated are described as *fair* quality rock.

Average Q rock mass ratings shown in the Table 13 indicate about 1000 meters of *fair* quality rock, (Sta. 28+00 to 34+00, 37+00 to 39+00, and 42+00 to 44+00). The remaining 1700 meters falls in the *poor* quality range. Average block size varies within domains with slightly smaller average block sizes indicated in domains two and three. Inner-block shear strength drops

gradually through the Main Drift. Active stress factor indicates greater fault and shear impact in domains 3 and 4 than rated in domains 1 and 2.

Between Sta. 28+00 and 39+00, average Q ratings show a *fair* quality rock mass with zones of *poor* quality rock.

Between Sta. 39+00 and 55+00, the average Q ratings show a generally *poor* quality rock mass.

Conclusions

- The rock mass quality encountered in the Main Drift is poor to fair quality, based upon Q and RMR ratings.
- Shotcrete was not used for ground support, the actual installed support is category 1 or category 4. About 78 percent of the tunnel requires category 3 ground support based on rated Q values. Therefore, about 62 percent of the Main Drift could be considered for additional ground support.
- Given the beneficial effects of machine excavation on the stability of the opening, intended application of empirical design systems, and somewhat different parameter determination, reaches of tunnel that theoretically need more support are actually adequately supported.
- The decision to use shotcrete for additional ground support should be made in conjunction with consideration of final support.

SUMMARY and CONCLUSIONS

Bureau of Reclamation personnel on behalf of the U.S. Geological Survey are engaged in a program of geologic mapping and collection of detailed information on the lithology, structure, and geotechnical properties of the rock units in the Main Drift of the ESF at Yucca Mountain. These data were studied, plotted, and analyzed with a variety of techniques. The results summarized in this report are part of a continuing program of data collection and analysis to characterize the geology and hydrologic properties of the site. This report will contribute to a better understanding of the regional geology and tectonics, assist in identifying directions for future studies, and assist in repository design.

The Main Drift of the ESF, Sta. 28+00 to 55+00, is almost entirely in the Tptpmn with minor exposures of the Tptpll beyond Sta. 53+00. The Topopah Spring Tuff consists of multiple pyroclastic-flow units more or less vertically symmetrical, with respect to welding and vapor-phase alteration, about the middle nonlithophysal zone. The middle nonlithophysal zone is composed of moderately to densely welded, devitrified pyroclastic-flow material and contains from 1 to 7 percent pumice that tends to occur in zones of aligned pumice clasts. It also contains 1 to 2 percent phenocrysts of tridymite, sanidine, plagioclase and partially oxidized biotite as well as 1 to 3 percent lithic fragments. Vapor-phase alteration is present throughout most of the Tptpmn but is concentrated near the overlying and underlying lithophysal zones. Vapor-phase alteration includes deposits of vapor-phase minerals, tridymite and sanidine, that form vapor-phase partings, line lithophysal cavities, and fracture surfaces, as well as purplish reaction rims that extend a few millimeters from surfaces coated with vapor-phase minerals. These minerals are sometimes covered by secondary minerals; calcite and opal are the most common with some occurrences of specular hematite and one zone where fluorite occurs. Vapor-phase partings and lithophysal cavities are concentrated near the beginning of the Main Drift, near the contact with the upper lithophysal zone at Sta. 27+30. Throughout the rest of the Main Drift, vapor-phase alteration is limited to isolated vapor-phase partings and vapor-phase mineral coatings on fracture surfaces.

Compilation and analysis of the data collected in the Main Drift reveal the presence of four

fracture sets, and a "random" category made up of fractures that do not fall within the bounds of the four sets. The most numerous and well defined set, Set 1, is oriented approximately $120^{\circ}/80^{\circ}$. Set 2 is oriented approximately $220^{\circ}/80^{\circ}$. Set 3 is oriented approximately $310^{\circ}/30^{\circ}$. Set 3 is present in most of the Main Drift with the exception of the interval between Sta. 42+00 and 49+00 where there is a near complete absence of these fractures. Set 4 is intermediate in orientation between Sets 1 and 3, and occurs only between Sta. 28+00 and 37+00. Set 4 fractures strike between 270° and 330° and dip between 40° and 60° . A significant number of fractures, especially between Sta. 28+00 and 42+00, cannot be included in any of the fracture sets within geologically significant limits. These fractures are designated as "random."

Cluster analysis was performed with the computer program Clustran. Cluster analysis resulted in identifying of four sets of data. These results not only generally agree with but also expand on the results obtained through other analytical methods. Clustran grouped all the discontinuities into four sets; whereas the other approaches identified groups or clusters of data and designated data outside those groups as random. The other major difference in the Clustran analysis is the placement of the set boundaries. The sets identified by cluster analysis include a wider range of orientations both in terms of strike and dip than the sets identified through the other methods. This difference is no doubt due to Clustran's inclusion of all the fractures into one of the four sets.

A compilation of shear and fault data shows essentially the same sets seen in the fracture distribution. However, the relative abundance of faults and shears within those sets differs from those of the fractures. In addition, the relative abundance of faults and shears changes along the Main Drift. Set 2 faults and shears are the most numerous overall. Set 3 faults and shears outnumber the others in the First and Second Domains. Set 1 is the smallest group of faults and shears.

Four large domains were identified in the Main Drift. The domains were identified based on their structural characteristics, both in terms of changing patterns of fracturing and faulting. However, the precise location of some of the domain boundaries differs slightly depending on whether fracturing or faulting characteristics are used. Only the First Domain has all four sets of fractures, and all three sets of shears. The First Domain also has a more even distribution of fractures, and a

large number of random fractures and shears. The fracture sets are not particularly well clustered. The Second Domain has three fracture sets and three shear sets. There are few random fractures and the data clusters are well defined. The end of the Second Domain based on fracture data is at the beginning of the fracture zone at Sta. 42+00. Based on shear data, the end of the Second Domain is at the last occurrence of a Set 3 shear, Sta. 42+60. The Third Domain is the fracture zone and is defined by very intense Set 1 fracturing. Set 3 fractures are rare in the Third Domain. The Fourth Domain extends from the end of the fracture zone to the end of the Main Drift, Sta. 51+50 to 55+00. This domain is characterized by high densities of Sets 1 and 2 fracturing with relatively few Set 3 fractures. Essentially all faults and shears are Sets 1 and 2 and they occur in equal numbers. This is the only area where Set 1 shears even approach the numbers of Set 2 shears.

The domains have the same or very similar boundaries as those identified in the analysis of the fracture data. As with the fractures, the orientations of the fault and shear Sets 1 and 2 shift to the right going down station. Set 1 and 2 faults and shears are present throughout the Main Drift. Set 3 faults and shears occur only in the first and Second Domains.

The discontinuous nature of the faults and shears suggests that these features are not through-going structures but rather complex zones of shearing and faulting that accommodated stresses exerted on the body of rock. This style of deformation may be restricted to the brittle rock of the Tptpmn and may or may not extend into the adjacent, mechanically different lithophysal zones.

The pattern of offsets in the sets changes somewhat in the different domains but can be generalized. Set 1 faults and shears have mixed offsets, both in dip-slip and strike-slip components. Set 2 faults and shears are strongly left-lateral except in the Fourth Domain where there are roughly equal numbers of left-lateral and normal offsets. Set 3 faults and shears invariably have reverse offset with two left-lateral offsets and one right-lateral offset.

The exposures in the Main Drift confirmed and clarified what was previously inferred from surface geologic mapping and drill-core logs. Geologic mapping of the Main Drift expanded on the knowledge of faults known from surface mapping. The geologic mapping and the DLS data

identified and quantified the fracture zone between Sta. 42+00 and 51+50. The correlation of subzones within the fracture zone with changes along the Ghost Dance fault suggests a relationship. There is a general correspondence between changes in offset, both gradual and abrupt along the Ghost Dance and subzone boundaries. In addition, faults mapped on the surface adjacent to the Ghost Dance have similar orientations to fractures, faults, and shears mapped in the Main Drift. The most compelling evidence is the correspondence between the clockwise rotation of Set 1 fractures between Sta. 46+00 and 49+00 and a similar change in orientation of the Ghost Dance fault.

One of the puzzling aspects of fracturing in the Main Drift is the multitude of Set 1 fractures.

Whether cooling joints can be attributed simply to thermal stresses in the cooling pyroclastic sheet is questionable. How similarly oriented, closely spaced cooling joints could form in the absence of opposing set cooling joints is not known. How the stress of contraction could act in only one direction is also not known.

That cooling joints and fractures have the same distribution suggests that the fractures and cooling joints may have formed under the influence of the same stress regime.

One possible explanation is that stresses other than the simple thermal stress were acting on the volcanic sheet as it cooled. It seems likely that the tectonic regime resulting in the system of fracturing and faulting was acting during the emplacement and cooling of the Topopah Spring Tuff.

The Set 3 faults and shears occur only in the First and Second Domains. Their consistent reverse offset indicates of south southwest-north northeast directed compressional stress. Compressional stress in that orientation is counter to stresses indicated by the Set 1 cooling joints which is extensional in the south southwest-north northeast direction. The restricted occurrence of Set 3 faults and shears may indicate a localized stress field. Offset on the Ghost Dance fault as shown on the geologic map of Yucca Mountain (Day and others, 1996) is not uniform but varies, gradually in some areas and abruptly in others. A zone of compression could have been induced

by flexure in the hanging wall of the fault because of changes in offset.

The southerly end of the Ghost Dance fault, south of the splay, is a Set 2 fault. The strong left-lateral offset on Set 2 faults and shears and the mixed left-lateral and normal offsets on Set 2 in the Fourth Domain indicates that the hanging wall of the fault is dropping down with clockwise rotation. This pattern of offset is seen in blocks adjacent to Yucca Mountain and most obviously in the more southerly parts of Yucca Mountain in the aerial photo (photo 14).

Geotechnical characterization of the Main Drift focused primarily on rock mass quality and rock mass mechanical properties. Descriptions are based on two empirical rock mass classification systems, rock quality (Q system) and rock mass rating (RMR). The rock mass quality encountered in the Main Drift is generally low quality. Average Q ratings range from fair in the First Domain to poor within the fracture zone. Average RQD values fall in the poor rock to fair rock category. The typical pattern throughout the Main Drift is of areas of wide fracture spacing and high RQD ratings alternating with areas of intensely fractured rock and low RQD. Average RMR ratings are very near 60 throughout the Main Drift, indicating fair quality. Shotcrete was not used for ground support, so the actual installed support is category 1 or category 4. About 78 percent of the Main Drift requires category 3 ground support based on rated Q values. Therefore, about 62 percent of the tunnel could be considered for additional ground support. However, given the beneficial effects of machine excavation on the stability of the opening and borderline conditions for calculation of support, some reaches of the tunnel which theoretically require additional support may be considered adequately supported. The decision on use of shotcrete for additional ground support should be made in conjunction with consideration of a final lining.

An r-mode, maximum variance, principle component analysis was performed on the Main Drift DLS data to identify diagnostic structural heterogeneities. The variables judged to be continuous--maximum aperture, minimum aperture, fracture length, mineral infilling thickness and dip--were selected for multivariate statistical analysis. The analysis indicated that the most useful DLS parameters for characterizing the Tptpmn are mineral-infilling thickness, followed by maximum aperture, and then fracture length. Factor 1 and 2 scores are used to divide the Main Drift into zones with significant structural heterogeneities. These zones correlate with lithostratigraphic

data. Correlations between factor scores and strike were also examined. The genetic and/or tectonic significance of these correlations should be examined in future studies.

REFERENCES

- Barr, D. L., Moyer, T. C., Singleton, W. L., Albin, A. L., Lung, R. C., Lee, A. C., Beason, S. C., and Eatman, G. L. W., 1996, Geology of the North Ramp - Stations 4+00 to 28+00, Exploratory Studies Facility, Yucca Mountain Project, Yucca Mountain, Nevada.
- Barton, N., Lien, R., Lunde, J., 1974, Engineering classification of rock masses for the design of tunnel support: *Rock Mechanics* vol. 6 no. 4.
- Beason, S. C., Bowen, J. C., Ryter, D. W., 1994, Technical procedure for underground mapping: NWM-USGS-GP-32, R0
- Bieniawski, Z.T., 1989, *Engineering rock mass classifications*: New York, John Wiley and Sons
- Broxton, D.E., Chipera, S.J., Byers, F.M., Jr., and Rautman, C.A., 1993. Geologic evaluation of six nonwelded tuff sites in the vicinity of Yucca Mountain, Nevada, for a surface-based test facility for the Yucca Mountain Project: Los Alamos National Laboratory Report LA-12542-MS, 83 p.
- Buesch, D.C., Spengler, R.W., Moyer, T.C., and Geslin, J.K., 1996, Proposed stratigraphic nomenclature and macroscopic identification of lithostratigraphic units of the Paintbrush Group exposed at Yucca Mountain, Nevada: U.S. Geological Survey Open-File Report 94-469, 47 p.
- Bureau of Reclamation, 1988, *Engineering geology field manual*: Government Printing Office, p. 91-93.
- Byers, F.M. Jr., Carr, M.J., Orkild, P.P., Quinlivan, W.D., and Sargent, K.A., 1976, Volcanic suites and related cauldrons of the Timber Mountain-Oasis Valley caldera complex, southern Nevada: U.S. Geological Survey Professional Paper 919, 70 p.

Christiansen, R.L., Lipman, P.W., Carr, M.J., Byers, F.M., Jr., Orkild, P.P., and Sargent, K.A., 1977, The Timber Mountain-Oasis Valley caldera complex of southern Nevada: Geological Society of America Bulletin, v. 88, p.943-959.

Day, W. C., Potter, C. J., Sweetkind, D. S., Dickerson, R. P., San Juan, C. A., 1996, Bedrock geologic map of the central block area, Yucca Mountain, Nye County, Nevada: USGS Administrative Report.

Deere, D.U., 1989, Rock quality designation (RQD) after twenty years, U.S. Corps of Engineers, Washington, DC

Dixon, W.J., 1995, BMDP Statistical software manual, V. 1, University of California Press, Los Angeles, p. 337-355.

Fabryka-Martin, J. T., Dixon, P. R., Levy, S., Liu, B., Turin, H. J., and Wolfsberg, A. V., 1996, Summary report of Chlorine-36 studies: Systematic sampling for Chlorine-36 in the Exploratory Studies Facility: Los Alamos National Laboratory Milestone Report 3783AD, 53p.

Geological Society of America, 1991, Rock-color chart: Boulder, Colorado, Geological Society of America

Geslin, J.K. and Moyer, T.C., 1994, Summary of lithologic logging of new and existing boreholes at Yucca Mountain, Nevada, March 1994 to June 1994: Geological Survey Open-File Report 94-451, 16 p.

Geslin, J.K., Moyer, T.C., and Buesch, D.C., 1994, Summary of lithologic logging of new and existing boreholes at Yucca Mountain, Nevada, August 1993 to February 1994: Geological Survey Open-File Report 94-342, 39 p.

- Gibson, J.D., Shephard, L.E., Swan, F.H., Wesling, J.R., and Kerl, F.A., 1990, Synthesis of studies for the potential of fault rupture at the proposed surface facilities, Yucca Mountain, Nevada: Proceedings of International Topical Meeting, High Level Radioactive Waste management, April 8-12, v. 1, p. 109-116.
- Gillett, S.L., 1987, Online users manual: Extract clusters from axial data sets using the algorithm of Shanley and Mahtab.
- Harman, H.H., 1976, Modern factor analysis, 3rd Ed., The University of Chicago Press, Chicago and London, p.290-299.
- Hudson, M.R., and Sawyer, D.A., 1994, Paleomagnetism and rotation constraints for the middle Miocene, southwestern Nevada volcanic field: Tectonics, v. 13 No. 2 p. 258-277.
- Jolliffe, I.T., 1986. Principal component analysis, Springer-Verlag, New York, p. 41-42.
- Kicker, D. C., Martin, E. R., Brechtel, C. E., Stone, C. A., and Kessel D. S., 1995, Geotechnical characterization for the Main Drift of the Exploratory Studies Facility: Sandia National Laboratories Report SAND952183.
- Lipman, P.W., Christiansen, R.L., and O'Connor, J.T., 1966, A compositionally zoned ash-flow sheet in southern Nevada: U.S. Geological Survey Professional Paper, 524-F, 47 p.
- Minor, S. A., 1995, Superimposed local and regional paleostresses--fault-slip analysis of Neogene Basin-and-Range faulting near a middle Miocene caldera complex, Yucca Flat, southern Nevada: Journal of Geophysical Research, v. 100, p. 10,507-10,528.
- Moyer, T.C., Geslin, J.K., and Buesch, D.C., 1995, Summary of lithologic logging of new and existing boreholes at Yucca Mountain, Nevada, July 1994 to November 1994: Geological Survey Open-File Report 95-102, 22 p.

- Ramsey, J. G., Huber, M. I., 1983, The techniques of modern structural geology: London U. K., Academic Press, p.50.
- Rosenbaum, J. G., Hudson, M. R., Scott, R.B., 1991, Paleomagnetic Constraints on the Geometry and Timing of Deformation at Yucca Mountain, Nevada: Journal of Geophysical Research, V 96, No B2, p 1963-1979.
- Sawyer, D.A., Fleck, R.J., Lanphere, M.A., Warren, R.G., and Broxton, D.E., 1994, Episodic caldera volcanism in the Miocene southwestern Nevada volcanic field: Revised stratigraphic framework, $^{40}\text{Ar}/^{39}\text{Ar}$ geochronology, and implications for magmatism and extension: Geologic Society of America Bulletin, v.106, p. 1304-1318.
- Schuraytz, B.C., Vogel, T.A., and Younker, L.W., 1989, Evidence for dynamic withdrawal from a layered magma body: The Topopah Spring Tuff, southwestern Nevada: Journal of Geophysical Research, v. 94, p. 5925-5942.
- Scott, R.B., 1990, Tectonic setting of Yucca Mountain, southwest Nevada, in Wernicke, B.P., ed., Basin and Range extensional tectonics near the latitude of Las Vegas, Nevada: Boulder, Colorado, Geological Society of America Memoir 176, p. 251-282.
- Scott, R.B., and Bonk, J., 1984, Preliminary geologic map of Yucca Mountain, Nye County, Nevada, with geologic sections: U.S. Geologic Survey Open-File Report 84-494, (map scale 1:12,000)
- Suppe, J., 1985, Principles of structural geology: Englewood Cliffs, N. J., Prentice-Hall, p.268.
- Terzaghi, R.D., 1965, Sources of error in joint surveys: Geotechnique 15:287-304
- Wackernagel, H., Multivariate geostatistics, Springer-Verlag, New York, Chapter 17-Principal component analysis.

APPENDIX 1

Data Tracking Numbers for Review Packages

APPENDIX 1. Data Tracking Numbers for Review Packages

Drawing OA-46-291	Comparative Geologic Cross Section Along Main Drift	GS960908314224.022
Drawing OA-46-222	General Geologic Explanation and Notes, For Stations 26+00 to 30+00	GS960808314224.012
Drawing OA-46-225	As Built Geology and Geotechnical Data, Stations 28+00 to 29+00	GS960808314224.012
Drawing OA-46-226	As Built Geology and Geotechnical Data, Stations 28+00 to 30+00	GS960808314224.012
Drawing OA-46-227	General Geologic Explanation and Notes, For Stations 30+00 to 35+00	GS960908314224.015
Drawing OA-46-228	As Built Geology and Geotechnical Data, Stations 30+00 to 31+00	GS960908314224.015
Drawing OA-46-229	General Geologic Explanation and Notes, For Stations 31+00 to 32+00	GS960908314224.015
Drawing OA-46-230	As Built Geology and Geotechnical Data, Stations 32+00 to 33+00	GS960908314224.015
Drawing OA-46-231	As Built Geology and Geotechnical Data, Stations 33+00 to 34+00	GS960908314224.015
Drawing OA-46-232	As Built Geology and Geotechnical Data, Stations 34+00 to 35+00	GS960908314224.015
Drawing OA-46-233	General Geologic Explanation and Notes, For Stations 35+00 to 40+00	GS960908314224.015
Drawing OA-46-234	As Built Geology and Geotechnical Data, Stations 35+00 to 36+00	GS960908314224.015
Drawing OA-46-235	As Built Geology and Geotechnical Data, Stations 36+00 to 37+00	GS960908314224.015
Drawing OA-46-236	As Built Geology and Geotechnical Data, Stations 37+00 to 38+00	GS960908314224.015
Drawing OA-46-237	As Built Geology and Geotechnical Data, Stations 38+00 to 39+00	GS960908314224.015
Drawing OA-46-238	As Built Geology and Geotechnical Data, Stations 39+00 to 40+00	GS960908314224.015

Drawing OA-46-239	General Geologic Explanation and Notes, For Stations 40+00 to 45+00	GS960908314224.016
Drawing OA-46-240	As Built Geology and Geotechnical Data, Stations 40+00 to 41+00	GS960908314224.016
Drawing OA-46-241	As Built Geology and Geotechnical Data, Stations 41+00 to 42+00	GS960908314224.016
Drawing OA-46-242	As Built Geology and Geotechnical Data, Stations 42+00 to 43+00	GS960908314224.016
Drawing OA-46-243	As Built Geology and Geotechnical Data, Stations 43+00 to 44+00	GS960908314224.016
Drawing OA-46-244	As Built Geology and Geotechnical Data, Stations 44+00 to 45+00	GS960908314224.016
Drawing OA-46-245	General Geologic Explanation and Notes, For Stations 45+00 to 50+00	GS960908314224.016
Drawing OA-46-246	As Built Geology and Geotechnical Data, Stations 45+00 to 46+00	GS960908314224.016
Drawing OA-46-247	As Built Geology and Geotechnical Data, Stations 46+00 to 47+00	GS960908314224.016
Drawing OA-46-248	As Built Geology and Geotechnical Data, Stations 47+00 to 48+00	GS960908314224.016
Drawing OA-46-249	As Built Geology and Geotechnical Data, Stations 48+00 to 49+00	GS960908314224.016
Drawing OA-46-250	General Geologic Explanation and Notes, For Stations 49+00 to 50+00	GS960908314224.016
Drawing OA-46-251	General Geologic Explanation and Notes, For Stations 50+00 to 55+00	GS960908314224.017
Drawing OA-46-252	As Built Geology and Geotechnical Data, Stations 50+00 to 51+00	GS960908314224.017
Drawing OA-46-253	As Built Geology and Geotechnical Data, Stations 51+00 to 52+00	GS960908314224.017
Drawing OA-46-254	As Built Geology and Geotechnical Data, Stations 52+00 to 53+00	GS960908314224.017
Drawing OA-46-255	As Built Geology and Geotechnical Data, Stations 53+00 to 54+00	GS960908314224.017

Drawing OA-46-256	As Built Geology and Geotechnical Data, Stations 54+00 to 55+00	GS960908314224.017
N/A	Detailed Line Survey, Stations 26+00 to 30+00	GS960608314224.007
N/A	Detailed Line Survey, Stations 30+00 to 35+00	GS960708314224.008
N/A	Detailed Line Survey, Stations 35+00 to 40+00	GS960808314224.011
N/A	Detailed Line Survey, Stations 40+00 to 45+00	GS960708314224.010
N/A	Detailed Line Survey, Stations 45+00 to 50+00	GS960808314224.013
N/A	Detailed Line Survey, Stations 50+00 to 55+00	GS960908314224.014
N/A	Detailed Line Survey, Alcove 5	GS960908314224.018

APPENDIX 2

Photogrammetric Negative Numbers and Camera Locations

Sta. 28+00 to 55+00

Date	Body #	Lens #	Pos #1	Posi. #2	PG #s	ID	Comments
11/16/95							
	210660004	7155685	27+13.58	27+15.38	9393/9402	Wehner	ESF Tunnel
	210660004	7155685	27+17.18	27+18.98	9403/9412	Wehner	ESF Tunnel; Contact of TPTPUL and TPTPMN at 27+20 R. Rib
	210660004	7155685	27+20.78	27+22.58	9413/9422	Wehner	ESF Tunnel; Contact of TPTPUL and TPTPMN at 27+20 R. Rib
	210660004	7155685	27+24.38	27+26.18	9423/9432	Wehner	ESF Tunnel
	210660004	7155685	27+27.98	27+29.78	9433/9442	Wehner	ESF Tunnel
	210660004	7155685	27+31.58	27+33.38	9443/9452	Wehner	ESF Tunnel
	210660004	7155685	27+35.18	27+36.98	9453/9462	Wehner	ESF Tunnel
	210660004	7155685	27+38.78	27+40.58	9463/9472	Wehner	ESF Tunnel
11/17/95							
	210660004	7155685	27+40.58	27+42.38	9473/9482	USBR	ESF Tunnel
	210660004	7155685	27+44.18	27+45.98	9483/9492	USBR	ESF Tunnel
	210660004	7155685	27+47.78	27+49.58	9493/9502	USBR	ESF Tunnel
	210660004	7155685	27+51.38	27+53.18	9503/9512	USBR	ESF Tunnel
	210660004	7155685	27+54.98	27+56.78	9513/9522	USBR	ESF Tunnel
	210660004	7155685	27+58.58	27+60.38	9523/9532	USBR	ESF Tunnel
	210660004	7155685	27+62.18	27+63.98	9533/9542	USBR	ESF Tunnel
	210660004	7155685	27+65.78	27+67.58	9543/9552	USBR	ESF Tunnel
	210660004	7155685	27+69.38		9553/9557	USBR	ESF Tunnel
11/20/95							
	210660004	7155685	27+69.38	27+71.18	9558/9567	Wehner	ESF Tunnel
	210660004	7155685	27+72.98	27+74.78	9568/9577	Wehner	ESF Tunnel

Date	Body #	Lens #	Pos #1	Posi. #2	PG #s	ID	Comments
	210660004	7155685	27+76.58	27+78.38	9578/9587	Wehner	ESF Tunnel
	210660004	7155685	27+80.18	27+81.98	9588/9597	Wehner	ESF Tunnel
	210660004	7155685	27+83.78	27+85.58	9598/9607	Wehner	ESF Tunnel
	210660004	7155685	27+87.38	27+89.18	9608/9617	Wehner	ESF Tunnel
	210660004	7155685	27+90.98	27+92.78	9618/9627	Wehner	ESF Tunnel
	210660004	7155685	27+94.58	27+96.38	9628/9637	Wehner	ESF Tunnel
	210660004	7155685	27+98.18	27+99.98	9638/9647	Wehner	ESF Tunnel
11/21/95							
	210660004	7155685	27+99.98	28+01.78	9648/9657	Wehner	ESF Tunnel
	210660004	7155685	28+03.58	28+05.38	9658/9667	Wehner	ESF Tunnel; End of Curve at 28+04.32
	210660004	7155685	28+07.18	28+08.98	9668/9677	Wehner	ESF Tunnel
	210660004	7155685	28+10.78	28+12.58	9678/9687	Wehner	ESF Tunnel
	210660004	7155685	28+14.38	28+16.18	9688/9697	Wehner	ESF Tunnel
	210660004	7155685	28+17.98	28+19.78	9698/9707	Wehner	ESF Tunnel
	210660004	7155685	28+21.58	28+23.38	9708/9717	Wehner	ESF Tunnel
	210660004	7155685	28+25.18	28+26.98	9718/9727	Wehner	ESF Tunnel
	210660004	7155685	28+28.78	28+30.58	9728/9737	Wehner	ESF Tunnel
	210660004	7155685	28+32.38	28+34.18	9738/9747	Wehner	ESF Tunnel
11/22/95							
	210660004	7155685	28+34.18	28+35.98	9748/9757	Wehner	ESF Tunnel
	210660004	7155685	28+37.78	28+39.58	9758/9767	Wehner	ESF Tunnel
	210660004	7155685	28+41.38	28+43.18	9768/9777	Wehner	ESF Tunnel
	210660004	7155685	28+44.98	28+46.78	9778/9787	Wehner	ESF Tunnel

Date	Body #	Lens #	Pos #1	Posi. #2	PG #s	ID	Comments
	210660004	7155685	28+48.58	28+50.38	9788/9797	Wehner	ESF Tunnel
	210660004	7155685	28+52.18	28+53.98	9798/9807	Wehner	ESF Tunnel
	210660004	7155685	28+55.78	28+57.58	9808/9817	Wehner	ESF Tunnel
	210660004	7155685	28+59.38	28+61.18	9818/9827	Wehner	ESF Tunnel
	210660004	7155685	28+62.98	28+64.78	9828/9837	Wehner	ESF Tunnel
	210660004	7155685	28+66.58		9838/9842	Wehner	ESF Tunnel
11/27/95							
	210660004	7155685	28+66.58	28+68.38	9843/9852	Wehner	ESF Tunnel
	210660004	7155685	28+70.18	28+71.98	9853/9862	Wehner	ESF Tunnel
	210660004	7155685	28+73.78	28+75.58	9863/9872	Wehner	ESF Tunnel
	210660004	7155685	28+77.38	28+79.18	9873/9882	Wehner	ESF Tunnel
11/28/95							
	210660004	7155685	28+80.98	28+82.78	9883/9892	Wehner	ESF Tunnel
	210660004	7155685	28+84.58	28+86.38	9893/9902	Wehner	ESF Tunnel
	210660004	7155685	28+88.18	28+89.98	9903/9912	Wehner	ESF Tunnel
	210660004	7155685	28+91.78	28+93.58	9913/9922	Wehner	ESF Tunnel
	210660004	7155685	28+95.38	28+97.18	9923/9932	Wehner	ESF Tunnel
	210660004	7155685	28+98.98	29+00.78	9933/9942	Wehner	ESF Tunnel
	210660004	7155685	29+02.58	29+04.38	9943/9952	Wehner	ESF Tunnel
	210660004	7155685	29+06.18	29+07.98	9953/9962	Wehner	ESF Tunnel
	210660004	7155685	29+09.78	29+11.58	9963/9972	Wehner	ESF Tunnel
	210660004	7155685	29+13.38	29+15.18	9973/9982	Wehner	ESF Tunnel
	210660004	7155685	29+16.98	29+18.78	9983/9992	Wehner	ESF Tunnel

Date	Body #	Lens #	Pos #1	Posi. #2	PG #s	ID	Comments
11/29/95	210660004	7155685	29+18.78	29+20.58	9993/10002	Wehner	ESF Tunnel
	210660004	7155685	29+22.38	29+24.18	10003/10012	Wehner	ESF Tunnel
	210660004	7155685	29+25.98	29+27.78	10013/10022	Wehner	ESF Tunnel
	210660004	7155685	29+29.58	29+31.38	10023/10032	Wehner	ESF Tunnel
	210660004	7155685	29+33.18	29+34.98	10033/10042	Wehner	ESF Tunnel
	210660004	7155685	29+36.78	29+38.58	10043/10052	Wehner	ESF Tunnel
	210660004	7155685	29+40.38	29+42.18	10053/10062	Wehner	ESF Tunnel
	210660004	7155685	29+43.98	29+45.78	10063/10072	Wehner	ESF Tunnel
	210660004	7155685	29+47.58	29+49.38	10073/10082	Wehner	ESF Tunnel
	210660004	7155685	29+51.18	29+52.98	10083/10092	Wehner	ESF Tunnel
	210660004	7155685	29+54.78		10093/10097	Wehner	ESF Tunnel
11/30/95	210660004	7155685	29+63.78	29+65.58	10098/10107	Wehner	ESF Tunnel; 4.6 meters of tunnel missed due to mining progress (exceeded 45 meter window)
	210660004	7155685	29+67.38	29+69.18	10108/10117	Wehner	ESF Tunnel
	210660004	7155685	29+70.98	29+72.78	10118/10127	Wehner	ESF Tunnel
	210660004	7155685	29+74.58	29+76.38	10128/10137	Wehner	ESF Tunnel
	210660004	7155685	29+78.18	29+79.98	10138/10147	Wehner	ESF Tunnel
	210660004	7155685	29+81.78	29+83.58	10148/10157	Wehner	ESF Tunnel
	210660004	7155685	29+85.38	29+87.18	10158/10167	Wehner	ESF Tunnel
	210660004	7155685	29+88.98	29+90.78	10168/10177	Wehner	ESF Tunnel
	210660004	7155685	29+92.58	29+94.38	10178/10187	Wehner	ESF Tunnel
	210660004	7155685	29+96.18	29+97.98	10188/10197	Wehner	ESF Tunnel

Date	Body #	Lens #	Pos #1	Posi. #2	PG #s	ID	Comments
	210660004	7155685	29+09.78	30+01.58	10198/10207	Wehner	ESF Tunnel
	210660004	7155685	30+03.38	30+05.18	10208/10217	Wehner	ESF Tunnel
	210660004	7155685	30+06.98	30+08.78	10218/10227	Wehner	ESF Tunnel; Rock Not Cleaned
	210660004	7155685	30+10.58		10228/10232	Wehner	ESF Tunnel; Rock Not Cleaned
12/1/95							
	210660004	7155685	30+06.98	30+08.78	10233/10242	USBR	ESF Tunnel; Same as 10218-10232 Except Rock Has Been Cleaned
	210660004	7155685	30+10.58	30+12.38	10243/10252	USBR	ESF Tunnel; Same as 10218-10232 Except Rock Has Been Cleaned
	210660004	7155685	30+14.18	30+15.98	10253/10262	USBR	ESF Tunnel
	210660004	7155685	30+17.78	30+19.58	10263/10272	USBR	ESF Tunnel
	210660004	7155685	30+21.38	30+23.18	10273/10282	USBR	ESF Tunnel
	210660004	7155685	30+24.98	30+26.78	10283/10292	USBR	ESF Tunnel
	210660004	7155685	30+28.58	30+30.38	10293/10302	USBR	ESF Tunnel
	210660004	7155685	30+32.18	30+33.98	10303/10312	USBR	ESF Tunnel
	210660004	7155685	30+35.78	30+37.58	10313/10322	USBR	ESF Tunnel
	210660004	7155685	30+39.38	30+41.18	10323/10332	USBR	ESF Tunnel
	210660004	7155685	30+42.98		10333/10337	USBR	ESF Tunnel
12/4/95							
	210660004	7155685	30+55.58	30+57.38	10338/10347	Wehner	ESF Tunnel; 12.6 meters lost due to rapid mining progress
	210660004	7155685	30+59.18	30+60.98	10348/10357	Wehner	ESF Tunnel
	210660004	7155685	30+62.78	30+64.58	10358/10367	Wehner	ESF Tunnel
	210660004	7155685	30+66.38	30+68.18	10368/10377	Wehner	ESF Tunnel
	210660004	7155685	30+69.98	30+71.78	10378/10387	Wehner	ESF Tunnel

Date	Body #	Lens #	Pos #1	Posi. #2	PG #s	ID	Comments
	210660004	7155685	30+73.58	30+75.38	10388/10397	Wehner	ESF Tunnel; Stop Change to F11.5
	210660004	7155685	30+77.18	30+78.98	10398/10407	Wehner	ESF Tunnel
	210660004	7155685	30+80.78	30+82.58	10408/10417	Wehner	ESF Tunnel
	210660004	7155685	30+84.38	30+86.18	10418/10427	Wehner	ESF Tunnel
	210660004	7155685	30+87.98	30+89.78	10428/10437	Wehner	ESF Tunnel
	210660004	7155685	30+91.58	30+93.38	10438/10447	Wehner	ESF Tunnel
	210660004	7155685	30+95.18	30+96.98	10448/10457	Wehner	ESF Tunnel
	210660004	7155685	30+98.78		10458/10462	Wehner	ESF Tunnel
12/12/95							
	210660004	7155685	30+98.78	31+00.58	10463/10472	Wehner	TBM 1000 Hour Maintenance Period 12-5 thru 12-12-95; ESF Tunnel
	210660004	7155685	31+02.38	31+04.18	10473/10482	Wehner	ESF Tunnel
	210660004	7155685	31+05.98	31+07.78	10483/10492	Wehner	ESF Tunnel
	210660004	7155685	31+09.58	31+11.38	10493/10502	USBR	ESF Tunnel
	210660004	7155685	31+13.18	31+14.98	10503/10512	USBR	ESF Tunnel
	210660004	7155685	31+16.78	31+18.58	10513/10522	USBR	ESF Tunnel
	210660004	7155685	31+20.38	31+22.18	10523/10532	USBR	ESF Tunnel
	210660004	7155685	31+23.98	31+25.78	10533/10542	USBR	ESF Tunnel
	210660004	7155685	31+27.58	31+29.38	10543/10552	USBR	ESF Tunnel
12/13/95							
	210660004	7155685	31+31.18	31+32.98	10553/10562	Wehner	ESF Tunnel
	210660004	7155685	31+34.78	31+36.58	10563/10572	Wehner	ESF Tunnel
	210660004	7155685	31+38.38	31+40.18	10573/10582	Wehner	ESF Tunnel
	210660004	7155685	31+41.98	31+43.78	10583/10592	Wehner	ESF Tunnel

Date	Body #	Lens #	Pos #1	Posl. #2	PG #s	ID	Comments
	210660004	7155685	31+45.58	31+47.38	10593/10602	Wehner	ESF Tunnel
	210660004	7155685	31+49.18		10603/10607	Wehner	ESF Tunnel
	210660004	7155685	31+49.18	31+50.98	10608/10617	USBR	ESF Tunnel
	210660004	7155685	31+52.78	31+54.58	10618/10627	USBR	ESF Tunnel
	210660004	7155685	31+56.38	31+58.18	10628/10637	USBR	ESF Tunnel
	210660004	7155685	31+59.98	31+61.78	10638/10647	USBR	ESF Tunnel
	210660004	7155685	31+63.58	31+65.38	10648/10657	USBR	ESF Tunnel
	210660004	7155685	31+67.18	31+68.98	10658/10667	USBR	ESF Tunnel
	210660004	7155685	31+70.78	31+72.58	10668/10677	USBR	ESF Tunnel
	210660004	7155685	31+74.38	31+76.18	10678/10687	USBR	ESF Tunnel
12/14/95							
	210660004	7155685	31+74.38	31+76.18	10688/10697	Wehner	ESF Tunnel; Rib Cleaned
	210660004	7155685	31+77.98	31+79.78	10698/10707	Wehner	ESF Tunnel
	210660004	7155685	31+81.58	31+83.38	10708/10717	Wehner	ESF Tunnel
	210660004	7155685	31+85.18	31+86.98	10718/10727	Wehner	ESF Tunnel
	210660004	7155685	31+88.78	31+90.58	10728/10737	Wehner	ESF Tunnel
	210660004	7155685	31+92.38		10738/10742	Wehner	ESF Tunnel
	210660004	7155685	31+92.38	31+94.18	10743/10752	USBR	ESF Tunnel
	210660004	7155685	31+95.98	31+97.78	10753/10762	USBR	ESF Tunnel
	210660004	7155685	31+99.58	32+01.38	10763/10772	USBR	ESF Tunnel
	210660004	7155685	32+03.18	32+04.98	10773/10782	USBR	ESF Tunnel
	210660004	7155685	32+06.78	32+08.58	10783/10792	USBR	ESF Tunnel
	210660004	7155685	32+10.38	32+12.18	10793/10802	USBR	ESF Tunnel

Date	Body #	Lens #	Pos #1	Posl. #2	PG #s	ID	Comments
	210660004	7155685	32+13.98	32+15.78	10803/10812	USBR	ESF Tunnel
12/15/95							
	210660004	7155685	32+15.78	32+17.58	10813/10822	USBR	ESF Tunnel
	210660004	7155685	32+19.38	32+21.18	10823/10832	USBR	ESF Tunnel
	210660004	7155685	32+22.98	32+24.78	10833/10842	USBR	ESF Tunnel
	210660004	7155685	32+26.58	32+28.38	10843/10852	USBR	ESF Tunnel
	210660004	7155685	32+30.18	32+31.98	10853/10862	USBR	ESF Tunnel
	210660004	7155685	32+33.78	32+35.58	10863/10872	USBR	ESF Tunnel
	210660004	7155685	32+37.38	32+39.18	10873/10882	USBR	ESF Tunnel
	210660004	7155685	32+40.98	32+42.78	10883/10892	USBR	ESF Tunnel
	210660004	7155685	32+42.78	32+44.58	10893/10902	USBR	ESF Tunnel
	210660004	7155685	32+46.38	32+48.18	10903/10912	USBR	ESF Tunnel
	210660004	7155685	32+49.98	32+51.78	10913/10922	USBR	ESF Tunnel
	210660004	7155685	32+53.58	32+55.38	10923/10932	USBR	ESF Tunnel
12/18/95							
	310660004	7155685	32+55.38	32+57.18	10933/10942	Wehner	ESF Tunnel
	210660004	7155685	32+58.98	32+60.78	10943/10952	Wehner	ESF Tunnel
	210660004	7155685	32+62.58	32+64.38	10953/10962	Wehner	ESF Tunnel
	210660004	7155685	32+66.18	32+67.98	10963/10972	Wehner	ESF Tunnel
	210660004	7155685	32+67.98	32+69.78	10973/10982	USBR	ESF Tunnel
	210660004	7155685	32+71.58	32+73.38	10983/10992	USBR	ESF Tunnel
	210660004	7155685	32+75.18	32+76.98	10993/11002	USBR	ESF Tunnel
	210660004	7155685	32+78.78	32+80.58	11003/11012	USBR	ESF Tunnel

Date	Body #	Lens #	Pos #1	Posi. #2	PG #s	ID	Comments
	210660004	7155685	32+82.38	32+84.18	11013/11022	USBR	ESF Tunnel
12/19/95							
	210660004	7155685	32+82.38	32+84.18	11023/11032	Wehner	ESF Tunnel; Rock Cleaned
	210660004	7155685	32+85.98	32+87.78	11033/11042	Wehner	ESF Tunnel
	210660004	7155685	32+89.58	32+91.38	11043/11052	Wehner	ESF Tunnel
	210660004	7155685	32+93.18	32+94.98	11053/11062	Wehner	ESF Tunnel
	210660004	7155685	32+96.78	32+98.58	11063/11072	Wehner	ESF Tunnel
	210660004	7155685	33+00.38	33+02.18	11073/11082	Wehner	ESF Tunnel
12/20/95							
	210660004	7155685	33+02.18	33+03.98	11083/11092	Wehner	ESF Tunnel
	210660004	7155685	33+05.78	33+07.58	11093/11102	Wehner	ESF Tunnel
	210660004	7155685	33+09.38	33+11.18	11103/11112	Wehner	ESF Tunnel
	210660004	7155685	33+12.98		11113/11117	Wehner	ESF Tunnel
	210660004	7155685	33+12.98	33+14.78	11118/11127	USBR	ESF Tunnel
	210660004	7155685	33+16.58	33+18.38	11128/11137	USBR	ESF Tunnel
	210660004	7155685	33+20.18	33+21.98	11138/11147	USBR	ESF Tunnel
	210660004	7155685	33+23.78	33+25.58	11148/11157	USBR	ESF Tunnel
	210660004	7155685	33+27.38	33+29.18	11158/11167	USBR	ESF Tunnel
	210660004	7155685	33+30.98		11168/11172	USBR	ESF Tunnel
12/21/95							
	210660004	7155685	33+30.98	33+32.78	11173/11182	Wehner	ESF Tunnel
	210660004	7155685	33+34.58	33+36.38	11183/11192	Wehner	ESF Tunnel
	210660004	7155685	33+38.18	33+39.98	11193/11202	Wehner	ESF Tunnel

Date	Body #	Lens #	Pos #1	Posi. #2	PG #s	ID	Comments
	210660004	7155685	33+41.78		11203/11207	Wehner	ESF Tunnel
	210660004	7155685	33+41.78	33+43.58	11208/11217	USBR	ESF Tunnel
	210660004	7155685	33+45.38	33+47.18	11218/11227	USBR	ESF Tunnel
	210660004	7155685	33+48.98	33+50.78	11228/11237	USBR	ESF Tunnel
	210660004	7155685	33+52.58	33+54.38	11238/11247	USBR	ESF Tunnel
	210660004	7155685	33+56.18	33+57.98	11248/11257	USBR	ESF Tunnel
	210660004	7155685	33+59.78		11258/11262	USBR	ESF Tunnel
12/22/95							
	210660004	7155685	33+59.78	33+61.58	11263/11272	USBR	ESF Tunnel
	210660004	7155685	33+63.38	33+65.18	11273/11282	USBR	ESF Tunnel
	210660004	7155685	33+66.98	33+68.78	11283/11292	USBR	ESF Tunnel
	210660004	7155685	33+70.58	33+72.38	11293/11302	USBR	ESF Tunnel
	210660004	7155685	33+74.18		11303/11307	USBR	ESF Tunnel
12/26/95							
	210660004	7155685	33+74.18	33+77.78	11308/11317	USBR	ESF Tunnel
	210660004	7155685	33+79.58	33+81.38	11318/11327	USBR	ESF Tunnel
	210660004	7155685	33+83.18	33+84.98	11328/11337	USBR	ESF Tunnel
	210660004	7155685	33+86.78	33+88.58	11338/11347	USBR	ESF Tunnel
	210660004	7155685	33+90.38	33+92.18	11348/11357	USBR	ESF Tunnel
	210660004	7155685	33+93.98	33+95.78	11358/11367	USBR	ESF Tunnel
12/27/95							
	210660004	7155685	33+93.98	33+95.78	11368/11377	USBR	ESF Tunnel
	210660004	7155685	33+97.58	33+99.38	11378/11387	USBR	ESF Tunnel

Date	Body #	Lens #	Pos #1	Posi. #2	PG #s	ID	Comments
	210660004	7155685	34+01.18	34+02.98	11388/11397	USBR	ESF Tunnel
	210660004	7155685	34+04.78	34+06.58	11398/11407	USBR	ESF Tunnel
	210660004	7155685	34+08.38	34+10.18	11408/11417	USBR	ESF Tunnel
	210660004	7155685	34+11.98	34+13.78	11418/11427	USBR	ESF Tunnel
	210660004	7155685	34+15.58	34+17.38	11428/11437	USBR	ESF Tunnel
	210660004	7155685	34+19.18	34+20.98	11438/11447	USBR	ESF Tunnel
	210660004	7155685	34+22.78	34+24.58	11448/11457	USBR	ESF Tunnel
	210660004	7155685	34+26.38	34+28.18	11458/11467	USBR	ESF Tunnel
12/29/95							
	210660004	7155685	34+28.18	34+29.98	11468/11477	USBR	ESF Tunnel
	210660004	7155685	34+31.78	34+33.58	11478/11487	USBR	ESF Tunnel
	210660004	7155685	34+35.38	34+37.18	11488/11497	USBR	ESF Tunnel
	210660004	7155685	34+38.98	34+40.78	11498/11507	USBR	ESF Tunnel
	210660004	7155685	34+42.58	34+44.38	11508/11517	USBR	ESF Tunnel
1/2/96							
	210660004	7155685	34+44.38	34+46.18	11518/11527	Wehner	ESF Tunnel
	210660004	7155685	34+47.98	34+49.78	11528/11537	Wehner	ESF Tunnel
	210660004	7155685	34+51.58	34+53.38	11538/11547	Wehner	ESF Tunnel
	210660004	7155685	34+55.18	34+56.98	11548/11557	Wehner	ESF Tunnel
	210660004	7155685	34+58.78	34+60.58	11558/11567	Wehner	ESF Tunnel
	210660004	7155685	34+62.38	34+64.18	11568/11577	Wehner	ESF Tunnel
	210660004	7155685	34+65.98	34+67.78	11578/11587	Wehner	ESF Tunnel
	210660004	7155685	34+69.58	34+71.38	11588/11597	Wehner	ESF Tunnel

Date	Body #	Lens #	Pos #1	Posi. #2	PG #s	ID	Comments
	210660004	7155685	34+73.18	34+74.98	11598/11607	Wehner	ESF Tunnel
	210660004	7155685	34+76.78		11608/11612	Wehner	ESF Tunnel
1/3/96							
	210660004	7155685	34+76.78	34+78.58	11613/11622	Wehner	ESF Tunnel
	210660004	7155685	34+80.38	34+82.18	11623/11632	Wehner	ESF Tunnel
	210660004	7155685	34+83.98	34+85.78	11633/11642	Wehner	ESF Tunnel
	210660004	7155685	34+87.58	34+89.38	11643/11652	Wehner	ESF Tunnel
	210660004	7155685	34+91.18	34+92.98	11653/11662	Wehner	ESF Tunnel
	210660004	7155685	34+94.78	34+96.58	11663/11672	Wehner	ESF Tunnel
	210660004	7155685	34+98.38	35+00.18	11673/11682	Wehner	ESF Tunnel
	210660004	7155685	35+01.98	35+03.78	11683/11692	Wehner	ESF Tunnel
	210660004	7155685	35+05.58	35+07.38	11693/11702	Wehner	ESF Tunnel
	210660004	7155685	35+09.18	35+10.98	11703/11712	Wehner	ESF Tunnel
	210660004	7155685	35+12.78		11713/11717	Wehner	ESF Tunnel
1/4/96							
	210660004	7155685	35+12.78	35+14.58	11718/11727	Wehner	ESF Tunnel
	210660004	7155685	35+16.38	35+18.18	11728/11737	Wehner	ESF Tunnel
	210660004	7155685	35+19.98	35+21.78	11738/11747	Wehner	ESF Tunnel
	210660004	7155685	35+23.58	35+25.38	11748/11757	Wehner	ESF Tunnel
1/5/96							
	210660004	7155685	35+25.38	35+27.18	11758/11767	USBR	ESF Tunnel
	210660004	7155685	35+28.98	35+30.78	11768/11777	USBR	ESF Tunnel
	210660004	7155685	35+32.58	35+34.38	11778/11787	USBR	ESF Tunnel

Date	Body #	Lens #	Pos #1	Posi. #2	PG #s	ID	Comments
	210660004	7155685	35+36.18	35+37.98	11788/11797	USBR	ESF Tunnel
	210660004	7155685	35+39.78	35+41.58	11798/11807	USBR	ESF Tunnel
	210660004	7155685	35+43.38	35+45.18	11808/11817	USBR	ESF Tunnel
	210660004	7155685	35+46.98	35+48.78	11818/11827	USBR	ESF Tunnel
	210660004	7155685	35+50.58	35+52.38	11828/11837	USBR	ESF Tunnel
	210660004	7155685	35+54.18	35+55.98	11838/11847	USBR	ESF Tunnel
	210660004	7155685	35+57.78	35+59.58	11848/11857	USBR	ESF Tunnel
	210660004	7155685	35+61.38	35+63.18	11858/11867	USBR	ESF Tunnel
	210660004	7155685	35+64.98	35+66.78	11868/11877	USBR	ESF Tunnel
	210660004	7155685	35+66.78	35+68.58	11878/11887	USBR	ESF Tunnel
	210660004	7155685	35+70.38	35+72.18	11888/11897	USBR	ESF Tunnel
	210660004	7155685	35+73.98	35+75.78	11898/11907	USBR	ESF Tunnel
	210660004	7155685	35+77.58	35+79.38	11908/11917	USBR	ESF Tunnel
	210660004	7155685	35+81.18	35+82.98	11918/11927	USBR	ESF Tunnel
	210660004	7155685	35+84.78	35+86.58	11928/11937	USBR	ESF Tunnel
1/8/96							
	210660004	7155685	35+84.78	35+86.58	11938/11947	Wehner	ESF Tunnel
	210660004	7155685	35+88.38	35+90.18	11948/11957	Wehner	ESF Tunnel
	210660004	7155685	35+91.98	35+93.78	11958/11967	Wehner	ESF Tunnel
	210660004	7155685	35+95.58	35+97.38	11968/11977	Wehner	ESF Tunnel
	210660004	7155685	35+99.18	36+00.98	11978/11987	Wehner	ESF Tunnel
	210660004	7155685	36+02.78	36+04.58	11988/11997	Wehner	ESF Tunnel

Date	Body #	Lens #	Pos #1	Posi. #2	PG #s	ID	Comments
1/9/96							
	210660004	7155685	36+08.18	36+09.98	11998/12007	Wehner	ESF Tunnel; 3.6 Meters Lost Due to Mining Progress on Graveyard Shift
	210660004	7155685	36+11.78	36+13.58	12008/12017	USBR	ESF Tunnel
	210660004	7155685	36+11.78	36+13.58	12018/12027	Wehner	ESF Tunnel
	210660004	7155685	36+15.38	36+17.18	12028/12037	Wehner	ESF Tunnel
	210660004	7155685	36+18.98	36+20.78	12038/12047	Wehner	ESF Tunnel
	210660004	7155685	36+22.58	36+24.38	12048/12057	Wehner	ESF Tunnel
	210660004	7155685	36+26.18	36+27.98	12058/12067	Wehner	ESF Tunnel
	210660004	7155685	36+29.78	36+31.58	12068/12077	Wehner	ESF Tunnel
	210660004	7155685	36+33.38	36+35.18	12078/12087	Wehner	ESF Tunnel
	210660004	7155685	36+36.98	36+38.78	12088/12097	Wehner	ESF Tunnel
	210660004	7155685	36+40.58	36+42.38	12098/12107	Wehner	ESF Tunnel
	210660004	7155685	36+44.18	36+45.98	12108/12117	Wehner	ESF Tunnel
	210660004	7155685	36+47.78	36+49.58	12118/12127	Wehner	ESF Tunnel
	210660004	7155685	36+51.38	36+53.18	12128/12137	Wehner	ESF Tunnel
	210660004	7155685	36+44.18	36+45.98	12138/12147	USBR	ESF Tunnel; Rock Cleaned
	210660004	7155685	36+47.78	36+49.58	12148/12157	USBR	ESF Tunnel
	210660004	7155685	36+51.38	36+53.18	12158/12167	USBR	ESF Tunnel
	210660004	7155685	36+54.98	36+56.78	12168/12177	USBR	ESF Tunnel
	210660004	7155685	36+58.58	36+60.38	12178/12187	USBR	ESF Tunnel
	210660004	7155685	36+62.18	36+63.98	12188/12197	USBR	ESF Tunnel
	210660004	7155685	36+65.78	36+67.58	12198/12207	USBR	ESF Tunnel
	210660004	7155685	36+69.38	36+71.18	12208/12217	USBR	ESF Tunnel

Date	Body #	Lens #	Pos #1	Posl. #2	PG #s	ID	Comments
1/10/96	210660004	7155685	36+72.98		12218/12222	USBR	ESF Tunnel
	210660004	7155685	36+74.78	36+76.58	12223/12232	Wehner	ESF Tunnel
	210660004	7155685	36+78.38	36+80.18	12233/12242	Wehner	ESF Tunnel
	210660004	7155685	36+81.98	36+83.78	12243/12252	Wehner	ESF Tunnel
	210660004	7155685	36+85.58	36+87.38	12253/12262	Wehner	ESF Tunnel
	210660004	7155685	36+89.18	36+90.98	12263/12272	Wehner	ESF Tunnel
	210660004	7155685	36+90.98	36+92.78	12273/12282	USBR	ESF Tunnel
	210660004	7155685	36+94.58	36+96.38	12283/12292	USBR	ESF Tunnel
	210660004	7155685	36+98.18	36+99.98	12293/12302	USBR	ESF Tunnel
	210660004	7155685	37+01.78	37+03.58	12308/12312	USBR	ESF Tunnel
	210660004	7155685	37+05.38		12313/12317	USBR	ESF Tunnel
1/11/96							
	210660004	7155685	37+05.54	37+07.34	12318/12327	Wehner	ESF Tunnel; New Survey Locations
	210660004	7155685	37+09.14	37+10.94	12328/12337	Wehner	ESF Tunnel
	210660004	7155685	37+12.74	37+14.54	12338/12347	Wehner	ESF Tunnel
	210660004	7155685	37+16.34	37+18.14	12348/12357	Wehner	ESF Tunnel
	210660004	7155685	37+19.94		12358/12362	Wehner	ESF Tunnel
1/12/96							
	210660004	7155685	37+19.94	37+21.74	12363/12372	USBR	ESF Tunnel
	210660004	7155685	37+23.54	37+25.34	12383/12392	USBR	ESF Tunnel
	210660004	7155685	37+27.14	37+28.94	12383/12392	USBR	ESF Tunnel
	210660004	7155685	37+30.74	37+32.54	12393/12402	Wehner	ESF Tunnel

Date	Body #	Lens #	Pos #1	Posl. #2	PG #s	ID	Comments
	210660004	7155685	37+34.34	37+36.14	12403/12412	USBR	ESF Tunnel; PG 12403 is Blank Frame
	210660004	7155685	37+37.94	37+39.74	12413/12422	USBR	ESF Tunnel
	210660004	7155685	37+41.54	37+43.34	12423/12432	USBR	ESF Tunnel; PG 12423 is Blank Frame
	210660004	7155685	37+45.14	37+46.94	12433/12442	USBR	ESF Tunnel
	210660004	7155685	37+48.74	37+50.54	12443/12452	USBR	ESF Tunnel
	210660004	7155685	37+52.34		12453/12457	USBR	ESF Tunnel
1/16/96							
	210660004	7155685	37+50.54	37+52.34	12458/12467	Wehner	ESF Tunnel
	210660004	7155685	37+54.14	37+55.94	12468/12477	Wehner	ESF Tunnel
	210660004	7155685	37+57.74	37+59.54	12478/12487	Wehner	ESF Tunnel
	210660004	7155685	37+61.34	37+63.14	12488/12497	Wehner	ESF Tunnel
	210660004	7155685	37+64.94	37+66.74	12498/12507	Wehner	ESF Tunnel
1/17/96							
	210660004	7155685	37+66.74	37+68.54	12508/12517	Wehner	ESF Tunnel
	210660004	7155685	37+70.34	37+72.14	12518/12527	Wehner	ESF Tunnel
	210660004	7155685	37+73.94	37+75.74	12528/12537	Wehner	ESF Tunnel
	210660004	7155685	37+77.54	37+79.34	12538/12547	Wehner	ESF Tunnel
	210660004	7155685	37+81.14	37+82.94	12548/12557	Wehner	ESF Tunnel
	210660004	7155685	37+84.74	37+86.54	12558/12567	Wehner	ESF Tunnel
	210660004	7155685	37+88.34	37+90.14	12568/12577	Wehner	ESF Tunnel
	210660004	7155685	37+91.94	37+93.74	12578/12587	Wehner	ESF Tunnel
	210660004	7155685	37+95.54	37+97.34	12588/12597	Wehner	ESF Tunnel
	210660004	7155685	37+99.14	38+00.94	12598/12607	Wehner	ESF Tunnel

Date	Body #	Lens #	Pos #1	Posi. #2	PG #s	ID	Comments
	210660004	7155685	38+02.74	38+04.54	12608/12617	Wehner	ESF Tunnel
	210660004	7155685	38+04.54	38+06.34	12618/12627	USBR	ESF Tunnel
	210660004	7155685	38+08.14	38+09.94	12628/12637	USBR	ESF Tunnel
	210660004	7155685	38+11.74	38+13.54	12638/12647	USBR	ESF Tunnel
	210660004	7155685	38+15.34	38+17.14	12648/12657	USBR	ESF Tunnel
1/25/96							
	210660004	7155685	38+17.14	38+18.94	12658/12667	USBR	ESF Tunnel; No Mining 1-17-96 to 1-25-96
	210660004	7155685	38+20.74	38+22.54	12668/12677	USBR	ESF Tunnel
	210660004	7155685	38+24.34	38+26.14	12678/12687	USBR	ESF Tunnel
	210660004	7155685	38+27.94	38+29.74	12688/12697	USBR	ESF Tunnel
	210660004	7155685	38+31.54	38+33.34	12698/12707	USBR	ESF Tunnel
1/26/96							
	210660004	7155685	38+31.54	38+33.34	12708/12717	USBR	ESF Tunnel; Same Positlons as Record #1271 Reshot After Rock Cleaning had Taken Place
	210660004	7155685	38+35.14	38+36.94	12718/12727	USBR	ESF Tunnel
	210660004	7155685	38+38.74	38+40.54	12728/12737	USBR	ESF Tunnel
	210660004	7155685	38+42.34	38+44.14	12738/12747	USBR	ESF Tunnel
	210660004	7155685	38+45.94	38+47.74	12748/12757	USBR	ESF Tunnel
	210660004	7155685	38+49.54	38+51.34	12758/12767	USBR	ESF Tunnel
	210660004	7155685	38+51.34	38+53.14	12768/12777	USBR	ESF Tunnel
	210660004	7155685	38+54.94	38+56.74	12778/12787	USBR	ESF Tunnel
	210660004	7155685	38+58.54	38+60.34	12788/12797	USBR	ESF Tunnel
	210660004	7155685	38+62.14	38+63.94	12798/12807	USBR	ESF Tunnel
	210660004	7155685	38+65.74	38+67.54	12808/12817	USBR	ESF Tunnel

Date	Body #	Lens #	Pos #1	Posi. #2	PG #s	ID	Comments
1/29/96							
	210660004	7155685	38+67.60	38+69.40	12818/12827	Wehner	ESF Tunnel; New Survey Locations
	210660004	7155685	38+71.20	38+73.00	12828/12837	Wehner	ESF Tunnel
	210660004	7155685	38+74.80	38+76.60	12838/12847	Wehner	ESF Tunnel
	210660004	7155685	38+78.40	38+80.20	12848/12857	Wehner	ESF Tunnel
	210660004	7155685	38+82.00	38+83.80	12858/12867	Wehner	ESF Tunnel
	210660004	7155685	38+85.60		12868/12872	Wehner	ESF Tunnel
	210660004	7155685	38+85.60	38+87.40	12873/12882	USBR	ESF Tunnel
	210660004	7155685	38+89.20	38+91.00	12883/12892	USBR	ESF Tunnel
	210660004	7155685	38+92.80	38+94.60	12893/12902	USBR	ESF Tunnel
	210660004	7155685	38+96.40		12903/12907	USBR	ESF Tunnel
1/30/96							
	210660004	7155685	38+96.40	38+98.20	12908/12917	Wehner	ESF Tunnel
	210660004	7155685	39+00.00	39+01.80	12918/12927	Wehner	ESF Tunnel
	210660004	7155685	39+03.60	39+05.40	12928/12937	Wehner	ESF Tunnel
	210660004	7155685	39+05.40	39+07.20	12938/12947	USBR	ESF Tunnel
	210660004	7155685	39+09.00	39+10.80	12948/12957	USBR	ESF Tunnel
	210660004	7155685	39+12.60	39+14.40	12958/12967	USBR	ESF Tunnel
	210660004	7155685	39+16.20	39+18.00	12968/12977	USBR	ESF Tunnel
	210660004	7155685	39+19.80	39+21.60	12978/12987	USBR	ESF Tunnel
	210660004	7155685	39+23.40	39+25.20	12988/12997	USBR	ESF Tunnel
1/31/96							
	210660004	7155685	39+27.00	39+28.80	12998/13007	Wehner	ESF Tunnel

Date	Body #	Lens #	Pos #1	Posi. #2	PG #s	ID	Comments
	210660004	7155685	39+30.60	39+32.40	13008/13017	Wehner	ESF Tunnel
	210660004	7155685	39+34.20	39+36.00	13018/13027	Wehner	ESF Tunnel
	210660004	7155685	39+37.80	39+39.60	13028/13037	Wehner	ESF Tunnel
2/1/96							
	210660004	7155685	39+39.60	39+41.40	13038/13047	Wehner	ESF Tunnel
	210660004	7155685	39+43.20	39+45.00	13048/13057	Wehner	ESF Tunnel
	210660004	7155685	39+46.80	39+48.60	13058/13067	Wehner	ESF Tunnel
	210660004	7155685	39+50.40	39+52.20	13068/13077	Wehner	ESF Tunnel
	210660004	7155685	39+54.00	39+55.80	13078/13087	Wehner	ESF Tunnel
	210660004	7155685	39+57.60	39+59.40	13088/13097	Wehner	ESF Tunnel
	210660004	7155685	39+61.20	39+63.00	13098/13107	Wehner	ESF Tunnel
	210660004	7155685	39+64.80	39+66.40	13108/13117	Wehner	ESF Tunnel
	210660004	7155685	39+66.40	39+68.20	13118/13127	USBR	ESF Tunnel
	210660004	7155685	39+70.00	39+71.80	13128/13137	USBR	ESF Tunnel
	210660004	7155685	39+73.60	39+75.40	13138/13147	USBR	ESF Tunnel
2/5/96							
	210660004	7155685	39+75.40	39+77.20	13148/13157	Wehner	ESF Tunnel
	210660004	7155685	39+79.00	39+80.80	13158/13167	Wehner	ESF Tunnel
	210660004	7155685	39+82.60	39+84.40	13168/13177	Wehner	ESF Tunnel
	210660004	7155685	39+86.20	39+88.00	13178/13187	Wehner	ESF Tunnel
	210660004	7155685	39+89.80	39+91.60	13188/13197	Wehner	ESF Tunnel
2/6/96							
	210660004	7155685	39+91.60	39+93.40	13198/13207	Wehner	ESF Tunnel

Date	Body #	Lens #	Pos #1	Posi. #2	PG #s	ID	Comments
	210660004	7155685	39+95.20	39+97.00	13208/13217	Wehner	ESF Tunnel
	210660004	7155685	39+98.80	40+00.60	13218/13227	Wehner	ESF Tunnel
	210660004	7155685	40+02.40	40+04.20	13228/13237	Wehner	ESF Tunnel
	210660004	7155685	40+06.00	40+07.80	13238/13247	Wehner	ESF Tunnel
	210660004	7155685	40+09.60		13248/13252	Wehner	ESF Tunnel
2/7/96							
	210660004	7155685	40+09.60	40+11.40	13253/13262	Wehner	ESF Tunnel
	210660004	7155685	40+13.20	40+15.00	13263/13272	Wehner	ESF Tunnel
	210660004	7155685	40+16.80	40+18.60	13273/13282	Wehner	ESF Tunnel
	210660004	7155685	40+20.40		13283/13287	Wehner	ESF Tunnel
	210660004	7155685	40+20.40	40+22.20	13288/13297	USBR	ESF Tunnel
	210660004	7155685	40+24.00	40+25.80	13298/13307	USBR	ESF Tunnel
	210660004	7155685	40+27.60	40+29.40	13308/13317	USBR	ESF Tunnel
	210660004	7155685	40+31.20	40+33.00	13318/13327	USBR	ESF Tunnel
	210660004	7155685	40+34.80	40+36.60	13328/13337	USBR	ESF Tunnel
2/8/96							
	210660004	7155685	40+36.60	40+38.40	13338/13347	Wehner	ESF Tunnel
	210660004	7155685	40+40.20	40+42.00	13348/13357	Wehner	ESF Tunnel
	210660004	7155685	40+43.80	40+45.60	13358/13367	Wehner	ESF Tunnel
	210660004	7155685	40+47.40	40+49.20	13368/13377	Wehner	ESF Tunnel
	210660004	7155685	40+51.00	40+52.80	13378/13387	Wehner	ESF Tunnel
	210660004	7155685	40+54.60	40+56.40	13388/13397	Wehner	ESF Tunnel
	210660004	7155685	40+58.20		13398/13402	Wehner	ESF Tunnel

Date	Body #	Lens #	Pos #1	Posi. #2	PG #s	ID	Comments
2/9/96							
	210660004	7155685	40+58.20	40+60.00	13403/13412	USBR	ESF Tunnel
	210660004	7155685	40+61.80	40+63.60	13413/13422	USBR	ESF Tunnel
	210660004	7155685	40+65.40	40+67.20	13423/13432	USBR	ESF Tunnel
2/12/96							
	210660004	7155685	40+67.20	40+69.00	13433/13442	Wehner	ESF Tunnel
	210660004	7155685	40+70.80	40+72.60	13443/13452	Wehner	ESF Tunnel
	210660004	7155685	40+74.40	40+76.20	13453/13462	Wehner	ESF Tunnel
	210660004	7155685	40+78.00	40+79.80	13463/13472	Wehner	ESF Tunnel
	210660004	7155685	40+81.60	40+83.40	13473/13482	Wehner	ESF Tunnel
2/13/96							
	210660004	7155685	40+83.40	40+85.20	13483/13492	Wehner	ESF Tunnel
	210660004	7155685	40+87.00	40+88.80	13493/13502	Wehner	ESF Tunnel
	210660004	7155685	40+90.60	40+92.40	13503/13512	Wehner	ESF Tunnel
2/14/96							
	210660004	7155685	40+92.40	40+94.20	13513/13522	Wehner	ESF Tunnel
	210660004	7155685	40+96.00	40+97.80	13523/13532	Wehner	ESF Tunnel
	210660004	7155685	40+99.60	41+01.40	13533/13542	Wehner	ESF Tunnel
	210660004	7155685	41+03.20	41+05.00	13543/13552	Wehner	ESF Tunnel
	210660004	7155685	41+06.80	41+08.60	13553/13562	Wehner	ESF Tunnel
	210660004	7155685	41+10.40	41+12.20	13563/13572	Wehner	ESF Tunnel
	210660004	7155685	00+05.	00+07.	13573/13582	Wehner	Heat Test Alcove, ESF Tunnel
	210660004	7155685	00+09.	00+11.	13583/13592	Wehner	Heat Test Alcove, ESF Tunnel

Date	Body #	Lens #	Pos #1	Posi. #2	PG #s	ID	Comments
	210660004	7155685	00+13.	00+15.	13593/13602	Wehner	Heat Test Alcove, ESF Tunnel
	210660004	7155685	00+17.	00+19.	13603/13612	Wehner	Heat Test Alcove, ESF Tunnel
	210660004	7155685	41+12.20	41+14.00	13613/13622	USBR	ESF Tunnel
	210660004	7155685	41+15.80	41+17.60	13623/13632	USBR	ESF Tunnel
	210660004	7155685	41+19.40	41+21.20	13633/13642	USBR	ESF Tunnel
	210660004	7155685	41+23.00	41+24.80	13643/13652	USBR	ESF Tunnel
	210660004	7155685	41+26.60	41+28.40	13653/13662	USBR	ESF Tunnel
	210660004	7155685	41+30.20	41+32.00	13663/13672	USBR	ESF Tunnel
	210660004	7155685	41+33.80		13673/13677	USBR	ESF Tunnel
2/15/96							
	210660004	7155685	41+33.80	41+35.60	13678/13687	Wehner	ESF Tunnel
	210660004	7155685	41+37.40	41+39.20	13688/13697	Wehner	ESF Tunnel
	210660004	7155685	41+41.00	41+42.80	13698/13707	Wehner	ESF Tunnel
	210660004	7155685	41+44.60	41+46.40	13708/13717	Wehner	ESF Tunnel
	210660004	7155685	41+48.20	41+50.00	13718/13727	Wehner	ESF Tunnel
2/16/96							
	210660004	7155685	41+50.00	40+51.80	13728/13737	USBR	ESF Tunnel
	210660004	7155685	41+53.60	41+55.40	13738/13747	USBR	ESF Tunnel
	210660004	7155685	41+57.20	41+59.00	13748/13757	USBR	ESF Tunnel
	210660004	7155685	41+60.80	41+62.60	13758/13767	USBR	ESF Tunnel
	210660004	7155685	41+64.40	41+66.20	13768/13777	USBR	ESF Tunnel
2/22/96							
	210660004	7155685	41+66.20	41+68.00	13778/13787	Wehner	ESF Tunnel

Date	Body #	Lens #	Pos #1	Posi. #2	PG #s	ID	Comments
	210660004	7155685	41+69.80	41+71.60	13788/13797	Wehner	ESF Tunnel
	210660004	7155685	41+73.40	41+75.20	13798/13807	Wehner	ESF Tunnel
2/23/96							
	210660004	7155685	41+75.20	41+77.00	13808/13817	USBR	ESF Tunnel
	210660004	7155685	41+78.80	41+80.60	13818/13827	USBR	ESF Tunnel
	210660004	7155685	41+82.40	41+84.20	13828/13837	USBR	ESF Tunnel
	210660004	7155685	41+86.00	41+87.80	13838/13847	USBR	ESF Tunnel
	210660004	7155685	41+89.60	41+91.40	13848/13857	USBR	ESF Tunnel
	210660004	7155685	41+93.20	41+95.00	13858/13867	USBR	ESF Tunnel
	210660004	7155685	41+96.80	41+98.60	13868/13877	USBR	ESF Tunnel
	210660004	7155685	42+00.60	42+02.20	13878/13887	USBR	ESF Tunnel
	210660004	7155685	42+04.00	42+05.80	13888/13897	USBR	ESF Tunnel
	210660004	7155685	42+07.60	42+09.40	13898/13907	USBR	ESF Tunnel
2/26/96							
	210660004	7155685	42+09.40	42+11.20	13908/13917	Wehner	ESF Tunnel
	210660004	7155685	42+13.00	42+14.80	13918/13927	Wehner	ESF Tunnel
	210660004	7155685	42+16.60	42+18.40	13928/13937	Wehner	ESF Tunnel
	210660004	7155685	42+20.20		13938/13942	Wehner	ESF Tunnel
2/27/96							
	210660004	7155685	42+20.20	42+22.00	13943/13952	Wehner	ESF Tunnel
	210660004	7155685	42+23.80	42+25.60	13953/13962	Wehner	ESF Tunnel
	210660004	7155685	42+27.40	42+29.20	13963/13972	Wehner	ESF Tunnel
	210660004	7155685	42+31.00	42+32.80	13973/13982	Wehner	ESF Tunnel

Date	Body #	Lens #	Pos #1	Posl. #2	PG #s	ID	Comments
2/28/96	210660004	7155685	42+34.60	42+36.40	13983/13992	Wehner	ESF Tunnel
	210660004	7155685	42+36.40	42+38.20	13993/14002	Wehner	ESF Tunnel
	210660004	7155685	42+40.00	42+41.80	14003/14012	Wehner	ESF Tunnel
	210660004	7155685	42+43.60	42+45.40	14013/14022	Wehner	ESF Tunnel
	210660004	7155685	42+47.20		14023/14027	Wehner	ESF Tunnel
2/29/96	210660004	7155685	42+47.20	42+49.00	14028/14037	Wehner	ESF Tunnel
	210660004	7155685	42+50.80	42+52.60	14038/14047	Wehner	ESF Tunnel
	210660004	7155685	42+54.40	42+56.20	14048/14057	Wehner	ESF Tunnel
	210660004	7155685	42+58.00	42+59.80	14058/14067	Wehner	ESF Tunnel
	210660004	7155685	42+61.60	42+63.40	14068/14077	Wehner	ESF Tunnel
	210660004	7155685	42+65.20	42+67.00	14078/14087	Wehner	ESF Tunnel
	210660004	7155685	42+68.80	42+70.60	14088/14097	Wehner	ESF Tunnel
	210660004	7155685	42+72.40	42+74.20	14098/14107	Wehner	ESF Tunnel
	210660004	7155685	42+76.00	42+77.80	14108/14117	Wehner	ESF Tunnel
	3/1/96	210660004	7155685	42+77.80	42+79.60	14118/14127	USBR
210660004		7155685	42+81.40	42+83.20	14128/14137	USBR	ESF Tunnel
210660004		7155685	42+85.00	42+86.80	14138/14147	USBR	ESF Tunnel
210660004		7155685	42+88.60	42+90.40	14148/14157	USBR	ESF Tunnel
210660004		7155685	42+92.20	42+94.00	14158/14167	USBR	ESF Tunnel
210660004		7155685	42+95.80		14168/14172	USBR	ESF Tunnel

Date	Body #	Lens #	Pos #1	Posi. #2	PG #s	ID	Comments
	210660004	7155685	42+95.80	42+97.60	14173/14182	USBR	ESF Tunnel
	210660004	7155685	42+99.40	43+01.20	14183/14192	USBR	ESF Tunnel
	210660004	7155685	43+03.00	43+04.80	14193/14202	USBR	ESF Tunnel
	210660004	7155685	43+06.60		14203/14207	USBR	ESF Tunnel
3/5/96							
	210660004	7155685	43+06.60	43+08.40	14208/14217	Wehner	ESF Tunnel
	210660004	7155685	43+10.20	43+12.00	14218/14227	Wehner	ESF Tunnel
	210660004	7155685	43+13.80	43+15.60	14228/14237	Wehner	ESF Tunnel
	210660004	7155685	43+17.40	43+19.20	14238/14247	Wehner	ESF Tunnel
	210660004	7155685	43+21.00	43+22.80	14248/14257	Wehner	ESF Tunnel
	210660004	7155685	43+24.60	43+26.40	14258/14267	Wehner	ESF Tunnel
	210660004	7155685	43+28.20		14268/14272	Wehner	ESF Tunnel
3/6/96							
	210660004	7155685	43+28.20	43+30.00	14273/14282	Unglesbee	ESF Tunnel
	210660004	7155685	43+31.80	43+33.60	14283/14292	Unglesbee	ESF Tunnel
	210660004	7155685	43+35.40	43+37.20	14293/14302	Unglesbee	ESF Tunnel
	210660004	7155685	43+39.00	43+40.80	14303/14312	Unglesbee	ESF Tunnel
	210660004	7155685	43+42.60	43+44.40	14313/14322	Unglesbee	ESF Tunnel
	210660004	7155685	43+46.20	43+48.00	14323/14332	Unglesbee	ESF Tunnel
	210660004	7155685	43+49.80		14333/14337	Unglesbee	ESF Tunnel
3/7/96							
	210660004	7155685	43+49.80	43+51.60	14338/14347	Wehner	ESF Tunnel
	210660004	7155685	43+53.40	43+55.20	14348/14357	Wehner	ESF Tunnel

Date	Body #	Lens #	Pos #1	Posi. #2	PG #s	ID	Comments
3/11/96							
	210660004	7155685	43+55.20	43+57.00	14358/14367	Wehner	ESF Tunnel
	210660004	7155685	43+58.80	43+60.60	14368/14377	Wehner	ESF Tunnel
	210660004	7155685	43+62.40	43+64.20	14378/14387	Wehner	ESF Tunnel
	210660004	7155685	43+66.00	43+67.80	14388/14397	Wehner	ESF Tunnel
	210660004	7155685	43+69.60	43+71.40	14398/14407	Wehner	ESF Tunnel
	210660004	7155685	43+73.20	43+75.00	14408/14417	Wehner	ESF Tunnel
	210660004	7155685	43+76.80	43+78.60	14418/14427	Wehner	ESF Tunnel
3/13/96							
	210660004	7155685	43+76.80	43+78.60	14428/14437	Wehner	ESF Tunnel; Rock Cleaned
	210660004	7155685	43+80.40	43+82.20	14438/14447	Wehner	ESF Tunnel
	210660004	7155685	43+84.00	43+85.80	14448/14457	Wehner	ESF Tunnel
	210660004	7155685	43+87.60	43+89.40	14458/14467	Wehner	ESF Tunnel
	210660004	7155685	43+91.20	43+93.00	14468/14477	Wehner	ESF Tunnel
	210660004	7155685	43+94.80	43+96.60	14478/14487	Wehner	ESF Tunnel
	210660004	7155685	43+98.40	44+00.20	14488/14497	Wehner	ESF Tunnel
	210660004	7155685	44+02.00	44+03.80	14498/14507	Wehner	ESF Tunnel
3/14/96							
	210660004	7155685	44+03.80	44+05.60	14508/14517	Wehner	ESF Tunnel
	210660004	7155685	44+07.40	44+09.20	14518/14527	Wehner	ESF Tunnel
	210660004	7155685	44+11.00	44+12.80	14528/14537	Wehner	ESF Tunnel
	210660004	7155685	44+14.60	44+16.40	14538/14547	Wehner	ESF Tunnel
	210660004	7155685	44+18.20	44+20.00	14548/14557	Wehner	ESF Tunnel

Date	Body #	Lens #	Pos #1	Posi. #2	PG #s	ID	Comments
	210660004	7155685	44+21.80	44+23.60	14558/14567	Wehner	ESF Tunnel
	210660004	7155685	44+25.40	44+27.20	14568/14577	Wehner	ESF Tunnel
	210660004	7155685	44+29.00		14578/14582	Wehner	ESF Tunnel
3/15/96							
	210660004	7155685	44+29.00	44+30.80	14583/14592	USBR	ESF Tunnel
	210660004	7155685	44+32.60	44+34.40	14593/14602	USBR	ESF Tunnel
	210660004	7155685	44+36.20	44+38.00	14603/14612	USBR	ESF Tunnel
	210660004	7155685	44+39.80	44+41.60	14613/14622	USBR	ESF Tunnel
	210660004	7155685	44+43.40	44+45.20	14623/14632	USBR	ESF Tunnel
	210660004	7155685	44+47.00	44+48.80	14633/14642	USBR	ESF Tunnel
3/18/96							
	210660004	7155685	44+47.00	44+48.80	14643/14652	Wehner	ESF Tunnel; Rock Cleaned
	210660004	7155685	44+50.60	44+52.40	14653/14662	Wehner	ESF Tunnel
	210660004	7155685	44+54.20	44+56.00	14663/14672	Wehner	ESF Tunnel
	210660004	7155685	44+57.80	44+59.60	14673/14682	Wehner	ESF Tunnel
	210660004	7155685	44+61.40	44+63.20	14683/14692	Wehner	ESF Tunnel
3/19/96							
	210660004	7155685	44+63.20	44+65.00	14693/14702	USBR	ESF Tunnel
	210660004	7155685	44+66.80	44+68.60	14703/14712	USBR	ESF Tunnel
	210660004	7155685	44+70.40	44+72.20	14713/14722	USBR	ESF Tunnel
	210660004	7155685	44+74.00	44+75.80	14723/14732	USBR	ESF Tunnel
	210660004	7155685	44+77.60	44+79.40	14733/14742	USBR	ESF Tunnel
	210660004	7155685	44+81.20	44+83.00	14743/14752	USBR	ESF Tunnel

Date	Body #	Lens #	Pos #1	Posi. #2	PG #s	ID	Comments
3/20/96							
	210660004	7155685	44+83.00	44+84.80	14753/14762	Wehner	ESF Tunnel
	210660004	7155685	44+86.60	44+88.40	14763/14772	Wehner	ESF Tunnel
	210660004	7155685	44+90.20	44+92.00	14773/14782	Wehner	ESF Tunnel
	210660004	7155685	44+93.80	44+95.60	14783/14792	Wehner	ESF Tunnel
	210660004	7155685	44+97.40	44+99.20	14793/14802	Wehner	ESF Tunnel
3/21/96							
	210660004	7155685	44+99.20	45+01.00	14803/14812	Wehner	ESF Tunnel
	210660004	7155685	45+02.80	45+04.60	14813/14822	Wehner	ESF Tunnel
	210660004	7155685	45+06.40	45+08.20	14823/14832	Wehner	ESF Tunnel
	210660004	7155685	45+10.00	45+11.80	14833/14842	Wehner	ESF Tunnel
	210660004	7155685	45+13.60	45+15.40	14843/14852	Wehner	ESF Tunnel
	210660004	7155685	45+17.20		14853/14857	Wehner	ESF Tunnel
3/22/96							
	210660004	7155685	45+17.20	45+19.00	14858/14867	USBR	ESF Tunnel
	210660004	7155685	45+20.80	45+22.60	14868/14877	USBR	ESF Tunnel
	210660004	7155685	45+24.40	45+26.20	14878/14887	USBR	ESF Tunnel
	210660004	7155685	45+28.00	45+29.80	14888/14897	USBR	ESF Tunnel
	210660004	7155685	45+31.60	45+33.40	14898/14907	USBR	ESF Tunnel
	210660004	7155685	45+35.20	45+37.00	14908/14917	USBR	ESF Tunnel
	210660004	7155685	45+38.80	45+40.60	14918/14927	USBR	ESF Tunnel
	210660004	7155685	45+42.40	45+44.20	14928/14937	USBR	ESF Tunnel

Date	Body #	Lens #	Pos #1	Posi. #2	PG #s	ID	Comments
3/28/96							
	210660004	7155685	45+44.20	45+46.00	14938/14947	Wehner	ESF Tunnel
	210660004	7155685	45+47.80	45+49.60	14948/14957	Wehner	ESF Tunnel
	210660004	7155685	45+51.40	45+53.20	14958/14967	Wehner	ESF Tunnel
	210660004	7155685	45+55.00	45+56.80	14968/14977	Wehner	ESF Tunnel
	210660004	7155685	45+58.60	45+60.40	14978/14987	Wehner	ESF Tunnel
	210660004	7155685	45+62.20	45+64.00	14988/14997	Wehner	ESF Tunnel
	210660004	7155685	45+65.80	45+67.60	14998/15007	Wehner	ESF Tunnel
	210660004	7155685	45+69.40	45+71.20	15008/15017	Wehner	ESF Tunnel
3/29/96							
	210660004	7155685	45+71.20	45+73.00	15018/15027	USBR	ESF Tunnel
	210660004	7155685	45+74.80	45+76.60	15028/15037	USBR	ESF Tunnel
	210660004	7155685	45+78.40	45+80.20	15038/15047	USBR	ESF Tunnel
	210660004	7155685	45+82.00	45+83.80	15048/15057	USBR	ESF Tunnel
4/1/96							
	210660004	7155685	45+83.80	45+85.60	15058/15067	Wehner	ESF Tunnel
	210660004	7155685	45+87.40	45+89.20	15068/15077	Wehner	ESF Tunnel
	210660004	7155685	45+91.00	45+92.80	15078/15087	Wehner	ESF Tunnel
4/2/96							
	210660004	7155685	45+92.80	45+94.60	15088/15097	Wehner	ESF Tunnel
	210660004	7155685	45+96.40	45+98.20	15098/15107	Wehner	ESF Tunnel
	210660004	7155685	46+00.00	46+01.80	15108/15117	Wehner	ESF Tunnel
	210660004	7155685	46+03.60	46+05.40	15118/15127	Wehner	ESF Tunnel

Date	Body #	Lens #	Pos #1	Posi. #2	PG #s	ID	Comments
4/3/96	210660004	7155685	46+07.20	46+09.00	15128/15137	Wehner	ESF Tunnel
	210660004	7155685	46+09.00	46+10.80	15138/15147	Wehner	ESF Tunnel
	210660004	7155685	46+12.60	46+14.40	15148/15157	Wehner	ESF Tunnel
	210660004	7155685	46+16.20	46+18.00	15158/15167	Wehner	ESF Tunnel
	210660004	7155685	46+19.80	46+21.60	15168/15177	Wehner	ESF Tunnel
	210660004	7155685	46+23.40	46+25.20	15178/15187	Wehner	ESF Tunnel
4/4/96	210660004	7155685	46+27.00	46+28.80	15188/15197	Wehner	ESF Tunnel
	210660004	7155685	46+28.80	46+30.60	15198/15207	Wehner	ESF Tunnel
	210660004	7155685	46+32.40	46+34.20	15208/15217	Wehner	ESF Tunnel
	210660004	7155685	46+36.00	46+37.80	15218/15227	Wehner	ESF Tunnel
	210660004	7155685	46+39.60	46+41.40	15228/15237	Wehner	ESF Tunnel
	210660004	7155685	46+43.20	46+45.00	15238/15247	Wehner	ESF Tunnel
	210660004	7155685	46+46.80	46+48.60	15248/15257	Wehner	ESF Tunnel
4/5/96	210660004	7155685	46+50.40	46+52.20	15258/15267	Wehner	ESF Tunnel
	210660004	7155685	46+52.20	46+54.00	15268/15277	USBR	ESF Tunnel
	210660004	7155685	46+55.80	46+57.60	15278/15287	USBR	ESF Tunnel
	210660004	7155685	46+59.40	46+61.20	15288/15297	USBR	ESF Tunnel
	210660004	7155685	46+63.00	46+64.80	15298/15307	USBR	ESF Tunnel
	210660004	7155685	46+66.60	46+68.40	15308/15317	USBR	ESF Tunnel
	210660004	7155685	46+70.20	46+72.00	15318/15327	USBR	ESF Tunnel

Date	Body #	Lens #	Pos #1	Posi. #2	PG #s	ID	Comments
	210660004	7155685	46+73.80	46+75.60	15328/15337	USBR	ESF Tunnel
	210660004	7155685	46+77.40	46+79.20	15338/15347	USBR	ESF Tunnel
	210660004	7155685	46+81.00	46+82.80	15348/15357	USBR	ESF Tunnel
4/8/96							
	210660004	7155685	46+82.80	46+84.60	15358/15367	Wehner	ESF Tunnel
	210660004	7155685	46+86.40	46+88.20	15368/15377	Wehner	ESF Tunnel
	210660004	7155685	46+90.00	46+91.80	15378/15387	Wehner	ESF Tunnel
	210660004	7155685	46+93.60	46+95.40	15388/15397	Wehner	ESF Tunnel
	210660004	7155685	46+97.20	46+99.00	15398/15407	Wehner	ESF Tunnel
	210660004	7155685	47+00.80	47+02.60	15408/15417	Wehner	ESF Tunnel
	210660004	7155685	47+04.40	47+06.20	15418/15427	Wehner	ESF Tunnel
	210660004	7155685	47+08.00	47+09.80	15428/15437	Wehner	ESF Tunnel
	210660004	7155685	47+11.60		15438/15442	Wehner	ESF Tunnel
4/9/96							
	210660004	7155685	47+11.60	47+13.40	15443/15452	Unglesbee	ESF Tunnel
	210660004	7155685	47+15.20	47+17.00	15453/15462	Unglesbee	ESF Tunnel
	210660004	7155685	47+18.80	47+20.60	15463/15472	Unglesbee	ESF Tunnel
	210660004	7155685	47+22.40	47+24.20	15473/15482	Unglesbee	ESF Tunnel
	210660004	7155685	47+26.00	47+27.80	15483/15492	Unglesbee	ESF Tunnel
	210660004	7155685	47+29.60	47+31.40	15493/15502	Unglesbee	ESF Tunnel
4/10/96							
	210660004	7155685	47+31.40	47+33.20	15503/15512	Unglesbee	ESF Tunnel
	210660004	7155685	47+35.00	47+36.80	15513/15522	Unglesbee	ESF Tunnel

Date	Body #	Lens #	Pos #1	Posi. #2	PG #s	ID	Comments
	210660004	7155685	47+38.60	47+40.40	15523/15532	Unglesbee	ESF Tunnel
	210660004	7155685	47+42.20		15533/15537	Unglesbee	ESF Tunnel
4/11/96							
	210660004	7155685	47+44.00	47+45.80	15538/15547	Unglesbee	ESF Tunnel
	210660004	7155685	47+47.60	47+49.40	15548/15557	Unglesbee	ESF Tunnel
	210660004	7155685	47+51.20	47+53.00	15558/15567	Unglesbee	ESF Tunnel
	210660004	7155685	47+54.80	47+56.60	15568/15577	Unglesbee	ESF Tunnel
	210660004	7155685	47+58.40	47+60.20	15578/15587	Unglesbee	ESF Tunnel
	210660004	7155685	47+62.00	47+63.80	15588/15597	Unglesbee	ESF Tunnel
	210660004	7155685	47+65.60	47+67.40	15598/15607	Unglesbee	ESF Tunnel
4/12/96							
	210660004	7155685	47+67.40	47+69.20	15608/15617	Unglesbee	ESF Tunnel
	210660004	7155685	47+71.00	47+72.80	15618/15627	Unglesbee	ESF Tunnel
	210660004	7155685	47+74.60	47+76.40	15628/15637	Unglesbee	ESF Tunnel
	210660004	7155685	47+78.20	47+80.00	15638/15647	Unglesbee	ESF Tunnel
	210660004	7155685	47+81.80	47+83.60	15648/15657	Unglesbee	ESF Tunnel
	210660004	7155685	47+85.40	47+87.20	15658/15667	Unglesbee	ESF Tunnel
	210660004	7155685	47+89.00	47+90.80	15668/15677	Unglesbee	ESF Tunnel
4/17/96							
	210660004	7155685	00+21.	00+23.	15678/15687	Wehner	ESF Tunnel; Heat Test Alcove;
	210660004	7155685	00+25.	00+27.	15688/15697	Wehner	ESF Tunnel; Heat Test Alcove;
	210660004	7155685	00+29.	00+31.	15698/15707	Wehner	ESF Tunnel; Heat Test Alcove;
	210660004	7155685	00+33.	00+35.	15708/15717	Wehner	ESF Tunnel; Heat Test Alcove;

Date	Body #	Lens #	Pos #1	Posl. #2	PG #s	ID	Comments
	210660004	7155685	00+37.		15718/15722	Wehner	ESF Tunnel; Heat Test Alcove,
	210660004	7155685	00+04.	00+06.	15723/15732	Wehner	ESF Tunnel; Thermo Mechanical Drift;
	210660004	7155685	00+08.	00+10.	15733/15742	Wehner	ESF Tunnel; Thermo Mechanical Drift;
	210660004	7155685	00+12.	00+14.	15743/15752	Wehner	ESF Tunnel; Thermo Mechanical Drift;
	210660004	7155685	00+16.	00+18.	15753/15762	Wehner	ESF Tunnel; Thermo Mechanical Drift;
	210660004	7155685	00+20.	00+22.	15763/15772	Wehner	ESF Tunnel; Thermo Mechanical Drift;
4/18/96							
	210660004	7155685	00+03.	00+05.	15773/15782	Wehner	ESF Tunnel; Thermo Mechanical Ext;
	210660004	7155685	00+07.	00+09.	15783/15792	Wehner	ESF Tunnel; Thermo Mechanical Ext;
	210660004	7155685	00+11.		15793/15797	Wehner	ESF Tunnel; Thermo Mechanical Ext;
4/24/96							
	210660004	7155685	47+90.80	47+92.60	15798/15807	Wehner	ESF Tunnel
	210660004	7155685	47+94.40	47+96.20	15808/15817	Wehner	ESF Tunnel
	210660004	7155685	47+98.00	47+99.80	15818/15827	Wehner	ESF Tunnel
	210660004	7155685	48+01.60	48+03.40	15828/15837	Wehner	ESF Tunnel
	210660004	7155685	48+05.20	48+07.00	15838/15847	Wehner	ESF Tunnel
	210660004	7155685	48+08.80	48+10.60	15848/15857	Wehner	ESF Tunnel
	210660004	7155685	48+12.40	48+14.20	15858/15867	Wehner	ESF Tunnel
	210660004	7155685	48+16.00		15868/15872	Wehner	ESF Tunnel
4/25/96							
	210660004	7155685	48+16.00	48+17.80	15873/15882	Wehner	ESF Tunnel
	210660004	7155685	48+19.60	48+21.40	15883/15892	Wehner	ESF Tunnel
	210660004	7155685	48+23.20	48+25.00	15893/15902	Wehner	ESF Tunnel

Date	Body #	Lens #	Pos #1	Posi. #2	PG #s	ID	Comments
	210660004	7155685	48+26.80	48+28.60	15903/15912	Wehner	ESF Tunnel
	210660004	7155685	48+30.40	48+32.20	15913/15922	Wehner	ESF Tunnel
	210660004	7155685	48+34.00	48+35.80	15923/15932	Wehner	ESF Tunnel
4/26/96							
	210660004	7155685	48+35.80	48+37.60	15933/15942	USBR	ESF Tunnel
	210660004	7155685	48+39.40	48+41.20	15943/15952	USBR	ESF Tunnel
	210660004	7155685	48+43.00	48+44.80	15953/15962	USBR	ESF Tunnel
	210660004	7155685	48+46.60	48+48.40	15963/15972	USBR	ESF Tunnel
	210660004	7155685	48+50.20	48+52.00	15973/15982	USBR	ESF Tunnel
	210660004	7155685	48+53.80	48+55.60	15983/15992	USBR	ESF Tunnel
	210660004	7155685	48+57.40	48+59.20	15993/16002	USBR	ESF Tunnel
	210660004	7155685	48+61.00	48+62.80	16003/16012	USBR	ESF Tunnel
	210660004	7155685	48+64.60	48+66.40	16013/16022	USBR	ESF Tunnel
4/29/96							
	210660004	7155685	48+66.40	48+68.20	16023/16032	Wehner	ESF Tunnel
	210660004	7155685	48+70.00	48+71.80	16033/16042	Wehner	ESF Tunnel
	210660004	7155685	48+73.60	48+75.40	16043/16052	Wehner	ESF Tunnel
	210660004	7155685	48+77.20	48+79.00	16053/16062	Wehner	ESF Tunnel
	210660004	7155685	48+80.80	48+82.60	16063/16072	Wehner	ESF Tunnel
	210660004	7155685	48+84.40	48+86.20	16073/16082	Wehner	ESF Tunnel
	210660004	7155685	48+88.00	48+89.80	16083/16092	Wehner	ESF Tunnel
	210660004	7155685	48+91.60	48+93.40	16093/16102	Wehner	ESF Tunnel
	210660004	7155685	48+95.20	48+97.00	16103/16112	Wehner	ESF Tunnel

Date	Body #	Lens #	Pos #1	Posi. #2	PG #s	ID	Comments
	210660004	7155685	48+98.80	49+00.60	16113/16122	Wehner	ESF Tunnel
4/30/96							
	210660004	7155685	49+00.60	49+02.40	16123/16132	Wehner	ESF Tunnel
	210660004	7155685	49+04.20	49+06.00	16133/16142	Wehner	ESF Tunnel
	210660004	7155685	49+07.80	49+09.60	16143/16152	Wehner	ESF Tunnel
	210660004	7155685	49+11.40	49+13.20	16153/16162	Wehner	ESF Tunnel
	210660004	7155685	49+15.00	49+16.80	16163/16172	Wehner	ESF Tunnel
	210660004	7155685	49+18.60	49+20.40	16173/16182	Wehner	ESF Tunnel
	210660004	7155685	49+22.20	49+24.00	16183/16192	Wehner	ESF Tunnel
	210660004	7155685	49+25.80	49+27.60	16193/16202	Wehner	ESF Tunnel
	210660004	7155685	49+29.40	49+31.20	16203/16212	Wehner	ESF Tunnel
5/1/96							
	210660004	7155685	49+31.20	49+33.00	16213/16222	Wehner	ESF Tunnel
	210660004	7155685	49+34.80	49+36.60	16223/16232	Wehner	ESF Tunnel
	210660004	7155685	49+38.40	49+40.20	16233/16242	Wehner	ESF Tunnel
	210660004	7155685	49+42.00	49+43.80	16243/16252	Wehner	ESF Tunnel
	210660004	7155685	49+45.60	49+47.40	16253/16262	Wehner	ESF Tunnel
	210660004	7155685	49+49.20	49+51.00	16263/16272	Wehner	ESF Tunnel
	210660004	7155685	49+52.80	49+54.60	16273/16282	Wehner	ESF Tunnel
	210660004	7155685	49+56.40	49+58.20	16283/16292	Wehner	ESF Tunnel
	210660004	7155685	49+60.00	49+61.80	16293/16302	Wehner	ESF Tunnel
	210660004	7155685	49+63.60	49+65.40	16303/16312	Wehner	ESF Tunnel
	210660004	7155685	49+67.20	49+69.00	16313/16322	Wehner	ESF Tunnel

Date	Body #	Lens #	Pos #1	Posl. #2	PG #s	ID	Comments
5/2/96							
	210660004	7155685	49+69.00	49+70.80	16323/16332	Wehner	ESF Tunnel
	210660004	7155685	49+72.60	49+74.40	16333/16342	Wehner	ESF Tunnel
	210660004	7155685	49+76.20	49+78.00	16343/16352	Wehner	ESF Tunnel
	210660004	7155685	49+79.80	49+81.60	16353/16362	Wehner	ESF Tunnel
	210660004	7155685	49+83.40	49+85.20	16363/16372	Wehner	ESF Tunnel
	210660004	7155685	49+87.00	49+88.80	16373/16382	Wehner	ESF Tunnel
	210660004	7155685	49+90.60	49+92.40	16383/16392	Wehner	ESF Tunnel
	210660004	7155685	49+94.20	49+96.00	16393/16402	Wehner	ESF Tunnel
5/3/96							
	210660004	7155685	49+96.00	49+97.80	16403/16412	Unglesbee	ESF Tunnel
	210660004	7155685	49+99.60	50+01.40	16413/16422	Unglesbee	ESF Tunnel
	210660004	7155685	50+03.20	50+05.00	16423/16432	Unglesbee	ESF Tunnel
	210660004	7155685	50+06.80	50+08.60	16433/16442	Unglesbee	ESF Tunnel
	210660004	7155685	50+10.40	50+12.20	16443/16452	Unglesbee	ESF Tunnel
	210660004	7155685	50+14.00	50+15.80	16453/16462	Unglesbee	ESF Tunnel
	210660004	7155685	50+17.60	50+19.40	16463/16472	Unglesbee	ESF Tunnel
	210660004	7155685	50+21.20	50+23.00	16473/16482	Unglesbee	ESF Tunnel
	210660004	7155685	50+24.80	50+26.60	16483/16492	Unglesbee	ESF Tunnel
	210660004	7155685	50+28.40	50+30.20	16493/16502	Unglesbee	ESF Tunnel
	210660004	7155685	50+32.00	50+33.80	16503/16512	Unglesbee	ESF Tunnel
	210660004	7155685	50+35.60		16513/16517	Unglesbee	ESF Tunnel

Date	Body #	Lens #	Pos #1	Posl. #2	PG #s	ID	Comments
5/6/96							
	210660004	7155685	50+35.60	50+37.40	16518/16527	Wehner	ESF Tunnel
	210660004	7155685	50+39.20	50+41.00	16528/16537	Wehner	ESF Tunnel
	210660004	7155685	50+42.80	50+44.60	16538/16547	Wehner	ESF Tunnel
	210660004	7155685	50+46.40	50+48.20	16548/16557	Wehner	ESF Tunnel
	210660004	7155685	50+50.00	50+51.80	16558/16567	Wehner	ESF Tunnel
	210660004	7155685	50+53.60	50+55.40	16568/16577	Wehner	ESF Tunnel
	210660004	7155685	50+57.20	50+59.00	16578/16587	Wehner	ESF Tunnel
	210660004	7155685	50+60.80	50+62.60	16588/16597	Wehner	ESF Tunnel
5/7/96							
	210660004	7155685	50+62.60	50+64.40	16598/16607	USBR	ESF Tunnel
	210660004	7155685	50+66.20	50+68.00	16608/16617	USBR	ESF Tunnel
	210660004	7155685	50+69.80	50+71.60	16618/16627	USBR	ESF Tunnel
	210660004	7155685	50+73.40	50+75.20	16628/16637	USBR	ESF Tunnel
	210660004	7155685	50+77.00	50+78.80	16638/16647	USBR	ESF Tunnel
	210660004	7155685	50+80.60	50+82.40	16648/16657	USBR	ESF Tunnel
	210660004	7155685	50+84.20	50+86.00	16658/16667	USBR	ESF Tunnel
5/8/96							
	210660004	7155685	50+87.80	50+89.60	16668/16677	Wehner	ESF Tunnel
	210660004	7155685	50+91.40	50+93.20	16678/16687	Wehner	ESF Tunnel
	210660004	7155685	50+95.00	50+96.80	16688/16697	Wehner	ESF Tunnel
	210660004	7155685	50+98.60	51+00.40	16698/16707	Wehner	ESF Tunnel
	210660004	7155685	51+02.20	51+04.00	16708/16717	Wehner	ESF Tunnel

Date	Body #	Lens #	Pos #1	Posi. #2	PG #s	ID	Comments
	210660004	7155685	51+05.80	51+07.60	16718/16727	Wehner	ESF Tunnel
	210660004	7155685	51+09.40	51+11.20	16728/16737	Wehner	ESF Tunnel
	210660004	7155685	51+13.00	51+14.80	16738/16747	Wehner	ESF Tunnel
	210660004	7155685	51+16.60	51+18.40	16748/16757	Wehner	ESF Tunnel
	210660004	7155685	51+20.20	51+22.00	16758/16767	Wehner	ESF Tunnel
	210660004	7155685	51+23.80	51+25.60	16768/16777	Wehner	ESF Tunnel
	210660004	7155685	51+27.40	51+29.20	16778/16787	Wehner	ESF Tunnel
	210660004	7155685	51+31.00		16788/16792	Wehner	ESF Tunnel
5/9/96							
	210660004	7155685	51+31.00	51+32.80	16793/16802	Wehner	ESF Tunnel
	210660004	7155685	51+34.60	51+36.40	16803/16812	Wehner	ESF Tunnel
	210660004	7155685	51+38.20	51+40.00	16813/16822	Wehner	ESF Tunnel
	210660004	7155685	51+41.80	51+43.60	16823/16832	Wehner	ESF Tunnel
	210660004	7155685	51+45.40	51+47.20	16833/16842	Wehner	ESF Tunnel
	210660004	7155685	51+49.00	51+50.80	16843/16852	Wehner	ESF Tunnel
	210660004	7155685	51+52.60	51+54.40	16853/16862	Wehner	ESF Tunnel
	210660004	7155685	51+56.20	51+58.00	16863/16872	Wehner	ESF Tunnel
	210660004	7155685	51+59.80	51+61.60	16873/16882	Wehner	ESF Tunnel
	210660004	7155685	51+63.40		16883/16887	Wehner	ESF Tunnel
5/10/96							
	210660004	7155685	51+63.40	51+65.20	16888/16897	USBR	ESF Tunnel
	210660004	7155685	51+67.00	51+68.80	16898/16907	USBR	ESF Tunnel
	210660004	7155685	51+70.60	51+72.40	16908/16917	USBR	ESF Tunnel

Date	Body #	Lens #	Pos #1	Posi. #2	PG #s	ID	Comments
	210660004	7155685	51+74.20	51+76.00	16918/16927	USBR	ESF Tunnel
	210660004	7155685	51+77.80	51+79.60	16928/16937	USBR	ESF Tunnel
	210660004	7155685	51+81.40	51+83.20	16938/16947	USBR	ESF Tunnel
	210660004	7155685	51+85.00	51+86.80	16948/16957	USBR	ESF Tunnel
	210660004	7155685	51+88.60	51+90.40	16958/16967	USBR	ESF Tunnel
	210660004	7155685	51+92.20	51+94.00	16968/16977	USBR	ESF Tunnel
	210660004	7155685	51+95.80		16978/16982	USBR	ESF Tunnel
5/14/96							
	210660004	7155685	51+95.80	51+97.60	16983/16992	Wehner	ESF Tunnel
	210660004	7155685	51+99.40	52+01.20	16993/17002	Wehner	ESF Tunnel
	210660004	7155685	52+03.00	52+04.80	17003/17012	Wehner	ESF Tunnel
	210660004	7155685	52+06.60	52+08.40	17013/17022	Wehner	ESF Tunnel
5/15/96							
	210660004	7155685	52+08.40	52+10.20	17023/17032	Wehner	ESF Tunnel
	210660004	7155685	52+12.00	52+13.80	17033/17042	Wehner	ESF Tunnel
	210660004	7155685	52+15.60	52+17.40	17043/17052	Wehner	ESF Tunnel
	210660004	7155685	52+19.20	52+21.00	17053/17062	Wehner	ESF Tunnel
	210660004	7155685	52+22.80	52+24.60	17063/17072	Wehner	ESF Tunnel
	210660004	7155685	52+26.40	52+28.20	17073/17082	Wehner	ESF Tunnel
	210660004	7155685	52+30.00		17083/17087	Wehner	ESF Tunnel
5/16/96							
	210660004	7155685	52+30.00	52+31.80	17088/17097	Wehner	ESF Tunnel
	210660004	7155685	52+33.60	52+35.40	17098/17107	Wehner	ESF Tunnel

Date	Body #	Lens #	Pos #1	Posi. #2	PG #s	ID	Comments
5/17/96	210660004	7155685	52+37.20		17108/17112	Wehner	ESF Tunnel
	210660004	7155685	52+40.80	52+42.60	17113/17122	USBR	ESF Tunnel
	210660004	7155685	52+44.40	52+46.20	17123/17132	USBR	ESF Tunnel
	210660004	7155685	52+48.00	52+49.80	17133/17142	USBR	ESF Tunnel
	210660004	7155685	52+51.60	52+53.40	17143/17152	USBR	ESF Tunnel
	210660004	7155685	52+55.20	52+57.00	17153/17162	USBR	ESF Tunnel
	210660004	7155685	52+58.80	52+60.60	17163/17172	USBR	ESF Tunnel
	210660004	7155685	52+62.40	52+64.20	17173/17182	USBR	ESF Tunnel
	210660004	7155685	52+66.00	52+67.80	17183/17192	USBR	ESF Tunnel
	210660004	7155685	52+69.60	52+71.40	17193/17202	USBR	ESF Tunnel
	210660004	7155685	52+73.20	52+75.00	17203/17212	USBR	ESF Tunnel
	210660004	7155685	52+76.80	52+78.60	17213/17222	USBR	ESF Tunnel
	210660004	7155685	52+80.40	52+82.20	17223/17232	USBR	ESF Tunnel
	210660004	7155685	52+84.00		17233/17242	USBR	ESF Tunnel
5/20/96							
	210660004	7155685	52+84.00	52+85.80	17243/17252	Wehner	ESF Tunnel
	210660004	7155685	52+87.60	52+89.40	17253/17262	Wehner	ESF Tunnel
	210660004	7155685	52+91.20	52+93.00	17263/17272	Wehner	ESF Tunnel
	210660004	7155685	52+94.80	52+96.60	17273/17282	Wehner	ESF Tunnel
	210660004	7155685	52+98.40	53+00.20	17283/17292	Wehner	ESF Tunnel
	210660004	7155685	53+02.00		17293/17297	Wehner	ESF Tunnel

Date	Body #	Lens #	Pos #1	Posi. #2	PG #s	ID	Comments
5/21/96							
	210660004	7155685	53+02.00	53+03.80	17298/17307	Wehner	ESF Tunnel
	210660004	7155685	53+05.60	53+07.40	17308/17317	Wehner	ESF Tunnel
	210660004	7155685	53+09.20	53+11.00	17318/17327	Wehner	ESF Tunnel
	210660004	7155685	53+12.80		17328/17332	Wehner	ESF Tunnel
5/22/96							
	210660004	7155685	53+12.80	53+14.60	17333/17342	Wehner	ESF Tunnel
	210660004	7155685	53+16.40	53+18.20	17343/17352	Wehner	ESF Tunnel
	210660004	7155685	53+20.00	53+21.80	17353/17362	Wehner	ESF Tunnel
	210660004	7155685	53+23.60	53+25.40	17363/17372	Wehner	ESF Tunnel
	210660004	7155685	53+27.20	53+29.00	17373/17382	Wehner	ESF Tunnel
	210660004	7155685	53+30.80	53+32.60	17383/17392	Wehner	ESF Tunnel
	210660004	7155685	53+34.40	53+36.20	17393/17402	Wehner	ESF Tunnel
	210660004	7155685	53+38.00	53+39.80	17403/17412	Wehner	ESF Tunnel
	210660004	7155685	53+41.60		17413/17417	Wehner	ESF Tunnel
5/23/96							
	210660004	7155685	53+41.60	53+43.40	17418/17427	Wehner	ESF Tunnel
	210660004	7155685	53+45.20	53+47.00	17428/17437	Wehner	ESF Tunnel
	210660004	7155685	53+48.80	53+50.60	17438/17447	Wehner	ESF Tunnel
5/24/96							
	210660004	7155685	53+50.60	53+52.40	17448/17457	USBR	ESF Tunnel
	210660004	7155685	53+54.20	53+56.00	17458/17467	USBR	ESF Tunnel
	210660004	7155685	53+57.80	53+59.60	17468/17477	USBR	ESF Tunnel

Date	Body #	Lens #	Pos #1	Posl. #2	PG #s	ID	Comments
	210660004	7155685	53+61.40	53+63.20	17478/17487	USBR	ESF Tunnel
	210660004	7155685	53+65.00	53+66.80	17488/17497	USBR	ESF Tunnel
	210660004	7155685	53+68.60	53+70.40	17498/17507	USBR	ESF Tunnel
	210660004	7155685	53+72.20	53+74.00	17508/17517	USBR	ESF Tunnel
	210660004	7155685	53+75.80	53+77.60	17518/17527	USBR	ESF Tunnel
	210660004	7155685	53+79.40	53+81.20	17528/17537	USBR	ESF Tunnel
5/28/96							
	210660004	7155685	53+81.20	53+83.00	17538/17547	USBR	ESF Tunnel
	210660004	7155685	53+84.80	53+86.60	17548/17557	USBR	ESF Tunnel
	210660004	7155685	53+88.40	53+90.20	17558/17567	USBR	ESF Tunnel
	210660004	7155685	53+92.00	53+93.80	17568/17577	USBR	ESF Tunnel
	210660004	7155685	53+95.60	53+97.40	17578/17587	USBR	ESF Tunnel
	210660004	7155685	53+99.20		17588/17592	USBR	ESF Tunnel
5/29/96							
	210660004	7155685	53+99.20	54+01.00	17593/17602	Unglesbee	ESF Tunnel
	210660004	7155685	54+02.80	54+04.60	17603/17612	Unglesbee	ESF Tunnel
	210660004	7155685	54+06.40	54+08.20	17613/17622	Unglesbee	ESF Tunnel
	210660004	7155685	54+10.00	54+11.80	17623/17632	Unglesbee	ESF Tunnel
	210660004	7155685	54+13.60	54+15.40	17633/17642	Unglesbee	ESF Tunnel
	210660004	7155685	54+17.20	54+19.00	17643/17652	Unglesbee	ESF Tunnel
	210660004	7155685	54+20.80	54+22.60	17653/17662	Unglesbee	ESF Tunnel
	210660004	7155685	54+24.40	54+26.20	17663/17672	Unglesbee	ESF Tunnel
	210660004	7155685	54+28.00		17673/17677	Unglesbee	ESF Tunnel

Date	Body #	Lens #	Pos #1	Posi. #2	PG #s	ID	Comments
5/30/96							
	210660004	7155685	54+28.00	54+29.80	17678/17687	USBR	ESF Tunnel
	210660004	7155685	54+31.60	54+33.40	17688/17697	USBR	ESF Tunnel
	210660004	7155685	54+35.20	54+37.00	17698/17707	USBR	ESF Tunnel
	210660004	7155685	54+38.80	54+40.60	17708/17717	USBR	ESF Tunnel
	210660004	7155685	54+42.40	54+44.20	17718/17727	USBR	ESF Tunnel
	210660004	7155685	54+56.00	54+47.80	17728/17737	USBR	ESF Tunnel
	210660004	7155685	54+49.60	54+51.40	17738/17747	USBR	ESF Tunnel
5/31/96							
	210660004	7155685	54+51.40	54+53.20	17748/17757	USBR	ESF Tunnel
	210660004	7155685	54+55.00	54+56.80	17758/17767	USBR	ESF Tunnel
	210660004	7155685	54+58.60	54+60.40	17768/17777	USBR	ESF Tunnel
	210660004	7155685	54+62.20	54+64.00	17778/17787	USBR	ESF Tunnel
	210660004	7155685	54+65.80	54+67.60	17788/17797	USBR	ESF Tunnel
	210660004	7155685	54+69.40	54+71.20	17798/17807	USBR	ESF Tunnel
	210660004	7155685	54+73.00	54+74.80	17808/17817	USBR	ESF Tunnel
	210660004	7155685	54+76.60	54+78.40	17818/17827	USBR	ESF Tunnel
	210660004	7155685	54+80.20		17828/17832	USBR	ESF Tunnel
6/3/96							
	210660004	7155685	54+80.20	54+82.00	17833/17842	Wehner	ESF Tunnel
	210660004	7155685	54+83.80	54+85.60	17843/17852	Wehner	ESF Tunnel
	210660004	7155685	54+87.40	54+89.20	17853/17862	Wehner	ESF Tunnel
	210660004	7155685	54+91.00	54+92.80	17863/17872	Wehner	ESF Tunnel

Date	Body #	Lens #	Pos #1	Posi. #2	PG #s	ID	Comments
6/4/96	210660004	7155685	54+94.60	54+96.40	17873/17882	Wehner	ESF Tunnel
	210660004	7155685	54+96.40	54+98.20	17883/17892	Wehner	ESF Tunnel
	210660004	7155685	55+00.00	55+01.80	17893/17902	Wehner	ESF Tunnel
	210660004	7155685	55+03.60	55+05.40	17903/17912	Wehner	ESF Tunnel
	210660004	7155685	55+07.20	55+09.00	17913/17922	Wehner	ESF Tunnel
6/5/96	210660004	7155685	55+10.80		17923/17927	Wehner	ESF Tunnel
	210660004	7155685	55+10.80	55+12.60	17928/17937	Wehner	ESF Tunnel
	210660004	7155685	55+14.40	55+16.20	17938/17947	Wehner	ESF Tunnel
	210660004	7155685	55+18.00	55+19.80	17948/17957	Wehner	ESF Tunnel
	210660004	7155685	55+21.60	55+23.40	17958/17967	Wehner	ESF Tunnel
6/6/96	210660004	7155685	55+23.40	55+25.20	17968/17977	Wehner	ESF Tunnel
	210660004	7155685	55+27.00	55+28.80	17978/17987	Wehner	ESF Tunnel
	210660004	7155685	55+30.60	55+32.40	17988/17997	Wehner	ESF Tunnel
	210660004	7155685	55+34.20	55+36.00	17998/18007	Wehner	ESF Tunnel
	6/7/96	210660004	7155685	55+36.00	55+37.80	18008/18017	Wehner
210660004		7155685	55+39.60	55+41.40	18018/18027	Wehner	ESF Tunnel
210660004		7155685	55+43.20	55+45.00	18028/18037	Wehner	ESF Tunnel
6/10/96		210660004	7155685	55+45.00	55+46.80	18038/18047	Wehner

APPENDIX 3

Photographs

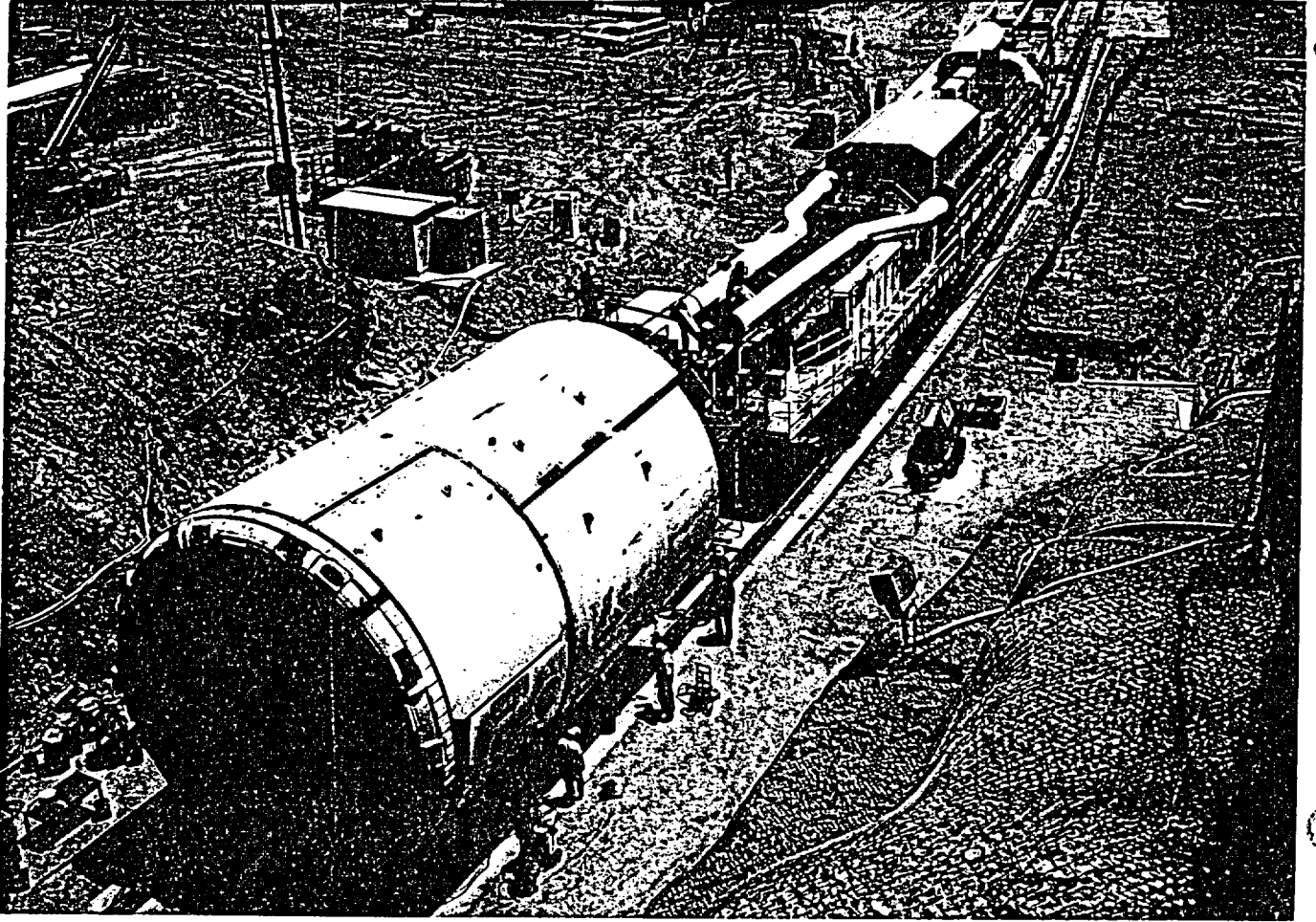


Photo 1 The TBM positioned to enter the ESF. YMP photo-YM8085

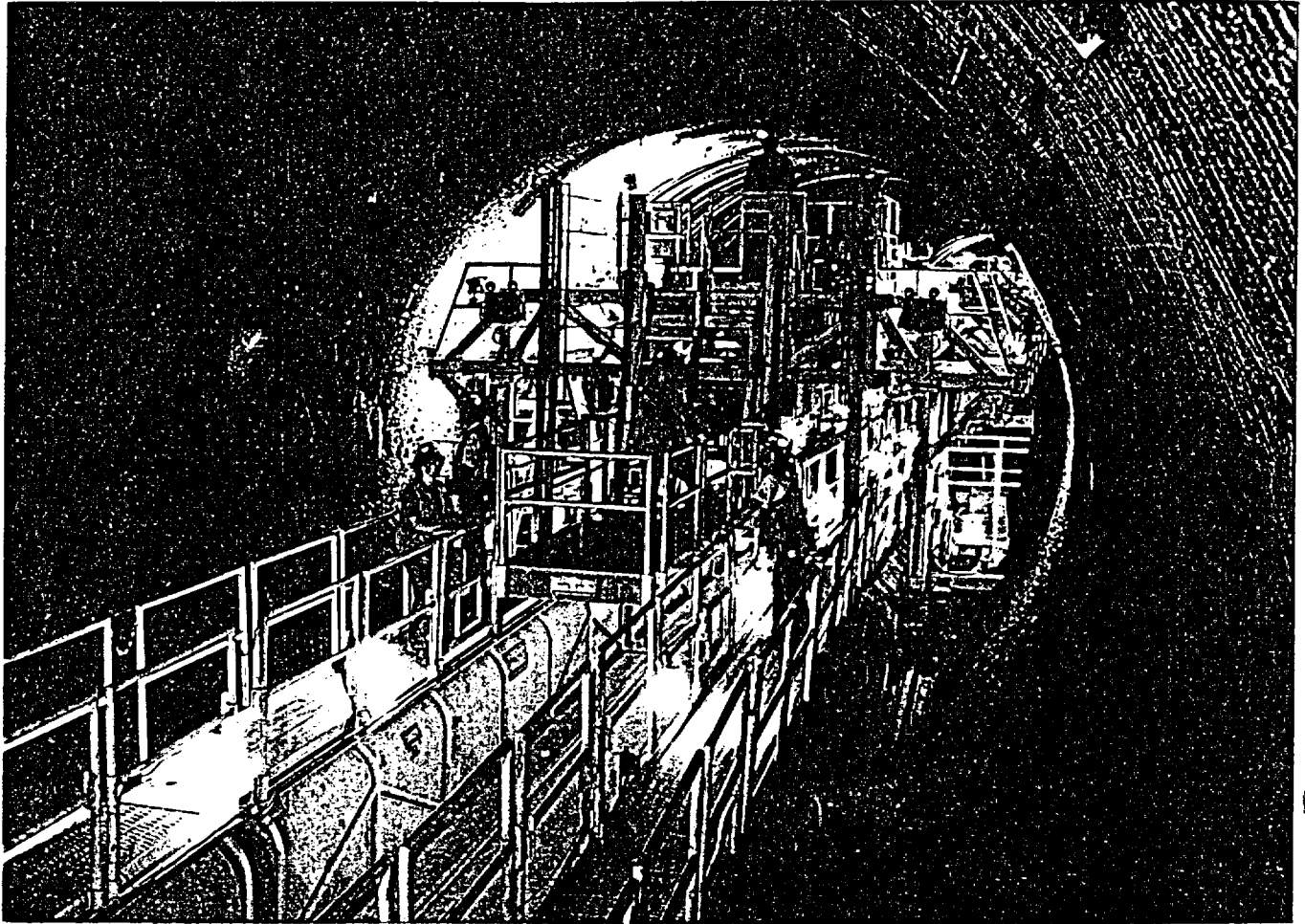


Photo 2 Geologists working in the mapping area on the trailing gear. The gantry, in the background, is capable of moving back and forth in this 45-m-long mapping area. YMP photo-YM11095

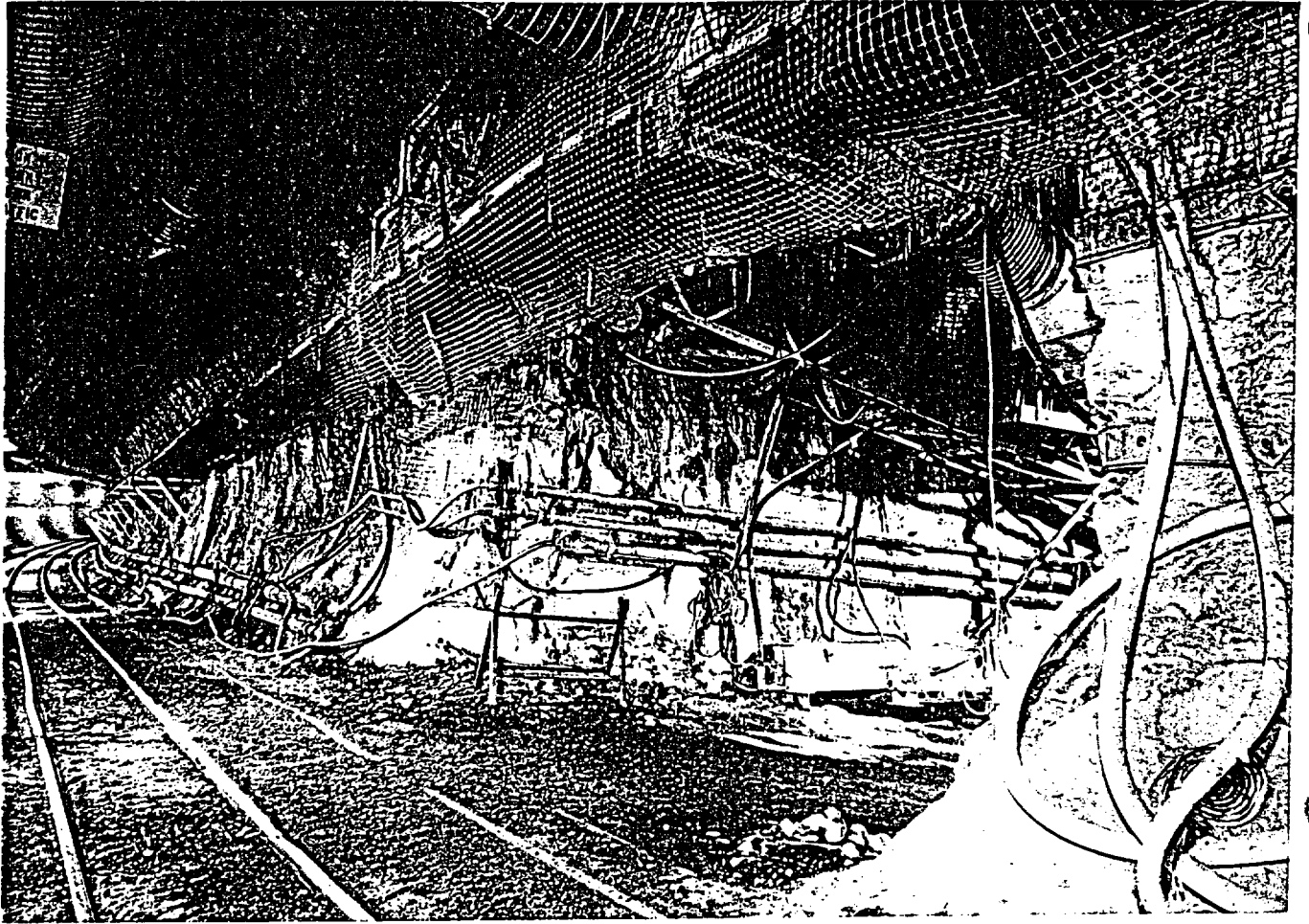


Photo 3 The entrance of Alcove 5 looking toward the North Ramp curve. YMP
photo-YM12625

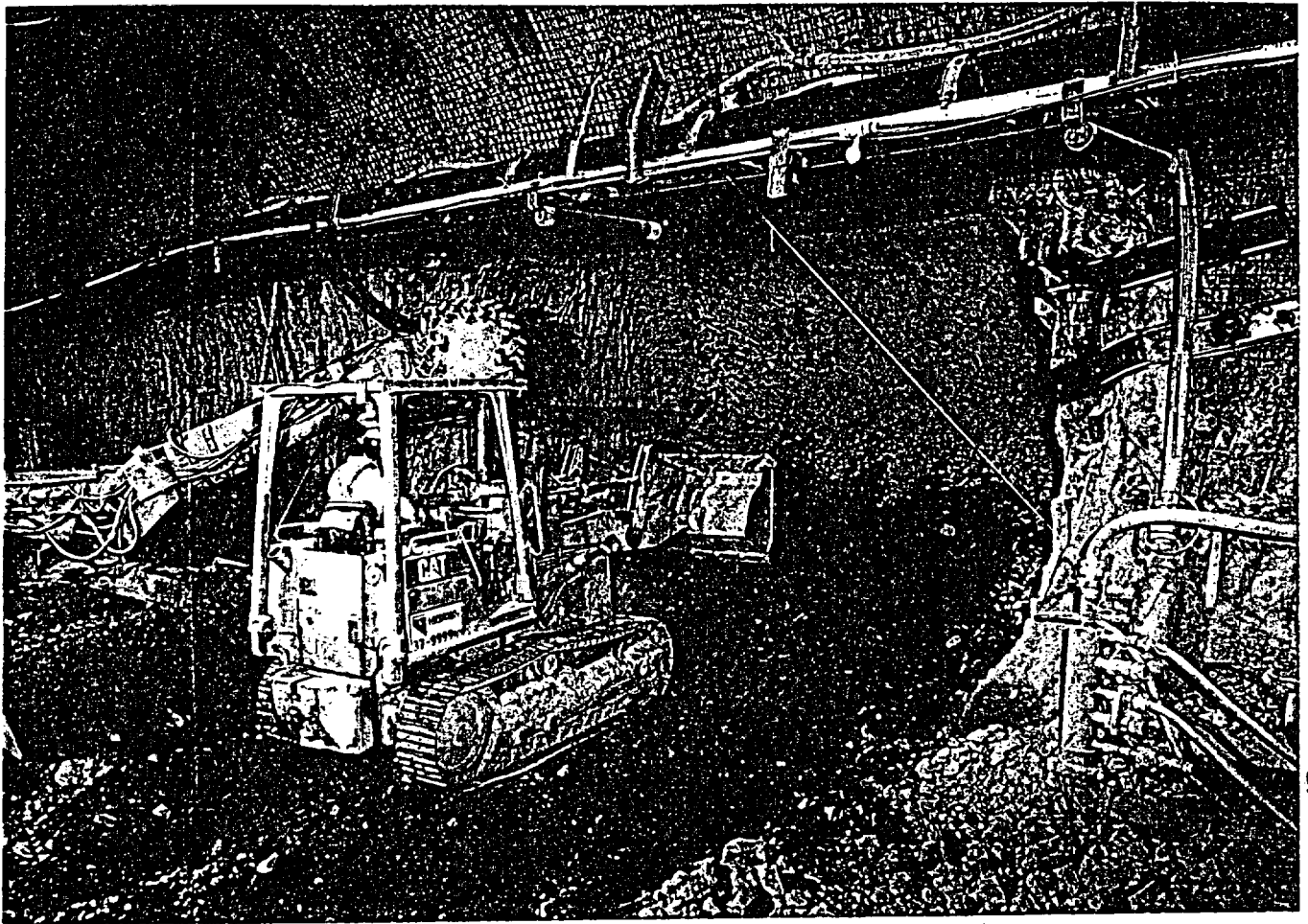


Photo 4 Initial excavation in Alcove 7 (10/29/96) at Sta. 50+64, within the fracture zone. Closely spaced Set 1 fractures are visible in the walls of the alcove.
YMP photo-YM13139

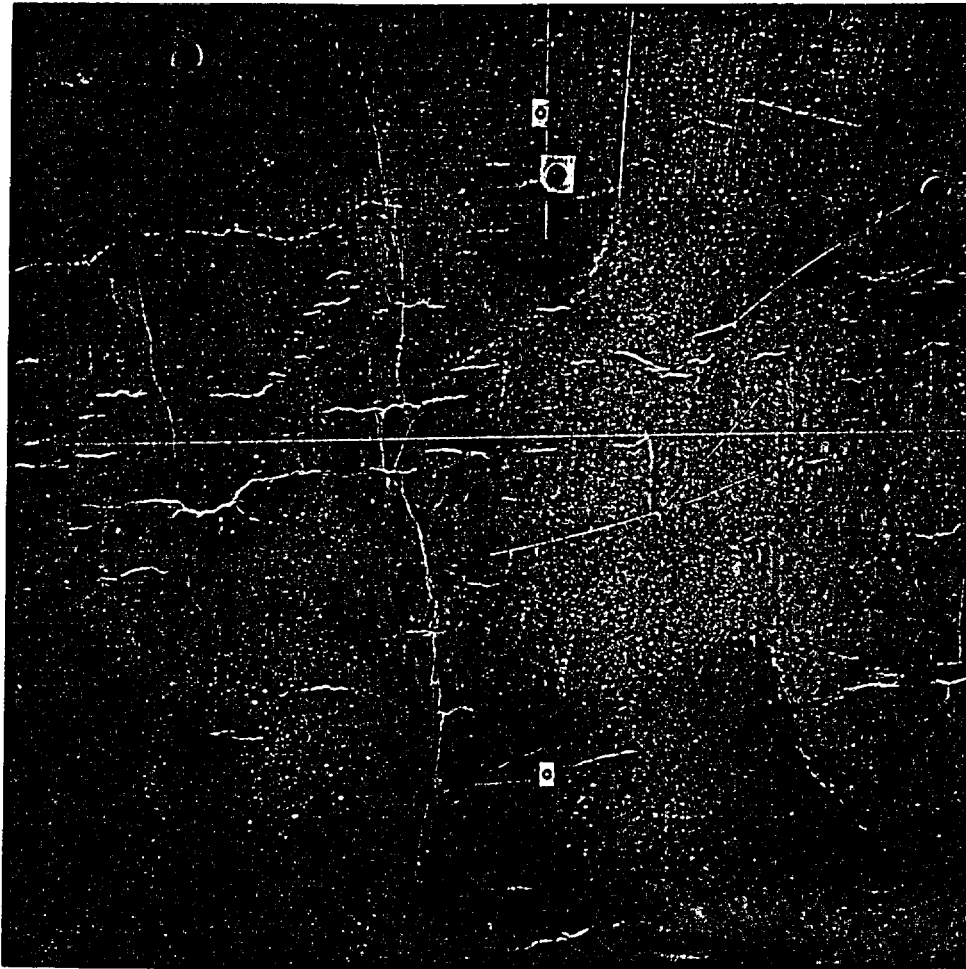


Photo 5 Typical rock matrix color changes shown on
the left wall of the tunnel at Sta. 34+55.
PG15552

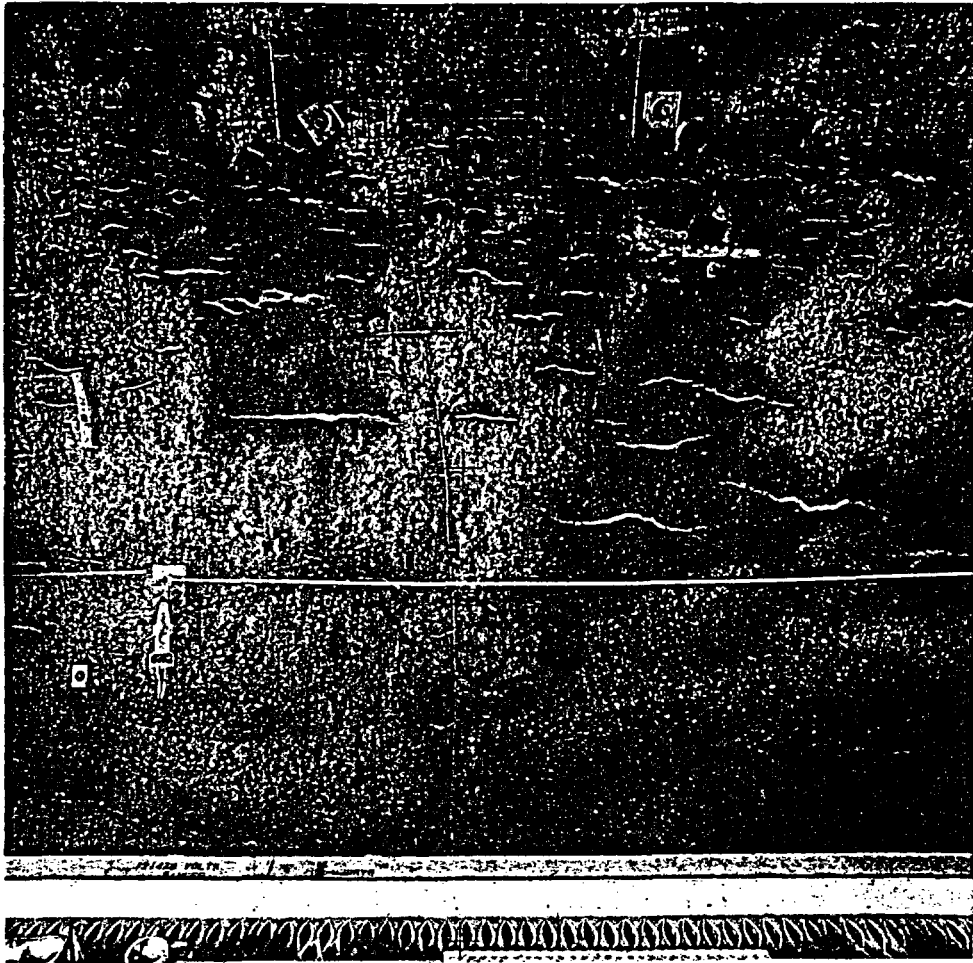


Photo 6 A variety of vapor-phase alteration and lithophysal cavities exposed on the right wall of the tunnel at Sta. 28+49. Vapor-phase alteration becomes more intense toward the crown. PG9788

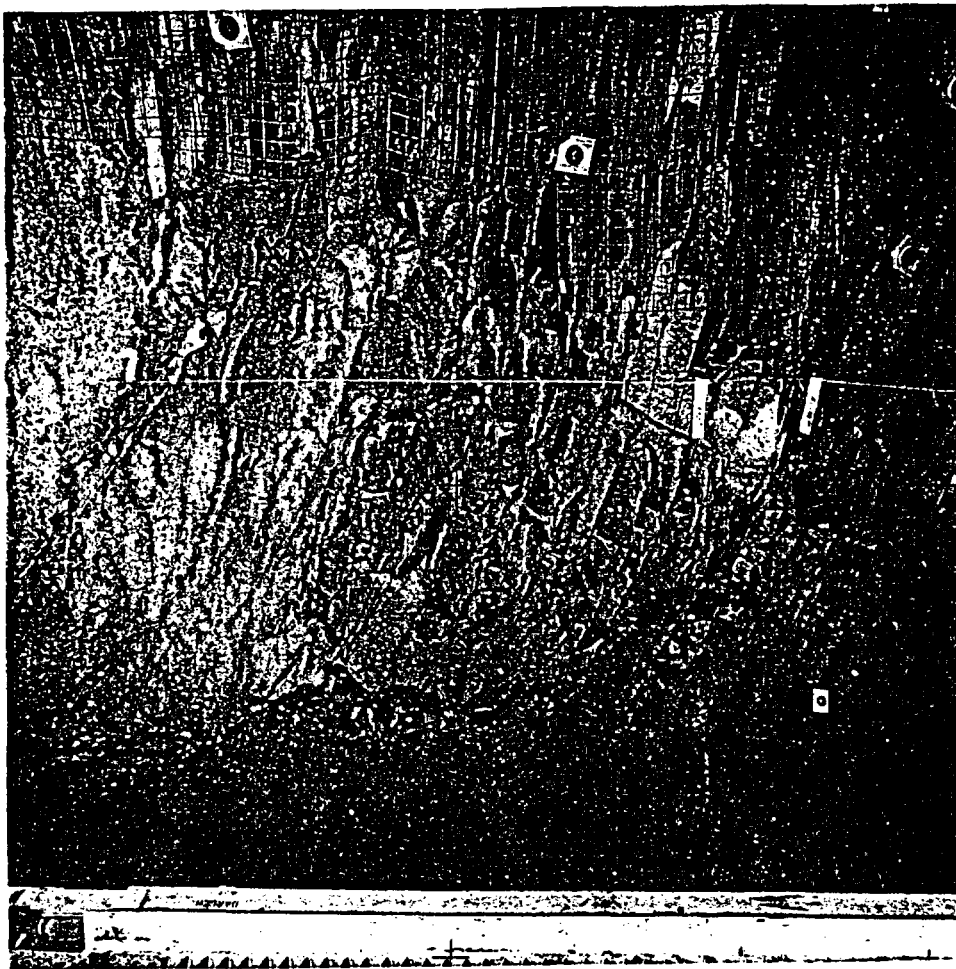


Photo 7 A curved cooling joint is exposed above the right springline at Sta. 47+49. The cooling joint is shown as the dark smooth surface in the upper right corner of the photo. Springline is marked by the white string in the center of the photo. PG15558

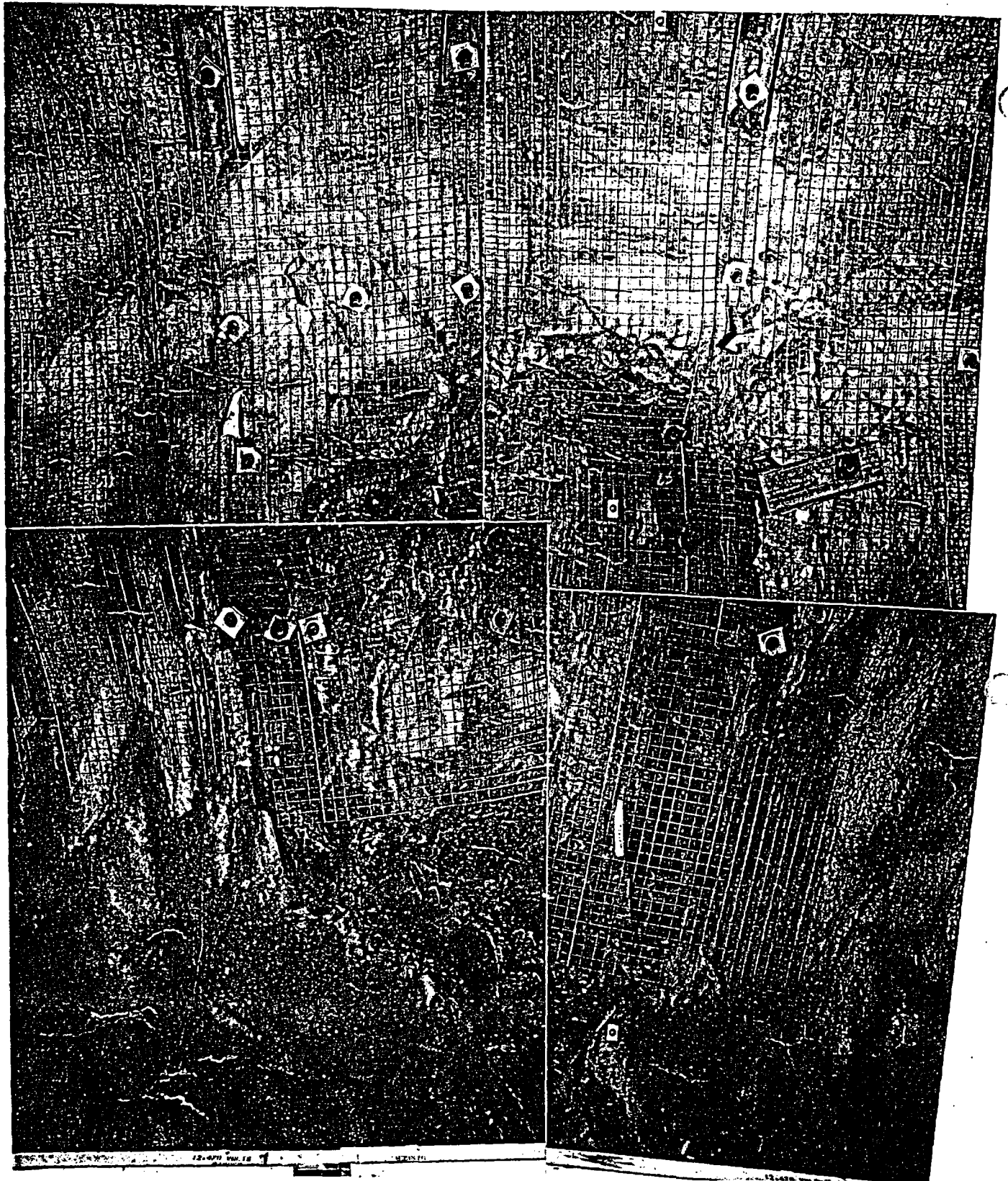


Photo 8. This photo mosaic shows the broad conical form exposed on the right wall at Sta. 34+12. The form is approximately 3-m wide and extends from the lower edge of the photo. The yellow lines are the outside edge of the trailing gear is visible along the yellow lines springline. For scale, the steel channels are shown in the photo mosaic and PG11419

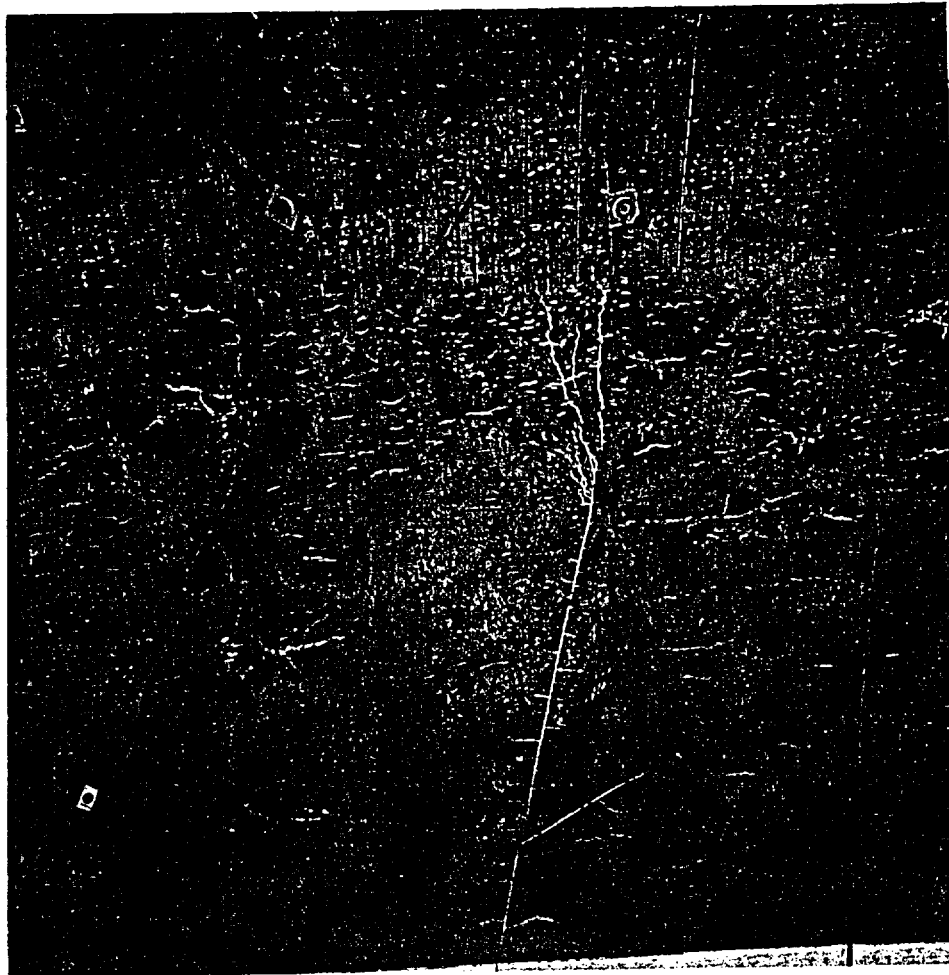


Photo 9 Vapor-phase partings project at right angles from a cooling joint located on the left wall at Sta. 28+54. Features of this kind are relatively common in areas of the Main Drift with prominent vapor-phase alteration. Also note, vapor-phase alteration increases going up the wall. The left edge of the trailing gear is visible along the bottom edge of the photo. PG9817

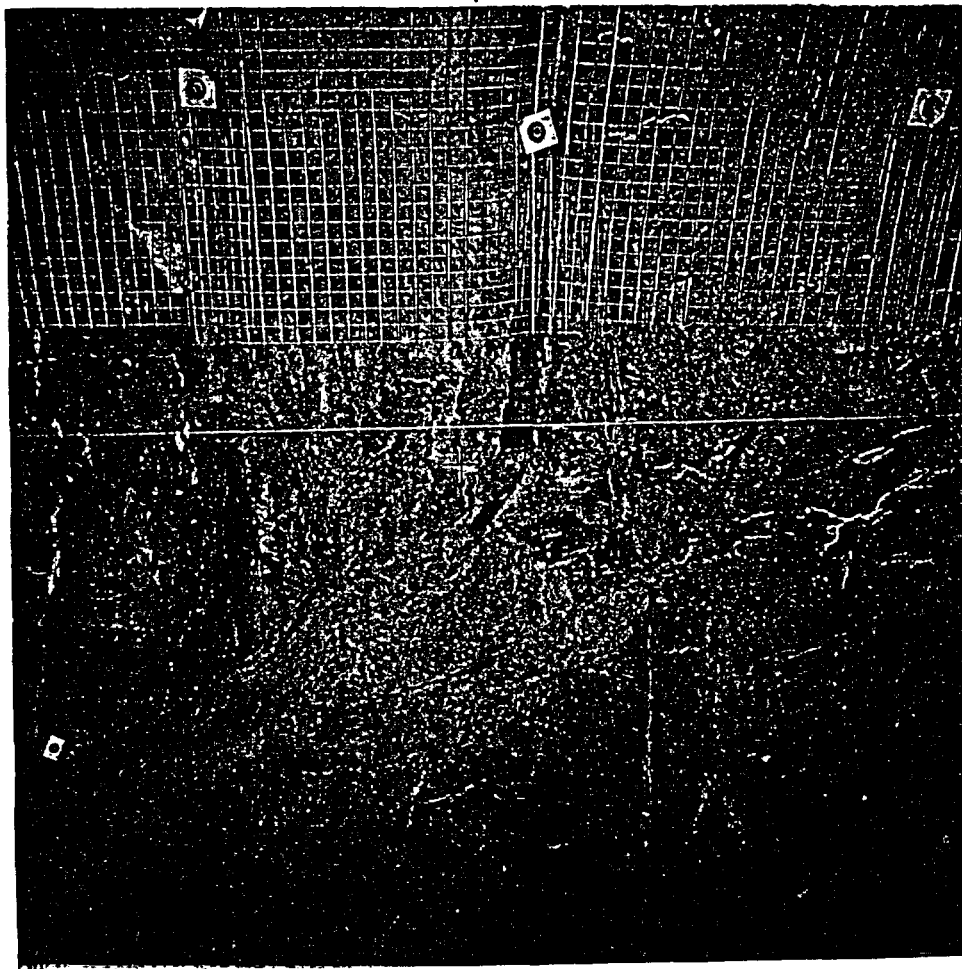


Photo 10 A segment of the Sundance fault is exposed in the left wall at Sta. 36+24. Slickensides are visible on the brown surface extending from the top, center of the photo downward. Left springline is marked by the white line through the center of the photo. PG12057

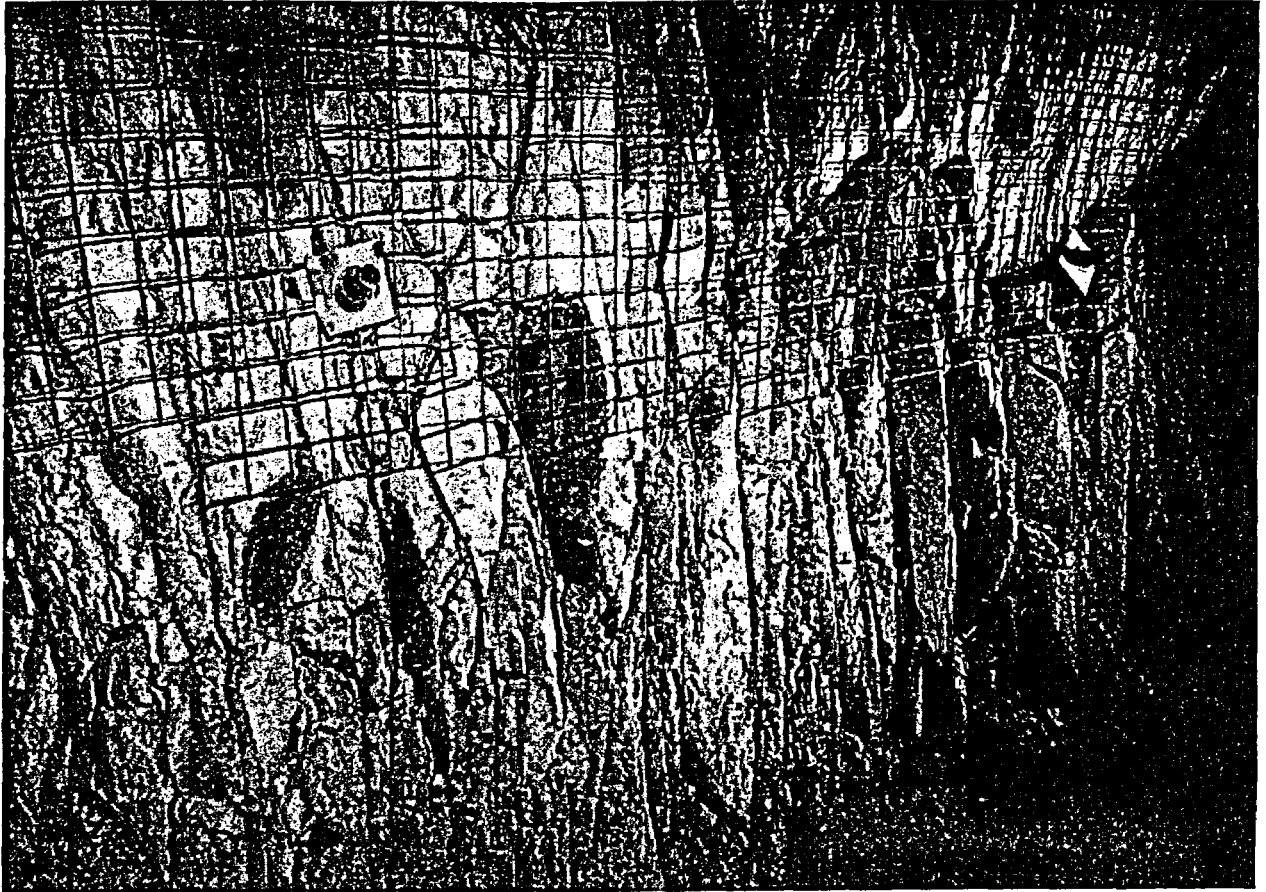


Photo 11 Photograph of intensely fractured rock on the right wall at Sta. 47+65 in the Fracture Zone. Welded wire fabric is 8cm by 8cm. YMP photo - YM11731

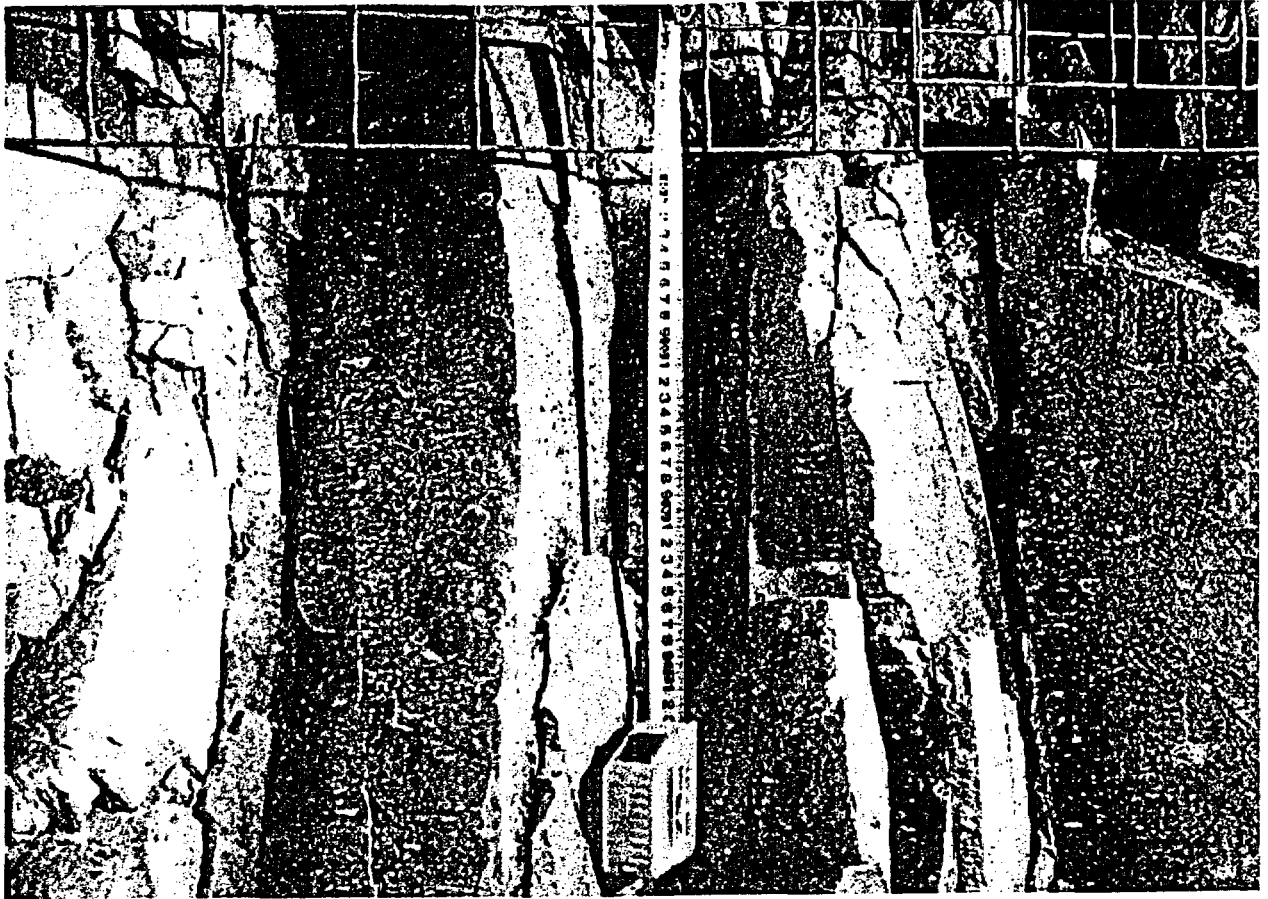


Photo 12 Close up of intensely fractured rock on the right wall at Sta. 47+65 in the Fracture Zone. YMP photo - YM11739

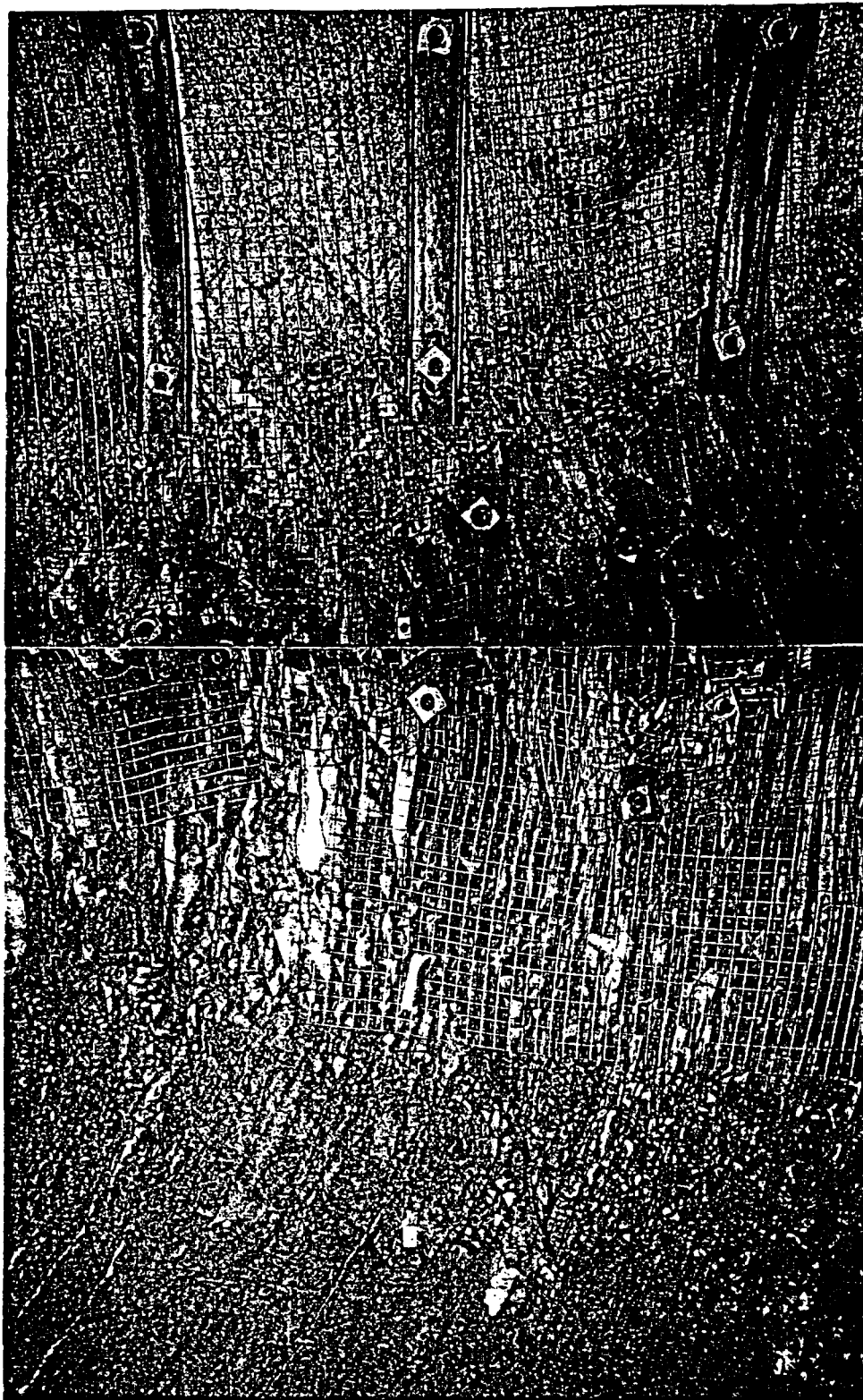


Photo 13. Intense fracturing on the walls giving way to apparent moderate fracturing across the crown. The traces of Set 1 fractures form arcs that are concave to the left. One well defined Set 2 fracture arcs from the upper right corner, through the center, and back toward the lower right. The edge of the trailing gear is visible along the bottom of the photo. Springline is marked by the white flag. For scale, the steel channels m wide. PG16263 and PG16264

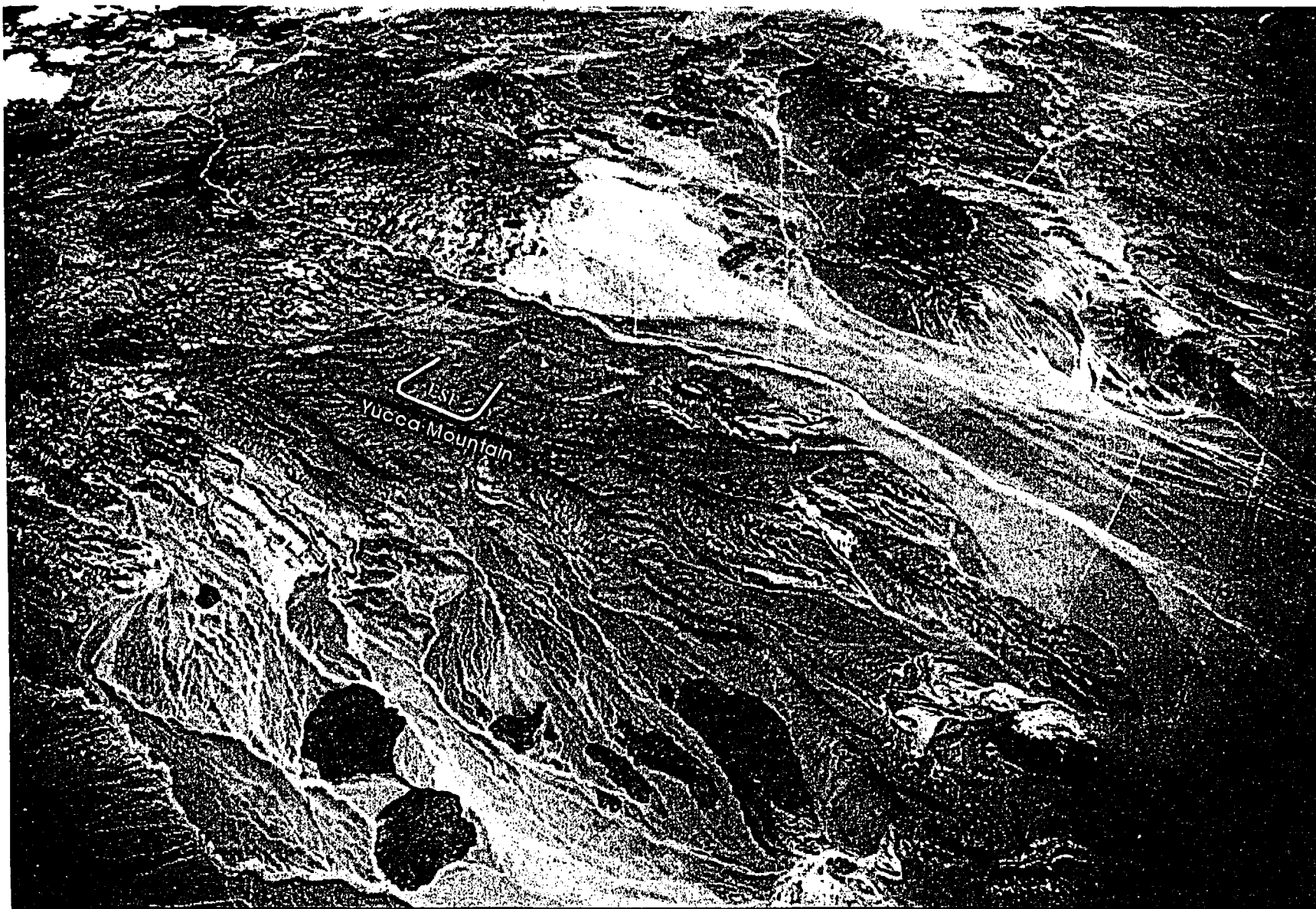


Photo 14 Oblique, high altitude aerial photo of Yucca Mountain, view to the northeast. EG&G88B187L (photo, USAF/USGS)